Adjuvant drug therapy to overcome antibiotic resistances: drug target evaluation in multidrug resistant pathogens

Inauguraldissertation
zur
Erlangung der Würde eines Doktors der Philosophie
vorgelegt der
Philosophisch-Naturwissenschaftlichen Fakultät
der Universität Basel

von

Vincent Trebosc

aus Huningue, France

Basel, 2017

Genehmigt von der Philosophisch-Naturwissenschaftlichen Fakultät auf Antrag von

Prof. Dr. Dirk Bumann

Prof. Dr. Urs Jenal

Dr. Christian Kemmer

Basel, 23.05.2017

Prof. Dr. Martin Spiess

Dekan der Philosophisch-Naturwissenschatlichen Fakultät

Abstract

Antimicrobial resistance is one of the biggest threats to human health globally. Alarmingly, multidrug-resistant, extensively drug-resistant and even pan-drug resistant pathogens have emerged worldwide and constantly spread in healthcare centers. These bacteria are resistant to most, if not all currently available antibiotics. If no actions are taken to tackle the antimicrobial resistance issue there is a high risk to enter into a post-antibiotic era, where standard surgeries provide a high risk to the patient and people died from simple infections due to a lack of treatment options. In the last decades, many big pharmaceutical companies pulled away from antibiotic discovery due to a lower expectation of profits compared to other therapeutic areas, leading to empty pipelines and a lack of innovation in the antibiotic field. To overcome this development gap, novel innovative therapeutic strategies may be needed. Adjuvant drug therapy to overcome antibiotic resistances is one of these innovative approaches. This therapy combines an antibiotic with an adjuvant drug, which specifically switches off the resistance mechanisms directed against the antibiotic. Such approach can potentially expand the life time of antibiotics by switching off an already developed resistance path or by delaying the onset of resistance. This work aimed to investigate the adjuvant therapy approach in *Acinetobacter baumannii* and *Mycobacterium tuberculosis*, which are two pathogens of great importance with constantly increasing drug resistance rates.

Acknowledgement

First, I would like to thank Christian for everything you did. For your support, for your guidance, for your openness, for your knowledge, and above all for your patience with my Frenglish, which is gone now! I probably do not show it that much, but I am aware of everything you have brought to me and I am very grateful for this.
I would like to thank Marc and Marcel. I am very grateful for the chance you gave me to work in this great company which is BioVersys. I want to thank Assaf, which whom everything started for me in BioVersys and which shared his virus for microbiology with me.
I would like to thank Prof. Dirk Bumann to have hosted me in his research group and the other member of my PhD committee Prof. Urs Jenal. I really appreciated the nice discussions and advices you both gave during the committee meetings.
Big thanks to the BioVersys team, Birgit, Michel, Sergio, Tina, Valentina, Peter, and all the intern students for all the fun we shared! Special thanks to Sarah, Marcus, Kevin, the adorable Kevin and Laura that helped me a lot in this work.
I thank all my friends here in Basel (Pauline, Pamela, the French connection, the rugby team) with whom I could easily escape from work. I also thank my friends from Baraqueville and the Toulousaing that are always present, I love you guys!
Last but not least, I would like to thank my parents, my sister, my brothers and all my family. I am convinced that everything we shared together have shaped the person I am today, and I am very glad about it! Of course Alexia, thank you to be here, thank you for your patience, thank you for your trust, thank you for your help, thank you for everything you give to me! We made it and I am not sure I could have done it without you.

Content

1. Introduction

1.1. Part A

Acinetobacter baumannii

1.1.1. *Acinetobacter baumannii* species

1.1.1.1. History

Acinetobacter baumannii is an opportunistic pathogen that belongs to the *Acinetobacter* genus. The history of the genus started in 1911 when Beijerinck, a dutch microbiologist, described an organism isolated from soil, named *Micrococcus calcoaceticus* (Beijerinck, 1911). The taxonomy history of the genus is complex with similar organisms assigned to at least 15 different genera and species (Peleg et al., 2008). The designation *Acinetobacter* was first proposed by Brisou and Prévot in 1954 and was definitely accepted in 1984 in the Bergey's Manual (Bergogne-Bérézin, 2008; Brisou and Prevot, 1954). *Acinetobacter* spp. are strict aerobic, non-fermenting, Gram-negative coccobacilli. The *Acinetobacter* species differentiation was enabled by the work of Bouvet and Grimont on DNA-DNA hybridization studies in 1986 (Bouvet and Grimont, 1986). This work allowed to name different "genomic species" in the *Acinetobacter* genus with, among others, the assignment of *A. baumannii* species. Although few species of the *Acinetobacter* genus may cause infections, *A. baumannii* is the most relevant species causing different human infectious disease (Bergogne-Bérézin, 2008).

1.1.1.2. Habitats

Acinetobacter spp. have been isolated from diverse sources including environment, food, animal and are commonly present among the human skin flora (Al Atrouni et al., 2016). However, non-*baumannii Acinetobacter* spp. account for the major part of this human colonization whereas *A. baumannii* is rarely detected (Berlau et al., 1999a; Patil and Chopade, 2001; Seifert et al., 1997). Similarly, *A. baumannii* have been recovered at low frequency in fecal samples of healthy volunteers indicating that the human intestine does not constitute an important community reservoir of this organism (Dijkshoorn et al., 2005). Importantly, *A. baumannii* have been reporter in food animal, meat, vegetables, milk and cheese, which could be vectors for subsequent human infections (Berlau et al., 1999b; Lupo et al., 2014; Rafei et al., 2015; Zhang et al., 2013).

1.1.2.Clinical manifestation and global epidemiology of *A. baumannii*

Although the identification of *A. baumannii* as cause of infection emerged in the 1960s, it was considered a low virulence pathogen with minimal significance until the 1990s (Spellberg and Bonomo, 2014). Since then, the frequency and the severity of *A. baumannii* infections have increased progressively and this emergence is mainly due to its high ability to acquire resistance to multiple antibiotics (Dijkshoorn et al., 2007). Nowadays, *A. baumannii* belongs to the most relevant pathogens causing nosocomial infections and is member of the so-called ESKAPE pathogens group, which includes *Enterobacter* spp., *Staphylococcus aureus/epidermidis*, *Klebsiella pneumoniae*, *Acinetobacter baumannii*, *Pseudomonas aeruginosa*, and *Enterococcus faecalis/faecium* (Pendleton et al., 2013). In 2013, the United States Centre for Disease Control and Prevention (CDC) classified multidrug resistant (MDR) *A. baumannii* as a "serious" threat (CDC, 2013). The same year, a study estimated that 45,000 and 1 million *A. baumannii* infections occurred in the United States and worldwide, respectively (Spellberg and Rex, 2013). In 2017, the World Health Organization (WHO) published its global priority

pathogens list where carbapenem resistant *A. baumannii* were assigned as top priority for the research and development of new and effective antibiotic treatments (WHO, 2017). Altogether, these reports highlight the importance of *A. baumannii* as a serious human pathogen.

For convenience, most of the following data on clinical manifestation are described for *Acinetobacter* spp. infections since most of the surveillance reports do not specifically differentiate *A. baumannii* from others *Acinetobacter* species. However, it is important to note that non-*baumannii Acinetobacter* infections are rare and therefore most of these data can be attributed to *A. baumannii* infections (Dijkshoorn et al., 2007).

1.1.2.1. Healthcare-associated infections

A. baumannii is mainly causing infections in critically ill patients hospitalized in intensive care units (ICUs). These infections emerged through the increase practise of modern intensive care medicine, such as mechanical ventilation, catheterisation and extensive antibiotic use. Foreign bodies enable pathogens to cross anatomical barriers, while antibiotic therapies alter the normal human microbiota allowing resistant *A. baumannii* to establish infection in hospitalized patients (Spellberg and Bonomo, 2014).

The most common clinical manifestations of *Acinetobacter* spp. are ventilator-associated pneumonias (VAPs), central line-associated bloodstream infections (CLABSIs) and catheter-associated urinary tract infections (CAUTIs) (Table 1 and Table 2). *Acinetobacter* spp. has a lower incidence in CAUTIs than in VAPs and CLABSIs.

1.1.2.1.1. Europe and United States

In Europe, the surveillance of healthcare-associated infections (HAIs) is reported by the European CDC (ECDC). Data related to *Acinetobacter* spp. HAIs in three different ECDC reports are presented in the Table 1. The reports of 2007 and 2012 refer to ICU facilities data whereas the third report covers the period 2011-2012 with incidence in acute care hospitals. The *Acinetobacter* spp. CAUTI rates remained stable in the three studies while the CLABSI rates in ICUs increased from 2007 to 2012. In 2012, the *Acinetobacter* spp. VAP rates in acute care hospitals were approximatively twice higher than in ICU facilities. However, *Acinetobacter* spp. VAP cases reported in ICU facilities were approximatively 8 times greater than in acute care hospitals.

In 2012, *Acinetobacter* spp were associated with 3.6 % of all HAIs in European acute care hospitals with a rate superior to 8 % in Bulgaria, Greece, Latvia and Romania (Figure 1). In ICU facilities in 2012, the country with the highest rates of *Acinetobacter* spp. HAIs were Estonia, Italy, Lithuania, Portugal, Romania and Slovakia with *Acinetobacter* spp. the major cause of VAP in Lithuania and Romania and the major cause of CLABSI in Romania (ECDC, 2015). Finally, the rate of carbapenem resistant *Acinetobacter* spp. isolates is very high in the three European reports (Table 1). This elevated carbapenem resistance rate is alarming considering that carbapenems are recognized as last resort antibiotics to treat MDR *A. baumannii* infections.

Table 1: Prevalence of *Acinetobacter* spp. hospital acquired infections in Europe and USA.

			Infection types			Carbapenem resistant	Source
			VAP	CLABSI	CAUTI		
Europe	ICU (2007)	N *	9,749	4,911	5,117	73.3 %	(ECDC, 2012)
		rate **	4.3 %	0.5 %	1.2 %		
	ICU (2012)	N *	13,672	6,313	3,174	68.8 %	(ECDC, 2015)
		rate **	4.8 %	3.5 %	1.5 %		
	non-ICU (2011-2012)	N *	1,777	1,722	2,168	81.2 %	(ECDC, 2013)
		rate **	8.7 %	4.1 %	1.5 %		
USA	non-ICU (2011-14)	N *	8,805	96,532	153,805	46.6 – 69 %	(Weiner et al., 2016)
		rate **	6.1 %	2.2 %	0.7 %		

* number of *Acinetobacter* spp. infection cases

** rates of *Acinetobacter* spp infection as a percentage of all microorganisms reported

CAUTI: catheter-associated urinary tract infection, CLABSI: central line-associated bloodstream infections, ICU: intensive care unit, VAP: ventilator-associated pneumonia.

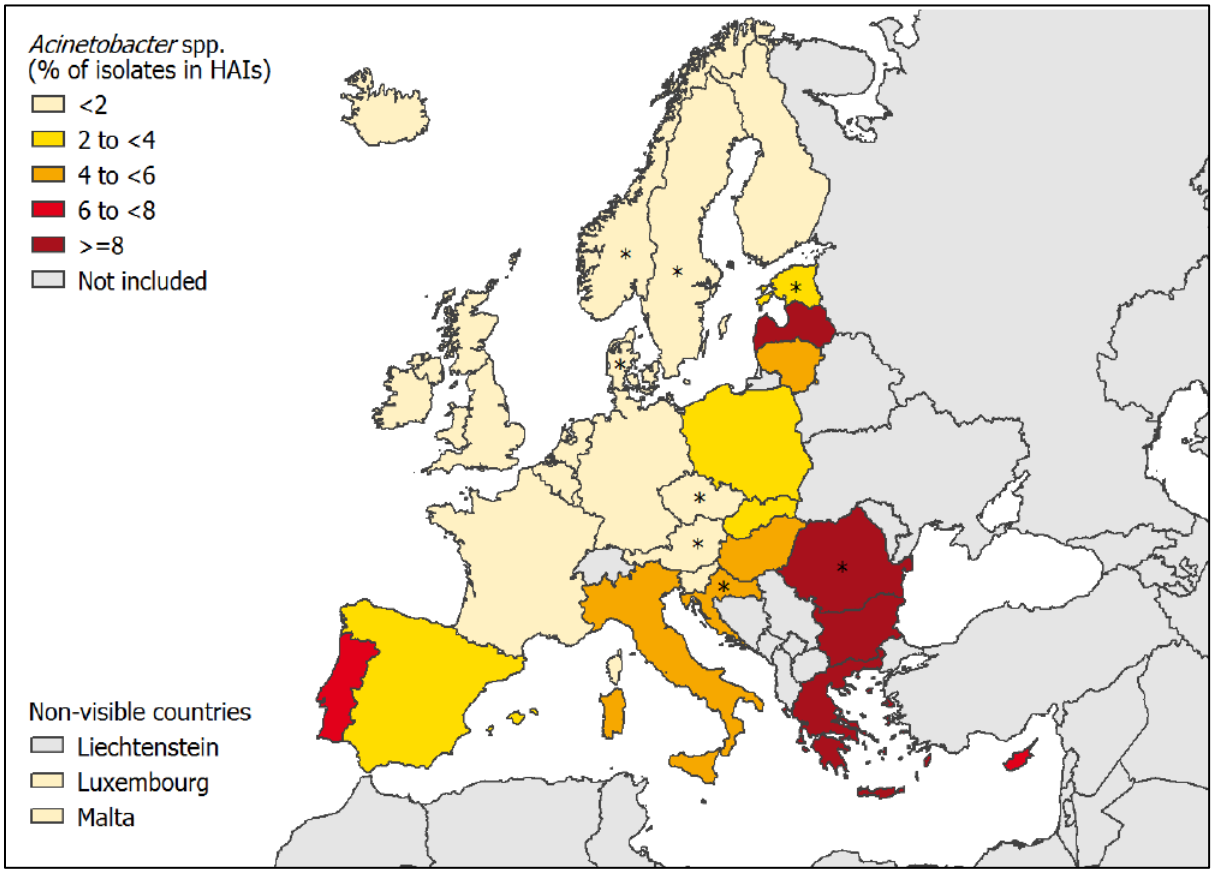

Figure 1: Relative frequency of *Acinetobacter* spp. causing HAIs as a percentage of all microorganisms (n=366 isolates) (ECDC, 2013).

* Poor data representativeness in these countries.

In the United States, the National Healthcare Safety Network reported the cases of HAIs from non-ICU facilities (acute care hospitals, long-term acute care hospitals and inpatient rehabilitation facilities) from 2011 to 2014 (Weiner et al., 2016). *Acinetobacter* spp. VAP, CLABSI and CAUTI cases are reported in Table 1. This report indicates that 46.6 to 69 % (depending on year and infection type) of *Acinetobacter* spp. VAPs, CLABIs and CAUTIs were caused by strains resistant to carbapenem, which is in accordance with the rates observed in

Europe. Similarly, 47.3 to 75.6 % of *Acinetobacter* spp. VAPs, CLABIs and CAUTIs were caused by MDR strains. These resistance rates are extremely high compared to those of other Gram-negative pathogens such as *P. aeruginosa*, *K. pneumoniae* and *E. coli* (Weiner et al., 2016). The CDC estimated that MDR *A. baumannii* infections caused 500 deaths per year in United States (CDC, 2013).

1.1.2.1.2. Other regions

Acinetobacter spp. pathogens are a global issue with infections reported worldwide. Since 2003, the International Nosocomial Infection Control Consortium (INICC) has published surveillance reports on device-associated HAIs in ICU facilities from individual countries (Rosenthal, 2016). The rates of *Acinetobacter* spp. HAIs from these reports are summarized in the Table 2. Overall, *Acinetobacter* spp. are more isolated from VAPs and CLABSIs than from CAUTIs as seen in USA and in Europe. The rates of *Acinetobacter* spp. HAIs in Latin America countries are similar to those seen in USA and Europe. However, *Acinetobacter* spp. HAI rates in Asia, Middle East and Morocco (the only representative of Africa in these reports) are significantly higher than those reported for the USA and Europe. According to these reports, *Acinetobacter* spp. are the first pathogens causing HAIs in China, Philippines, Iran, Morocco and the second in Lebanon.

Table 2: Prevalence of *Acinetobacter* spp hospital acquired infections expressed as a percentage of all microorganisms reported.

Region	Country	HAIs (%)	VAPs (%)	CLABSI (%)	CAUTI (%)	Source
Latin America	**Brazil**	14.6	N.D.	N.D.	N.D.	(Salomao et al., 2008)
	Mexico	2.8	2.9	3.3	1.6	(Ramirez Barba et al., 2006)
	Colombia	4.5	N.D.	N.D.	N.D.	(Moreno et al., 2006)
	Cuba	10.3	15.4	33.3	0	(Guanche-Garcell et al., 2011)
	Peru	4.7	4.2	6.3	5	(Cuellar et al., 2008)
	El Salvador	4	N.D.	N.D.	N.D.	(Dueñas et al., 2011)
Asia	**China**	19.1	25.4	12.3	3	(Tao et al., 2011)
	Philippines	21.1	25.5	18.2	11.1	(Navoa-Ng et al., 2011)
	India	N.D.	N.D.	N.D.	N.D.	(Mehta et al., 2007)
Middle East	**Lebanon**	29.1	37.5	27.3	20	(Kanj et al., 2012)
	Iran	27.5	60	N.D.	N.D.	(Jahani-Sherafat et al., 2015)
	Turkey	22.6	29.2	23.2	7.5	(Leblebicioglu et al., 2007)
Africa	**Morocco**	31.9	45.8	14.3	18.8	(Madani et al., 2009)

CAUTI: catheter-associated urinary tract infection, CLABSI: central line-associated bloodstream infections, HAI: hospital acquired infection, VAP: ventilator-associated pneumonia.

1.1.2.2. Other clinical manifestations

Acinetobacter spp. can cause infection in other organ systems, including endocarditis, meningitis, intraabdominal abscess, osteomyelitis, soft tissue, and surgical site infections (Glew et al., 1977).

Acinetobacter spp. have been reported as one of the major cause of osteomyelitis and wound infections during the military operations in the Middle East (Davis et al., 2005; Yun et al., 2008). *A. baumannii* was the second most isolated Gram-negative pathogen from osteomyelitis infections from 2007 to 2009 in Sao Paulo, Brazil (Carvalho et al., 2012). The incidence of endocarditis caused by *A. baumannii* is rather low but the outcome can be dramatic with sudden

patient death (Laganà et al., 2015). A recent study indicates that, although *S. aureus* is the most common cause of meningitis following neurosurgical procedure, the rate of *A. baumannii* causing meningitis is increasing (Chen et al., 2016). Indeed, *A. baumannii* has been reported in 31.8 % of the meningitis cases in a Taiwan hospital from 2008 to 2012, (Chen et al., 2016). Other studies further reported *A. baumannii* as the most common pathogen causing postneurosurgical meningitis in a private hospital of Tehran (Iran) from 2010 to 2012 and in Turkey from 2004 to 2013 (Sipahi et al., 2017; Yadegarynia et al., 2014).

1.1.2.3. Community-acquired infections

Community-acquired *A. baumannii* infections typically occur in tropical regions during the wet season (Dexter et al., 2015). Community-acquired pneumonia caused by *A. baumannii* is rare but it is fulminant and generally extremely severe with a mortality rate as high as 64 % (Anstey et al., 1992; Chen et al., 2001; Leung et al., 2006; Ong et al., 2009). This high mortality rate has been associated to non-appropriate treatment since an appropriate initial therapy reduced the mortality rate to 11 % (Davis et al., 2014). It appears that hazardous alcohol consumption, smoking and chronic lung disease are important risk factors for community-acquired *A. baumannii* infections (Davis et al., 2014).

1.1.3. *A. baumannii* pathogenesis

1.1.3.1. Virulence and mortality rate

A. baumannii is generally considered as a low virulence pathogen when compared to the other microorganisms of the ESKAPE group (Paterson and Harris, 2015). The mortality rate of *A. baumannii* infections is controversial due to the difficulty to attribute the cause of mortality to the infection per se or to underlying diseases. In 2003, a study concluded that *A. baumannii* bacteremia is not associated with increased mortality in ICU patients (Blot et al., 2003). The mortality rate of *A. baumannii* bacteremia was 42.2 % while the mortality rate of controls was 34.4 % indicating an attributable mortality of 7.8 %. The same conclusions were drawn on *A. baumannii* pneumonia, which was not significantly associated with an attributable mortality rate (Garnacho et al., 2003). However, in 2006, a review of six matched case-control studies indicated that the attributable mortality rates of *A. baumannii* infection ranged from 7.8 % to 23 % in hospital and from 10 % to 43 % in ICU facilities, indicating that *A. baumannii* infection might be associated with considerably increased mortality (Falagas et al., 2006).

Hypervirulent *A. baumannii* causing outbreaks have been isolated, such as the LAC-4 strain that was isolated from nosocomial outbreaks in Los Angeles in 1997 (Valentine et al., 2008). This strain was considered as hypervirulent based on immunocompetent *in vivo* mouse model, but there are no clinical or epidemiologic data available for this strain (Harris et al., 2013). Recently, hypervirulent strains were isolated from fatal outbreaks in the northwest of United States (Jones et al., 2015). Interestingly, the most virulent strains in this study belong to the same clonal lineage than the LAC-4 strain. In contrast to the LAC-4 strain, clinical history is available for the strains reported by Jones and colleagues and they showed that patients had only minor underlying disease, suggesting that patient death was mainly caused by the *A. baumannii* infection.

Other data suggest *A. baumannii* isolates with enhanced virulence. A case of severe pneumonia was reported in a healthcare worker due to occupational transmission (Whitman et al., 2008). The strain recovered from the healthcare worker was most likely transmitted from a patient during endotracheal suctioning. Fulminant sepsis with patient death 6-days after transplantation have been reported (Patel et al., 2015). The autopsy revealed endocarditis, myocarditis, splenic and renal emboli, peritonitis, and pneumonia, highlighting the potential of *A. baumannii* to develop strong virulence.

A. baumannii virulence has been assessed in different mouse models (de Breij et al., 2012; Bruhn et al., 2015; Eveillard et al., 2010). These studies demonstrated that virulence is highly strain dependant with some strains being hypervirulent and others being hypovirulent. Bruhn and colleagues tested different strains from the International Clonal Complex (ICC) 2, which is the most widespread clonal complex in hospital, in a bacteremia mouse model (Bruhn et al., 2015). They showed that some strains inoculated at 2 x 10^7 colony forming units (CFUs) develop a lethal infection within seven days whereas other strains require an inoculum of 5 x 10^7 CFUs to achieve the same outcome. These results suggest that factors independent of the clonal lineage are involved in *A. baumannii* virulence.

1.1.3.2. Persistence in hospital environment

Long-term persistence in hospital environment most likely contributes to the success of *A. baumannii.* Clinical isolates can survive up to one month in simulated hospital conditions independently of the strain source (Jawad et al., 1998). A prospective cohort study examined the presence of *A. baumannii* in intensive care unit rooms with patient colonized or infected with this pathogen (Thom et al., 2011). Approximately half of the rooms sampled were positive for the bacteria and most of the strains were similar to the patient isolates. A recent study showed that 54 % of healthy health care worker were *A. baumannii* nasal carriers in long-term-care facilities in Taiwan (Liou et al., 2017). Altogether, these data indicate that persistence in hospital environment and health care worker may play a major role in *A. baumannii* nosocomial infection. This persistence behaviour is associated with the ability of *A. baumannii* to resist desiccation and adhere to abiotic surfaces, which are both discussed below.

1.1.3.2.1. Resistance to desiccation

A. baumannii is intrinsically more resistant to desiccation than other Gram-negatives pathogens, as demonstrated by a 2-log CFU reduction after 25 days compared to *K. pneumoniae*, *P. aeruginosa* and *E. coli* that showed a 5-log CFU reduction after 1 h, 2 h and 7 h, respectively (Hirai, 1991). Under dry conditions, *A. baumannii* undergoes morphological changes, including transition from rod to round shaped cells and significantly thickening of the cell wall, which most likely contribute to desiccation resistance (Houang et al., 1998). Interestingly, these morphological changes make *A. baumannii* phenotypically more resembling Gram-positive bacteria, which are more desiccation resistant than Gram-negative bacteria (Hirai, 1991).

Boll and colleagues suggested that the hepta-acylated lipid A present in the outer membrane of *A. baumannii* renders the membrane less fluid than the hexa-acylated lipid A present in most Gram-negative (Boll et al., 2015). Consequently, a decrease in membrane fluidity may reduce the leakage of essential growth factors therefore increasing long-term survival. They showed that a penta-acylated *A. baumannii* mutant strain could not survive desiccation conditions

compared to the hepta-acylated wild type strain, indicating that a specific outer membrane composition may explain the differences between *A. baumannii* and other Gram-negative bacteria in their ability to resist desiccation.

Besides morphological changes, the RecA recombinase is required for *A. baumannii* desiccation resistance. It has been suggested that RecA, which is involved in several DNA repair mechanisms, allows to cope with DNA damages caused by desiccation stress (Aranda et al., 2011). However, this does not explain the differences in desiccation resistance between *A. baumannii* and other Gram-negative bacteria, because they all encode *recA*.

1.1.3.2.2. Adherence to abiotic surface

A. baumannii has the capacity to attach to glass or plastic surfaces and to form biofilms. The ability to adhere and survive on abiotic surfaces plays an important role in nosocomial infections due to *A. baumannii* colonization of medical devices, such as urinary catheters, central venous catheters and endotracheal tubes (Longo et al., 2014).

Different mechanisms appear to be involved in this process. Tomaras and colleague have demonstrated that adherence to abiotic surfaces and subsequent biofilm formation is dependent on the expression of the *csuE* gene in *A. baumannii* ATCC-19606 strain (Tomaras et al., 2003). CsuE is part of the CsuA/BABCDE chaperone–usher pili assembly system, and pili formation promotes *A. baumannii* adherence to and biofilm formation on abiotic surfaces. Transposon mutagenesis on *A. baumannii* 307-0294 strain revealed that a protein homolog to the *S. aureus* biofilm-associated protein (Bap) is required for the stabilization of *A. baumannii* biofilms formed on glass (Loehfelm et al., 2008). Another transposon mutagenesis study on ATCC-19606 strain demonstrated that deletion of the outer membrane protein A gene (*ompA*) hampered biofilm formation on plastic surface (Gaddy et al., 2009).

This section specifically discussed abiotic surfaces adherence and biofilm mechanisms. Other mechanisms are observed for adherence to biotic surfaces and some of them will be discussed in the next section on virulence determinants.

1.1.3.3. Virulence determinants

The mechanisms involved in *A. bamaunnii* virulence and pathogenesis have been only partially elucidated (Gordon and Wareham, 2010; McConnell et al., 2013). This lack of knowledge can be attributed to the paucity of tools to genetically manipulate *A. baumannii* clinical isolates to study virulence factors (Wong et al., 2017). In addition, virulence studies were often performed on avirulent lab-adapted strains and/or non-relevant infections models (Wong et al., 2017). Therefore, virulence studies must be interpreted carefully keeping in mind the strains and models that were used and their potential limitations. Nevertheless, Wong and colleagues recently compiled all the studies related to *A. baumannii* virulence and separated the different virulence factors in function of the model used for their identification (Wong et al., 2017). This work highlights cell surface components, such as outer membrane proteins, pili, capsule and protein secretion systems, as important *A. baumannii* virulence factors.

1.1.3.3.1. OmpA

OmpA is the most abundant outer membrane protein in *A. baumannii*. This protein is involved in several virulence mechanisms, such as adherence and invasion of host epithelial cells, cell cytotoxicity and biofilm formation (McConnell et al., 2013). Adherence to host cells is an important bacterial virulence factor as it is the initial step of the colonization process. In 2006, light and scanning electron microscopy experiments showed the first evidence of *A. baumannii* attachment to human bronchial epithelial cells (Lee et al., 2006). Later, the work of Gaddy and colleagues revealed that OmpA is involved in epithelial cell attachment (Gaddy et al., 2009). *A. baumannii* ATCC-19606 OmpA-deficient mutant cells were drastically impaired in their ability to attach and invade A549 human alveolar epithelial cells compared to the parental strain. Same findings were obtained with the *A. baumannii* AB5075 clinical strain (Schweppe et al., 2015). Moreover, it has been shown that OmpA protein is able to translocate to the nucleus of host cells, to target mitochondria and to induces cell death (Choi et al., 2005, 2008). OmpA mediated cell death was also demonstrated in dendritic cells suggesting that this virulence mechanism allows *A. baumannii* to prevent the adaptive immune system response (Lee et al., 2010). Finally, the importance of OmpA for *A. baumannii* pathogenesis was demonstrated *in vivo* in lung infection mouse models (Schweppe et al., 2015; Wang et al., 2014).

1.1.3.3.2. Pili

Pilis are filamentous appendages at the surface of bacteria mediating interactions with their environment. The role of pili in *A. baumannii* virulence has not been completely decoded (Weber et al., 2015a).

The most studied pili structure in *A. baumannii* is the chaperone/usher Csu pili. As previously mentioned, this system is involved in attachment and biofilm formation on abiotic surfaces (Tomaras et al., 2003). In addition, Csu pili subunits have been identified as major components in the matrix of the pellicle, which is the biofilm that *A. baumannii* forms at the air-liquid surface (Chabane et al., 2014; Marti et al., 2011). However, the Csu pili system is not required for attachment of *A. baumannii* ATCC-19606 to biotic surfaces, such as epithelial cells (de Breij et al., 2009). In addition, the *A. baumannii* clinical isolate ACICU harbours a non-functional Csu system due to transposon insertion (Eijkelkamp et al., 2014). Therefore, it appears that the *A. baumannii* Csu pili system is important for biofilm formation but its role in virulence needs to be confirmed *in vivo*.

1.1.3.3.3. Capsule

Bacterial capsules are composed by extracellular polysaccharides forming a protection layer around bacterial cells. Most *A. baumannii* clinical isolates produce a capsule without distinction between epidemic or sporadic strains (Koeleman et al., 2001). The biosynthesis pathway of capsules is encoded by a cluster of genes called the K locus. The K locus is organized with modules encoding genes for polysaccharide export or UDP-linked sugar precursors synthesis at each ends (Kenyon and Hall, 2013). Genes present in between these two modules code for sugar synthesis enzymes, glycosyltransferases, glycan modification enzymes, and repeat unit processing enzymes. Although the two modules flanking the K locus are relatively conserved, the genes present in between are highly variable leading to high diversity and complexity in

capsule sugar composition and capsule organization in *A. baumannii* strains (Hu et al., 2013; Kenyon and Hall, 2013). Nevertheless, glycoproteome analysis revealed that the capsule is composed by glycans with similar characteristics across all *A. baumannii* (Scott et al., 2014). In general, *A. baumannii* capsular polysaccharides are short (three to five residue), unbranched glycans and contain negatively charged amino-containing sugars that contribute to host immunity protection. Capsule production has been associated with *A. baumannii* defence against complement-mediated opsonisation and destruction, as well as phagocytic uptake (Geisinger and Isberg, 2015; Lees-Miller et al., 2013; Russo et al., 2010). Two different studies performed on a laboratory and a clinical strain indicated that capsule deficient *A. baumannii* mutants were negatively affected during *in vitro* serum survival and in *in vivo* mouse experiments (Lees-Miller et al., 2013; Russo et al., 2010). Sub-inhibitory concentration of antibiotics may trigger an increased production of capsule exopolysaccharides due to activation of the BfmRS two component system (TCS) (Geisinger and Isberg, 2015). Capsule hyperproduction confers increased virulence in bloodstream infection mouse model. Finally, hypervirulent strains with an unusual capsule harbouring legionamic acid residue have been reported (Hu et al., 2013; Jones et al., 2015; Ou et al., 2015). The similarity between legionamic acid and sialic acid, which is present on mammalian surface glycoproteins, suggests a role for legionamic acid containing capsules in immune system escape (Ou et al., 2015).

1.1.3.3.4. Secretion systems

Protein secretion systems have been associated with virulence in Gram-negative bacteria. *A. baumannii* encodes two different types of secretion systems, the type II secretion system (T2SS) and the type VI secretion system (T6SS).

The T2SS has been recently identified in *A. baumannii* and it was suggested to be commonly present in this species (Weber et al., 2015a). *A. baumannii* T2SS is involved in lipase secretion, which is required for growth on long-chain fatty acids as a sole carbon source (Johnson et al., 2016). Exogenous lipid metabolism is broadly accepted as a virulence factor suggesting a role for T2SS in *A. baumannii* pathogenesis (Singh et al., 2010). A T2SS deficient *A. baumannii* mutant was outcompeted by its respective parental strain in a bacteremia mouse model confirming the role of T2SS in *A. baumannii* virulence (Johnson et al., 2016).

T6SSs were first described as toxin secretion systems used to compete with and kill surrounding eukaryotic cells. T6SS deficient *A. baumannii* mutants are significantly attenuated in a *Galleria mellonella* killing assay indicating the role of T6SS in pathogenesis (Repizo et al., 2015). Additionally, it appears that T6SSs are important for infection establishment by killing competing bacteria (Weber et al., 2015a). Indeed, T6SS expressing *A. baumannii* strains compete with and kill a wide range of bacteria *in vitro*, including other *A. baumannii* strains (Repizo et al., 2015; Weber et al., 2015b). T6SS expression is generally tightly regulated due to the considerable energy requirement of a functional system (Basler, 2015). In *A. baumannii* ATCC-17978 and Ab04 strains, T6SS expression is controlled by a transcriptional repressor present on a plasmid harbouring multiple resistance genes (Weber et al., 2015b). Weber and colleagues suggest that *A. baumannii* takes advantage of this regulation system to simultaneously associate infection establishment with antibiotic resistance. Indeed, spontaneous plasmid loss in a population subpart would enable T6SS expression and niche

establishment while the rest of the population harbouring the plasmid resists antibiotic treatment.

1.1.3.3.5. Iron acquisition

Iron sequestration is used by the host to fight against bacterial infections (Mortensen and Skaar, 2013). Successful pathogens including *A. baumannii*, have developed efficient iron acquisition systems to access iron from their hosts. *A. baumannii* iron acquisition mainly resides on two systems.

The first system uses the uptake of bacterial or host proteins that bind iron with high affinity. Indeed, *A. baumannii* can secrete and take up several siderophores, which are proteins that scavenge iron, or directly ingest iron-bound hemes that are released during erythrocytes lysis (Mortensen and Skaar, 2013). In both cases, the uptake of iron-bound proteins is dependent on an energy-transducing system mediated by TonB dependent-receptors. The most studied *A. baumannii* siderophore is acinetobactin. Its biosynthesis pathway and uptake systems are required for *A. baumannii* virulence as demonstrated in *G. mellonella* and mouse infection models indicating that iron acquisition plays an important role in *A. baumannii* pathogenesis (Fiester et al., 2015; Gaddy et al., 2012; Penwell et al., 2012; Zimbler et al., 2013).

The second *A. baumannii* iron acquisition mechanism resides in the direct uptake of reduced ferrous iron. The ferrous iron import system relies on FoeAB transporters, which are ubiquitous in *A. baumannii* clinical isolates (Antunes et al., 2011). Transposon sequencing experiment conducted in a bacteremia mouse model indicated that mutants in the FeoAB transport system have a fitness defect compared to wildtype strains (Subashchandrabose et al., 2016). Altogether, it appears that iron acquisition mechanisms are important for *A. baumannii* virulence.

1.1.3.4. Immune system response to *A. baumannii* infection

Host defence mechanisms involved in the control of *A. baumannii* infections as well as factors involved in clinical outcome were recently elucidated (Wong et al., 2017). Virulence assessment of multiple strains in a bacteremia mouse model showed that bacterial growth inhibition and infection clearance require the concerted action of the three innate immunity components, which are the complement system, neutrophils and macrophages (Bruhn et al., 2015). Indeed, only the combined depletion of the three innate immunity effectors significantly increases bacterial density in blood triggering lethal sepsis. Consequently, early host defence mechanisms are essential to control the bacterial load enabling subsequent *A. baumannii* infection clearance (Figure 2.A). However, *A. baumannii* virulent strains, such as capsule hyperproducers, may escape complement mediated killing and phagocytosis leading to increased bacterial density (Figure 2.B). An increased bacterial load activates the second line of defence consisting in toll-like receptor 4 (TLR4) mediated macrophages recognition of bacterial lipopolysaccharide (LPS) that triggers an inflammation response (Knapp et al., 2006). In a non-lethal pneumonia model, bacterial burden was increased in TLR4 deficient mice leading to bacteremia. Therefore, the TLR4 mediated inflammatory response has been suggested as a key player in the elimination of *A. baumannii* infection. In contrast, in a lethal bloodstream mouse model TLR4 deficient mice survived *A. baumannii* infections while wildtype mice died from septic shock (Lin et al., 2012). Additionally, mice treated with LpxC inhibitors blocking the LPS production survived *A. baumannii* infections while non-treated

mice died from septic shock. These results suggest that TLR4 mediated LPS recognition, which triggers inflammatory response, negatively drives the clinical outcome of *A. baumannii* infection.

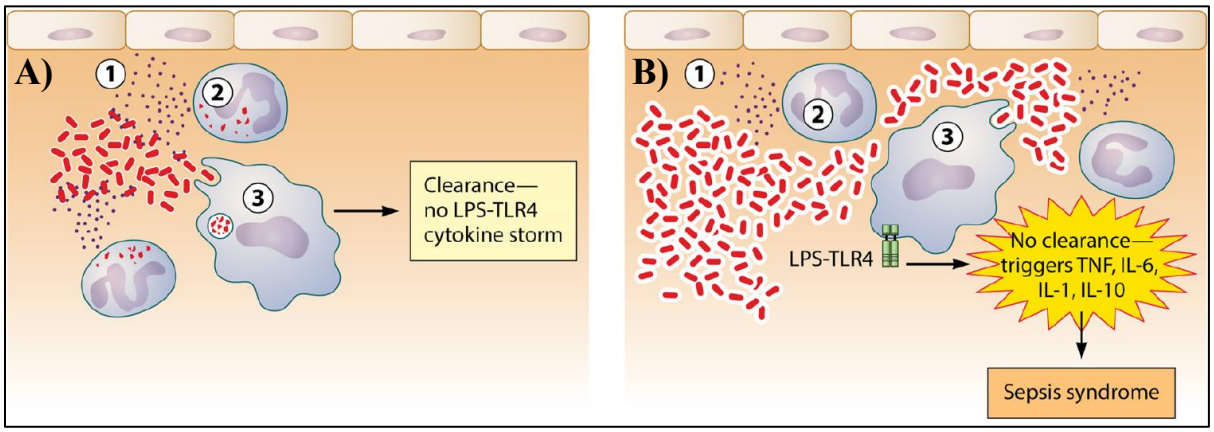

Figure 2: Host response to *A. baumannii* infection can follow two scenarios (Wong et al., 2017). A) The innate immune effectors (1, complement; 2, neutrophils; 3, macrophages) are efficient in controlling and clearing the infection. **B)** The innate immune effectors fail to control infection, which induces LPS-TLR4 mediated inflammatory response leading to a macrophage induced cytokine storm and sepsis.

Altogether, these data indicate that the host response to *A. baumannii* infections may follow two scenarios (Figure 2). In the first scenario, the innate immune effectors are efficient in controlling the infection by lowering the bacterial density and this prevents a strong deleterious inflammatory response and leads to final infection clearance. The second scenario happens in infections caused by highly virulent *A. baumannii* strains that escape the primary innate immune effectors killing triggering a damaging TLR4-LPS mediated inflammatory response. This finally leads to a cytokine storm, sepsis syndrome and death (Wong et al., 2017).

1.1.4. Antibiotic resistance

A. baumannii is characterized by its high ability to acquire resistance to multiple antimicrobial agents. A case of *A. baumannii* nosocomial outbreak caused by a pan drug resistant (PDR) strain in a Spanish hospital illustrates the ability of this pathogen to resist all available antibiotics (Valencia et al., 2009).

Until recently, criteria to classify *A. baumannii* strains as MDR, extensively drug resistant (XDR) and PDR were not standardized leading to a lack of consistence between different studies. Currently, the standard and broadly accepted definition of resistance types is based on nine clinically relevant antibacterial categories that include one to four antimicrobial agents (Table 3) (Magiorakos et al., 2012). MDR *A. baumannii* are defined as non-susceptible to at least one agent in three or more antimicrobial categories. XDR *A. baumannii* are non-susceptible to at least 1 agent in all but two or fewer categories. Finally, PDR *A. baumannii* are non-susceptible to all 22 antimicrobial agents present in the list. This definition allows precise resistance classification that is consistent between different studies.

Table 3: Antimicrobial categories and agents used to define *A. baumannii* resistance types (Magiorakos et al., 2012).

Antimicrobial categories	Antimicrobial agents	Mode of action
Aminoglycosides	Gentamicin, Tobramycin, Amikacin, Netilmicin	Inhibition of protein synthesis
Antipseudomonal carbapenems	Imipenem, Meropenem, Doripenem	Inhibition of cell wall synthesis
Antipseudomonal fluoroquinolones	Ciprofloxacin, Levofloxacin	Inhibition of DNA synthesis
Antipseudomonal penicilins + β-lactamase inhibitors	Piperacillin-tazobactam, Ticarcillin-clavulanic acid	Inhibition of cell wall synthesis
Extended-spectrum cephalosporins	Cefotaxime, Ceftriaxone, Ceftazidime, Cefepime	Inhibition of cell wall synthesis
Folate pathway inhibitors	Trimethoprim-sulfamethoxazole	Inhibition of folate synthesis
Penicillins + β-lactamase inhibitors	Ampicillin-sulbactam	Inhibition of cell wall synthesis
Polymyxins	Colistin, Polymyxin B	Cell membrane disruption
Tetracyclines	Tetracycline, Doxycycline, Minocycline	Inhibition of protein synthesis

A. baumannii infections are predominantly caused by a few successful lineages worldwide, which belong to the international clonal cluster (ICC) ICC1, ICC2 and ICC3 lineages (Higgins et al., 2010). Multilocus sequence typing (MLST), a PCR based method that relies on the sequence variation of internal portion of seven housekeeping genes, is the gold standard method for *A. baumannii* typing. The first MLST scheme to be developed for *A. baumannii*, named Oxford MLST, was published in 2005 and it relies on the sequence of the *gltA*, *gyrB*, *gdhB*, *recA*, *cpn60*, *gpi*, and *rpoD* genes (Bartual et al., 2005). Five years later, Diancourt and colleagues used a modified MLST scheme, named Pasteur MLST, to evaluate the phylogenetic relatedness of 154 *A. baumannii* clinical strains isolated in Europe (Diancourt et al., 2010). The Pasteur scheme introduced four new genes, namely *fusA*, *pyrG, rpoB* and *rplB,* and conserved the *cpn60*, *gltA* and *recA* genes of the Oxford scheme. Both schemes are now hosted in the same database (https://pubmlst.org/abaumannii/) but the Pasteur MLST represents the standard scheme to type *A. baumannii* clonal lineage (Zarrilli et al., 2013).

A. baumannii successful clonal lineages are more likely to resist multiple antibiotics including carbapenems, which are last resort antibiotics for the treatment of MDR *A. baumannii* infections (Diancourt et al., 2010; Higgins et al., 2010; Zarrilli et al., 2013). Among the three international clonal complexes, the ICC2 is the most successful pathogenic lineage. A recent study evaluating biofilm formation in 114 *A. baumannii* clinical isolates demonstrated that 95.7 % of the MDR isolate belonged to the ICC2 lineage and that ICC2 isolates produced less biofilm than other isolates (Hu et al., 2016). Consequently, the ability to resist antibiotic treatment might be a determinant for the *A. baumannii* epidemic spread.

A recent global surveillance study indicated that *A. baumannii* has the highest rate of MDR among the major Gram-negative pathogens (Giammanco et al., 2017). The study described a dramatic increase in *A. baumannii* MDR rates from 23% (309/1,323) in 2004 to 63% (447/712) in 2014. This trend was confirmed by the 2015 ECDC report on antimicrobial resistance in Europe with several countries having a MDR rate above 50 % (Figure 3). These data are

alarming considering that *A. baumannii* MDR infections are associated with increased hospital stay and higher mortality rate than infections with drug susceptible *A. baumannii* (Lee et al., 2007; Sunenshine et al., 2007).

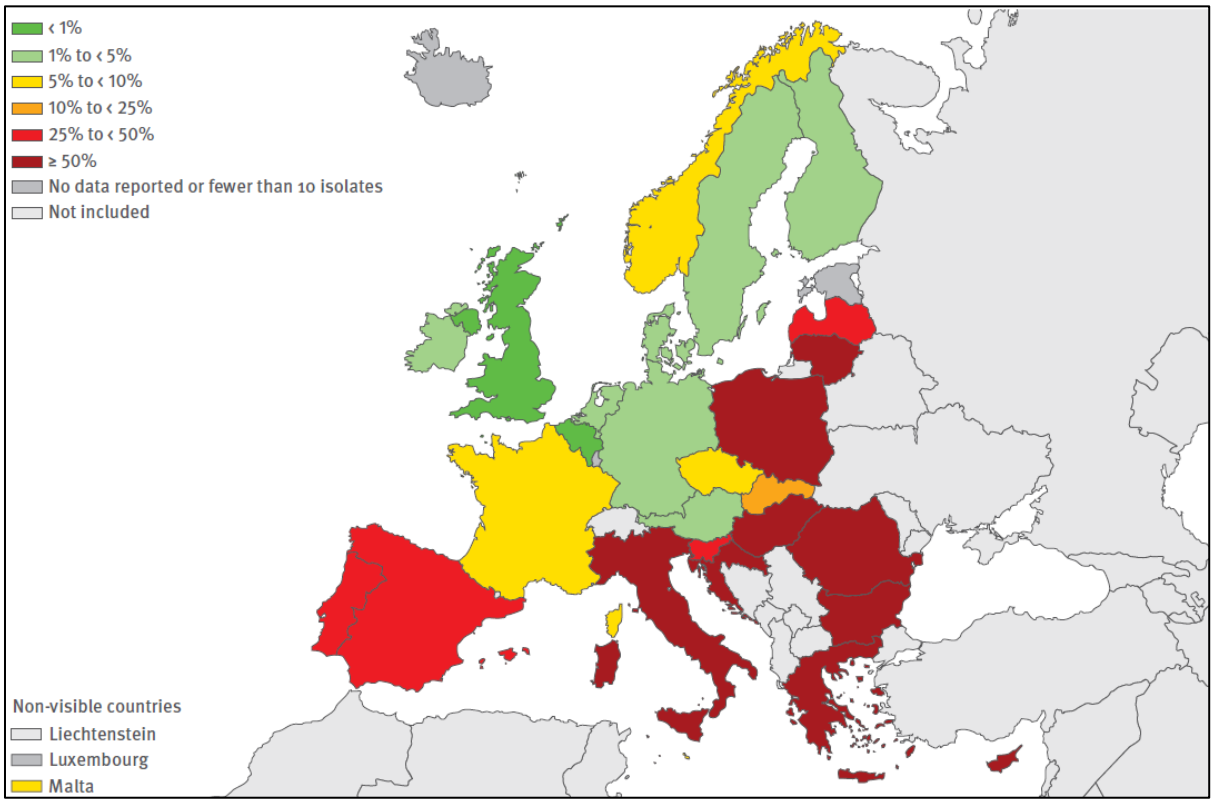

Figure 3: Percentage of MDR *Acinetobacter* spp. per country in 2015 (ECDC, 2017).

1.1.4.1. Mechanisms of antibiotic resistance

Bacteria exploit several diverse mechanisms to resist antibiotic, including modification/inactivation of antibiotics, protection/modification/bypass of drug targets and increasing the cellular efflux or decreasing the influx to lower the intracellular antibiotic concentration (Figure 4) (Blair et al., 2015). Each of these mechanisms is represented in the *A. baumannii* arsenal of innate and acquired resistance determinants used to overcome antibiotic action. Genomic plasticity together with the high DNA acquisition capacity account for the broad-spectrum resistance of *A. baumannii*.

Despite the predominance of few successful clonal lineages, the genome of *A. baumannii* strains causing infections is rather diverse (Imperi et al., 2011; Liu et al., 2014; Snitkin et al., 2011). The high degree of genome plasticity is based on the presence of genomic islands and transposons that can move and re-organize across the genome by homologous recombination. Several genomic islands containing resistance determinants (AbaR resistance islands) have been identified in MDR isolates (Adams et al., 2008; Fournier et al., 2006; Iacono et al., 2008; Kim et al., 2013; Lean et al., 2015; Li et al., 2015; Ou et al., 2015; Post et al., 2010). AbaR-type resistance island are in general integrated in the *comM* gene coding for an ATPase and the resistance genes were most probably acquired from other Gram-negative species. The plasticity and transfer capacity of AbaR-type resistance islands is highlighted by the presence of multiple mobile elements inside and around these gene clusters, such as insertion sequence (IS) elements. In addition to their role in genome plasticity, IS elements play an important role in

A. baumannii antibiotic resistance. Indeed, IS elements encode a strong promoter at the edge of their sequence that may drive the expression of surrounding antibiotic resistance genes, such as efflux pumps and β-lactamases (Lopes and Amyes, 2012; Mugnier et al., 2009; Sun et al., 2012).

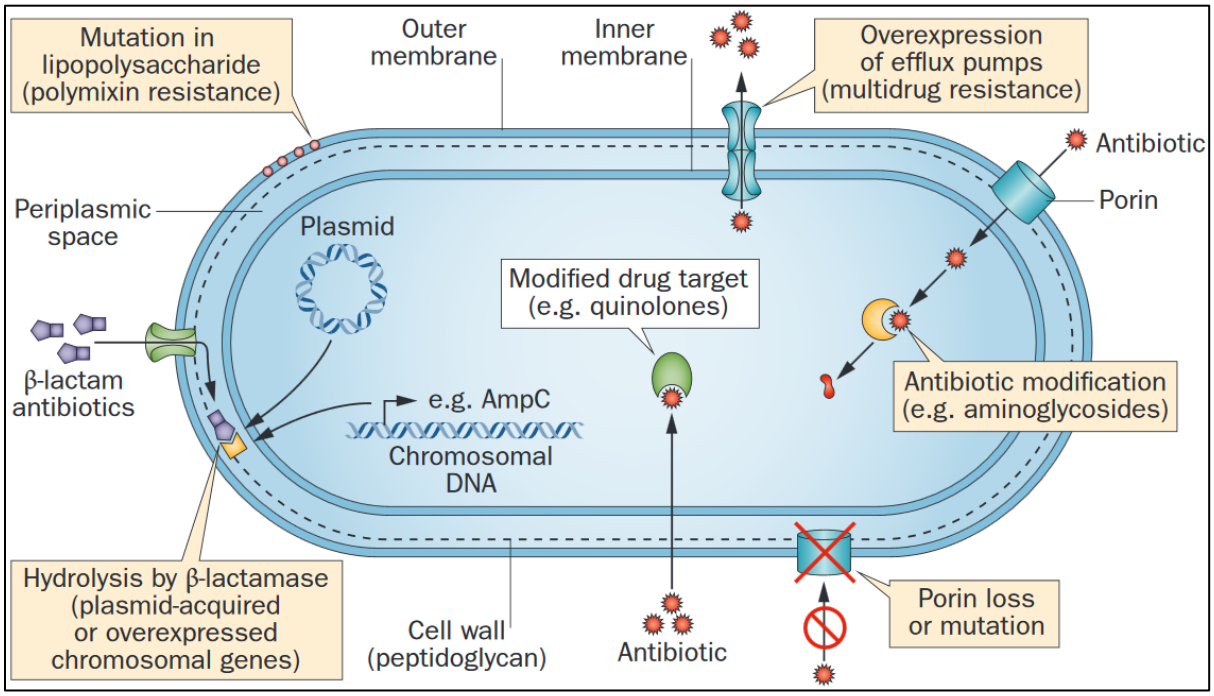

Figure 4: Overview of Gram-negative antimicrobial resistance mechanisms (Zowawi et al., 2015).
The main antibiotic resistance mechanisms are represented. These mechanisms include modification/inactivation of antibiotics, protection/modification/bypass of drug targets and increase efflux or decrease influx to lower intracellular antibiotic concentration.

1.1.4.1.1. β-Lactams

The most significant mechanism of β-lactam resistance consists in antibiotic degradation due to the expression of β-lactamases encoding genes (*bla*) (Figure 4). *A. baumannii* naturally encodes two β-lactamases, the AmpC cephalosporinase and the OXA-51 class D oxacillinase. In addition, *A. baumannii* may acquire a multitude of other chromosomally or plasmid encoded β-lactamases.

A. baumannii chromosomally encoded *ampC* (bla_{ADC}) is expressed at low level and its expression is not inducible in contrast to other AmpC producing pathogens (Bou and Martínez-Beltrán, 2000). The insertion of an IS element upstream bla_{ADC} is required to confer AmpC mediated β-lactam resistance in *A. baumannii*. Transposon driven AmpC expression confers resistance to 3rd and 4th generation of extended-spectrum-cephalosporins, such as cefotaxime, ceftazidime and cefepime (Héritier et al., 2006; Lopes and Amyes, 2012).

In addition to bla_{ADC}, *A. baumannii* may acquire other extended-spectrum-β-lactamases (ESBLs) conferring resistance to cephalosporins. The most frequently found ESBLs correspond to the Amber class A β-lactamases of the PER and VEB types. Notably, VEB-1 producing *A. baumannii* were responsible for an outbreak in 53 French hospitals in 2003-2004 (Naas et al., 2006a). This ESBL has been also reported in cephalosporin resistant *A. baumannii* clinical isolates from Belgium and Argentina (Naas et al., 2006b; Pasterán et al., 2006). More recently,

39.5 % (39 / 108) of *A. baumannii* clinical strains isolated from two hospitals in Teheran harboured bla_{VEB-1}, which was the second most identified ESBL after bla_{PER-1} identified in 78 % of the strains (Fallah et al., 2014). *A. baumannii* isolates producing PER types of ESBL have been reported worldwide: in Europe (Belgium, Bulgaria, Hungary, France and Romania), America (Argentina and USA), Asia (China, Russia, Korea and India) and Middle-East (Iran, Egypt, Turkey and Saudi Arabia) (Al-Agamy et al., 2014; Bonnin et al., 2011; Fallah et al., 2014; Hujer et al., 2006; Jeong et al., 2005; Litake et al., 2009; Naas et al., 2006b, 2007a, 2007b; Pasterán et al., 2006; Strateva et al., 2008; Szabó et al., 2008; Vahaboglu et al., 1997; Yezli et al., 2015; Zhang et al., 2010). Other ESBLs commonly found in *A. baumannii* include, TEM, SHV and CTX-M types (Alyamani et al., 2015; Endimiani et al., 2007; Naas et al., 2007c; Potron et al., 2011). Noteworthy, GES type ESBLs have been identified in *A. baumannii* and some of these GES-type enzymes possess additional carbapenemase activity (Bonnin et al., 2013; Chihi et al., 2016; Moubareck et al., 2009).

Carbapenems are the antibiotics of choice to treat *A. baumannii* infections (Maragakis and Perl, 2008; Peleg and Hooper, 2010). However, there is an increase in *A. baumannii* infections caused by carbapenem resistant isolates as illustrated by the ECDC map representing the rate of carbapenem resistant *A. baumannii* in Europe in 2015 (Figure 5). The major cause of carbapenem resistance consists of OXA type carbapenemases expression. *A. baumannii* ubiquitously encodes an OXA-51 like carbapenemase in its chromosome. Indeed, bla_{OXA-51} was used as specific marker for *A. baumannii* species genotyping (Turton et al., 2006a). Similarly to AmpC, OXA-51 confers carbapenem resistance only when an IS element is present upstream bla_{OXA-51} to drive its expression (Figueiredo et al., 2009; Turton et al., 2006b). In addition to the intrinsic OXA-51 like carbapenemases, *A. baumannii* may acquire several others OXA subclasses that are found both chromosomally or on plasmids (Poirel et al., 2010). Among them, the OXA-23 like, OXA-24(40) like, OXA-58 like, OXA-143 like and OXA-235 like are the most represented subclasses with OXA-23 being widespread in worldwide successful ICC2 isolates (Mugnier et al., 2009; Potron et al., 2015).

Different non-oxacillinase carbapenemases may be also present in carbapenem resistant *A. baumannii*. The *Klebsiella pneumoniae* carbapenemases (KPCs), which are widespread in *Enterobacteriaceae* and confer resistance to all β-lactams, have been only rarely identified in *A. baumannii* (Potron et al., 2015). Indeed, *A. baumannii* ICC2 isolates carrying KPC carbapenemases have been reported to date only in Puerto Rico (Martinez et al., 2016; Robledo et al., 2010). Metallo-β-lactamases (MBLs) with carbapenemase activity have been reported in *A. baumannii* isolates. The most worrisome MBL is the NDM-1 β-lactamase that was rather recently identified but spread widely among *Enterobacteriaceae.* NDM-1 carbapenemase was identified in *A. baumannii* isolated from several countries in Europe (Potron et al., 2015). In 2013, an outbreak due to NDM-1 producing *A. baumannii* was reported in France (Decousser et al., 2013). *A. baumannii* harbouring NDM-1 carbapenemase are increasingly reported worldwide with a majority of cases coming from Asia and Middle-East (Dortet et al., 2014). Others MBLs, such as IMP-like, VIM-like or SIM-1 have been reported with a lower rate than the previously mentioned carbapenemases (Poirel and Nordmann, 2006; Potron et al., 2015).

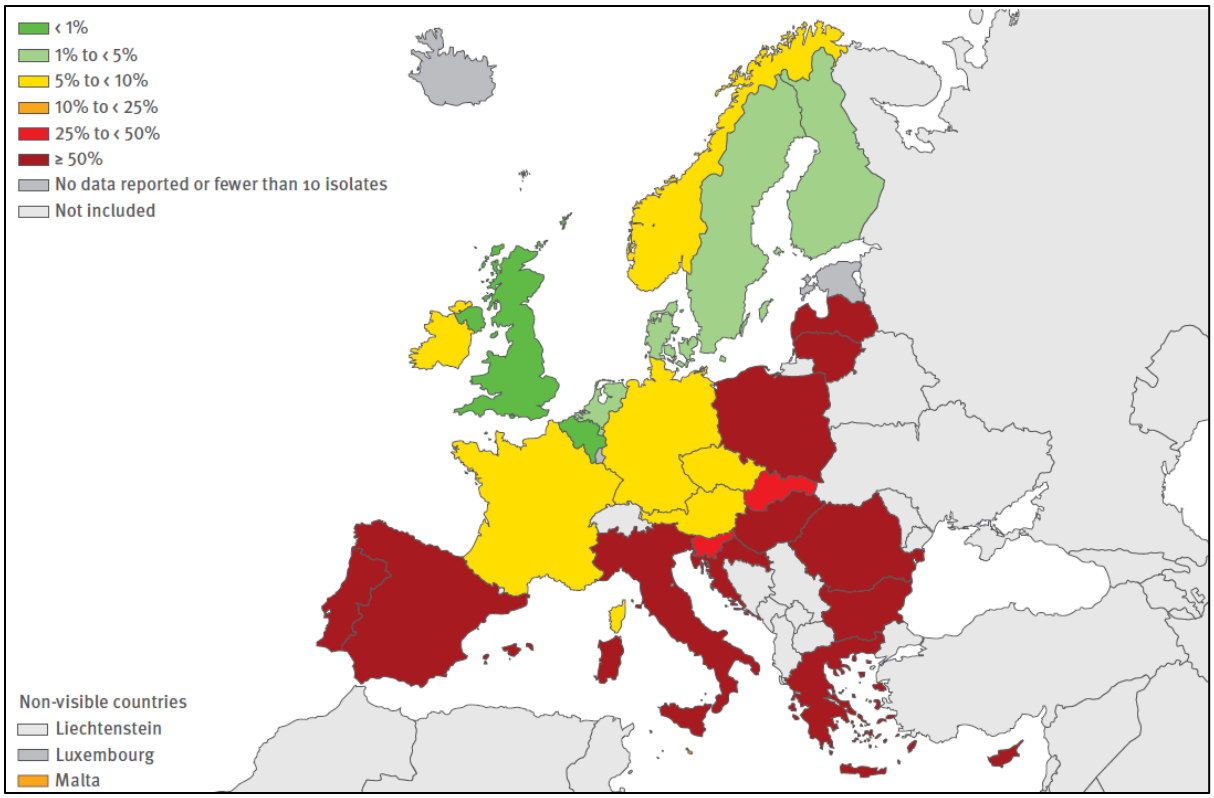

Figure 5: Percentage of carbapenem resistant *Acinetobacter* spp. per country in 2015 (ECDC, 2017)

The presence of non-β-lactamase resistance mechanisms have been suggested in *A. baumannii*. Loss of porins through which β-lactams permeate to reach the periplasm is a common resistance mechanism (Figure 4). However, this mechanism only slightly increases *A. baumannii* resistance to β-lactams and its clinical relevance is still debated (Catel-Ferreira et al., 2012; Clark, 1996; Dupont et al., 2005; Fonseca et al., 2013; del Mar Tomás et al., 2005).

1.1.4.1.2. Aminoglycosides

Aminoglycosides are an important class of antibiotics to treat infections caused by Gram-negative pathogens, including *A. baumannii* (Maragakis and Perl, 2008; Peleg and Hooper, 2010). *A. baumannii* has developed a wide range of diverse aminoglycoside resistance mechanisms consisting in antibiotic modification, target modification and antibiotic efflux mechanisms (Figure 4). This led to a rapid emergence of aminoglycoside resistant *A. baumannii* isolates with a rate exceeding 50 % in several European countries in 2015 (Figure 6).

The most common aminoglycoside resistance mechanism resides in antibiotic inactivation due to aminoglycoside modifying enzymes (AMEs). AMEs were detected in 94 % (79 / 84) of aminoglycoside non-sensitive *A. baumannii* strains isolated in Iran in 2014 indicating the major role of AMEs in *A. baumannii* aminoglycoside resistance (Sheikhalizadeh et al., 2017). *A. baumannii* may acquire a wide array of genes encoding AMEs that catalyse different type of modifications with more or less activity in function of the aminoglycosidic agent (Nemec et al., 2004; Ramirez and Tolmasky, 2010). The three types of AMEs, namely acetyltransferases (AACs), phosphotransferases (APHs) and nucleotidyltransferases (ANTs), have been identified in *A. baumannii.* There is no clear hierarchy in the prevalence of AACs, APHs and ANTs with different preponderance observed in different studies (Akers et al., 2010; Atasoy et al., 2015;

Cho et al., 2009; Miller et al., 1995; Noppe-Leclercq et al., 1999; Sheikhalizadeh et al., 2017). Nevertheless, these enzymes are each specific to certain aminoglycosides and do not confer broad aminoglycoside resistance like 16S rRNA methyltransferases and efflux pumps.

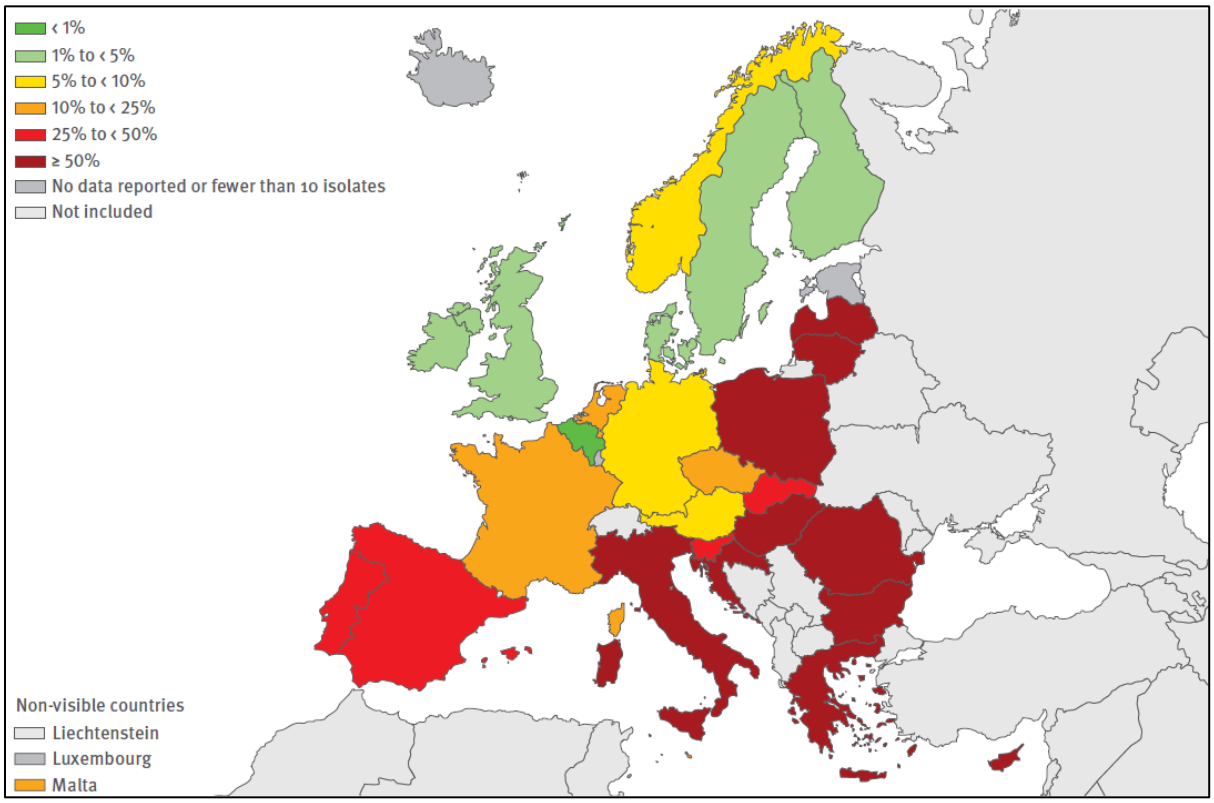

Figure 6: Percentage of aminoglycoside resistant *Acinetobacter* spp. per country in 2015 (ECDC, 2017)

Aminoglycosides block bacterial protein production by binding to the conserved 16S rRNA in the ribosome. Therefore, modification of 16S rRNA conformation mediated by methyltransferases confers broad and high level aminoglycoside resistance (Doi and Arakawa, 2007). The ArmA methyltransferase is the most identified in *A. baumannii* isolates worldwide (Potron et al., 2015). Studies from Iran, China and Vietnam have reported a strong prevalence of *armA* in highly aminoglycoside resistant *A. baumannii* strains (94.4 %, 98 % and 87.1 %, respectively) (Nie et al., 2014; Sheikhalizadeh et al., 2017; Tada et al., 2013). Noteworthy, *A. baumannii* strains co-producing carbapenemases and ArmA are emerging worldwide (Bakour et al., 2014; Brigante et al., 2012; El-Sayed-Ahmed et al., 2015; Hong et al., 2013; Karah et al., 2011; Milan et al., 2016; Shen et al., 2016a; Strateva et al., 2012; Tada et al., 2014, 2015; Wang et al., 2016).

The last aminoglycoside resistance mechanism identified in *A. baumannii* consists in active efflux. The AdeABC efflux pump is involved in aminoglycoside resistance in the MDR *A. baumannii* BM4454 strain isolated from a patient with urinary tract infection (Magnet et al., 2001). Kanamycin and gentamycin, two aminoglycosides, were further identified as substrate of the *A. baumannii* AbeM efflux pump (Su et al., 2005). However, only few studies have looked at the relation between aminoglycoside resistance phenotype and AdeABC or AbeM expression in *A. baumannii* clinical isolates. A recent study indicates that AdeABC and AbeM efflux pumps play only a minor role in aminoglycoside resistance in clinically isolated *A. baumannii* strains (Sheikhalizadeh et al., 2017).

1.1.4.1.3. Fluoroquinolones

Fluoroquinolones, such as ciprofloxacin and levofloxacin, played a major role in the treatment of *A. baumannii* infections (Peleg and Hooper, 2010). However, fluoroquinolones are no longer a valid option to treat *A. baumannii* infections in many countries due to high rate of resistance as illustrated in Greece with 94.9 % of resistance among the 946 isolates tested in 2015 (Figure 7).

The primary fluoroquinolone resistance mechanism consists in antibiotic target modification (Figure 4). Mutations in the subunits of the gyrase (*gyrA*) and topoisomerase IV (*parC*) confer high fluoroquinolone resistance in *A. baumannii* due to decreased fluoroquinolone affinity to the enzyme-DNA complex (Adams-Haduch et al., 2008; Hamouda and Amyes, 2004; Higgins et al., 2004; Lee et al., 2005; Park et al., 2011a; Vila et al., 1995, 1997). More recently, mutations in the second gyrase subunit (*gyrB*) were associated with fluoroquinolone resistance (Park et al., 2011a). The authors described that triple mutations (*gyrA*, *gyrB* and *parC*) may confer even higher ciprofloxacin resistance than *gyrA* and *parC* mutations.

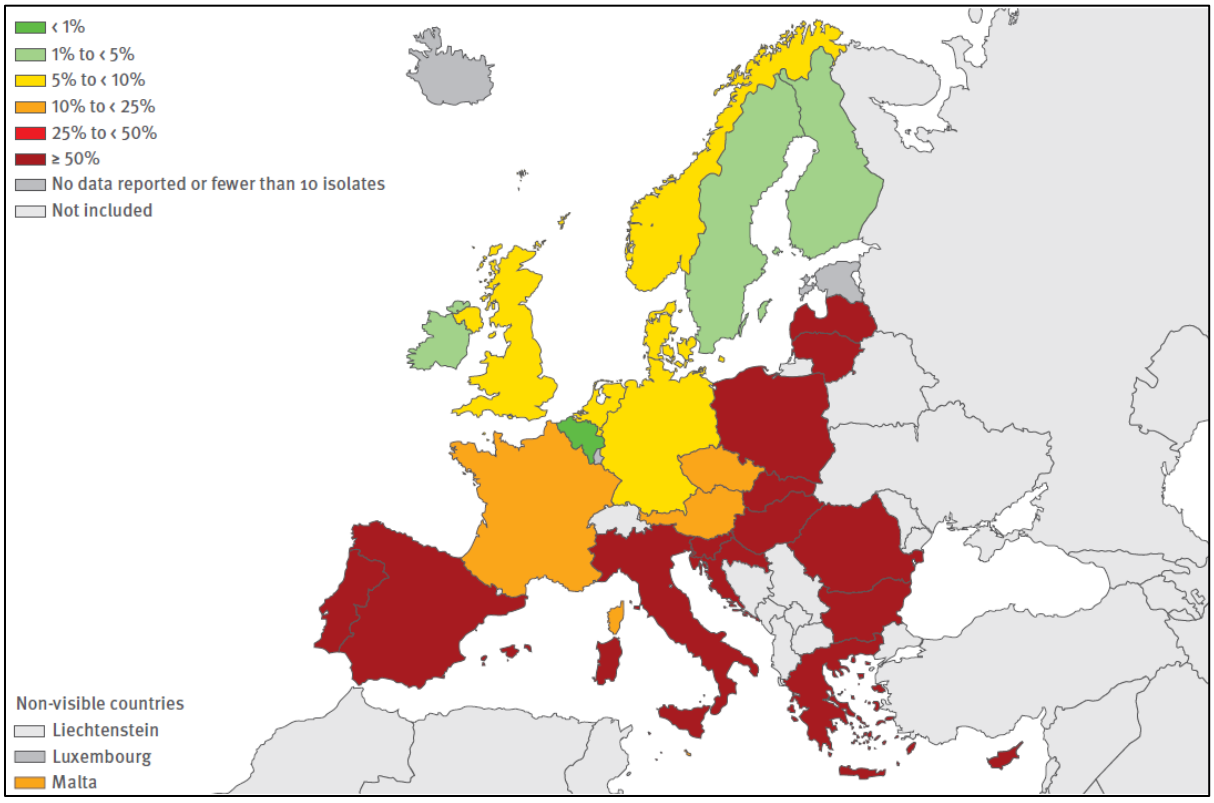

Figure 7: Percentage of fluoroquinolone resistant *Acinetobacter* spp. per country in 2015 (ECDC, 2017)

The second fluoroquinolone resistance mechanism consists in active efflux. Expression of AdeABC, AdeFGH, AbeM and AbeS efflux pumps have been associated with fluoroquinolones resistance in *A. baumannii* (Coyne et al., 2010; Magnet et al., 2001; Srinivasan et al., 2009; Su et al., 2005). In accordance to what is observed with aminoglycoside resistance, the expression of efflux pumps may play a secondary and minor role in *A. baumannii* fluoroquinolone resistance compared to antibiotic target mutations that represent the predominant resistance mechanism.

1.1.4.1.4. Tetracyclines

Tetracycline agents, such as minocycline and its glycylcycline derivative tigecycline, are potent antibiotics used to treat *A. baumannii* infections (Peleg and Hooper, 2010). Indeed, tigecycline has the lowest MIC_{90} (2 µg/ml) and minocycline the lowest resistance rate (12.6 %) among 11 antimicrobial agents tested on 8,294 MDR *A. baumannii* collected globally between 2004 and 2014 (Giammanco et al., 2017).

Tetracycline antibiotics target the 30S ribosomal subunit and prevent the attachment of aminoacyl-tRNA to the ribosomal acceptor site leading to protein synthesis inhibition (Chopra and Roberts, 2001). The major tetracycline resistance mechanisms reside in active efflux and target protection (Figure 4). *A. baumannii* active efflux systems that confer tetracycline resistance are encoded by *tet*(A) and *tet*(B) (Guardabassi et al., 2000; Ribera et al., 2003). An old study carried out on 35 tetracycline resistant *A. baumannii* strains isolated from European hospitals from 1981 to 1998 showed a similar ratio between *tet*(A) and *tet*(B) harbouring strains, whereas more recent studies showed a predominance of strains encoding *tet*(B) (Guardabassi et al., 2000; Mak et al., 2009; Vilacoba et al., 2016). The emergence of *tet*(B) harbouring strains might be due to minocycline selection. Indeed, *tet*(B) confers resistance to both tetracycline and minocycline, whereas *tet*(A) confers resistance mainly to tetracycline (Chopra and Roberts, 2001). In contrast, the ribosome protection gene *tet*(M) has been only rarely identified in *A. baumannii* clinical isolates although it confers resistance to minocycline (Huys et al., 2005a, 2005b; Ribera et al., 2003).

The recently approved antibiotic tigecycline escapes the *tet*(A)/(B) and *tet*(M) mediated efflux and protection resistance mechanism, respectively (Esterly et al., 2011). However, overexpression of the AdeABC efflux pumps have been associated with *A. baumannii* tigecycline resistance. This AdeABC mediated tigecycline resistance mechanism is the scope of the section 2.1.1.

1.1.4.1.5. Polymyxins

Polymyxin antibiotics, which consists of polymyxin E (colistin) and polymyxin B, are old antibiotics that were put aside due to their high-level nephrotoxicity (Brown et al., 1970; Koch-Weser et al., 1970; Ryan et al., 1969). However, with increasing Gram-negative antibiotic resistance rates, polymyxins were re-introduced and are now considered as last resort antibiotic to treat carbapenem resistant Gram-negative infections, such as the one caused by *A. baumannii* (Falagas and Kasiakou, 2005; Li et al., 2006; Maragakis and Perl, 2008; Peleg and Hooper, 2010; Zavascki et al., 2007).

Polymyxins are cationic polypeptides that bind to the negatively charged LPS and disturb the bacterial cell membrane, thus increasing permeability and leakiness, leading to cell death (Falagas and Kasiakou, 2005). Polymyxin resistance is conferred by lipid A modifications that lower the outer membrane negative charge and decrease polymyxin affinity (Figure 4) (Olaitan et al., 2014). The *A. baumannii* polymyxin resistance mechanism is the scope of the section 2.1.2.

1.2. Part B

Mycobacterium tuberculosis

1.2.1. History

Tuberculosis is an airborne infectious disease caused by the bacterial pathogen *Mycobacterium tuberculosis*. Tuberculosis has been a plague for humanity from ancient times up to present days (Daniel, 2006). The *Mycobacterium* genus may have originated more than 150 million years ago, while *M. tuberculosis* origin was estimated at 3 million years ago based on mutation rate studies (Gutierrez et al., 2005; Hayman, 1984). There are evidences of the presence of *M. tuberculosis* in Egypt 5000 years ago. Egyptian mummies skeletal bones presented abnormalities that are characteristic of tuberculosis disease and *M. tuberculosis* DNA has been identified on these Egyptian mummies (Crubézy et al., 1998; Nerlich et al., 1997; Zimmerman, 1979). Similarly, *M. tuberculosis* DNA has been identified in a 1000-years-old pre-Columbian Peruvian mummy indicating its presence in America before European colonization (Salo et al., 1994). Tuberculosis became endemic in Europe and America in the 18th and 19th centuries were it caused enormous amount of death (Daniel, 2006; Holmberg, 1990). In the early 19th century, Theophile Laennec first described with precision tuberculosis pathogenesis (Daniel, 2004). In 1865, Jean-Antoine Villemin demonstrated the transmissibility of tuberculosis indicating the infectious nature of the disease (Keshavjee and Farmer, 2012). A major step in tuberculosis understanding was enabled in 1882 by Robert Koch who discovered the tubercle bacillus as the etiologic agent of tuberculosis (Daniel, 2006; Keshavjee and Farmer, 2012). Despite advance in tuberculosis understanding, appropriate treatments were missing until 1944, when streptomycin as the first antibiotic agent active on *M. tuberculosis* was isolated (Group, 1948; Hinshaw et al., 1946; Jellinek, 1949; Schatz et al., 2005). In 1952, isoniazid was discovered followed by ethionamide in 1956 and rifampicin in 1957, which are still used to treat *M. tuberculosis* infections nowadays (Keshavjee and Farmer, 2012).

1.2.2. Epidemiology

Two to three billion people, which represents one-third of the world's population, are estimated to be latently infected with *M. tuberculosis* according to the latest annual report on tuberculosis by the WHO (WHO, 2016). However, it is estimated that only 5 to 15 % of people carrying *M. tuberculosis* will develop tuberculosis in their lifetime. In 2015, 10.4 million new tuberculosis cases were estimated and 1.8 million people died from tuberculosis making the disease one of the top 10 causes of death worldwide. Sixty percent of new tuberculosis cases in 2015 originate from six countries: India, Indonesia, China, Nigeria, Pakistan and South Africa. Globally, low income countries in southern Africa, southern Asia and Oceania are the most affected (Figure 8).

In 2015, 11 % of estimated incident tuberculosis patients were HIV positive making HIV infection the major risk factor for tuberculosis. The proportion of HIV positive tuberculosis cases exceeded 50 % in parts of southern Africa (Figure 9). Twenty two percent (0.4 million) of tuberculosis deaths occured in HIV-positive people in 2015 indicating that tuberculosis-HIV co-infection is a factor increasing mortality.

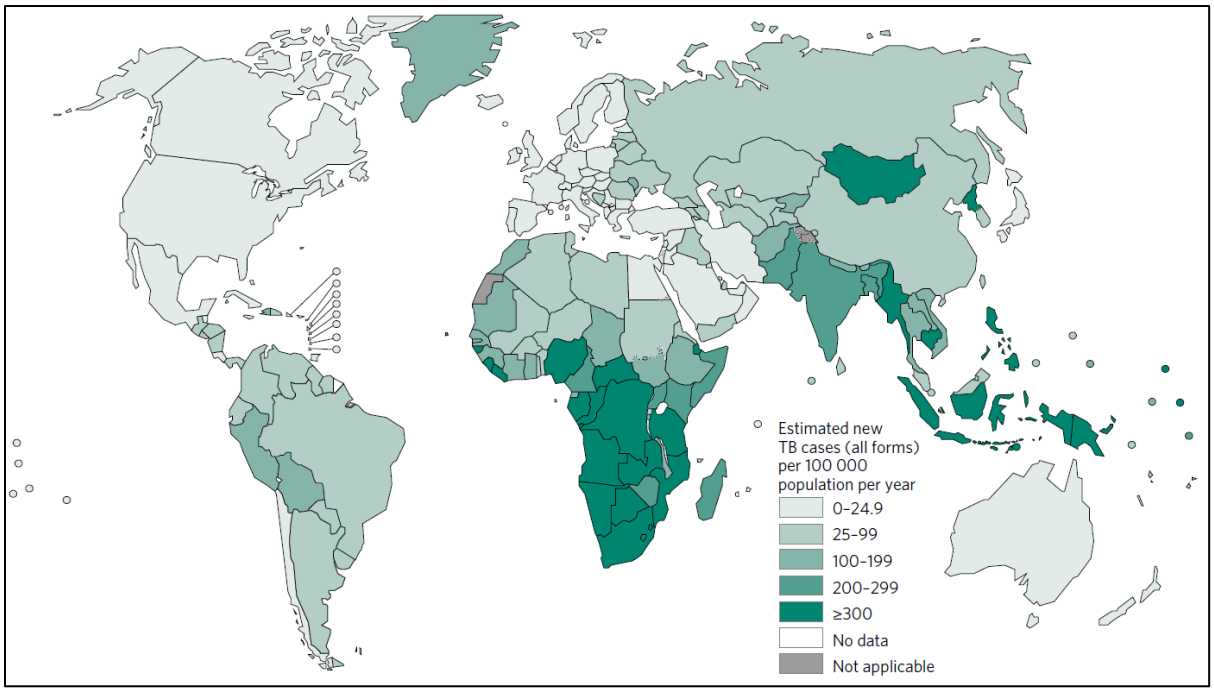

Figure 8: Estimated tuberculosis incidence rates in 2015 (WHO, 2016)

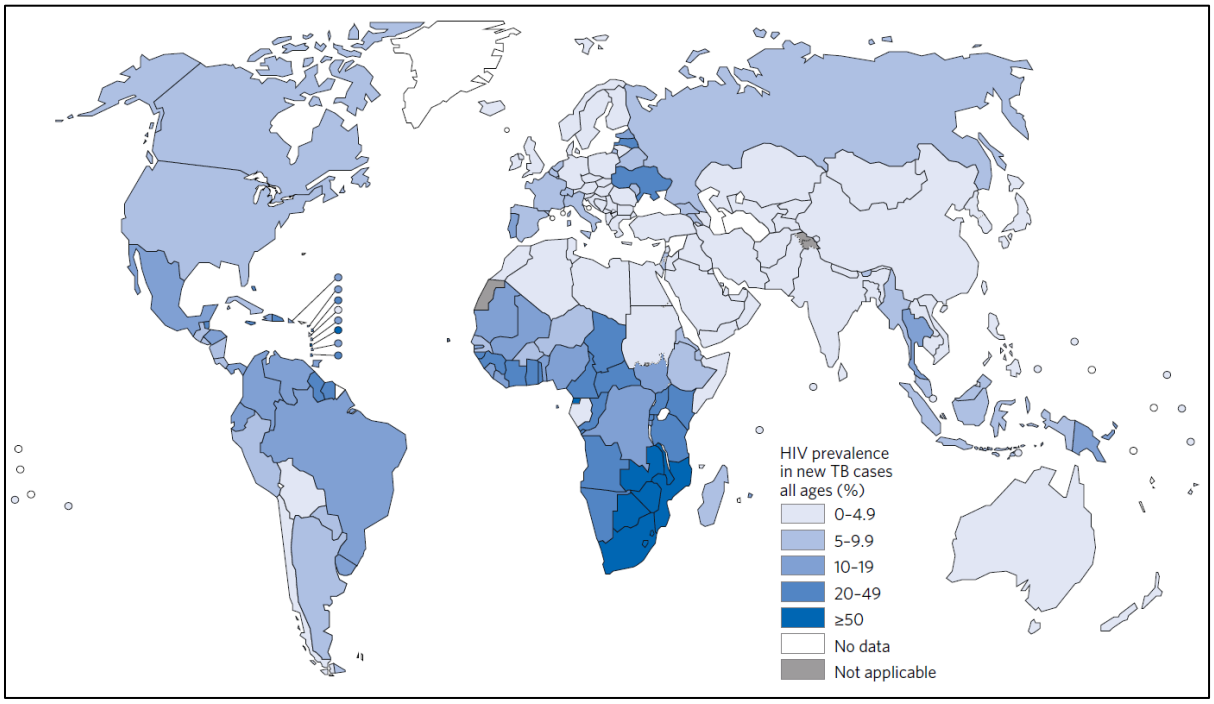

Figure 9: Estimated HIV prevalence in tuberculosis cases in 2015 (WHO, 2016)

In 2015, the incidence of MDR *M. tuberculosis*, which is defined as resistance to rifampicin and isoniazid, was estimated at 480 000 new cases and the incidence of rifampicin resistant (RR) *M. tuberculosis,* which are newly eligible for MDR treatment regiment (see section 1.2.3.), was estimated at 100 000 new cases. Globally, MDR and RR *M. tuberculosis* represented 5 % of new cases of tuberculosis. The highest rate of MDR and RR *M. tuberculosis* was observed in the Russian Federation with rates superior to 18 % (Figure 10).

Although the overall rate of MDR and RR *M. tuberculosis* was low, India is by far the country with the highest incidence of MDR and RR *M. tuberculosis* followed by China and the Russian

Federation, which together accounted for 45 % of those cases (Figure 11). Deaths from MDR and RR *M. tuberculosis* were estimated at 250 000 in 2015, which corresponds to 43 % of MDR and RR *M. tuberculosis* cases. Global tuberculosis mortality rate was 17 % in 2015 indicating that MDR and RR *M. tuberculosis* trigger increased tuberculosis mortality.

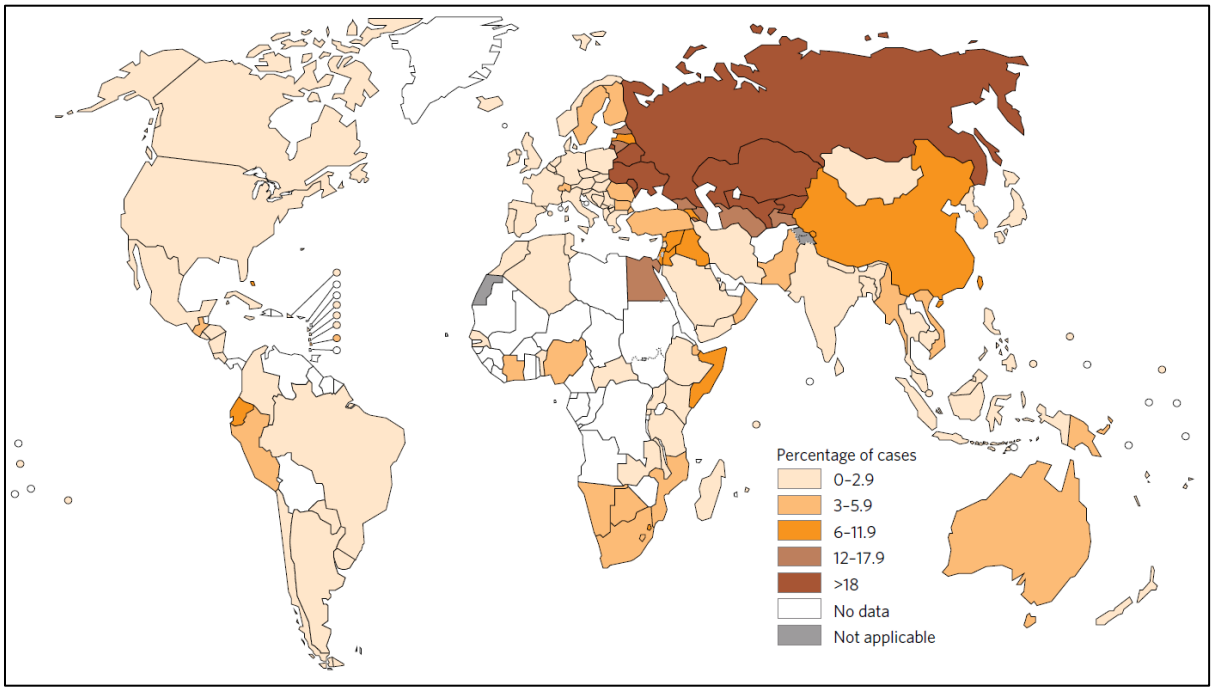

Figure 10: Percentage of new tuberculosis cases with MDR and RR *M. tuberculosis* in 2015 (WHO, 2016)

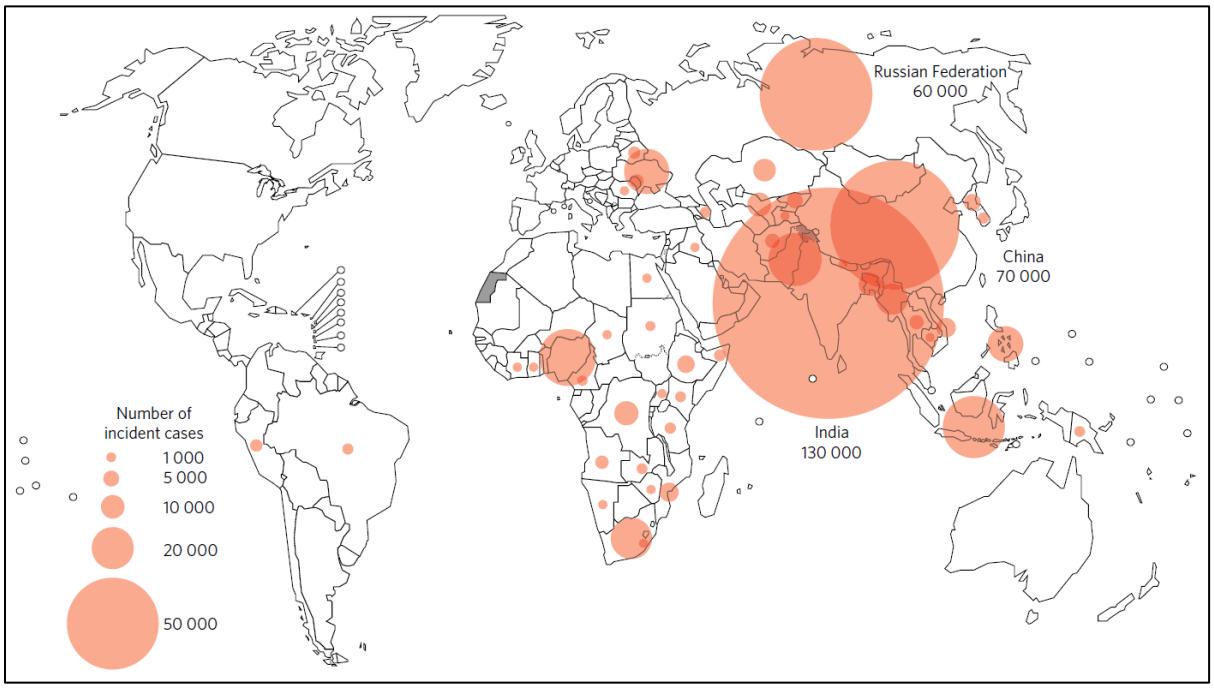

Figure 11: Incidence of MDR and RR *M. tuberculosis* in 2015 (WHO, 2016)

1.2.3. Antibiotic treatments and resistance mechanisms

1.2.3.1. Antibiotic treatments

Most of the drugs available to treat tuberculosis were discovered more than 50 years ago (Nguyen, 2016) (Table 4). The most potent anti-tuberculosis drugs represent the first-line treatment and include isoniazid, rifampicin, pyrazinamide and ethambutol. If these drugs are inefficient due to MDR or RR, second line drugs are used to fight the infection. However, the second-line drugs are generally less potent against *M. tuberculosis* and may have more severe toxic side effects. Second-line tuberculosis-drugs include cycloserine, ethionamide, p-Aminosalicylic acid (PAS), streptomycin, amikacin, capreomycin and broad-spectrum fluoroquinolones.

The standard treatment regimen recommended for tuberculosis is a 6-month therapy consisting in an intensive 2-month treatment with isoniazid, rifampicin, pyrazinamide and ethambutol followed by a 4-month treatment with isoniazid and rifampicin (Nahid et al., 2016). Treatment failure is defined as positive culture after 4 and 5 months of appropriate treatment in United States and Europe, respectively (Nahid et al., 2016). This regimen is very efficient in treating infections caused by drug-susceptible *M. tuberculosis* with a cure rate of 90 to 95 % (Nahid et al., 2016).

However, the prevalence of MDR and RR *M. tuberculosis* in certain regions of the world impairs the efficacy of the standard treatment regimen (Figure 10 and Figure 11). Treatment of MDR tuberculosis is built empirically in function of the resistance profile of the *M. tuberculosis* strain when this information is available. For MDR treatment regiment, the WHO recommends to use ethionamide combined with an injectable second-line drug, namely capreomycin or amikacin, a fluoroquinolone, at least another second-line drug, and the first-line drugs that are still active (World Health Organization, 2014). In contrast to drug susceptible, MDR tuberculosis treatment lasts up to 24 months and the cure rate is drastically reduced with only 50 % of MDR tuberculosis patients successfully treated in 2014. More worryingly, XDR *M. tuberculosis*, which is defined as MDR with additional resistance to fluoroquinolones and one of the injectable second-line drugs, and totally-drug resistant (TDR) *M. tuberculosis* are emerging (Dorman and Chaisson, 2007; Udwadia, 2012). Infections caused by XDR or TDR *M. tuberculosis* strains are essentially incurable by the current anti-tuberculosis drugs (Nguyen, 2016).

Table 4: Anti-tuberculosis drugs mode of action and resistance mechanisms (Palomino and Martin, 2014; Zhang and Yew, 2015)

	Drug (year of discovery)	Mode of action	Targets	Genes involved in resistance
First-line	Isoniazid (1952)	Inhibition of mycolic acid synthesis	Enoyl acyl carrier protein (ACP) reductase (InhA)	*katG*, inhA, ndh*
	Rifampicin (1957)	Inhibition RNA synthesis	RNA polymerase β subunit	*rpoB*
	Pyrazinamide (1952)	Inhibition of fatty acids synthesis and inhibition of tran-translation	Fatty acid synthetase I (FASI) and ribosomal protein 1 (RpsA)	*pncA*, rspA*
	Ethambutol (1961)	Inhibition of cell wall arabinogalactan synthesis	Arabinosyl transferase	*embCAB*
Second-line	Ethionamide (1956)	Inhibition of mycolic acid synthesis	Enoyl-ACP reductase (InhA)	*ethA*, ethR, inhA*
	Cycloserine (1952)	Inhibition of peptidoglycan synthesis	D-alanine racemase (AlrA)	*alrA, cycA, ddl*
	p-Aminosalicylic acid (PAS) (1946)	Inhibition of salicylic acid synthesis and folate pathway	Unknown	*thyA, folC*
	Aminoglycosides	Inhibition of protein synthesis		
	- Streptomycin (1944)		- Ribosomal S12 protein and16S rRNA	- *rpsL, rrs, gidB*
	- Amikacin (1972)		- 16S rRNA	- *rrs, eis, whiB7*
	- Capreomycin (1963)		- interface between small and large ribosomal subunits	- *rrs, eis, tlyA*
	Quinolones (1963)	Inhibition of DNA synthesis	DNA gyrase	*gyrA, gyrB*

* *katG*, *pncA*, and *ethA* encode proteins involved in the activation of the prodrugs isoniazid, pyrazinamide and ethionamide, respectively.

1.2.3.2. Resistance mechanisms

M. tuberculosis is generally more resistant to antibiotics than other bacteria. This high intrinsic resistance not only protects *M. tuberculosis* from most available antibiotics but also impairs the development of new drugs. Intrinsic resistance has largely been attributed to the presence of an impermeable mycolic-acid-rich cell envelope, which is specific for the *Mycobacterium* genus (Jarlier and Nikaido, 1994; Nguyen, 2016). In addition to low permeability, *M. tuberculosis* encodes a system involved in resistance to multiple antibiotics, which is dependent on the transcriptional activator WhiB7 (Morris et al., 2005). The *whiB7* multidrug-resistance system is ubiquitous in all species of the Actinomycetales order, including *M. tuberculosis*, which are known for their ability to produce antibiotics, such as *Streptomyces* (Eldholm and Balloux, 2016).

Anti-tuberculosis drugs may be grouped according to their spectrum, with tuberculosis specific drugs such as isoniazid, pyrazinamide, ethambutol, ethionamide and PAS, and broad-spectrum drugs such as rifampicin, cycloserine, the aminoglycosides and the fluoroquinolones. Interestingly, except ethambutol, all the tuberculosis specific drugs are prodrugs that need to be converted into active compound by the host or by *M. tuberculosis* itself. The prodrug approach increases the bioavailability and the effectiveness of the drugs while reducing potential toxicity (Mori et al., 2017). Prodrugs are prevalent in tuberculosis therapy in contrast to other therapeutic areas, where it is estimated that 10 % of the marketed drugs are prodrugs (Zawilska et al., 2013). However, anti-tuberculosis prodrug approach was not aimed and the prodrug feature of these agents were discovered only in 1992, 1996, 2000 and 2006 for isoniazid, pyrazinamide, ethionamide and PAS, respectively (Baulard et al., 2000; Scorpio and Zhang, 1996; Zhang et al., 1992; Zheng et al., 2013). The negative counterpart of prodrugs is the possibility for the pathogen to resist the action of the drug by disrupting the bioactivation pathway.

Another *M. tuberculosis* exception resides in its low ability of horizontal gene transfer, low recombination and mutation rates and therefore low genome diversity (Eldholm and Balloux, 2016). In theory, these features render *M. tuberculosis* unlikely to develop resistances compared to other successful pathogens that use horizontal gene transfer and genome plasticity to resist antibiotics. However, MDR, XDR and TDR *M. tuberculosis* are rapidly emerging indicating the ability of this pathogen to develop resistance mechanisms. *M. tuberculosis* resistance mostly arises through endogenous mechanisms that does not require acquisition of foreign DNA, such as mutations of the antibiotic target or inactivation of the bioactivation enzymes, which is a prevalent resistance mechanism in *M. tuberculosis* (Table 4).

The mode of actions and antibiotic resistance mechanisms of first- and second-line anti-tuberculosis drugs have recently been reviewed and are summarized in the Table 4 (Palomino and Martin, 2014; Zhang and Yew, 2015).

1.2.3.2.1. Ethionamide resistance

Ethionamide is a second-line anti-tuberculosis drug analogue to the first-line drug isoniazid (Vilchèze and Jacobs, 2014). Both molecules are prodrugs, ethionamide is activated by the *M. tuberculosis* monooxygenase EthA whereas isoniazid is activated by the *M. tuberculosis* catalase-peroxidase KatG (Baulard et al., 2000; Fraaije et al., 2004; Lei et al., 2000; Zhang et

al., 1992). In both case, the resulting activated drugs inhibit the enoyl-ACP reductase InhA by forming NAD^+ adducts that sit in the active site of the NADH dependent enzyme (Figure 12) (Banerjee et al., 1994; Rawat et al., 2003; Wang et al., 2007). InhA is part of the fatty acid synthase type II system and its inhibition stops mycolic acid biosynthesis, which is one of the major components of *M. tuberculosis* cell wall therefore resulting in mycobacteria cell death (Marrakchi et al., 2000; Takayama et al., 1972; Vilchèze et al., 2000; Winder et al., 1971).

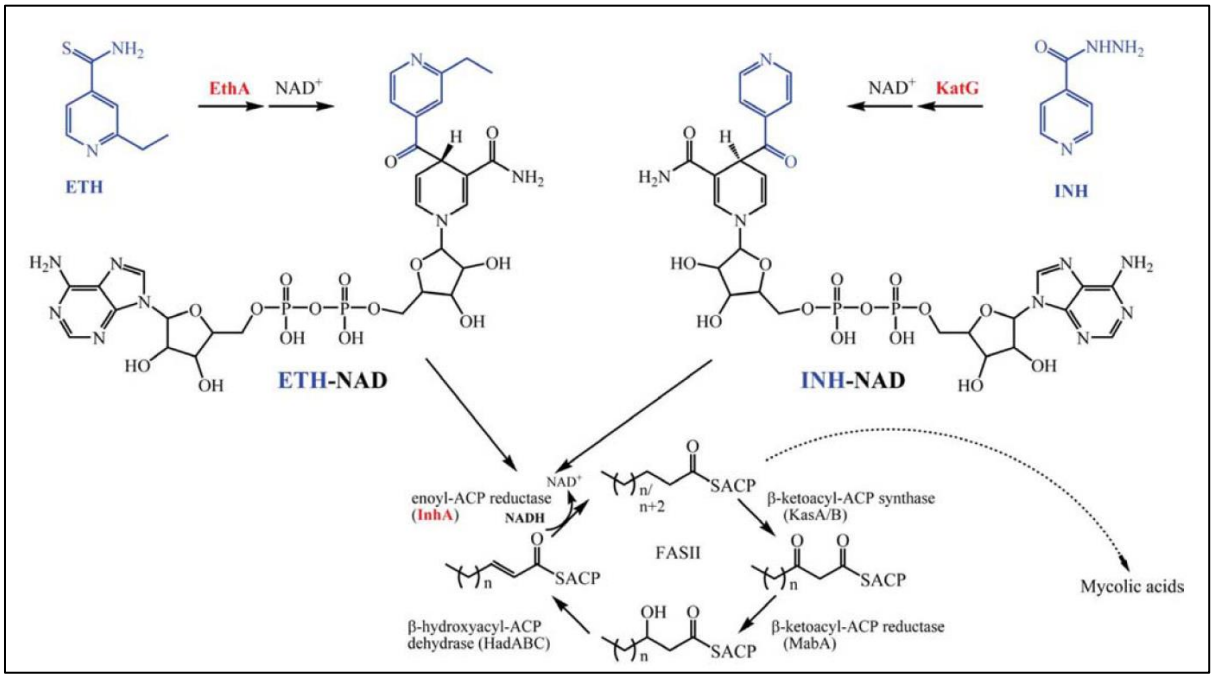

Figure 12: Ethionamide and isoniazid mode of action (Vilchèze and Jacobs, 2014).
Ethionamide (ETH) and isoniazid (INH) are activated by the monooxygenase EthA and the catalase peroxidase KatG, respectively, to form a reactive species that binds to NAD^+. The resulting adducts, ETH-NAD or INH-NAD, inhibit the enoyl-ACP reductase InhA of the FASII system, resulting in mycolic acid biosynthesis inhibition.

The predominant ethionamide resistance mechanism in *M. tuberculosis* is the direct mutation of the target InhA or mutation in the promoter region of *inhA*. Mutations in InhA result in a lower affinity for the ethionamide- and isoniazid-NAD^+ adducts leading to increased drug resistance (Vilchèze et al., 2006). On the other hand, mutations in the promoter region of *inhA* result in InhA overexpression leading to increased ethionamide and isoniazid resistance (Vilchèze et al., 2006). In a panel of 38 ethionamide resistant *M. tuberculosis* strains isolated from United States, Russia and Brazil, 73 % of the strains harboured mutation in InhA and/or *inhA* promoter (Morlock et al., 2003). Mutations in *inhA* promoter were predominant (n = 26) over mutations in InhA (n = 9). Similarly, 62 % of 47 ethionamide resistant *M. tuberculosis* strains isolated from France harboured mutations in InhA and/or *inhA* promoter (Brossier et al., 2011). Again, mutations in *inhA* promoter were predominant (n = 26) over mutations in InhA (n = 6). Mutations in InhA are rare due to the essential role of this enzyme in *M. tuberculosis* mycolic acid biosynthesis pathway. Three different InhA mutations were reported in ethionamide resistant *M. tuberculosis* strains causing the amino acid substitutions I21T(or V), S94A and I95P (Morlock et al., 2003; Ristow et al., 1995). In contrast, mutation in *inhA* promoter leading to InhA overexpression are widespread. Three different *inhA* promoter mutations were reported in ethionamide resistant *M. tuberculosis* strains, namely the

t-8c, the c-15t and the g-17t, which are located 8 bp, 15 bp and 17 bp upstream the *inhA* start codon, respectively (Brossier et al., 2011; Morlock et al., 2003). Among them, the c-15t mutation is the most widespread and it leads to a 20-fold InhA overexpression and an 8-fold increase in ethionamide MIC (Vilchèze and Jacobs, 2014; Vilchèze et al., 2006).

The second ethionamide resistance mechanism in *M. tuberculosis* resides in the disruption of the prodrug bioactivation pathway. Ethionamide is activated by the *M. tuberculosis* monooxygenase EthA and *ethA* expression is negatively regulated by the TetR-type transcriptional regulator EthR (Baulard et al., 2000; Fraaije et al., 2004). Therefore, EthA and EthR mutations have been associated with ethionamide resistance in *M. tuberculosis* clinical isolates (Vilchèze and Jacobs, 2014). Indeed, EthA mutations that impair ethionamide bioactivation activity result in increased resistance. Ethionamide resistant *M. tuberculosis* clinical isolates have been reported with missense mutations and nucleotide deletions or insertions all over the coding sequence of *ethA* without any mutation hotspot (Boonaiam et al., 2010; Brossier et al., 2011; DeBarber et al., 2000; Leung et al., 2010; Morlock et al., 2003). EthA mutation was reported in 47 % of the 47 ethionamide resistant *M. tuberculosis* strains isolated in France and 39 % of the 38 ethionamide resistant *M. tuberculosis* strains isolated in United States, Russia and Brazil (Brossier et al., 2011; Morlock et al., 2003). In contrast, mutations in EthR were only rarely reported (Brossier et al., 2011). EthR mutations triggering an increased resistance would require protein modifications that tighten the binding of EthR to its operator site to increase promoter repression and consequently prevent *ethA* expression. The appearance of such EthR modifications is rather unlikely and may explain the low prevalence of EthR mutations.

2. Goal and aims of this Thesis

The goal of this thesis was to study the potential of adjuvant drug therapy to overcome antibiotic resistances in multidrug resistant pathogens. For this we followed two main projects that were focused on the *A. baumannii* and *M. tuberculosis* pathogens.

The overall goal of the first project is the identification of suitable therapeutic targets to overcome antibiotic resistance in *A. baumannii.*

To achieve this goal, I have followed several specific aims:

- generate a genome-editing method that can be applied to laboratory and clinical *A. baumannii* strains, independently of their resistance profile
- apply the genome editing method to characterize potential drug targets in *A. baumannii* clinical strains.

The overall goal of the second project is the development of an adjuvant drug to boost the ethionamide bioactivation pathway in *M. tuberculosis*. This project is part of a collaboration in between BioVersys and researchers from the University of Lille (France). During the project, we discovered an alternative ethionamide bioactivation pathway called EthA2-EthR2, which is analogue to the previously known EthA-EthR bioactivation pathway. My contribution in this project was to assist the development of EthR2 inhibitor compounds that are active on the novel bioactivation pathway to boost ethionamide efficacy against *M. tuberculosis*.

To achieve this goal, I have followed several specific aims:

- generate a synthetic mammalian gene circuit to sense EthR2-DNA interactions
- characterize the synthetic gene circuit
- apply this bioassay to evaluate the ability of compounds to inhibit EthR2-DNA interactions.

3. Results

3.1. Part A

Adjuvant drug targets to overcome antibiotic resistance in *A. baumannii*

3.1.1. A novel genome-editing platform for drug-resistant *Acinetobacter baumannii* reveals an AdeR-unrelated tigecycline resistance mechanism

Vincent Trebosc[1,2], Sarah Gartenmann[1], Kevin Royet[1], Pablo Manfredi[2], Marcus Tötzl[1], Birgit Schellhorn[1], Michel Pieren[1], Marcel Tigges[1], Sergio Lociuro[1], Peter C. Sennhenn[1], Marc Gitzinger[1], Dirk Bumann[2], and Christian Kemmer[1]

[1] BioVersys AG, Basel, Switzerland
[2] Biozentrum, University of Basel, Basel, Switzerland

Status of the paper: published in Antimicrobial Agents and Chemotherapy

3.1.1.1. Abstract of the paper

Infections with the Gram-negative coccobacillus *Acinetobacter baumannii* are a major threat in hospital settings. The progressing emergence of multidrug resistant clinical strains significantly reduces the treatment options for clinicians to fight *A. baumannii* infections. The current lack of robust methods to genetically manipulate drug resistant *A. baumannii* isolates impedes research on resistance and virulence mechanisms in clinically relevant strains. In this study, we developed a highly efficient and versatile genome editing platform enabling the markerless modification of the genome of *A. baumannii* clinical and laboratory strains, regardless of their resistance profile. We applied this method by deleting AdeR, a transcription factor that regulates the expression of the AdeABC efflux pump in tigecycline resistant *A. baumannii*, to evaluate its function as a putative drug target. Loss of *adeR* reduced the MIC90 of tigecycline from 25 µg/ml in the parental strains to 3.1 µg/ml in the Δ*adeR* mutants indicating its importance in the drug resistant phenotype. However, 60% of the clinical isolates remained non-susceptible to tigecycline after *adeR* deletion. Evolution of artificial tigecycline resistance in two strains followed by whole genome sequencing revealed loss of function mutations in *trm*, suggesting its role in an alternative AdeABC-independent tigecycline resistance mechanism. This finding was strengthened by the confirmation of *trm* disruption in the majority of the tigecycline resistant clinical isolates. This study highlights the development and application of a powerful genome editing platform for *A. baumannii* enabling future research on drug resistance and virulence pathways in clinical relevant strains.

3.1.1.2. Statement of my work

- Design of all experiments
- Design and construction of the genome editing platform
- Construction of gene deletion and point mutation *A. baumannii* mutants
- Determination of MIC
- qRT-PCR experiments and data analysis
- Genotyping of *adeR*, *adeS* and *trm*
- Writing of the manuscript

3.1.1.3. Published paper

AMERICAN SOCIETY FOR MICROBIOLOGY | Antimicrobial Agents and Chemotherapy

A Novel Genome-Editing Platform for Drug-Resistant *Acinetobacter baumannii* Reveals an AdeR-Unrelated Tigecycline Resistance Mechanism

Vincent Trebosc,[a,b] Sarah Gartenmann,[a] Kevin Royet,[a] Pablo Manfredi,[b] Marcus Tötzl,[a] Birgit Schellhorn,[a] Michel Pieren,[a] Marcel Tigges,[a] Sergio Lociuro,[a] Peter C. Sennhenn,[a] Marc Gitzinger,[a] Dirk Bumann,[b] Christian Kemmer[a]

BioVersys AG, Basel, Switzerland[a]; Biozentrum, University of Basel, Basel, Switzerland[b]

Infections with the Gram-negative coccobacillus *Acinetobacter baumannii* are a major threat in hospital settings. The progressing emergence of multidrug-resistant clinical strains significantly reduces the treatment options for clinicians to fight *A. baumannii* infections. The current lack of robust methods to genetically manipulate drug-resistant *A. baumannii* isolates impedes research on resistance and virulence mechanisms in clinically relevant strains. In this study, we developed a highly efficient and versatile genome-editing platform enabling the markerless modification of the genome of *A. baumannii* clinical and laboratory strains, regardless of their resistance profiles. We applied this method for the deletion of AdeR, a transcription factor that regulates the expression of the AdeABC efflux pump in tigecycline-resistant *A. baumannii*, to evaluate its function as a putative drug target. Loss of *adeR* reduced the MIC_{90} of tigecycline from 25 μg/ml in the parental strains to 3.1 μg/ml in the Δ*adeR* mutants, indicating its importance in the drug resistance phenotype. However, 60% of the clinical isolates remained nonsusceptible to tigecycline after *adeR* deletion. Evolution of artificial tigecycline resistance in two strains followed by whole-genome sequencing revealed loss-of-function mutations in *trm*, suggesting its role in an alternative AdeABC-independent tigecycline resistance mechanism. This finding was strengthened by the confirmation of *trm* disruption in the majority of the tigecycline-resistant clinical isolates. This study highlights the development and application of a powerful genome-editing platform for *A. baumannii* enabling future research on drug resistance and virulence pathways in clinically relevant strains.

One of the greatest global health problems results from the limited treatment options to fight bacterial infections caused by multidrug-resistant (MDR) organisms. The group of ESKAPE organisms that is comprised of *Enterobacter* spp., *Staphylococcus aureus/epidermidis*, *Klebsiella pneumonia*, *Acinetobacter baumannii*, *Pseudomonas aeruginosa*, and *Enterococcus faecalis/faecium* is considered to cause the vast majority of, often untreatable, nosocomial infections (1). Among these ESKAPE pathogens *A. baumannii* is most difficult to treat due to its multiple intrinsic and acquired resistance mechanisms that resulted in the development of MDR, extensively drug resistant (XDR), or even pan-drug-resistant (PDR) phenotypes (2–5).

Bacteria have evolved multiple ways to evade antibiotic-mediated cell death, such as (i) enzymatic modification/cleavage of the antibiotic (e.g., beta-lactams), (ii) modification/protection of the antibiotic target (e.g., fluoroquinolones), or (iii) reduction of the intracellular concentration by antibiotic efflux or reduced influx (e.g., tetracyclines) (6). The expression of such defense mechanisms may require an extensive metabolic investment, often leading to a reduced fitness of these resistant bacteria in the absence of the external selection pressure (7). To overcome these ecological drawbacks, bacteria have developed diverse transcriptional regulation mechanisms that ensure specific expression of the resistance genes only in the presence of poisoning antibiotics (8). The need for precise regulation of resistance gene cluster expression makes transcriptional regulators promising drug targets as part of a strategy to overcome antibiotic resistances. Small molecules that specifically interfere with the transcriptional regulator function may switch off the resistance mechanism. The combination of such inhibitors with a potent antibiotic as an adjuvant drug may provide a new tool to fight infections caused by MDR, XDR, or even PDR pathogens by restoring the efficacy of an approved antibiotic (9, 10).

In clinical settings the use of different and/or combinations of antibiotics to treat hazardous infections caused by the Gram-negative pathogen *A. baumannii* leads to a tremendous selection pressure toward the development of multidrug-resistant strains. Unfortunately, we currently have only limited understanding of the innate and acquired antibiotic resistance mechanisms of *A. baumannii* clinical isolates. This lack of knowledge is mainly based on the unavailability of robust methods that allow the genetic manipulation of MDR, XDR, and PDR patient-derived strains (11). In most studies investigating antibiotic resistance mechanisms in *A. baumannii*, laboratory strains were used, such as ATCC-19606 and ATCC-17978, which do not represent the problematic clonal lineages that are currently present in hospitals (12, 13).

In this study, we developed a novel method allowing the short-term construction of markerless gene knockouts in *A. baumannii*

Received 16 June 2016 **Returned for modification** 8 July 2016
Accepted 16 September 2016

Accepted manuscript posted online 26 September 2016

Citation Trebosc V, Gartenmann S, Royet K, Manfredi P, Tötzl M, Schellhorn B, Pieren M, Tigges M, Lociuro S, Sennhenn PC, Gitzinger M, Bumann D, Kemmer C. 2016. A novel genome-editing platform for drug-resistant *Acinetobacter baumannii* reveals an AdeR-unrelated tigecycline resistance mechanism. Antimicrob Agents Chemother 60:7263–7271. doi:10.1128/AAC.01275-16.

Address correspondence to Christian Kemmer, christian.kemmer@bioversys.com.

Supplemental material for this article may be found at http://dx.doi.org/10.1128/AAC.01275-16.

clinical isolates, regardless of their resistance profiles. We applied this powerful tool in 10 diverse *A. baumannii* strains that were resistant to multiple antibiotics to evaluate the transcriptional regulator AdeR as a potential drug target to rejuvenate the activity of tigecycline, a drug of last resort for treatment of XDR *A. baumannii* infections (14). We demonstrated that AdeR-regulated AdeABC-mediated drug efflux is not the exclusive tigecycline resistance mechanism in XDR *A. baumannii* clinical strains, disqualifying AdeR as a direct drug target.

MATERIALS AND METHODS

Bacterial strains, MICs, MLST, and oligonucleotides. Ten XDR *A. baumannii* clinical isolates from the BioVersys proprietary strain collection were used in this study. As a control the tigecycline-susceptible *A. baumannii* ATCC-17978 strain from the American Type Culture Collection (ATCC) was used. Multilocus sequence type (MLST) analysis was performed according to the Pasteur scheme by using specific primers (source: http://pubmlst.org/abaumannii/) (12). MICs were determined by the microdilution method in cation-adjusted Mueller-Hinton broth (CA-MHB) according to CLSI guidelines (15). Bacteria were grown using Luria-Bertani (LB) broth or agar at 37°C unless otherwise stated. All oligonucleotides used in this study are listed in Table S1 in the supplemental material and were synthesized at Microsynth AG (Balgach, Switzerland).

Cloning of the gene knockout vector backbone pVT77 suitable for genetic manipulation of drug-resistant *A. baumannii* strains. The vector pSEVA238 (Standard European Vector Assembly platform [http://seva.cnb.csic.es/]) was used as the starting backbone for cloning of the pVT77 knockout plasmid (16). First, the pUC19 origin of replication (ColE1) was PCR amplified from the pUC19 plasmid using the primers oVT01/oVT02 and cloned into the AscI and FseI restriction sites of pSEVA238, creating plasmid pVT52. A synthetic cassette containing the thiopurine *S*-methyltransferase (*tpm*) gene of *Acinetobacter baylyi* (locus tag ACIAD2922) driven by the *Burkholderia cenocepacia rpsL* PC_{S12} promoter was cloned with EcoRI and PacI into pVT52 to allow antibiotic-independent selection for genomic plasmid integration by sodium tellurite (pVT59). For counterselection with 3′-azido-3′-deoxythymidine (AZT), the thymidine kinase (*tdk*) gene was PCR amplified from *Escherichia coli* DH5α genomic DNA using primers oVT113/oVT114 flanked with an upstream ribosome binding site (RBS) and cloned into pSEVA234, creating plasmid pVT66. On this plasmid *tdk* is placed under the repression of LacI. The *lacI-tdk* cassette was excised from pVT66 with PacI and AscI restriction enzymes and subsequently cloned into pVT59, resulting in plasmid pVT67. Further modifications were done to maximize the cloning possibilities in the multiple cloning site (MCS). The EcoRI restriction site present in the *lacI-tdk* cassette was removed by PCR mutagenesis using primers oVT141/oVT142. The present MCS was also replaced with a more complete MCS, including StuI, XhoI, EcoRI, SacI, KpnI, SmaI, BamHI, XbaI, PstI, and HindIII restriction sites, by cloning annealed oligonucleotides oVT149 and oVT150 into EcoRI and HindIII restriction sites of pVT67. The resulting plasmid was named pVT77, and it was used as a backbone for the cloning of flanking regions to knock out any specific targets in *A. baumannii* clinical isolates (Fig. 1A).

Construction of *adeR* and *trm* gene deletions in *A. baumannii* isolates. Scarless deletions of the *adeR* and *trm* genes were done in *A. baumannii* using a two-step allelic exchange method adapted from Amin and colleagues (Fig. 1B) (17). DNA fragments corresponding to 700-bp up- and downstream genomic regions of the genes to be deleted were amplified by PCR using primers oVT154/oVT106 and oVT107/oVT155 for *adeR* and oVT412/oVT413 and oVT414/oVT415 for *trm*, respectively. The up- and downstream fragments of each gene were ligated and introduced into pVT77 previously digested with XhoI/XbaI and EcoRI/XbaI for *adeR* and *trm*, respectively, using Gibson assembly. The resulting knockout plasmids were transformed in the *E. coli* conjugative strain MFD*pir*, which is auxotrophic for diaminopimelic acid (DAP) (18). The transfer of the plasmid in *A. baumannii* isolates was achieved by conjugation, as previously described (17). Briefly, 0.2-ml overnight cultures from the donor (MFD*pir* cells containing the knockout plasmid) and receiver (*A. baumannii* isolate) strains were mixed and washed twice with 1 ml of LB broth to remove residual antibiotics. The cells were resuspended in 50 μl of medium and transferred onto a 0.45-μm-pore-size nitrocellulose filter placed on LB agar containing 300 μM DAP. After overnight incubation at 37°C for conjugative plasmid transfer, the cells were scraped off the filter and resuspended in 0.4 ml of 0.85% (wt/vol) NaCl, and 0.1-ml aliquots were plated on LB agar plates containing 100 μg/ml sodium tellurite. After overnight selection at 37°C, clones were screened for genomic plasmid integration by PCR using primers oVT93/oVT08 and oVT423/oVT8 for *adeR* and *trm*, respectively. Clones containing up- and downstream plasmid integrations were used to inoculate 2 ml of fresh LB broth containing 1 mM isopropyl-β-D-1-thiogalactopyranoside (IPTG) and cultured for 3 h at 37°C to express the heterologous thymidine kinase. Culture aliquots (0.1 ml) of a 1:10 dilution series (10^0 to 10^{-2}) were plated on LB agar plates containing 200 μg/ml AZT and incubated overnight at 37°C for plasmid removal from the genome. Clones were screened for gene deletion and plasmid removal by PCR using primers oVT93/oVT94 and oVT423/oVT424 for *adeR* and *trm*, respectively. The genomic gene deletions were finally confirmed by DNA sequencing (Microsynth AG, Balgach, Switzerland).

Restoration of a functional *trm* gene by chromosomal single nucleotide knock-in in *A. baumannii* isolates. For allelic replacement of the mutated *trm*, a 1.4-kb DNA fragment including the wild-type *trm* (lacking the A240 deletion) was PCR amplified from isolate BV186 using primers oVT416/oVT417. This fragment was cloned into pVT77 previously digested with KpnI/XbaI using Gibson assembly. The two-step allelic exchange method described above was used to restore wild-type *trm*, and the successful gene replacement was confirmed by sequencing using primers oVT312/oVT161.

qRT-PCR. The expression of the efflux pump operon *adeABC* was evaluated by quantifying *adeB* expression using adeB-qRT-F/adeB-qRT-R primers. *A. baumannii* isolates were grown in LB broth at 37°C to mid-log phase (optical density at 600 nm [OD_{600}] of 0.5), and total RNA was extracted using a PureLink RNA minikit (Ambion) according to the manufacturer's recommendations. Residual DNA contaminations were removed using a Turbo DNA-free kit (Ambion). Quantitative reverse transcription-PCR (qRT-PCR) was performed using a GoTaq 1-Step RT-qPCR System kit (Promega) on a StepOne Real-Time PCR Light-Cycler (Applied Biosystems). Extracted RNA (25 ng) was mixed with 10 μl of GoTaq MasterMix, 3 μl of 8 μM primers, 0.4 μl of GoScript RT mix, and 0.3 μl of carboxy-X-rhodamine (CXR) standard dye in a total volume of 20 μl. As a housekeeping gene, the RNA polymerase sigma factor D (*rpoD*) was quantified with primers rpoD-qRT-F/rpoD-qRT-R, and *adeB* expression was normalized to that of *rpoD* using the comparative $\Delta\Delta C_T$ (where C_T is threshold cycle) method. A detailed description of the DNA probes used for RNA detection is given in Table S1 in the supplemental material.

Genotyping of *adeR*, *adeS*, and *trm* in clinical isolates. A genomic sequence including *adeR* and *adeS* was PCR amplified from all *A. baumannii* isolates using primers oVT05 and oVT134 (except for ATCC-17978, for which the oVT151 primer was used instead of oVT134). A genomic sequence including *trm* was PCR amplified from all *A. baumannii* isolates using primers oVT160 and oVT161. The PCR products were subsequently sent for sequencing (Microsynth AG, Balgach, Switzerland).

***In vitro* evolution of tigecycline resistance.** *A. baumannii* ATCC-17978 and its Δ*adeR* mutant (ATCC-$17978_{\Delta adeR}$) were subjected to serial passages to develop tigecycline resistance *in vitro* (see Fig. S1 in the supplemental material). In brief, LB broth liquid cultures were passaged every 48 h starting with a tigecycline concentration of 0.2 μg/ml and incubated at 37°C. For passaging, the cultures were diluted 1/100 and exposed to double the tigecycline concentration of the preceding culture until a concentration of 6.4 μg/ml tigecycline was reached. The artificially evolved tigecycline-resistant strains derived from strain *A. baumannii* ATCC-

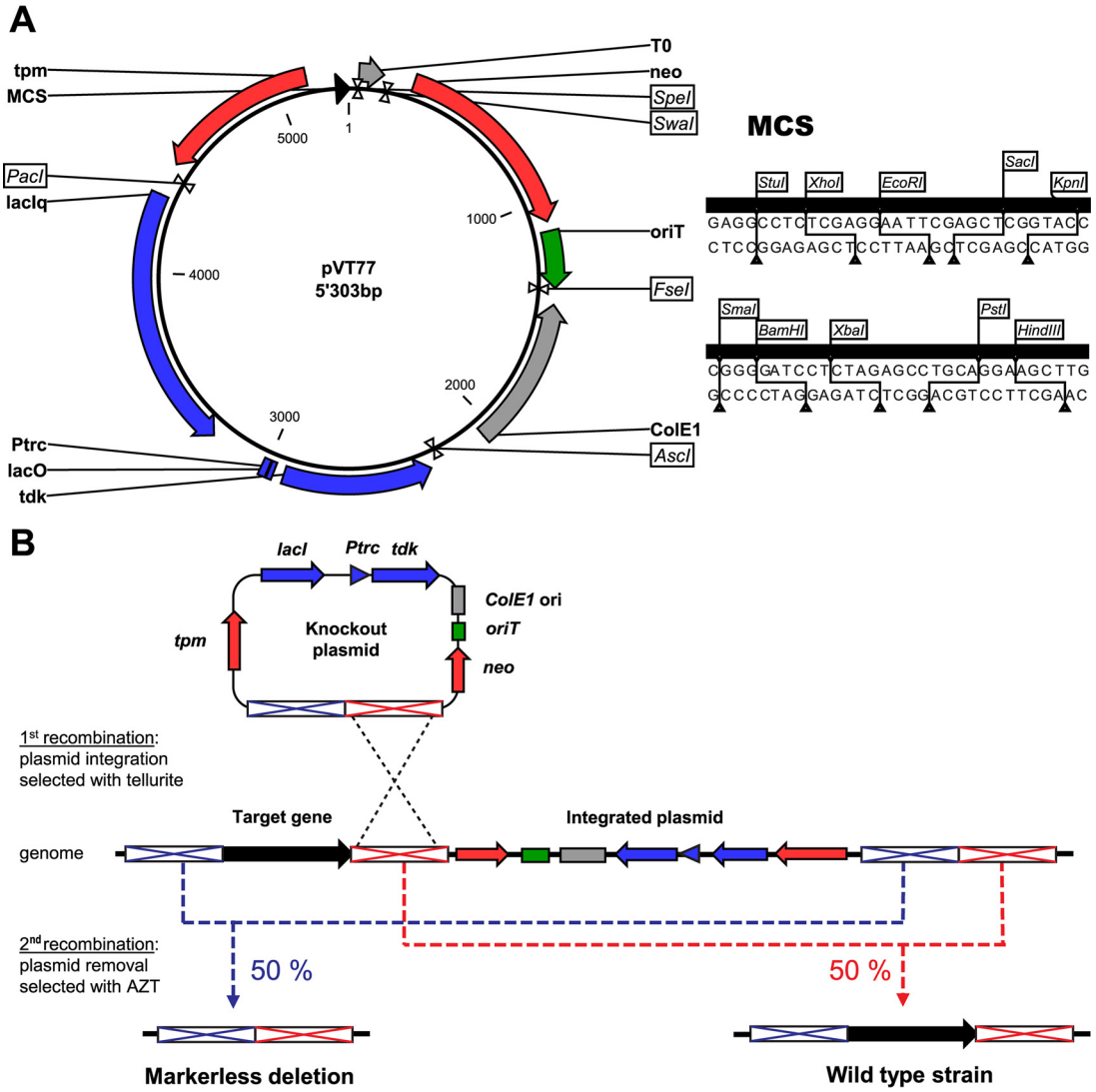

FIG 1 Schematic representation of the knockout platform developed for targeted gene deletion in XDR *A. baumannii*. (A) Representation of the modular pVT77 cloning vector. Important features of the vector platform are shown: (i) a thiopurine *S*-methyltransferase (*tpm*) for antibiotic-free selection of clones after plasmid integration and a kanamycin resistance cassette (*neo*) for selection in *E. coli* (in red); (ii) a functional counterselection cassette ($lacI_q$-P_{trc}-lacO-tdk; shown in blue) for genomic plasmid removal in the presence of IPTG and AZT; (iii) an origin of transfer (*oriT*; in green) for conjugative plasmid transfer from *E. coli* to *A. baumannii*; (iv) ColE1 *ori* for efficient plasmid replication in *E. coli* (please note that this origin of replication is not active in *A. baumannii*, resulting in a suicide vector for this pathogen) and the transcriptional terminator T0 (in gray); and (v) a multiple cloning site (MCS; black) allowing the integration of the up- and downstream regions of the target gene. The plasmid map was generated with CLC Main Workbench, version 6.9.1. (B) Representation of the two-step allelic exchange method for targeted gene deletion using derivatives of the knockout plasmid pVT77. The knockout plasmid is site-specifically integrated next to a target gene by an initial homologous recombination event, and clones are selected with potassium tellurite. Afterwards, a second recombination event for the subsequent plasmid removal is produced by the induction of the counterselection cassette, which triggers cytotoxicity in the presence of AZT, leading to 50% knockout mutants or wild-type revertants.

17978 and its Δ*adeR* mutant were designated ATCC-17978(TGC) and ATCC-17978$_{\Delta adeR}$(TGC), respectively.

Whole-genome sequencing. Genomic DNA (gDNA) of ATCC-17978(TGC), ATCC-17978$_{\Delta adeR}$(TGC), and their parental strains was extracted using a GeneJET genomic DNA purification kit (Thermo Scientific) according to the manufacturer's recommendations. The four gDNA samples were multiplex sequenced using a Illumina MiSeq system (Illumina, Inc.) using a paired-end 250-bp protocol at the Quantitative Genomics Facility (Department of Biosystems Science and Engineering, ETH Zurich, Basel, Switzerland). Four to eight million high-quality reads per sample were generated and mapped against the reference genome of *A. baumannii* ATCC-17978 (GenBank accession number CP000521.1) using Bowtie2, achieving an average coverage above ×100 (19). Small nucleotide variations were spotted using SAMtools (20). Recombination events were screened with a series of in-house perl scripts based on (i) coverage fluctuations, (ii) the distribution of start/end positions of mapped reads, and (iii) reads that significantly mapped to at least two noncontiguous regions of the reference chromosome (i.e., regions including the newly formed recombination boundaries). In addition, *de novo* assembly of reads with poor mapping score values was performed with SOAPdenovo 2 and identified insertion sequences (IS) were aligned with the ISFinder insertion sequence database (https://www-is.biotoul.fr/) (21, 22).

Accession number(s). The sequence of the pVT77 cloning vector has been deposited in the GenBank under accession number KX397287. Sequences of the *adeR* and *adeS* genes for the following isolates were deposited in GenBank under the indicated accession numbers: BV26 (KX819204),

TABLE 1 Characterization of the *A. baumannii* clinical isolate panel used in this study

Strain designation	Strain isolation		MLST	MIC (μg/ml)[a]									
	Location	Date		GEN	MEM	CIP	TIM*	CTX	SXT*	SAM*	CST	TET	TEL
ATCC-17978	France	1951	77	2	0.5	1	16/2	*16*	**>8/152**	4/2	0.5	2	4
BV26	Switzerland	1979	1	**>128**	1	**4**	**>256/2**	*16*	**>8/152**	**64/32**	0.5	**128**	4
BV94	USA	2011	2	**>128**	**32**	**256**	**>256/2**	**>256**	**>8/152**	*16/8*	**64**	**32**	8
BV173	Greece	2012	2	**>128**	**>64**	**128**	**>256/2**	**>256**	**>8/152**	**128/64**	**32**	**>256**	1
BV175	Turkey	2012	2	**128**	**32**	**256**	**>256/2**	**256**	**>8/152**	**32/16**	**>256**	**256**	0.5
BV185	Mexico	2013	2	**>128**	**>64**	**128**	**>256/2**	**>256**	**>8/152**	**64/32**	**>256**	**256**	1
BV186	USA	2013	2	**16**	**64**	**256**	**>256/2**	**>256**	**>8/152**	**32/16**	**16**	*8*	4
BV187	USA	2013	2	**32**	**64**	**256**	**>256/2**	**>256**	**>8/152**	*16/8*	**16**	*8*	4
BV189	Spain	2013	2	**128**	**32**	**128**	**>256/2**	**256**	**>8/152**	**32/16**	**64**	**16**	8
BV190	Greece	2012	1	**>128**	**64**	**64**	**>256/2**	**>256**	**>8/152**	**64/32**	**256**	**256**	4
BV191	China	2013	2	**>128**	**>64**	**256**	**>256/2**	**>256**	**>8/152**	**128/64**	**>256**	**>256**	2
ATCC-25922[b]				1	<0.06	<0.25	8/2	<0.25	0.125/2.34	4/2	1	2	4

[a] MLST, multilocus sequence type; CIP, ciprofloxacin; CST, colistin; CTX, cefotaxime; GEN, gentamicin; MEM, meropenem; SAM, ampicillin-sulbactam; SXT, trimethoprim-sulfamethoxazole; TIM, ticarcillin-clavulanate; TEL, tellurite (nonantibiotic compound); TET, tetracycline. Classification of antibiotic resistance was done according to breakpoints published by the Clinical and Laboratory Standards Institute and is indicated as follows: susceptible, underlining; intermediate, italics; resistant, boldface (46). *, values for the components are separated by a slash.

[b] Quality control.

BV94 (KX819205), BV173 (KX819206), BV175 (KX819207), BV185 (KX819208), BV186 (KX819209), BV187 (KX819210), BV189 (KX819211), BV190 (KX819212), and BV191 (KX819213). Sequences of the *trm* gene were deposited in GenBank under the indicated accession numbers: BV26 (KX819214), BV94 (KX819215), BV173 (KX819216), BV175 (KX819217), BV185 (KX819218), BV186 (KX819219), BV187 (KX819220), BV189 (KX819221), BV190 (KX819222), and BV191 (KX819223). The reads of the whole-genome sequencing have been deposited in the GenBank Sequence Read Archive (SRA) as follows: ATCC-17978 (GenBank accession number SRR4176247), ATCC-17978$_{\Delta adeR}$ (SRR4176248), ATCC-17978(TGC) (SRR4176249), and ATCC-17978$_{\Delta adeR}$(TGC) (SRR4176250).

RESULTS

Knockout technology for genetic manipulation of *A. baumannii* clinical isolates regardless of their antibiotic resistance profiles. *A. baumannii* is among the ESKAPE pathogens most difficult to treat because it often combines a multitude of intrinsic and acquired drug resistance mechanisms (2). In order to investigate the function of putative drug targets in clinically problematic drug-resistant isolates of *A. baumannii*, we had to develop a novel technology platform enabling the genome modification of these MDR isolates because traditional methods using antibiotic selection cassettes cannot be applied in these pathogens. We screened a collection of clinically relevant *A. baumannii* isolates for their susceptibilities to various chemical agents and demonstrated that all strains were sensitive to sodium tellurite (MIC ≤ 8 μg/ml) (Table 1). Our results suggested that a tellurite resistance cassette might be a powerful tool to select for genetic manipulation of MDR, XDR, and PDR *A. baumannii* isolates independently of their antibiotic resistance profiles. A two-step homologous recombination approach was developed to target clinical isolates (Fig. 1B). Traditional antibiotic selection cassettes were replaced by the *Acinetobacter baylyi*-derived tellurite resistance marker gene *tpm*, encoding a thiopurine *S*-methyltransferase, to allow selection for chromosomal plasmid integration with sodium tellurite (23). In bacteria, expression of Tpm enzymatically detoxifies tellurite by a reduction and methylation of tellurite to produce volatile dimethyl telluride (24). The *sacB* gene, widely used as a counterselection cassette to initiate a second recombination event in different bacteria, was shown not to be capable of efficiently removing the integrated plasmid from the genome of *A. baumannii* and *E. coli* (17, 25). During our design process we also noticed that SacB expression is slightly toxic even in the absence of sucrose, leading to the selection of inactivating mutations in the *sacB* gene. As an alternative, we PCR amplified the *E. coli*-derived thymidine kinase gene (*tdk*) and cloned it under the control of an isopropyl-β-D-thiogalactopyranoside (IPTG)-inducible promoter. The expression of thymidine kinase in the presence of the reverse transcriptase small-molecule inhibitor 3′-azido-3′-deoxythymidine (AZT) results in the incorporation of a chain-terminating thymidine analogue during DNA replication, which finally leads to cell death or removal of the *tdk*-expressing plasmid from the genome (26). This powerful setup selected for the second recombination event with an efficiency of >95% in *A. baumannii* clinical isolates. The application of our gene knockout platform enabled us to efficiently delete different target genes in *A. baumannii* strains of diverse origins that were antibiotic susceptible or that accumulated multiple antibiotic resistance mechanisms.

Deletion of genomic *adeR* reveals an AdeABC-independent tigecycline resistance mechanism. Tigecycline is considered to be a last-resort treatment regimen for infections with MDR/XDR *A. baumannii* (14). Resistance to tigecycline is mediated by the AdeABC efflux pump, which is controlled by the AdeRS two-component system (TCS) (27–31). This TCS was recently suggested as a putative drug target for small-molecule intervention to interfere with different antibiotic resistance pathways in *A. baumannii* (10). In order to evaluate the importance of the transcriptional regulator AdeR in mediating tigecycline resistance in clinical *A. baumannii* isolates, we customized our gene knockout platform (Fig. 1A) to produce genomic *adeR* deletions. We selected a diverse panel of 10 tigecycline-resistant clinical *A. baumannii* isolates using the following parameters: (i) their recent isolation from diverse geographic locations, (ii) their antibiotic resistance profile to first-, second-, and last-line drugs (carbapenems, colistin, and tigecycline, respectively), and (iii) their clonal lineage as determined by using MLST according to the Pasteur scheme (12). All strains were isolated between 2011 and 2013 (except for BV26, which was isolated in 1979) and classified as XDR according to the definition

TABLE 2 Tigecycline resistance profile and list of identified mutations in the clinical *A. baumannii* isolate panel and the corresponding Δ*adeR* strains

Strain designation	Tigecycline MIC (μg/ml)		AdeRS amino acid substitution(s)	Deletion in *trm*
	Wild type	Δ*adeR* strain		
ATCC-17978	0.4	0.4	Reference	
BV26	6.3	0.4	AdeS E201K E237K	
BV94	25	3.1	AdeS F170S	G1065
BV173	6.3	0.8	AdeR D21V D26N	A240
BV175	3.1	0.8		A240
BV185	6.3	3.1		A240
BV186	3.1	3.1		G1065
BV187	3.1	3.1		G1065
BV189	6.3	3.1		A240
BV190	6.3	0.8	AdeS Q339K	T1050
BV191	25	1.6	AdeS G79S	A240

given by Magiorakos and colleagues (32). MLST analysis revealed that eight of the clinical isolates belonged to clonal cluster 2 (CC2), and two belonged to clonal cluster 1 (CC1), clusters that represent the most prominent worldwide epidemic clonal lineages (12, 13) (Table 1). Conjugation from *E. coli* was used to introduce the knockout plasmid into *A. baumannii* isolates. The plasmid conjugation/integration efficiency was measured as the number of transconjugants per receiver cell and was similar among different clinical isolates ($1.8 \times 10^{-7} \pm 0.2 \times 10^{-7}$ transconjugants/cell; $n = 3$) and one order of magnitude lower than for the reference strain ATCC-17978 (3.2×10^{-6} transconjugants/cell). We successfully created scarless *adeR* knockout (Δ*adeR*) mutants of these 10 XDR *A. baumannii* strains and also deleted *adeR* in the reference strain ATCC-17978. We characterized the tigecycline resistance profile of the Δ*adeR* mutants and their parental strains using the microdilution method. Deletion of *adeR* in 10 XDR *A. baumannii* strains reduced the MIC_{90} of tigecycline from 25 μg/ml to 3.1 μg/ml, demonstrating a significant shift of Δ*adeR* mutants toward tigecycline susceptibility (Table 2). Our data indicate that AdeR is important for *A. baumannii* to develop tigecycline resistance. However, in clinical practice the tigecycline susceptibility breakpoint for *A. baumannii* infections is ≤1 μg/ml (33). Our results demonstrated that 60% of the tested clinical isolates remained tigecycline nonsusceptible after *adeR* deletion and suggest that AdeR-regulated AdeABC-mediated tigecycline resistance is not the exclusive resistance mechanism rendering tigecycline inactive in these strains. We propose the existence of at least one AdeR-unrelated resistance mechanism that may be developed in *A. baumannii* clinical isolates to render tigecycline ineffective.

AdeR was previously shown to activate the expression of the RND (resistance-nodulation-cell division)-type AdeABC efflux pump and most likely controls the extrusion of tigecycline from the cells (31). However, the presence of an alternative activating mechanism for AdeABC mediated by the TCS BaeSR was recently suggested (34). In order to determine if overexpression of AdeABC was mediating tigecycline resistance despite the deletion of *adeR*, we quantified the expression level of *adeB*, which is the main component of the RND efflux pump. By using quantitative real-time PCR, we demonstrated general overexpression of *adeB* in all tested tigecycline-resistant clinical isolates (Fig. 2). The overexpression of the *adeABC* efflux pump correlated with elevated tigecycline MICs, as demonstrated by 990-fold and 160-fold overexpression levels of *adeB* in strains BV94 and BV191 with the highest tigecycline resistance levels, respectively. In contrast, all Δ*adeR* mutants lost the ability to express *adeB*, suggesting that AdeR is the main transcriptional activator of the AdeABC efflux pump. These data further indicate that an AdeR-unrelated tigecycline resistance mechanism in *A. baumannii* clinical isolates is not based on deregulated expression of the AdeABC efflux pump.

To evaluate if the AdeABC efflux pump overexpression in tigecycline-resistant clinical isolates was triggered by mutations in the AdeRS TCS as previously described, we analyzed the genomic sequences of *adeR* and *adeS* (35). To distinguish between mutations involved in *adeABC* overexpression and those coming from clonal lineage evolution, we used as reference sequences the tigecycline-sensitive *A. baumannii* strains AYE and ACICU, which are representatives of clonal clusters CC1 and CC2, respectively (12). The only strain that contained mutations in the transcriptional regulator AdeR was BV173 (Table 2). One of the identified amino acid substitutions (D21V) in this strain was previously described to mediate *adeABC* overexpression (36). Mutations in the sensor kinase AdeS were much more abundant, and different amino acid substitutions were identified in four clinical isolates (Table 2). Interestingly, five tigecycline-resistant clinical isolates had wild-type AdeRS sequences without any amino acid substitutions. For these strains, we further analyzed the sequence of the intergenic regulatory region between *adeRS* and *adeABC* that encodes the AdeR DNA-binding site. However, we could not identify any mutations that could explain the overexpression of *adeABC*. These strains, with the exception of BV175, were not resensitized to tigecycline by the deletion of *adeR* (Table 2).

Taken together, these results indicate that the loss of *adeR* in XDR *A. baumannii* clinical isolates abolished the expression of *adeB*, leading to increased tigecycline sensitivity in 8 out of 10 Δ*adeR* mutants. However, 60% of the clinical isolates remained tigecycline nonsusceptible, with an MIC above the clinical susceptibility breakpoint of ≤1 μg/ml (33, 37). The requirement for AdeR to express the AdeABC efflux pump and the absence of mutation in four strains that were not resensitized to tigecycline indicate the presence of an alternative AdeR-AdeABC-independent tigecycline resistance pathway in these strains and disqualify AdeR as an adjuvant drug target.

Insights into alternative tigecycline resistance mechanisms. To investigate putative AdeRS-AdeABC-unrelated tigecycline resistance mechanisms in *A. baumannii*, we developed artificial tige-

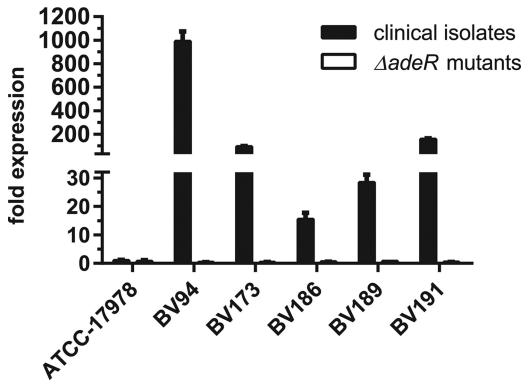

FIG 2 Quantification of *adeB* expression levels in tigecycline-resistant *A. baumannii* clinical isolates and their Δ*adeR* mutants. The *adeB* expression levels of the individual strains were determined by quantitative real-time PCR and normalized to the *adeB* expression of the reference strain ATCC-17978.

cycline-resistant strains by subjecting *A. baumannii* ATCC-17978 and its Δ*adeR* mutant (ATCC-17978$_{\Delta adeR}$) to liquid serial passage in the presence of increasing tigecycline concentrations (see Fig. S1 in the supplemental material). After 12 days (6 passages) we obtained wild-type and Δ*adeR*-derived strains able to grow at 6.4 μg/ml tigecycline and designated them ATCC-17978(TGC) and ATCC-17978$_{\Delta adeR}$(TGC), respectively. We analyzed the susceptibilities of these artificially evolved strains to various antibiotic classes. As expected, both strains were resistant to high tigecycline concentrations (see Table S2 in the supplemental material). In parallel with the tigecycline resistance, MICs of tetracycline increased to 32 μg/ml and 64 μg/ml, and MICs of ciprofloxacin increased to 2 μg/ml and 4 μg/ml for ATCC-17978(TGC) and ATCC-17978$_{\Delta adeR}$(TGC), respectively. In contrast, MICs to meropenem remained unchanged in both evolved strains. Both strains also showed a slight shift toward gentamicin susceptibility. To investigate if an alternative regulatory mechanism induced the *adeABC* expression, we analyzed the expression of *adeB* but could not detect an altered *adeB* expression pattern in the parental and evolved strains. This result was consistent with the presence of wild-type *adeS* and *adeRS* sequences in the evolved knockout and parental strains, respectively. In summary, our results suggest the presence of an AdeRS-unrelated tigecycline resistance mechanism leading to an increased resistance pattern to diverse antibiotics.

To unravel this new resistance mechanism, we sequenced the genome of the artificially evolved tigecycline-resistant strains ATCC-17978(TGC) and ATCC-17978$_{\Delta adeR}$(TGC) and compared the sequences with those of the parental strains. We identified the *trm* gene (A1S_2858) coding for a methyltransferase with unknown function as the only gene that was disrupted in both independently evolved strains (see Table S3 in the supplemental material). In ATCC-17978(TGC), we identified an insertion sequence (IS) of approximately 1 kb integrated into the *trm* gene at nucleotide position 747 (total *trm* length, 1,212 nucleotides [nt]). The IS shared 97% sequence identity with IS*Aba12*, a transposon that is present in two copies in the genome of ATCC-17978 (22). In ATCC-17978$_{\Delta adeR}$(TGC), an adenine deletion at *trm* nucleotide 311 caused a frameshift leading to a premature stop codon. In conclusion, both strains expressed a truncated Trm variant that is most likely nonfunctional. We also identified several other mutated genes in the two independently evolved strains. However, these genes were mutated in one or the other strain and therefore cannot represent a general alternative tigecycline resistance mechanism (see Table S3). To evaluate the relevance of *trm* disruption in clinical strains, we sequenced the *trm* gene in our tigecycline-resistant *A. baumannii* strain panel. Except for BV26, all clinical isolates carried a nucleotide deletion in *trm* leading to an early stop codon and therefore a nonfunctional methyltransferase (Table 2). These data suggest that loss of Trm may potentially confer tigecycline resistance by using a pathway independent of the efflux pump AdeABC. To our surprise, three Δ*adeR* mutant strains (BV173, BV175, and BV190) contained a disrupted Trm variant but remained susceptible to tigecycline.

To characterize the role of *trm* disruption in tigecycline resistance we (i) deleted *trm* from the genome of the reference strain ATCC-17978, and (ii) we restored the functionality of chromosomal *trm* by reintroducing the deleted nucleotide A240 in clinical isolates. Loss of Trm in ATCC-17978 marginally increased tigecycline resistance whereas *trm* restoration in clinical isolates slightly decreased tigecycline resistance (see Table S4 in the supplemental material). Although these MIC shifts are considered in the standard deviation of the method, the consistency of the results among the strains suggests that loss of Trm plays a general role in tigecycline resistance in *A. baumannii*.

DISCUSSION

In contrast to the use of conventional antibiotics that target conserved essential mechanisms, the adjuvant approach aims to modulate nonessential mechanisms, which may vary significantly within the same species. Consequently, the identification of new drug targets for adjuvant therapy requires extensive validation in diverse clinical strains to ensure target relevance. Unfortunately, methods to manipulate these drug-resistant strains are lacking, rendering drug target validation difficult. Recently, a method based on the recombineering technology has been developed to produce gene deletion mutants in *A. baumannii* (11). This method requires the plasmid-encoded expression of a recombinase to enhance the efficiency of homologous recombination and electroporation to incorporate foreign DNA into the cells (11). Unfortunately, clone selection is performed with two different antibiotic resistance cassettes, and electroporation may be very inefficient in clinical isolates, which prevents an adaptation of this method for the manipulation of drug-resistant strains. Moreover, the recombinase expression vector has to be cured from the cells to allow the subsequent introduction of another vector that expresses the FLP recombinase, which once again has to be cured to finally produce markerless mutants (11). Overall, this recombineering-based method is a time-consuming procedure and is incompatible with multidrug-resistant isolates.

Amin and colleagues previously developed a two-step method to construct scarless knockout mutants in MDR *A. baumannii* by implementation of a tellurite resistance operon into their knockout plasmids that allowed targeting *A. baumannii* isolates regardless of their antibiotic resistance profiles (17). The applied operon used as selection marker consisted of three consecutive genes (*kilA*, *telA*, and *telB*) carried by a 3-kb DNA sequence. Its expression requires an enormous metabolic investment and confers resistance to 30 μg/ml tellurite (17). A *sacB* cassette was further used to select for the second recombination event and plasmid removal from the genome. Several sucrose passages were required for successful plasmid removal, indicating the inefficiency of this counterselection cassette (17). SacB is also prone to accumulate inactivation mutations due to its slight cytotoxicity even in the absence of sucrose, making the use of this counterselection marker disadvantageous in *A. baumannii* (25).

Here, we report the design of a highly efficient knockout platform for *A. baumannii* isolates, regardless of their antibiotic resistance profiles. The knockout platform takes advantage of an efficient thiopurine *S*-methyltransferase encoded by a single *tpm* gene of *Acinetobacter baylyi* (Fig. 1A). This resistance marker confers resistance to ≥100 μg/ml tellurite and requires a low fitness investment from the cells. We combined this selection marker with an inducible variant of an *E. coli*-derived thymidine kinase (*tdk*) to select for the second recombination event, allowing plasmid removal with an efficiency of >95% in *A. baumannii* isolates in a one-step counterselection passage on AZT. The developed knockout technology enables us to perform markerless gene deletions in *A. baumannii* clinical and laboratory strains in only 3 days, with the capability for repetitive application of the process to delete

multiple genes from the same genome. The platform is suitable for a multitude of genome engineering techniques in drug-resistant bacteria. Besides producing targeted gene knockouts, we used this technology platform to do gene disruptions and targeted chromosomal insertions (knock-ins) of single nucleotides (point mutation) as well as longer DNA sequences to produce conditional knockout mutants in *A. baumannii*. Moreover, this platform has a modular architecture and allows the exchange of the individual genetic building blocks (e.g., origin of replication, selection marker, or counterselection cassette) by digestion/ligation reactions, enabling the potential for customization to target other pathogens (Fig. 1A). We successfully employed a modified version of the knockout platform to produce markerless gene deletions in MDR *P. aeruginosa*, highlighting the potential for expansion of the platform to other pathogenic species (data will be published elsewhere).

In a case study we demonstrated the efficient deletion of *adeR* from the genome of diverse XDR *A. baumannii* clinical isolates. We characterized these isolates with an antibiotic panel that was chosen to discriminate between non-MDR, MDR, and XDR strains and found that most of the strains were resistant to all tested antibiotics (Table 1) (32). Our data suggest that some of the strains may be even classified as PDR; however, further analyses are required to finalize this classification.

The analysis of AdeR as a potential adjuvant drug target confirmed the importance of AdeR in mediating tigecycline resistance in *A. baumannii*. Our data further suggest that there is at least one AdeR-unrelated mechanism that confers moderate resistance to tigecycline in *A. baumannii* clinical isolates (Table 2). The U.S. Food and Drug Administration (FDA) and the European Committee on Antimicrobial Susceptibility Testing (EUCAST) do not provide breakpoints for *A. baumannii* treatment with tigecycline. However, in clinical practice the susceptibility breakpoint of ≤1 μg/ml is commonly accepted (33, 37).

Because in the absence of AdeR the expression of *adeB* was abolished, this alternative resistance pathway is unrelated to AdeABC-mediated drug efflux (Fig. 2). It was recently shown that the TCS BaeSR may trigger the activation of *adeABC* expression in *A. baumannii* ATCC-17978 (34). Our results indicate that the BaeSR regulation of *adeABC* expression may occur through AdeR because the loss of *adeR* completely abolished *adeABC* expression under the tested conditions. This observation suggests a cross talk between both TCSs by either BaeS-mediated phosphorylation of AdeR or specific activation of *adeR* expression by BaeR. Further experiments are required to clarify a putative dynamic interaction between AdeRS and BaeSR.

Sequencing of *adeRS* in our strain panel revealed that five *A. baumannii* isolates contained mutations in AdeRS (Table 2). We found one strain with mutated AdeR, but four strains with alterations in the sequence of AdeS, suggesting that the sensor kinase is more prone to mutations, leading to an overexpression of AdeABC. With the exception of the D21V substitution mutation in AdeR of strain BV173, the identified mutations have not been previously described (27, 31, 35, 36, 38, 39). To our surprise, the tested XDR strain panel contained four tigecycline-resistant isolates with wild-type AdeRS that were not resensitized for tigecycline by deletion of *adeR* (Table 2). This finding highlights the presence of an alternative AdeABC-independent resistance mechanism mediating tigecycline protection in *A. baumannii*. The hypothesis of an alternative resistance pathway was further supported by the successful *in vitro* development of tigecycline resistance in ATCC-17978$_{\Delta adeR}$.

Whole-genome sequencing of artificially *in vitro*-evolved tigecycline-resistant strains identified the *trm* gene, coding for a methyltransferase, as the only gene that was disrupted in both independently evolved strains (see Table S3 in the supplemental material). Chen and colleagues recently developed artificial tigecycline resistance in *A. baumannii* ATCC-19606 and also found a mutated *trm* gene, suggesting an important role of this methyltransferase in conferring moderate tigecycline resistance (40). Methyltransferases are able to catalyze the methylation of ribosomal RNAs (rRNAs). The conformational modification of the rRNAs, which are the molecular targets of tigecycline, may result in an alteration of the antibiotic target interaction, suggesting that *trm* disruption could be a valid tigecycline resistance mechanism (41). We also sequenced the *trm* gene of our XDR strain panel and found in 9 out of 10 clinical isolates a disrupted *trm* gene (Table 2). Interestingly, the isolate that harbors a wild-type *trm* (BV26) was isolated in 1979, almost 25 years before tigecycline was approved by the FDA. Our finding suggests that in contrast to AdeABC efflux pump overexpression, which can be selected under pressure of different antibiotic classes, *trm* disruption may be a specific result of tigecycline selection pressure in clinical settings. We demonstrated that the disruption of *trm* plays only a moderate role in tigecycline resistance in clinical isolates, suggesting that loss of Trm may not be the only trigger for an alternative AdeABC-independent tigecycline resistance pathway.

Besides *trm*, we found other genes that were mutated in one of the two independently evolved strains (see Table S3 in the supplemental material) and that were previously linked to tigecycline resistance in *A. baumannii*, such as *rpsJ* (S10) or *adeN* (42–45). However, to our knowledge the identified mutations in the RNase E 23S rRNA pseudouridylate synthase and in the promoter of the MATE family efflux pump AbeM (see Table S3) were never linked to tigecycline resistance, and further studies are required to verify their impact on tigecycline resistance.

Since the development of our gene knockout platform enables efficient and quick genetic manipulation of *A. baumannii* clinical isolates regardless of their resistance profiles, this technology is a powerful tool to investigate the molecular nature of different pathways that allow *A. baumannii* to escape antibiotic-mediated killing. By using AdeR as an example, our study revealed the genetic variability of different tigecycline-resistant isolates, which may be a cause of the different selection pressures applied during patient treatment in clinical units, clearly demonstrating that the study of one model strain is not sufficient to obtain a global picture of species-related pathogenesis and antibacterial resistance.

ACKNOWLEDGMENT

We acknowledge funding for V.T. from the Marie Curie Initial Training Network ITN-2013-607694-Translocation.

FUNDING INFORMATION

This work, including the efforts of Vincent Trebosc, was funded by Marie Curie Initial Training Network (ITN-2013-607694-Translocation).

REFERENCES

1. **Pendleton JN, Gorman SP, Gilmore BF.** 2013. Clinical relevance of the ESKAPE pathogens. Expert Rev Anti Infect Ther **11**:297–308. http://dx.doi.org/10.1586/eri.13.12.
2. **Dijkshoorn L, Nemec A, Seifert H.** 2007. An increasing threat in hospi-

tals: multidrug-resistant *Acinetobacter baumannii*. Nat Rev Microbiol **5:**939–951. http://dx.doi.org/10.1038/nrmicro1789.
3. **Peleg AY, Seifert H, Paterson DL.** 2008. *Acinetobacter baumannii*: emergence of a successful pathogen. Clin Microbiol Rev **21:**538–582. http://dx.doi.org/10.1128/CMR.00058-07.
4. **Visca P, Seifert H, Towner KJ.** 2011. Acinetobacter infection—an emerging threat to human health. IUBMB Life **63:**1048–1054. http://dx.doi.org/10.1002/iub.534.
5. **Paterson DL, Harris PNA.** 2015. Editorial commentary: the new *Acinetobacter* equation: hypervirulence plus antibiotic resistance equals big trouble. Clin Infect Dis **61:**155–156. http://dx.doi.org/10.1093/cid/civ227.
6. **Blair JM, Webber MA, Baylay AJ, Ogbolu DO, Piddock LJ.** 2015. Molecular mechanisms of antibiotic resistance. Nat Rev Microbiol **13:**42–51. http://dx.doi.org/10.1038/nrmicro3380.
7. **Andersson DI, Hughes D.** 2010. Antibiotic resistance and its cost: is it possible to reverse resistance? Nat Rev Microbiol **8:**260–271. http://dx.doi.org/10.1038/nrmicro2319.
8. **Depardieu F, Podglajen I, Leclercq R, Collatz E, Courvalin P.** 2007. Modes and modulations of antibiotic resistance gene expression. Clin Microbiol Rev **20:**79–114. http://dx.doi.org/10.1128/CMR.00015-06.
9. **Pieren M, Tigges M.** 2012. Adjuvant strategies for potentiation of antibiotics to overcome antimicrobial resistance. Curr Opin Pharmacol **12:**551–555. http://dx.doi.org/10.1016/j.coph.2012.07.005.
10. **Worthington RJ, Blackledge MS, Melander C.** 2013. Small-molecule inhibition of bacterial two-component systems to combat antibiotic resistance and virulence. Future Med Chem **5:**1265–1284. http://dx.doi.org/10.4155/fmc.13.58.
11. **Tucker AT, Nowicki EM, Boll JM, Knauf GA, Burdis NC, Trent MS, Davies BW.** 2014. Defining gene-phenotype relationships in *Acinetobacter baumannii* through one-step chromosomal gene inactivation. mBio **5:**e01313-14. http://dx.doi.org/10.1128/mBio.01313-14.
12. **Diancourt L, Passet V, Nemec A, Dijkshoorn L, Brisse S.** 2010. The population structure of *Acinetobacter baumannii*: expanding multiresistant clones from an ancestral susceptible genetic pool. PLoS One **5:**e10034. http://dx.doi.org/10.1371/journal.pone.0010034.
13. **Zarrilli R, Pournaras S, Giannouli M, Tsakris A.** 2013. Global evolution of multidrug-resistant *Acinetobacter baumannii* clonal lineages. Int J Antimicrob Agents **41:**11–19. http://dx.doi.org/10.1016/j.ijantimicag.2012.09.008.
14. **Peleg AY, Hooper DC.** 2010. Hospital-acquired infections due to Gram-negative bacteria. N Engl J Med **362:**1804–1813. http://dx.doi.org/10.1056/NEJMra0904124.
15. **Clinical and Laboratory Standards Institute.** 2012. Methods for dilution antimicrobial susceptibility tests for bacteria that grow aerobically. Approved standard, 9th ed. CLSI document M07-A9. Clinical and Laboratory Standards Institute, Wayne, PA.
16. **Silva-Rocha R, Martínez-García E, Calles B, Chavarría M, Arce-Rodríguez A, de las Heras A, Páez-Espino AD, Durante-Rodríguez G, Kim J, Nikel PI, Platero R, de Lorenzo V.** 2013. The Standard European Vector Architecture (SEVA): a coherent platform for the analysis and deployment of complex prokaryotic phenotypes. Nucleic Acids Res **41:**D666–D675. http://dx.doi.org/10.1093/nar/gks1119.
17. **Amin IM, Richmond GE, Sen P, Koh TH, Piddock LJ, Chua KL.** 2013. A method for generating marker-less gene deletions in multidrug-resistant *Acinetobacter baumannii*. BMC Microbiol **13:**158. http://dx.doi.org/10.1186/1471-2180-13-158.
18. **Ferrières L, Hémery G, Nham T, Guérout A-M, Mazel D, Beloin C, Ghigo J-M.** 2010. Silent mischief: bacteriophage Mu insertions contaminate products of *Escherichia coli* random mutagenesis performed using suicidal transposon delivery plasmids mobilized by broad-host-range RP4 conjugative machinery. J Bacteriol **192:**6418–6427. http://dx.doi.org/10.1128/JB.00621-10.
19. **Langmead B, Salzberg SL.** 2012. Fast gapped-read alignment with Bowtie 2. Nat Methods **9:**357–359. http://dx.doi.org/10.1038/nmeth.1923.
20. **Li H, Handsaker B, Wysoker A, Fennell T, Ruan J, Homer N, Marth G, Abecasis G, Durbin R, 1000 Genome Project Data Processing Subgroup.** 2009. The Sequence Alignment/Map format and SAMtools. Bioinformatics **25:**2078–2079. http://dx.doi.org/10.1093/bioinformatics/btp352.
21. **Luo R, Liu B, Xie Y, Li Z, Huang W, Yuan J, He G, Chen Y, Pan Q, Liu Y, Tang J, Wu G, Zhang H, Shi Y, Liu Y, Yu C, Wang B, Lu Y, Han C, Cheung DW, Yiu S-M, Peng S, Xiaoqian Z, Liu G, Liao X, Li Y, Yang H, Wang J, Lam T-W, Wang J.** 2012. SOAPdenovo2: an empirically improved memory-efficient short-read de novo assembler. GigaScience **1:**18. http://dx.doi.org/10.1186/2047-217X-1-18.
22. **Siguier P, Perochon J, Lestrade L, Mahillon J, Chandler M.** 2006. ISfinder: the reference centre for bacterial insertion sequences. Nucleic Acids Res **34:**D32–D36. http://dx.doi.org/10.1093/nar/gkj014.
23. **Nowak J, Seifert H, Higgins P.** 2013. The tellurite-resistance determinant Tpm of the *Acinetobacter baylyi* strain ADP1 as a useful non-antibiotic selection marker for genetic manipulation in *Acinetobacter baumannii*, abstr p1356. Abstr 23rd Eur Soc Clin Microbiol Infect Dis Conf, Berlin, Germany, 27 to 30 April 2013.
24. **Prigent-Combaret C, Sanguin H, Champier L, Bertrand C, Monnez C, Colinon C, Blaha D, Ghigo J-M, Cournoyer B.** 2012. The bacterial thiopurine methyltransferase tellurite resistance process is highly dependent upon aggregation properties and oxidative stress response. Environ Microbiol **14:**2645–2660. http://dx.doi.org/10.1111/j.1462-2920.2012.02802.x.
25. **Wang H, Bian X, Xia L, Ding X, Müller R, Zhang Y, Fu J, Stewart AF.** 2014. Improved seamless mutagenesis by recombineering using *ccdB* for counterselection. Nucleic Acids Res **42:**e37. http://dx.doi.org/10.1093/nar/gkt1339.
26. **Holzer GW, Mayrhofer J, Gritschenberger W, Falkner FG.** 2005. Dominant negative selection of vaccinia virus using a thymidine kinase/thymidylate kinase fusion gene and the prodrug azidothymidine. Virology **337:**235–241. http://dx.doi.org/10.1016/j.virol.2005.04.009.
27. **Hornsey M, Ellington MJ, Doumith M, Thomas CP, Gordon NC, Wareham DW, Quinn J, Lolans K, Livermore DM, Woodford N.** 2010. AdeABC-mediated efflux and tigecycline MICs for epidemic clones of *Acinetobacter baumannii*. J Antimicrob Chemother **65:**1589–1593. http://dx.doi.org/10.1093/jac/dkq218.
28. **Ruzin A, Keeney D, Bradford PA.** 2007. AdeABC multidrug efflux pump is associated with decreased susceptibility to tigecycline in *Acinetobacter calcoaceticus-Acinetobacter baumannii* complex. J Antimicrob Chemother **59:**1001–1004. http://dx.doi.org/10.1093/jac/dkm058.
29. **Sun J-R, Chan M-C, Chang T-Y, Wang W-Y, Chiueh T-S.** 2010. Overexpression of the *adeB* gene in clinical isolates of tigecycline-nonsusceptible *Acinetobacter baumannii* without insertion mutations in *adeRS*. Antimicrob Agents Chemother **54:**4934–4938. http://dx.doi.org/10.1128/AAC.00414-10.
30. **Peleg AY, Adams J, Paterson DL.** 2007. Tigecycline efflux as a mechanism for nonsusceptibility in *Acinetobacter baumannii*. Antimicrob Agents Chemother **51:**2065–2069. http://dx.doi.org/10.1128/AAC.01198-06.
31. **Marchand I, Damier-Piolle L, Courvalin P, Lambert T.** 2004. Expression of the RND-type efflux pump AdeABC in *Acinetobacter baumannii* is regulated by the AdeRS two-component system. Antimicrob Agents Chemother **48:**3298–3304. http://dx.doi.org/10.1128/AAC.48.9.3298-3304.2004.
32. **Magiorakos A-P, Srinivasan A, Carey RB, Carmeli Y, Falagas ME, Giske CG, Harbarth S, Hindler JF, Kahlmeter G, Olsson-Liljequist B, Paterson DL, Rice LB, Stelling J, Struelens MJ, Vatopoulos A, Weber JT, Monnet DL.** 2012. Multidrug-resistant, extensively drug-resistant and pandrug-resistant bacteria: an international expert proposal for interim standard definitions for acquired resistance. Clin Microbiol Infect **18:**268–281. http://dx.doi.org/10.1111/j.1469-0691.2011.03570.x.
33. **Garnacho-Montero J, Dimopoulos G, Poulakou G, Akova M, Cisneros JM, De Waele J, Petrosillo N, Seifert H, Timsit JF, Vila J, Zahar J-R, Bassetti M.** 2015. Task force on management and prevention of *Acinetobacter baumannii* infections in the ICU. Intensive Care Med **41:**2057–2075. http://dx.doi.org/10.1007/s00134-015-4079-4.
34. **Lin M-F, Lin Y-Y, Yeh H-W, Lan C-Y.** 2014. Role of the BaeSR two-component system in the regulation of *Acinetobacter baumannii adeAB* genes and its correlation with tigecycline susceptibility. BMC Microbiol **14:**119. http://dx.doi.org/10.1186/1471-2180-14-119.
35. **Yoon E-J, Courvalin P, Grillot-Courvalin C.** 2013. RND-type efflux pumps in multidrug-resistant clinical isolates of *Acinetobacter baumannii*: major role for AdeABC overexpression and AdeRS mutations. Antimicrob Agents Chemother **57:**2989–2995. http://dx.doi.org/10.1128/AAC.02556-12.
36. **Higgins PG, Schneiders T, Hamprecht A, Seifert H.** 2010. In vivo selection of a missense mutation in *adeR* and conversion of the novel $bla_{OXA-164}$ gene into bla_{OXA-58} in carbapenem-resistant *Acinetobacter baumannii* isolates from a hospitalized patient. Antimicrob Agents Chemother **54:**5021–5027. http://dx.doi.org/10.1128/AAC.00598-10.
37. **Brink AJ, Bizos D, Boffard KD, Feldman C, Grolman DC, Pretorius J,**

Richards GA, Senekal M, Steyn E, Welkovic N, Association of Surgeons of South Africa, Critical Care Society of Southern Africa, Federation of Infectious Diseases Societies of Southern Africa, South African Thoracic Society, Trauma Society of South Africa. 2010. Guideline: appropriate use of tigecycline. S Afr Med J **100:**388–394. http://dx.doi.org/10.7196/SAMJ.4109.

38. **Rumbo C, Gato E, López M, Ruiz de Alegría C, Fernández-Cuenca F, Martínez-Martínez L, Vila J, Pachón J, Cisneros JM, Rodríguez-Baño J, Pascual A, Bou G, Tomás M, Spanish Group of Nosocomial Infections and Mechanisms of Action and Resistance to Antimicrobials (GEIH-GEMARA), Spanish Society of Clinical Microbiology and Infectious Diseases (SEIMC), Spanish Network for Research in Infectious Diseases (REIPI).** 2013. Contribution of efflux pumps, porins, and β-lactamases to multidrug resistance in clinical isolates of *Acinetobacter baumannii*. Antimicrob Agents Chemother **57:**5247–5257. http://dx.doi.org/10.1128/AAC.00730-13.
39. **Coyne S, Courvalin P, Périchon B.** 2011. Efflux-mediated antibiotic resistance in *Acinetobacter* spp. Antimicrob Agents Chemother **55:**947–953. http://dx.doi.org/10.1128/AAC.01388-10.
40. **Chen Q, Li X, Zhou H, Jiang Y, Chen Y, Hua X, Yu Y.** 2014. Decreased susceptibility to tigecycline in *Acinetobacter baumannii* mediated by a mutation in *trm* encoding SAM-dependent methyltransferase. J Antimicrob Chemother **69:**72–76. http://dx.doi.org/10.1093/jac/dkt319.
41. **Morić I, Savić M, Ilić-Tomić T, Vojnović S, Bajkić S, Vasiljević B.** 2010. rRNA methyltransferases and their role in resistance to antibiotics. J Med Biochem **29:**165–174.
42. **Beabout K, Hammerstrom TG, Perez AM, Magalhães B, de Prater FAG, Clements TP, Arias CA, Saxer G, Shamoo Y.** 2015. The ribosomal S10 protein is a general target for decreased tigecycline susceptibility. Antimicrob Agents Chemother **59:**5561–5566. http://dx.doi.org/10.1128/AAC.00547-15.
43. **Rosenfeld N, Bouchier C, Courvalin P, Périchon B.** 2012. Expression of the resistance-nodulation-cell division pump AdeIJK in Acinetobacter baumannii is regulated by AdeN, a TetR-type regulator. Antimicrob Agents Chemother **56:**2504–2510. http://dx.doi.org/10.1128/AAC.06422-11.
44. **Damier-Piolle L, Magnet S, Brémont S, Lambert T, Courvalin P.** 2008. AdeIJK, a resistance-nodulation-cell division pump effluxing multiple antibiotics in *Acinetobacter baumannii*. Antimicrob Agents Chemother **52:**557–562. http://dx.doi.org/10.1128/AAC.00732-07.
45. **Yoon E-J, Chabane YN, Goussard S, Snesrud E, Courvalin P, Dé E, Grillot-Courvalin C.** 2015. Contribution of resistance-nodulation-cell division efflux systems to antibiotic resistance and biofilm formation in *Acinetobacter baumannii*. mBio **6:**e00309-15. http://dx.doi.org/10.1128/mBio.00309-15.
46. **Clinical and Laboratory Standards Institute.** 2014. Performance standards for antimicrobial susceptibility testing; 24th informational supplement. CLSI document M100-S24. Clinical and Laboratory Standards Institute, Wayne, PA.

Supplementary information for:

A novel genome editing platform for drug resistant *Acinetobacter baumannii* revealed an AdeR-unrelated tigecycline resistance mechanism

Vincent Trebosc[1,2], Sarah Gartenmann[1], Kevin Royet[1], Pablo Manfredi[2], Marcus Tötzl[1], Birgit Schellhorn[1], Michel Pieren[1], Marcel Tigges[1], Sergio Lociuro[1], Peter C. Sennhenn[1], Marc Gitzinger[1], Dirk Bumann[2], and Christian Kemmer[1#]

[1] BioVersys AG, Basel, Switzerland
[2] Biozentrum, University of Basel, Basel, Switzerland

Running title: Genome editing platform for drug resistant *A. baumannii*

[#] Corresponding author: Christian Kemmer christian.kemmer@bioversys.com

Keywords: multidrug resistance, knockout, knockin, efflux pumps, *adeABC*, *trm*.

Table of content:

Figure S1: Development of artificial tigecycline resistance in A. baumannii using serial passages. *Strain ATCC-17978 and its ΔadeR mutant were grown for 12 days in medium containing indicated tigecycline concentrations. The cells were passaged every 48h into fresh medium containing a duplication in the tigecycline concentration. The artificially evolved tigecycline resistant strains derived from strain A. baumannii ATCC-17978 and its ΔadeR mutant were designated ATCC-17978(TGC) and ATCC-17978$_{\Delta adeR}$(TGC), respectively. The figure was produced, in part, by using Servier Medical Art.*

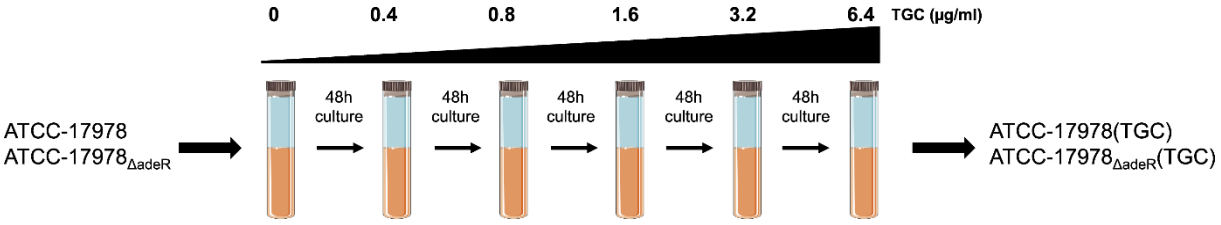

Table S1: Oligonuclotides used in this study.

Oligo name	Sequence (5'-3')
oVT01	GGCGCGCCCTGTCAGACCAAGTTTACTC
oVT02	GGCCGGCCTATCAGCTCACTCAAAGG
oVT05	ACTGACTTTAGCCGGTGGTG
oVT08	GTTTTCCCAGTCACGACGC
oVT93	GCAGCTTGTAGGCGTTCATAC
oVT94	AACTTGCTCAATACGACGGC
oVT106	TTTTAATATTATCCCGGGAGAAAATCTGGCTATAGAAAGTG
oVT107	GCCAGATTTTCTCCCGGGATAATATTAAAAAATAGCTAGGGAATATTTTATG
oVT113	CCGCTCGAGCCTAGGGAATTCAAAGAGGAGAAAATGGCACAGCTATATTTCTACTATTCCGC
oVT114	AACTGCAGAAGCTTGGCGCGCCAACCCCTTGGGGCCTCTAAACGGGTCTTGAGGGGTTTTTTG TTAATCGTGGCGATGCCTTTC
oVT134	TTTTTGCGGCCATTGGTGAG
oVT141	CATTTTCTCCTCTTTGTATTCGCGCGGCCGCG
oVT142	CGCGGCCGCGCGAATACAAAGAGGAGAAAATG
oVT149	AATTGAGGCCTCTCGAGGAATTCGAGCTCGGTA*CCCGGG*GATCCTCTAGAGCCTGCAGGAAGC TTCG
oVT150	GGCCCGAAGCTTCCTGCAGGCTCTAGAGGATC*CCCGGG*TACCGAGCTCGAATTCCTCGAGAGG CCTC
oVT151	AAAAGAGAGTGAGGGGGCAC
oVT154	GGAGAATTGAGGCCTCTCGAGTGCACCTTCAGTGACAAAAG
oVT155	AGCTTCCTGCAGGCTCTAGATTTAAGAACTTTTTCAACTACCG
oVT160	ACTGCCATAACCACACCAGC
oVT161	CCCATTCATCTTCGGGCTCA
oVT312	AAGGAGAGTTGACACAGCTG
oVT412	AGAATTGAGGCCTCTCGAGGAATTCGCACCTGCACCTAAAAGC
oVT413	CTGGTCTTGCCCGGGGGAGAAAACCGACACTGATATAC
oVT414	GGTTTTCTCCCCCGGGCAAGACCAGTTGCCGATC
oVT415	CCGCAAGCTTCCTGCAGGCTCTAGACGCTGTGCCCGTTATAATG
oVT416	GAGGAATTCGAGCTCGGTACCTTACAAAAACGGCAAGCC
oVT417	CCGCAAGCTTCCTGCAGGCTCTAGAAGCAATCATCACGTCCAG
oVT423	GGCTACTACAGGAGCAGCAG
oVT424	CTACTTTGATGGCGGCGTTG
adeB-qRT-F	GGATTATGGCGACAGAAGGA
adeB-qRT-R	AATACTGCCGCCAATACCAG
rpoD-qRT-F	GAGTCTAATGGCGGTGGTTC
rpoD-qRT-R	ATTGCTTCATCTGCTGGTTG

Table S2: Antibiotic resistance profile of the in vitro evolved tigecycline resistant strains and their parental strains.

MIC (µg/ml)	Tigecycline	Tetracycline	Meropenem	Ciprofloxacin	Gentamycin
ATCC-17978	0.4	2	0.5	0.5	2
ATCC-17978(TGC)	25	32	0.5	2	0.5
ATCC-17978$_{\Delta adeR}$	0.4	2	0.25	0.25	1
ATCC-17978$_{\Delta adeR}$(TGC)	6.3	64	0.5	4	0.5

Table S3: Important mutations identified by whole genome sequencing of in vitro evolved tigecycline resistant strains.

Mutated gene or region	Mutations		Protein function	References
	ATCC-17978(TGC)	ATCC-17978$_{\Delta adeR}$(TGC)		
trm (A1S_2858)	IS-17 like transposon inserted in the coding sequence	Adenine in position 311 of *trm* deleted leading to early stop codon	Methyltransferase potentially involved in rRNAs methylation	(1)
RNase E (A1S_0403)	58 bp deletion in the coding sequence	-	Ribonuclease involved in rRNAs processing and RNA decay	(2)
Intergenic region between *RNase E* (A1S_0403) and *23S rRNA pseudouridylate synthase* (A1S_0404)	IS*Aba11* element inserted at position 439,336 in the intergenic region	-	RNase E see above. 23S rRNA pseudouridylate synthase involved in modification of 23S rRNA	(3)
adeN (A1S_1979)	-	IS*Aba11* transposon inserted in the coding sequence	Transcriptional repressor of the *adeIJK* efflux pump	(4)
abeM (A1S_0395)	-	Cytosine to thymidine mutation (position 429,259) in the promoter region of *abeM*	MATE family efflux pump	(5)
rpsJ (A1S_3081)	-	S12F substitution in the coding sequence	30S ribosomal protein S10 part of tigecycline binding site in the ribosome	(6, 7)

Table S4: Tigecycline resistance profile of the trm knockout and trm restored strains.

	***trm* knockout**		***trm* wildtype recovery**					
	ATCC-17978		**BV185**		**BV186**		**BV191**	
Tigecycline MIC (µg/ml)	**WT**	**Δ*trm***	**WT**	***trm*+**	**WT**	***trm*+**	**WT**	***trm*+**
	0.4	0.8	3.1	1.6	3.1	1.6	12.5	6.3

References:

1. **Morić I**, **Savić M**, **Ilić-Tomić T**, **Vojnović S**, **Bajkić S**, **Vasiljević B**. 2010. rRNA Methyltransferases and their Role in Resistance to Antibiotics. J Med Biochem **29**:165–174.

2. **Mackie GA**. 2013. RNase E: at the interface of bacterial RNA processing and decay. Nat Rev Microbiol **11**:45–57.

3. **Gutgsell NS**, **Deutscher MP**, **Ofengand J**. 2005. The pseudouridine synthase RluD is required for normal ribosome assembly and function in Escherichia coli. RNA N Y N **11**:1141–1152.

4. **Rosenfeld N**, **Bouchier C**, **Courvalin P**, **Périchon B**. 2012. Expression of the resistance-nodulation-cell division pump AdeIJK in Acinetobacter baumannii is regulated by AdeN, a TetR-type regulator. Antimicrob Agents Chemother **56**:2504–2510.

5. **Su X-Z**, **Chen J**, **Mizushima T**, **Kuroda T**, **Tsuchiya T**. 2005. AbeM, an H+-coupled Acinetobacter baumannii multidrug efflux pump belonging to the MATE family of transporters. Antimicrob Agents Chemother **49**:4362–4364.

6. **Schedlbauer A**, **Kaminishi T**, **Ochoa-Lizarralde B**, **Dhimole N**, **Zhou S**, **López-Alonso JP**, **Connell SR**, **Fucini P**. 2015. Structural characterization of an alternative mode of tigecycline binding to the bacterial ribosome. Antimicrob Agents Chemother **59**:2849–2854.

7. **Beabout K**, **Hammerstrom TG**, **Perez AM**, **Magalhães B de F**, **Prater AG**, **Clements TP**, **Arias CA**, **Saxer G**, **Shamoo Y**. 2015. The ribosomal S10 protein is a general target for decreased tigecycline susceptibility. Antimicrob Agents Chemother.

3.1.2. Dissecting colistin resistance mechanisms in extensively drug resistant *Acinetobacter baumannii* clinical isolates

Vincent Trebosc[1,2], Sarah Gartenmann[1], Marcus Tötzl[1], Valentina Lucchini[1,2], Birgit Schellhorn[1], Michel Pieren[1], Sergio Lociuro[1], Marc Gitzinger[1], Marcel Tigges[1], Dirk Bumann[2], and Christian Kemmer[1]

[1] BioVersys AG, Basel, Switzerland
[2] Biozentrum, University of Basel, Basel, Switzerland

Status of the paper: manuscript in preparation

3.1.2.1. Abstract of the paper

Nosocomial infections with *Acinetobacter baumannii* are a global problem in intensive care units causing severe infections with high mortality rates. The rapid emergence of strains resistant to the first and second line antibiotics have forced the use of colistin as last resort treatment. However, increasing development of colistin resistance in *A. baumannii* has been reported and strategies to recover colistin efficacy are needed. In this study, we evaluated the transcriptional regulator PmrA as potential drug target to restore colistin efficacy in *A. baumannii*. Deletion of *pmrA* in a panel of extensively drug resistant *A. baumannii* clinical isolates reduced the MIC80 of colistin from 32 μg/mL in the parental strains to 1 μg/mL in the Δ*pmrA* strains, indicating its importance in the drug resistance phenotype. However, 17% of the clinical isolates remained highly resistant to colistin, indicating that PmrA-mediated overexpression of the phosphoethanolamine (PetN) transferase PmrC is not the exclusive colistin resistance mechanism in *A. baumannii*. A detailed genetic characterization revealed that colistin resistance in 2 clinical isolates was mediated by genetic integration of the transposon IS*AbaI* upstream of the PmrC homolog EptA leading to its overexpression. We found that *eptA* was ubiquitously present in clinical strains belonging to the international clone 2, but absent in the international clone 1, and that IS*AbaI* integration upstream of *eptA* was required to mediate the colistin resistant phenotype. To our surprise, we found three distinct genome-encoded *eptA* isoforms in one clinical isolate. Our data highlight the importance of PetN-transferase mediated colistin resistance in clinical strains and disprove PmrA as a direct drug target for adjuvant therapies. However, we suggest that direct targeting of the highly homologous PetN-transferases PmrC/EptA with small molecule inhibitors may have the potential to overcome colistin resistance in *A. baumannii*.

3.1.2.2. Statement of my work

- Design of all experiments
- Construction of gene deletion *A. baumannii* mutants
- Determination of MIC
- qRT-PCR experiments and data analysis
- Genotyping of *pmrA*, *pmrB* and the various *eptA* isoforms
- Writing of the manuscript

3.1.2.3. Draft paper

Dissecting colistin resistance mechanisms in extensively drug resistant *Acinetobacter baumannii* clinical isolates.

Short tittle: *A. baumannii* colistin resistance mechanisms.

Vincent Trebosc[1,2], Sarah Gartenmann[1], Marcus Tötzl[1], Valentina Lucchini[1,2], Birgit Schellhorn[1], Michel Pieren[1], Sergio Lociuro[1], Marc Gitzinger[1], Marcel Tigges[1], Dirk Bumann[2], and Christian Kemmer[1]*

[1] BioVersys AG, Basel, Switzerland
[2] Biozentrum, University of Basel, Basel, Switzerland

* Corresponding author

E-mail: christian.kemmer@bioversys.com (CK)

Abstract

Nosocomial infections with *Acinetobacter baumannii* are a global problem in intensive care units causing severe infections with high mortality rates. The rapid emergence of strains resistant to the first and second line antibiotics have forced the use of colistin as last resort treatment. However, increasing development of colistin resistance in *A. baumannii* has been reported and strategies to recover colistin efficacy are needed. In this study, we evaluated the transcriptional regulator PmrA as potential drug target to restore colistin efficacy in *A. baumannii*. Deletion of *pmrA* in a panel of extensively drug resistant *A. baumannii* clinical isolates reduced the MIC_{80} of colistin from 32 μg/mL in the parental strains to 1 μg/mL in the Δ*pmrA* strains, indicating its importance in the drug resistance phenotype. However, 17% of the clinical isolates remained highly resistant to colistin, indicating that PmrA-mediated overexpression of the phosphoethanolamine (PetN) transferase PmrC is not the exclusive colistin resistance mechanism in *A. baumannii*. A detailed genetic characterization revealed that colistin resistance in 2 clinical isolates was mediated by genetic integration of the transposon IS*AbaI* upstream of the PmrC homolog EptA leading to its overexpression. We found that *eptA* was ubiquitously present in clinical strains belonging to the international clone 2, but absent in the international clone 1, and that IS*AbaI* integration upstream of *eptA* was required to mediate the colistin resistant phenotype. To our surprise, we found three distinct genome-encoded *eptA* isoforms in one clinical isolate. Our data highlight the importance of PetN-transferase mediated colistin resistance in clinical strains and disprove PmrA as a direct drug target for adjuvant therapies. However, we suggest that direct targeting of the highly homologous PetN-transferases PmrC/EptA with small molecule inhibitors may have the potential to overcome colistin resistance in *A. baumannii*.

Author summary

Antibiotic resistance is a major and global threat for our health care system. The discovery of antibiotics revolutionized modern medicine and enabled to cure previously deadly bacterial infectious diseases. The risk to re-enter a pre-antibiotic era has been mentioned due to the emergence of the so-called “superbugs” that do not respond to most of antibiotics available. Colistin represents one of our last resort antibiotic that is still active against most of bacterial

pathogens. However, colistin resistance is increasingly reported worldwide, in particular due to the protein MCR-1 present in superbugs, such as *E. coli* and *K. pneumonieae*. In this study, we showed that colistin resistance in *A. baumannii*, a top priority superbug causing deadly nosocomial infections, is mediated through different avenues that all lead to the same end, which resides in the activity of a specific enzyme called PetN transferase. Considering that MCR-1 is also a PetN transferase, our findings indicate that PetN transferases might be the Achilles' heel of superbugs to restore colistin efficacy and like this preserve our most potent weapon against bacterial infections.

Introduction

Antimicrobial resistance is a serious threat to global health systems resulting in the loss of treatment options to fight a growing number of bacterial infections (1). Considering the paucity of newly developed antibiotics in the last decade, old antibiotics such as polymyxins have been re-introduced to treat infections caused by multidrug resistant (MDR) Gram-negative pathogens (2–4). Nowadays, the polymyxin antibiotics polymyxin E (colistin) and polymyxin B represent the last resort for the treatment of MDR Gram-negative infections, such as infections caused by carbapenem resistant *Enterobacterieaceae*, MDR *Pseudomonas aeruginosa* and MDR *Acinetobacter baumannii* (5,6). Unfortunately, the increasing use of polymyxins to treat serious infections caused by MDR pathogens leads to a spread of resistance to these last line drugs (7). There is a high unmet medical need for new drugs effective against Gram-negative bacteria to treat infections caused by these pathogens and to reserve colistin to fight MDR pathogens (8). Besides this, an alternative strategy resides in the recovery of colistin efficacy by blocking bacterial colistin resistance mechanisms. Antibiotic adjuvants therapies consist in the combination of a potent antibiotic with a non-antibiotic agent interfering with specific antibiotic resistance or virulence mechanisms. This strategy may provide a new tool to fight infections caused by drug resistant pathogens by restoring or boosting the efficacy of an approved antibiotic (9).

Colistin resistance is conferred by lipopolysaccharide (LPS) modifications at the outer cell envelope. Reduction of the negative charge on LPS results in a reduced affinity of colistin to LPS (10). The two main LPS modifications conferring colistin resistance are the addition of 4-amino-4-deoxy-L-arabinose (AraN) and phosphoethanolamine (PetN) to the lipid A (11). The expression of LPS modifying enzymes is regulated by the concerted action of several two-component systems (TCSs). In *Enterobacteriaceae* PhoPQ and PmrAB TCSs regulate the expression of colistin resistance mechanisms, whereas in *P. aeruginosa* the PhoPQ, PmrAB, ParRS, ColRS and CprRS TCSs seem to be involved (11). Plasmid mediated colistin resistance has been recently reported in *Enterobacteriaceae* due to the PetN transferase MCR-1. The presence of MCR-1 on a plasmid leads to its rapid geographical and interspecies spread (12,13). In *A. baumannii,* colistin resistance is mediated by PetN addition to the lipid A and this resistance mechanism is regulated by the PmrAB TCS. In contrast to other pathogens, AraN lipid A modification pathway is not present in *A. baumannii* (11), rendering *A. baumannii* a suitable pathogen to develop an adjuvant therapy approach to rejuvenate colistin efficacy by blocking the PmrAB TCS.

Colistin resistance in *A. baumannii* clinical isolates is associated with alterations in the *pmrCAB* operon. *pmrC* gene codes for a PetN transferase and *pmrA* and *pmrB* code for the TCS (14). It has been shown that mutations in the PmrAB TCS induce the overexpression of *pmrC* leading to the modification of lipid A with PetN and colistin resistance (14–18). Because PmrA is the transcriptional regulator that triggers PmrC overexpression, inhibition of PmrA with a small molecule may potentially block PmrC overexpression and therefore switch-off colistin resistance in *A. baumannii* (19). This study was designed to evaluate the relevance of PmrA as a drug target to restore colistin efficacy in *A. baumannii* clinical isolates. We demonstrate that in absence of PmrA-mediated expression of PmrC, transposition of an insertion sequence (IS) element can lead to overexpression of the alternative highly similar PetN transferase EptA that also confers colistin resistance. Our results show that in all studied clinical isolates overexpression of at least one PetN transferase (PmrC or various EptA variants) was responsible for colistin resistance indicating that PetN transferases may be a suitable drug target to overcome colistin resistance in *A. baumannii*.

Results

PmrA is not always essential for colistin resistance in *A. baumannii* clinical isolates.

We deleted *pmrA* from the genome of a panel of 12 colistin resistant *A. baumannii* strains to evaluate the transcriptional regulator PmrA as a potential drug target to rejuvenate colistin efficacy in *A. baumannii*. The strains in the panel consisted of recently isolated colistin resistant clinical strains collected at diverse geographical origins. They belong to three distinct and highly successful clonal lineages, the international clone 1 (ST1), international clone 2 (ST2) and ST25 clonal lineages (Table 1) (20–22). All strains were classified as extensively drug resistant according to criteria of Magiorakos and colleagues (23). These data underscore the clinical relevance and the diversity of the strain panel. The colistin susceptible *A. baumannii* ATCC-17978 strain was included as a reference strain. In all strains *pmrA* was deleted by applying a previously described method that allows efficient scarless genome engineering even in extensively resistant *A. baumannii* clinical isolates (24).

The colistin sensitivity of the parental clinical isolates and their corresponding *pmrA* knockout mutants (Δ*pmrA*) was determined by microdilution method. *pmrA* deletion reduced MICs 64- to 1024-fold in 10 out of 12 initially colistin resistant clinical isolates (83%) thus restoring susceptibility to colistin (MIC $\leq$ 2 μg/ml) (Table 2). To our surprise, however, two strains (BV94 and BV189) retained colistin resistance even in absence of *pmrA*.

We investigated the differences between strains that became susceptible after *pmrA* deletion and those that remained resistant by analysing the sequence variations of the PmrAB TCS in the strain panel. The PmrA and PmrB sequences of the *A. baumannii* AYE, ACICU and NIPH 146 strains were used as reference for ST1, ST2 and ST25 clonal lineages, respectively. Non-synonymous mutations were found only in the PmrB sensor kinase (Table 2). Interestingly, the two strains with an unaltered PmrB sequence were those that remained colistin resistant after *pmrA* deletion (BV94 and BV189). Our data suggest that colistin resistance in these two strains is not conferred by a PmrA-mediated PmrC overexpression. We confirmed this hypothesis by quantifying the expression of *pmrC* using quantitative reverse-transcription PCR (qRT-PCR) (Fig 1.A). The control strain ATCC-17978, and the two refractory strains BV94 and BV189

showed only marginal levels of *pmrC* expression. In contrast, the 10 other strains showed *pmrC* overexpression and this overexpression was abolished in the Δ*pmrA* mutant.

Table 1: Characterization of the *A. baumannii* clinical isolate panel used in this study.

Strain designation	Strain isolation		MLST	MICs (µg/ml)							
	location	date		GENT	MERO	CIP	TZP	CTX	SXT	SAM	TET
ATCC-17978	France	1951	77	2	0.5	1	8/4	16	> 8/152	4/2	2
BV94	USA	2011	2	> 128	32	256	> 256/4	> 256	> 8/152	16/8	32
BV95	Colombia	2010	25	1	64	128	256/4	32	> 8/152	16/8	> 256
BV172	Israel	2012	2	> 128	64	32	256/4	> 256	> 8/152	64/32	> 256
BV173	Greece	2012	2	> 128	> 64	128	> 256/4	> 256	> 8/152	128/64	> 256
BV174	USA	2012	2	8	64	256	256/4	256	> 8/152	32/16	32
BV175	Turkey	2012	2	128	32	256	> 256/4	256	> 8/152	32/16	256
BV185	Mexico	2013	2	> 128	> 64	128	> 256/4	> 256	> 8/152	64/32	256
BV186	USA	2013	2	16	64	256	> 256/4	> 256	> 8/152	32/16	8
BV187	USA	2013	2	32	64	256	> 256/4	> 256	> 8/152	16/8	8
BV189	Spain	2013	2	128	32	128	> 256/4	256	> 8/152	32/16	16
BV190	Greece	2012	1	> 128	64	64	> 256/4	> 256	> 8/152	64/32	256
BV191	China	2013	2	> 128	> 64	256	> 256/4	> 256	> 8/152	128/64	> 256
ATCC-25922 (Quality control)				1	< 0.06	< 0.25	4/4	< 0.25	0.125/2.34	4/2	2

Abbreviations: CIP: ciprofloxacin, CTX: cefotaxime, GENT: gentamycin, MERO: meropenem, MLST: Multilocus sequence type, SAM: ampicillin-sulbactam, SXT: trimethoprim-sulfamethoxazole, TET: tetracycline, TZP: piperacillin-tazobactam. Classification of antibiotic resistance was done according to breakpoints published by the Clinical and Laboratory Standards Institute: susceptible (green), Intermediate (yellow), resistant (red) (25).

Table 2: Effect of loss of PmrA on colistin susceptibility and PmrB mutations in the strain panel.

Strain designation	Colistin MIC (µg/ml) *		PmrB mutations (amino acid substitutions)
	wildtype	Δ*pmrA*	
ATCC-17978	0.25	0.25	reference
BV94	64	32	wildtype
BV95	32	0.5	L274W
BV172	256	1	Q43L and L267F
BV173	128	1	A138T and A226V
BV174	64	1	Q277R
BV175	256	0.5	L267W
BV185	256	0.25	P233S
BV186	16	0.25	Q277R
BV187	16	0.25	Q277R
BV189	64	64	wildtype
BV190	256	0.5	A138T and A226V
BV191	256	0.25	A138T and P233S

Red background indicates the strains that did not recover colistin susceptibility after *pmrA* deletion.
*susceptibility breakpoint ≤ 2 µg/ml.

Taken together, colistin resistance in *A. baumannii* is predominantly conferred by mutations in the PmrB TCS sensor kinase that lead to overexpression of PmrC, as shown in 10 out of 12 strains. However, some isolates (2 out of 12 strains in our panel) may use an alternative colistin resistance mechanism independent of PmrA mediated PmrC overexpression to resist the antibacterial activity of colistin.

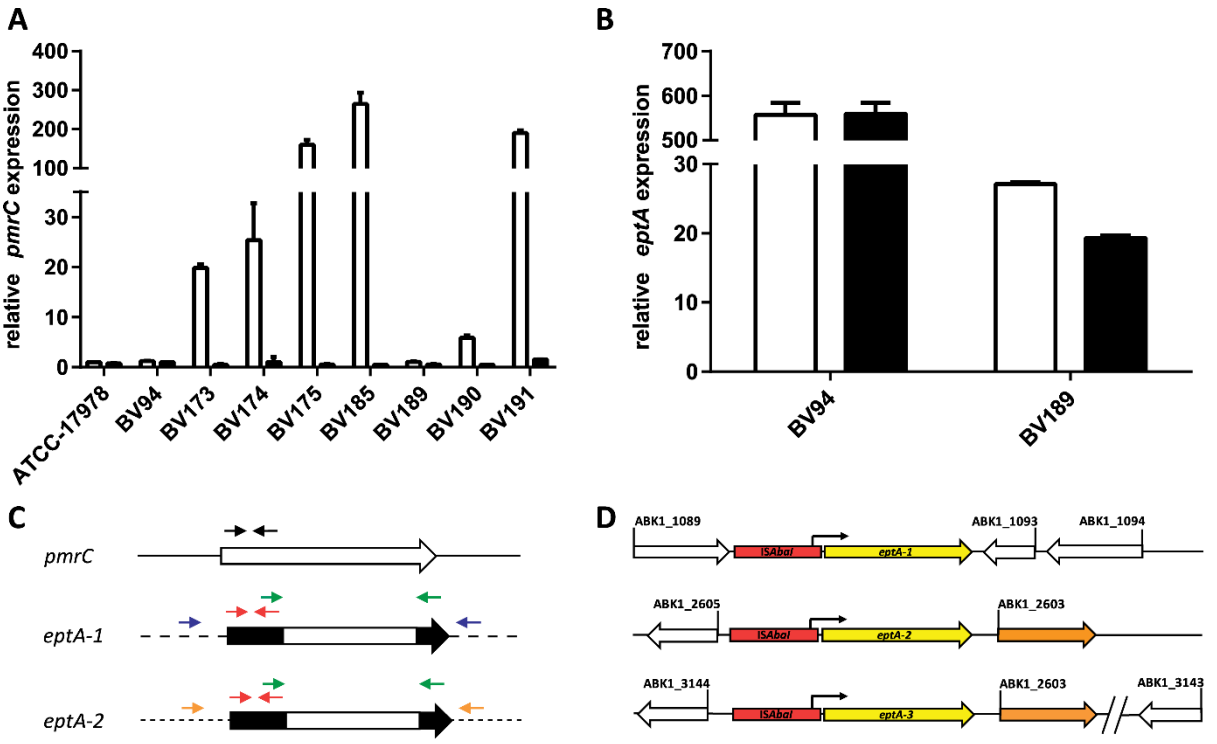

Fig 1: Discrimination and quantification of *pmrC* and *eptA*.
Expression levels of (A) *pmrC* and (B) *eptA* were quantified by qRT-PCR in colistin resistant *A. baumannii* isolates (white bars) and their Δ*pmrA* mutants (black bars). The expression levels were normalized to the *pmrC* expression in the ATCC-17978 reference strain. (C) Schematic representation of differences in the *pmrC*, *eptA-1* and *eptA-2* coding sequence. Black (oVT162/oVT163) and red primers (oVT164/oVT165) were used to detect *pmrC* and *eptA* in qRT-PCR experiments, respectively. The green primers (oVT152/oVT153) were used to genotype the *eptA* isoforms. Blue (oVT198/oVT199) and orange primers (oVT201/oVT202) were used to discriminate *eptA-1* and *eptA-2*, respectively. (D) Representation of IS*AbaI-eptA-1*, IS*AbaI-eptA-2* and the probably duplicated IS*AbaI-eptA-3* genomic sequence of clinical isolate BV94. The junction between ABK1_3144 and IS*AbaI-eptA3* has been sequenced while the sequence downstream ABK1_2603 could not be resolved. The ABK1 gene annotation is shown according to the genomic sequence of *A. baumannii* strain 1652-2 (Genbank accession number NC_017162).

EptA, a PmrC homolog, is present in the *A. baumannii* strains of international clone 2.

Lesho and colleagues described the presence of the alternative PetN transferase EptA in *A. baumannii* (17). EptA and PmrC are homologous proteins with 93% amino acid identity suggesting similar enzymatic activities. However, the role of EptA in *A. baumannii* colistin resistance is still unclear (17). To investigate the prevalence of *eptA* in *A. baumannii*, we took advantage of sequence differences between *pmrC* and *eptA* at the N- and C-terminal ends of the open reading frames and designed oligonucleotides (oVT152/oVT153) that can discriminate *eptA* from *pmrC* (Fig 1.C and Table S1). Using these *eptA* specific primers we detected *eptA* in all our international clone 2 strains, but not in international clone 1 strains. This finding was further confirmed by screening 12 additional isolates from the BioVersys strain collection (data not shown).

The integrated transposon IS*AbaI* causes *eptA* overexpression in BV94 and BV189.

Two isoforms of *eptA*, *eptA-1* and *eptA-2* (Genbank accession number KC700024 and KC700023, respectively), were previously described to be present at different locations in the genome of various *A. baumannii* strains (17). Taking advantage of the different flanking

regions, we designed primers able to discriminate *eptA-1* and *eptA-2* (oVT198/oVT199 and oVT201/oVT202, respectively) (Fig 1.C and Table S1). By genotyping the strain panel, we demonstrated that all strains that belong to the international clone 2 contained *eptA-1* and four of them contained an additional copy of *eptA-2* (Fig S1). Interestingly, the PCR products obtained for *eptA-2* in BV94 and *eptA-1* in BV189 were approximately 1 kilobase larger than the expected fragment size. Sequencing of the PCR products identified an insertion of transposon IS*AbaI* upstream of *eptA-2* and *eptA-1* in BV94 and BV189, respectively. The IS*AbaI* orientation enabled its strong promoter (P_{out}) to drive *eptA* overexpression as previously described for other antibiotic resistance determinants (Fig 1.D) (26,27).

Using probes specific for *eptA* and *pmrC* we quantified their expression levels in our strains. *eptA* was 550- and 25-fold higher expressed in BV94 and BV189, respectively, than the homologous isoform *pmrC* in the control strain ATCC-17978 (which does not encode *eptA*) (Fig 1.B). This *eptA* overexpression was not altered in the Δ*pmrA* mutant strains suggesting that *eptA* expression in both strains is regulated independently of the PmrAB TCS. These data suggest that an IS*AbaI*-driven *eptA* overexpression may represent an alternative and PmrAB-independent colistin resistance mechanism in BV94 and BV189.

IS*AbaI* driven *eptA* overexpression confers colistin resistance in *A. baumannii* clinical isolates.

To validate this hypothesis, we deleted *eptA-1* in the clinical isolates BV189 and BV94 and determined MIC values. Indeed, BV189 (which carries IS*AbaI* upstream of *eptA-1*) became colistin susceptible upon *eptA-1* deletion, indicating an essential role of IS*AbaI-eptA-1* in conferring colistin resistance in this strain (Table 3). In contrast, BV94, encoding both *eptA-1* and *eptA-2* isoforms, but carrying an IS*AbaI* insertion upstream of *eptA-2*, remained colistin resistant after deletion of *eptA-1* suggesting the key role of the position of IS*AbaI* insertion for colistin resistance in *A. baumannii*. To further confirm the importance of IS*AbaI*, we constructed the double mutant BV94$_{\Delta eptA\text{-}1/\Delta eptA\text{-}2}$ and evaluated its colistin susceptibility. A 4-fold MIC reduction was observed in BV94$_{\Delta eptA\text{-}1/\Delta eptA\text{-}2}$ mutant compared to BV94 and BV94$_{\Delta eptA\text{-}1}$ parental and single mutant, respectively, indicating that *eptA-2* with an upstream IS*AbaI* affects colistin resistance of BV94 (Table 3). However, we were surprised to see that BV94$_{\Delta eptA\text{-}1/\Delta eptA\text{-}2}$ remained resistant to colistin with a MIC of 16 µg/ml indicating that there must be yet another colistin resistance mechanism present in this isolate.

Table 3: Recovery of colistin susceptibility after deletion of different *eptA* isoforms.

	Colistin MIC (µg/ml)			
Strains	**wildtype**	**Δ*eptA-1***	**Δ*eptA-1*/Δ*eptA-2***	**Δ*eptA-1*/Δ*eptA-2* /Δ*eptA-3***
BV189	128	0.5	-	-
BV94	64	64	16	1

Three different *eptA* variants can confer colistin resistance in *A. baumannii*.

We genotyped the BV94$_{\Delta eptA\text{-}1/\Delta eptA\text{-}2}$ double mutant and confirmed the successful deletion of *eptA1* and *eptA2*. However, we detected the presence of at least one additional *eptA* copy (*eptA-3*) in the double mutant (Fig S2). We performed a fusion primer and nested integrated PCR experiment (FPNI-PCR) to amplify genomic flanking regions of the additional *eptA-3*

variant (28). Sequencing revealed an upstream IS*AbaI* and downstream gene ABK1_2603 showing an identical context of *eptA-3* as for *eptA-2* in strain 1652-2 (Genbank accession number NC_017162). However, further upstream there were marked differences. IS*AbaI-eptA-3* was adjacent to ABK1_3144 while IS*AbaI-eptA-2* had ABK1_2605 (Fig 1.D). We could not determine the downstream flanking region of IS*AbaI-eptA3* ABK1_2603 in multiple attempts. Our results suggest that *eptA-3* in BV94 might be a result of an IS*AbaI-eptA-2* cassette gene duplication.

We finally deleted the DNA fragment between ABK1_3144 and ABK1_3143 containing *eptA-3* to confirm that IS*AbaI-eptA-3* was responsible for the high residual colistin resistance in BV94$_{\Delta eptA\text{-}1/\Delta eptA\text{-}2}$. In addition, we performed PCR-based *eptA* genotyping on the resulting triple mutant BV94$_{\Delta eptA\text{-}1/\Delta eptA\text{-}2/\Delta eptA\text{-}3}$ to exclude the presence of yet another *eptA* copy (Fig S2). The loss of all 3 *eptA* isoforms in BV94$_{\Delta eptA\text{-}1/\Delta eptA\text{-}2/\Delta eptA\text{-}3}$ rendered this triple mutant susceptible to colistin, indicating that colistin resistance in BV94 was entirely conferred by the overexpression of EptA-isoforms (Table 3).

Targeting PetN transferases may overcome colistin resistance in *A. baumannii*.

In this study we have shown that colistin resistance was mediated in 10 out of 12 analysed clinical strains by PmrA mediated overexpression of PmrC. In the remaining two strains IS*AbaI* driven EptA expression conferred colistin resistance. Taken together, in all tested clinical isolates colistin resistance was mediated by the overexpression of PetN transferases, suggesting that inhibition of these homologous enzymes with small molecules may have the potential to overcome colistin resistance in *A. baumannii* (Fig 2). Chin and colleagues recently suggested that the acetyl-galactosamine (GalNAc) deacetylase NaxD plays a role in colistin resistance in *A. baumannii* (29). In this report, the expression of NaxD was regulated by the PmrAB TCS and NaxD mediated galactosamine (GalN) addition to lipid A finally conferred the colistin resistance phenotype. We performed additional experiments to exclude the possibility that the observed colistin re-sensitisation after deletion of PmrA was based on a modulation of *naxD* and not *pmrC*. We first confirmed the PmrAB controlled *naxD* expression based on qRT-PCR data for BV191 and BV191$_{\Delta pmrA}$ (Fig S3). BV191 has a PmrB mutation that likely triggers PmrA-mediated *pmrC* overexpression. Similarly, *naxD* expression was 15-fold higher in the colistin resistant strain BV191 compared to the susceptible strain ATCC-17978. In BV191$_{\Delta pmrA}$, lacking the response regulator PmrA, *pmrC* and *naxD* overexpression was abolished confirming that both genes were regulated by the PmrAB TCS. Notably, *pmrC* overexpression was 20-fold higher compared to *naxD* overexpression. To confirm the major role of PmrC in PmrA-mediated colistin resistance and to exclude that another PmrA-regulated gene is involved in colistin resistance, we directly deleted the effector *pmrC* from the genome of BV191. The loss of PmrC rendered BV191 susceptible to colistin (MIC of 0.5 µg/ml) and resulted in a similar phenotype as in BV191$_{\Delta pmrA}$ (Table 2). By contrast, *naxD* was still 15-fold overexpressed in BV191$_{\Delta pmrC}$ (Fig S3). This result suggests that overexpression of *naxD* is not sufficient to confer colistin resistance in BV191 and indicates that PmrC is the main effector of PmrA-mediated colistin resistant *A. baumannii* strains, such as BV191.

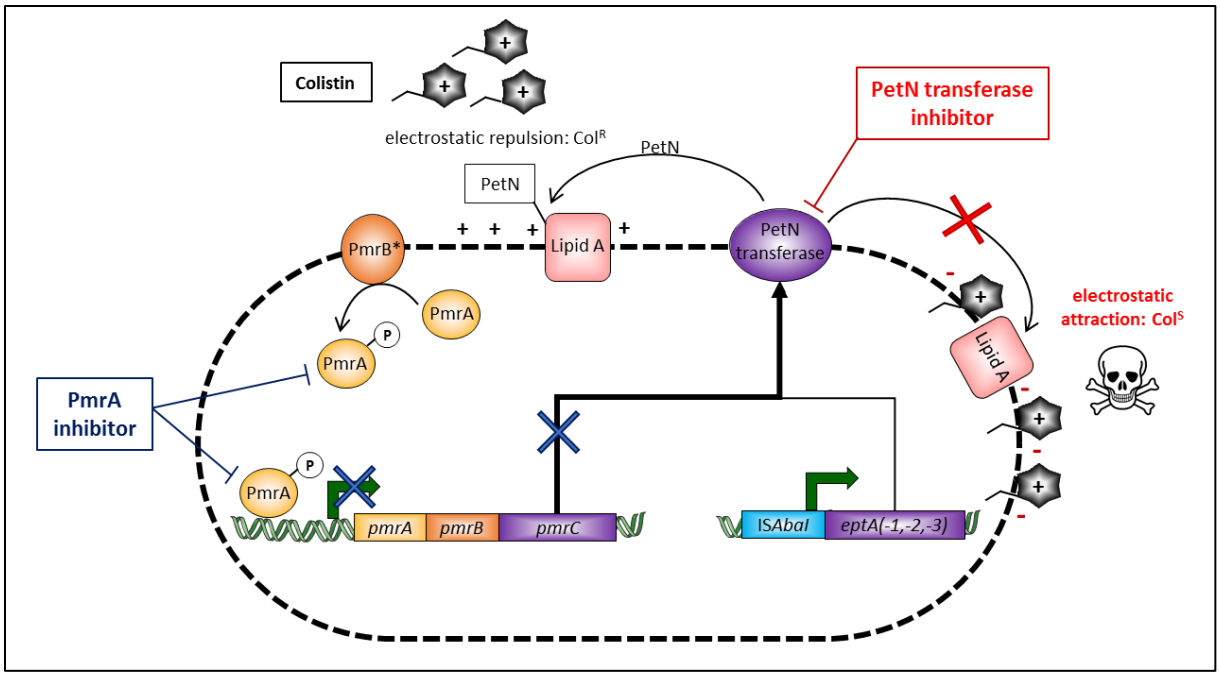

Fig 2: Schematic representation of *A. baumannii* colistin resistance mechanisms.
The two pathways leading to phosphoethanolamine (PetN) transferase overexpression and colistin resistance are represented. The major *A. baumannii* PetN transferase overexpression pathway results from *pmrC* expression, which is activated by the transcriptional regulator PmrA previously phosphorylated (activated) by a mutated variant of the sensor kinase PmrB (PmrB*). Alternatively, *A. baumannii* PetN transferase overexpression can result from the integration of IS*AbaI* transposon upstream of an *eptA* isoform. PetN transferase enzymes decorate the outer membrane lipid A with PetN thereby lowering the negative charge and preventing colistin binding. PmrA inhibitor would only block the *pmrC* pathway (dark blue cross), while PetN transferase inhibitor would block lipid A modification (red cross) and restore colistin efficacy against *A. baumannii*.

Discussion

Bacteria have evolved multiple ways to escape the hazardous action of antibiotics. In nosocomial infections, the individual strain history of antibiotic exposures during patient treatment may result in the development and accumulation of different resistance mechanisms in strains of the same species. Therefore, it is important to study resistance mechanism on multiple strains. Moreover, it is crucial to study these mechanisms on strains that developed resistance during patient treatment due to the discrepancy that may be observed between *in vitro* and *in vivo* developed mechanisms. For instance, *A. baumannii* polymyxin resistance is commonly mediated by LPS loss when *A. baumannii* is exposed to the drug *in vitro* but this mechanism is not viable *in vivo* due to the strong fitness cost it engenders (16,30).

In this study, we dissected the mechanisms conferring colistin resistance in 12 clinically relevant *A. baumannii* strains. To our knowledge, this is the first time that colistin resistance is genetically characterized in a panel of *A. baumannii* clinical strains that developed resistance during patient treatment. This gap in knowledge originates from the difficulties to manipulate the genome of *A. baumannii* colistin resistant clinical strains. Indeed, as exemplified in our strain panel, such strains are generally resistant to all other antibiotics because colistin is used as last option in the treatment of *A. baumannii* infections, only when other antibiotics failed. To break the barrier of antibiotic resistance in these strains, we applied a genome editing method

based on non-antibiotic resistance marker, which is efficient regardless of the resistance profile of the strain (24).

We demonstrated two different ways to overexpress PetN transferases that cause colistin resistance in *A. baumannii* clinical isolates (Fig 2). The predominant colistin resistance mechanism found in 83% of the studied clinical isolates was mediated by *pmrC* overexpression. The overexpression of *pmrC* in these strains was entirely caused by mutations in the sensor kinase PmrB, although previous studies also found mutations in the response regulator PmrA (14,15,17). We found 7 different PmrB variants among the 10 PmrC-mediated colistin resistant strains indicating the diversity of mutations that lead to PmrC overexpression. Except the A226V and P233S mutations, the identified PmrB mutations were not yet reported in *A. baumannii* (11,15,16).

Interestingly, we found two clinical isolates in which colistin resistance was conferred by a genomic insertion of the transposon IS*AbaI* resulting in a strong overexpression of the *pmrC* homolog *eptA*. *eptA-1* and *eptA-2* genes have been previously identified in *A. baumannii*, however, their distribution, expression regulation, and role in colistin resistance was not assessed (17). Our study revealed that *A. baumannii* strains of the international clone 2, which represent the most problematic strains in hospital, carry at least one *eptA* variant. In contrast, international clone 1 strains did not encode *eptA*. Our data further show that *eptA* expression is not regulated by the PmrAB TCS but, instead, integration of IS*AbaI* upstream of any *eptA* isoform is required to confer the resistance phenotype, presumably by IS*AbaI*-driven *eptA* overexpression. Consequently, detection of an *eptA* gene alone is not sufficient to classify *A. baumannii* strains as colistin resistant.

The analysis of PmrA as a potential drug target confirmed the importance of this protein in mediating colistin resistance in *A. baumannii*. However, the high prevalence of *eptA* and the ability of IS*AbaI* to integrate upstream of *eptA* and drive its expression independently of the PmrAB TCS disproved PmrA as a direct drug target for re-sensitisation of *A. baumannii* to colistin (Fig 2). An adjuvant therapy consisting of a PmrA inhibitor in combination with colistin would most likely select for IS*AbaI* driven EptA overexpressing colistin resistant strains. As demonstrated by the two clinical isolates BV94 and BV189, such strains are already present in the hospitals. One of the strains also contained a duplicated IS*AbaI-eptA* cassette suggesting that this functional cassette mediating colistin resistance was present on a mobile element. The presence of a mobile colistin resistance-mediating cassette increases the probability of intra- and interspecies transfer of the resistance pathways by the integration into plasmids. This phenomenon was recently illustrated with plasmid encoded PetN transferase *mcr-1*, which was initially found in China but rapidly spreads globally and in different species (12,13).

One of the major colistin resistance pathways in *Enterobacteriaceae* and *P. aeruginosa* is the addition of AraN to lipid A (11). Although we describe here two different ways to overexpress PetN transferases, our results suggest that colistin resistance in clinical *A. baumannii* isolates is exclusively conferred by PetN addition to lipid A. A recent study suggested that a GalN-based modification of lipid A may be involved in colistin resistance in *A. baumannii* (29). In contrast, our results suggest that alteration of the lipid A structure by addition of PetN plays the major role in colistin resistance in *A. baumannii*. It has been also described that loss of LPS may confers colistin resistance in *A. baumannii* (31). However, most of the LPS deficient colistin resistant mutants were obtained *in vitro* after colistin evolution and it has been shown that these

mutants are hypersusceptible to other antibiotic classes and are avirulent (16,30). Emergence of LPS-deficient colistin resistant mutants in patients is therefore unlikely.

In conclusion, the overexpression of homologous PetN transferases caused colistin resistance in all studied clinical isolates, but in some cases this occurred independently of PmrAB. Our data suggests that a direct inhibitor of homologous PetN transferases PmrC and EptA may have the potential to overcome colistin resistance in *A. baumannii* clinical strains (Fig 2).

Materials and methods

Bacterial strains, MIC, MLST and oligonucleotides. The *A. baumannii* reference strain ATCC-17978 and twelve extensively drug resistant *A. baumannii* clinical isolates from the BioVersys proprietary strain collection were used in this study. The microdilution method was used to determine MICs according to the CLSI guidelines (32). Multiple locus sequence type (MLST) was determined according to the Pasteur scheme using specific primers (source: http://pubmlst.org/abaumannii/) (20). Oligonucleotides used in this study are listed in Table S1.

Genomic deletions of *pmrA*, *eptA-1*, *eptA-2*, *eptA-3* and *pmrC* in *A. baumannii* clinical isolates. Scarless deletions of *pmrA*, *pmrC* and the *eptA* isoforms were performed using a two-step recombination method previously described (24).
DNA fragments corresponding to 700-bp up- and downstream genomic regions of the genes to be deleted were amplified by PCR and cloned in the multiple cloning site of the knockout platform pVT77. Oligonucleotides oVT49/oVT50 and oVT51/oVT52 were used to amplify the up- and downstream regions, respectively, of *pmrA*. The resulting DNA fragments were ligated and introduced into pVT77 previously digested by EcoRI and BamHI. Similarly, oligonucleotides oVT235/oVT236 and oVT237/oVT238 were used to amplify the flanking regions of *eptA-1* and oligonucleotides oVT305/oVT306 and oVT307/oVT242 were used to amplify the flanking regions of *eptA-2*. The resulting DNA fragments for *eptA-1* and *eptA-2* were introduced into pVT77 previously digested by XhoI and XbaI using NEBuilder HiFi DNA assembly (New England Biolabs). For *eptA-3* deletion, the genomic regions flanking the duplicated cassette were amplified using oVT390/oVT391 and oVT392/oVT393. The resulting DNA fragments were cloned into pVT77 previously digested with EcoRI and XbaI using NEBuilder HiFi DNA assembly. Lastly, the flanking regions of *pmrC* were amplified using oVT324/oVT325 and oVT326/oVT327 and the resulting DNA fragments were cloned into pVT77 previously digested with KpnI and PstI using NEBuilder HiFi DNA assembly.
The cloned knockout plasmids were transformed in *E. coli* conjugative strain MFD*pir* to proceed with the construction of markerless deletion in *A. baumannii,* as previously described (24). Briefly, after conjugation, genomic plasmid integration was selected on LB agar plates containing 100 µg/ml sodium tellurite. Clones were screened for up- or downstream integration by PCR using primers oVT8 that anneals on the plasmid and oVT91, oVT243, oVT311 or oVT328 that anneal upstream of *pmrA*, *eptA-1*, *eptA-2* and *pmrC*, respectively. For *eptA-3*, clones were screened using primers oVT8/oVT396 and oVT174/oVT397 for up- and downstream integration, respectively. Clones containing up- and downstream plasmid integrations were transferred on LB agar plates containing 1 mM isopropyl-β-D-1-thiogalactopyranoside and 200 µg/ml 3'-azido-3'-deoxythymidine to select for plasmid removal from the genome. Clones were screened for gene deletion and plasmid removal by

PCR using primers oVT91/oVT92, oVT243/oVT244, oVT246/oVT311, oVT396/oVT397 and oVT328/oVT14 for *pmrA*, *eptA-1*, *eptA-2*, *eptA-3* and *pmrC*, respectively. The genomic gene deletions were finally confirmed by DNA sequencing (Microsynth AG, Balgach, Switzerland).

Genotyping of *pmrA*, *pmrB* and *eptA*. A genomic DNA sequence including *pmrA* and *pmrB* was PCR amplified from all the strains of the panel using oVT91 and oCK292 and the PCR products were sent to sequencing (Microsynth AG, Balgach, Switzerland). The genotyping of *eptA* isoforms was performed by PCR using *eptA* specific primers oVT152 and oVT153 that anneal on all *eptA* isoforms but not on *pmrC* (Fig 1.C). PCR using primers oVT198/oVT199 and oVT201/oVT202 that anneal on the flanking sides of *eptA-1* and *eptA-2*, respectively, were used to discriminate between *eptA* isoforms (Fig 1.C).

qRT-PCR. Quantitative reverse transcription-PCR was performed as previously described (24). The specific expression of the PetN transferases *pmrC* and *eptA* was evaluated using oVT162/oVT163 and oVT164/oVT165 primers, respectively (Fig 1.C). The expression of *naxD* was evaluated using oVT314/oVT315 primers. Expressions were normalized to that of the housekeeping gene *rpoD* using the comparative $\Delta\Delta C_T$ method. The expression of *rpoD* was evaluated using rpoD-qRT-F/rpoD-qRT-R primers.

FPNI-PCR. Fusion primer and nested integrated PCR was performed as previously described (28). This method relies on a three-step PCR using arbitrary degenerated oligonucleotides fused to known adaptors and three sequence specific oligonucleotides, which consist in our case of *eptA* specific oligonucleotides. FPNI-PCR experiments was performed on the $BV94_{\Delta eptA\text{-}1/\Delta eptA\text{-}2}$ mutant with two sets of three *eptA* specific oligonucleotides oVT343, oVT344, oVT345 and oVT340, oVT341, oVT342 to identify the sequence up- and downstream of the new *eptA* copy, respectively. The degenerated primers and the known adaptor primers were directly taken from the previously described method (28). Briefly, the first round of PCRs was performed using the degenerated primers and oVT343 for upstream identification and oVT340 for downstream identification. The second round of PCRs were performed with the first adaptor primer FSP1 and oVT344 for upstream identification and oVT341 for downstream identification. The last round of PCRs was performed with the second adaptor primer FSP2 and oVT345 for upstream identification and oVT342 for downstream identification. The brightest and most isolated PCR products obtained were sent to sequencing (Microsynth AG, Balgach, Switzerland).

References

1. Thabit AK, Crandon JL, Nicolau DP. Antimicrobial resistance: impact on clinical and economic outcomes and the need for new antimicrobials. Expert Opin Pharmacother. 2015 Feb;16(2):159–77.

2. Bassetti M, Merelli M, Temperoni C, Astilean A. New antibiotics for bad bugs: where are we? Ann Clin Microbiol Antimicrob. 2013;12:22.

3. Boucher HW, Talbot GH, Benjamin DK, Bradley J, Guidos RJ, Jones RN, et al. 10 × ’20 Progress—Development of New Drugs Active Against Gram-Negative Bacilli: An Update From the Infectious Diseases Society of America. Clin Infect Dis. 2013 Jun 15;56(12):1685–94.

4. Li J, Nation RL, Turnidge JD, Milne RW, Coulthard K, Rayner CR, et al. Colistin: the re-emerging antibiotic for multidrug-resistant Gram-negative bacterial infections. Lancet Infect Dis. 2006 Sep;6(9):589–601.

5. Zavascki AP, Goldani LZ, Li J, Nation RL. Polymyxin B for the treatment of multidrug-resistant pathogens: a critical review. J Antimicrob Chemother. 2007 Dec 1;60(6):1206–15.

6. Peleg AY, Hooper DC. Hospital-Acquired Infections Due to Gram-Negative Bacteria. N Engl J Med. 2010 May 13;362(19):1804–13.

7. Gales AC, Jones RN, Sader HS. Contemporary activity of colistin and polymyxin B against a worldwide collection of Gram-negative pathogens: results from the SENTRY Antimicrobial Surveillance Program (2006–09). J Antimicrob Chemother. 2011 Sep 1;66(9):2070–4.

8. Pogue JM, Cohen DA, Marchaim D. Editorial commentary: Polymyxin-resistant Acinetobacter baumannii: urgent action needed. Clin Infect Dis Off Publ Infect Dis Soc Am. 2015 May 1;60(9):1304–7.

9. Pieren M, Tigges M. Adjuvant strategies for potentiation of antibiotics to overcome antimicrobial resistance. Curr Opin Pharmacol. 2012 Oct;12(5):551–5.

10. Needham BD, Trent MS. Fortifying the barrier: the impact of lipid A remodelling on bacterial pathogenesis. Nat Rev Microbiol. 2013 Jul;11(7):467–81.

11. Olaitan AO, Morand S, Rolain J-M. Mechanisms of polymyxin resistance: acquired and intrinsic resistance in bacteria. Front Microbiol. 2014;5:643.

12. Liu Y-Y, Wang Y, Walsh TR, Yi L-X, Zhang R, Spencer J, et al. Emergence of plasmid-mediated colistin resistance mechanism MCR-1 in animals and human beings in China: a microbiological and molecular biological study. Lancet Infect Dis. 2016 Feb;16(2):161–8.

13. Rolain J-M, Kempf M, Leangapichart T, Chabou S, Olaitan AO, Page SL, et al. Plasmid-mediated mcr-1 gene in colistin-resistant clinical isolates of Klebsiella pneumoniae in France and Laos. Antimicrob Agents Chemother. 2016 Aug 29;AAC.00960-16.

14. Adams MD, Nickel GC, Bajaksouzian S, Lavender H, Murthy AR, Jacobs MR, et al. Resistance to Colistin in Acinetobacter baumannii Associated with Mutations in the PmrAB Two-Component System. Antimicrob Agents Chemother. 2009 Sep 1;53(9):3628–34.

15. Arroyo LA, Herrera CM, Fernandez L, Hankins JV, Trent MS, Hancock REW. The pmrCAB operon mediates polymyxin resistance in Acinetobacter baumannii ATCC 17978 and clinical isolates through phosphoethanolamine modification of lipid A. Antimicrob Agents Chemother. 2011 Aug;55(8):3743–51.

16. Beceiro A, Moreno A, Fernández N, Vallejo JA, Aranda J, Adler B, et al. Biological cost of different mechanisms of colistin resistance and their impact on virulence in Acinetobacter baumannii. Antimicrob Agents Chemother. 2014;58(1):518–26.

17. Lesho E, Yoon E-J, McGann P, Snesrud E, Kwak Y, Milillo M, et al. Emergence of Colistin-Resistance in Extremely Drug-Resistant Acinetobacter baumannii Containing a Novel pmrCAB Operon During Colistin Therapy of Wound Infections. J Infect Dis. 2013 Oct 1;208(7):1142–51.

18. Park YK, Choi JY, Shin D, Ko KS. Correlation between overexpression and amino acid substitution of the PmrAB locus and colistin resistance in Acinetobacter baumannii. Int J Antimicrob Agents. 2011 Jun;37(6):525–30.

19. Harris TL, Worthington RJ, Hittle LE, Zurawski DV, Ernst RK, Melander C. Small molecule downregulation of PmrAB reverses lipid A modification and breaks colistin resistance. ACS Chem Biol. 2014 Jan 17;9(1):122–7.

20. Diancourt L, Passet V, Nemec A, Dijkshoorn L, Brisse S. The population structure of Acinetobacter baumannii: expanding multiresistant clones from an ancestral susceptible genetic pool. PloS One. 2010;5(4):e10034.

21. Sahl JW, Del Franco M, Pournaras S, Colman RE, Karah N, Dijkshoorn L, et al. Phylogenetic and genomic diversity in isolates from the globally distributed Acinetobacter baumannii ST25 lineage. Sci Rep. 2015 Oct 14;5:15188.

22. Zarrilli R, Pournaras S, Giannouli M, Tsakris A. Global evolution of multidrug-resistant Acinetobacter baumannii clonal lineages. Int J Antimicrob Agents. 2013 Jan;41(1):11–9.

23. Magiorakos A-P, Srinivasan A, Carey RB, Carmeli Y, Falagas ME, Giske CG, et al. Multidrug-resistant, extensively drug-resistant and pandrug-resistant bacteria: an international expert proposal for interim standard definitions for acquired resistance. Clin Microbiol Infect. 2012 Mar 1;18(3):268–81.

24. Trebosc V, Gartenmann S, Royet K, Manfredi P, Tötzl M, Schellhorn B, et al. A Novel Genome-Editing Platform for Drug-Resistant Acinetobacter baumannii Reveals an AdeR-Unrelated Tigecycline Resistance Mechanism. Antimicrob Agents Chemother. 2016 Dec 1;60(12):7263–71.

25. M100-S24: Performance Standards for Antimicrobial Susceptibility Testing; Twenty-Fourth Informational Supplement.

26. Mugnier PD, Poirel L, Nordmann P. Functional Analysis of Insertion Sequence ISAba1, Responsible for Genomic Plasticity of Acinetobacter baumannii. J Bacteriol. 2009 Apr1;191(7):2414-8.

27. Sun J-R, Perng C-L, Chan M-C, Morita Y, Lin J-C, Su C-M, et al. A Truncated AdeS Kinase Protein Generated by ISAba1 Insertion Correlates with Tigecycline Resistance in Acinetobacter baumannii. PLoS ONE. 2012 Nov 14;7(11):e49534.

28. Wang Z, Ye S, Li J, Zheng B, Bao M, Ning G. Fusion primer and nested integrated PCR (FPNI-PCR): a new high-efficiency strategy for rapid chromosome walking or flanking sequence cloning. BMC Biotechnol. 2011;11:109.

29. Chin C-Y, Gregg KA, Napier BA, Ernst RK, Weiss DS. A PmrB-Regulated Deacetylase Required for Lipid A Modification and Polymyxin Resistance in Acinetobacter baumannii. Antimicrob Agents Chemother. 2015 Dec;59(12):7911–4.

30. García-Quintanilla M, Carretero-Ledesma M, Moreno-Martínez P, Martín-Peña R, Pachón J, McConnell MJ. Lipopolysaccharide loss produces partial colistin dependence and collateral sensitivity to azithromycin, rifampicin and vancomycin in Acinetobacter baumannii. Int J Antimicrob Agents. 2015 Sep 7;

31. Moffatt JH, Harper M, Adler B, Nation RL, Li J, Boyce JD. Insertion sequence ISAba11 is involved in colistin resistance and loss of lipopolysaccharide in Acinetobacter baumannii. Antimicrob Agents Chemother. 2011 Jun;55(6):3022–4.

32. M07-A9: Methods for Dilution Antimicrobial Susceptibility Tests for Bacteria That Grow Aerobically; Approved Standard—Ninth Edition.

Supporting information

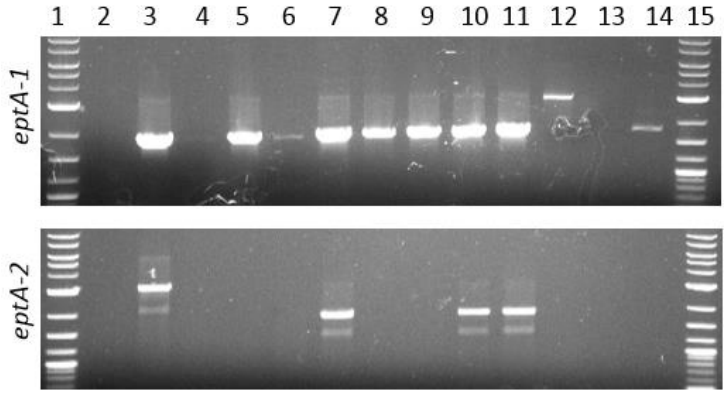

Fig S1: Agarose gel of *eptA-1* and *eptA-2* genotyping in the strain panel.
The genotyping of *eptA-1* (upper gel) and *eptA-2* (lower gel) was performed by PCR using primers oVT198/oVT199 and oVT201/oVT202, respectively. Lane 1: 2-log ladder (New England Biolabs), lane 2: ATCC-17978, lane 3: BV94, lane 4: BV95, lane 5: BV172, lane 6: BV173, lane 7: BV174, lane 8: BV175, lane 9: BV185, lane 10: BV186, lane 11: BV187, lane 12: BV189, lane 13: BV190, lane 14: BV191 and lane 15: 2-log ladder. Compared to the expected size of 1,862-bp and 1,827-bp, the PCR products for BV94 *eptA-2* and BV189 *eptA-1* genotyping are approximately 1 kilobase larger corresponding to the presence of IS*AbaI*.

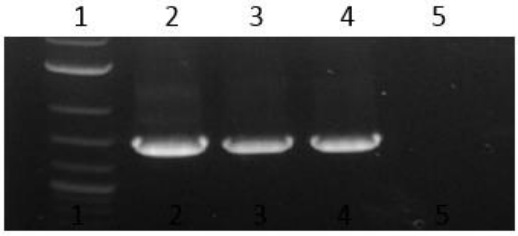

Fig S2: Gel agarose of *eptA* genotyping in the clinical isolate BV94 and its *eptA* knockout mutants.
The genotyping of *eptA* isoforms was performed by PCR using primers oVT152/oVT153. Lane 1: 2-log ladder (New England Biolabs), lane 2: BV94, lane 3: $BV94_{\Delta eptA\text{-}1}$, lane 4: $BV94_{\Delta eptA\text{-}1/\Delta eptA\text{-}2}$, lane 5: $BV94_{\Delta eptA\text{-}1/\Delta eptA\text{-}2/\Delta eptA\text{-}3}$. The triple mutant $BV94_{\Delta eptA\text{-}1/\Delta eptA\text{-}2/\Delta eptA\text{-}3}$ did not encode any other *eptA* isoform.

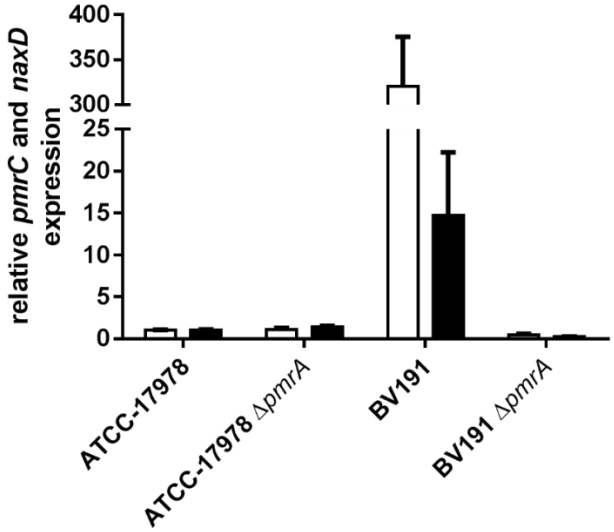

Fig S3: Quantification of *pmrC* and *naxD* expression levels in *A. baumannii* BV191 and its Δ*pmrA* mutants.
The expression of *pmrC* (white bars) and *naxD* (black bars) was quantified by qRT-PCR and normalized to the gene expression level in the reference strain ATCC-17978.

Table S1: Oligonucleotides used in this study

Oligo name	Sequence (5′-3′)
oVT8	GTTTTCCCAGTCACGACGC
oVT14	TGAGGTGCCCCAAATCAGTC
oVT49	GGAATTCCGGTTACCAAGTGACTTGG
oVT50	CGAAATTTTAAATCCCCCGGGGGAGTTCTAGGCTCGCTTTAGTTTAC
oVT51	CTCCCCCGGGGGATTTAAAATTTCGGGACTTC
oVT52	CGGATCCGTCGTAATTCATGAGCAGC
oVT91	CGGGTATGCCACGTGTAGAT
oVT92	CAAATGCTGAATACGCGCCA
oVT152	AGTTCTTTTCTTAGGGGCGACA
oVT153	ACATTGGCTCAACATATCAAGTTTGT
oVT162	CCATTTGGCTAGGTGCAATTT
oVT163	ACCGCATAATAGGTAGCAACA
oVT164	TGCTTTTATCTATCTGGCTAGGTT
oVT165	TGTCGCCCCTAAGAAAAGAACT
oVT174	ACCCAGCATGATATTCCGGA
oVT198	CTCAAGGAGCCATCGTCATAT
oVT199	GGGTTACGACTGCCCTCTTA
oVT201	AGTTTTACTAGCTAAGATTTCGAG
oVT202	TGATGCATAGCTGACGAAG
oVT235	GGAGAATTGAGGCCTCTCGAGCATTCAGGTGTTGCTGTG
oVT236	CCCTCTTACCCGGGATATGACGATGGCTCCTTG
oVT237	TCGTCATATCCCGGGTAAGAGGGCAGTCGTAACC
oVT238	AGCTTCCTGCAGGCTCTAGAAATGGGGGCTTCTGG
oVT242	AGCTTCCTGCAGGCTCTAGACGCCCTTTGGTCTCCTAAC
oVT243	TATGGCACAAGAAGAAGGCG
oVT244	ACAGCTTGGCCATAGGAAGC
oVT246	GCTTTTGTGAAGTTGGGGCC
oVT305	GGAGAATTGAGGCCTCTCGAGACGATTGCGAGCATCAGG
oVT306	ACGAAGGTCCCGGGCGAAACATCGGTCTGCAC
oVT307	GATGTTTCGCCCGGGACCTTCGTCAGCTATGCATC
oVT311	ATGTAAACCACTGCTCACCG
oVT314	TGGCAAAGGTGTGCTATTGC
oVT315	ATTTGGCAGCAGCAGTTTCC
oVT324	AATTCGAGCTCGGTACCAGAGGTTCTGCTTCAGCTC
oVT325	CTCGCTTTACCCGGGAAACAGGGAAATCTGTTTATTTC
oVT326	CCCTGTTTCCCGGGTAAAGCGAGCCTAGAACATG
oVT327	CGCAAGCTTCCTGCAGATTGAGGTGCCCCAAATC
oVT328	TCGACAAACATTGGTGGTGG
oVT340	AGCGGTTTCTGTGCCATGTA
oVT341	CCGCGTTTGATTGTTCTGCA
oVT342	TACAGGGCTGTTCGCAAACT
oVT343	GCAGGTCCATGACTACCCAC
oVT344	TGCAGAACAATCAAACGCGG
oVT345	CCGACCACTGCAAATGAAGC
oVT390	AGAATTGAGGCCTCTCGAGGAATTCATATGTGTTGTGGTCTGGG
oVT391	TGGGATTTTTCCCGGGGACCCACAAAATCTCTTTTC
oVT392	TTTGTGGGTCCCCGGGAAAAATCCCACCGAAGTG
oVT393	CCGCAAGCTTCCTGCAGGCTCTAGAAAACGTGCTCAAACTGC
oVT396	TAAATCCTGGCACTTGGTGG
oVT397	CCGGTGGTATGGAGTCGATG
oCK292	GGACAGGCTGGGTCGTTTG
rpoD-qRT-F	GAGTCTAATGGCGGTGGTTC
rpoD-qRT-R	ATTGCTTCATCTGCTGGTTG

3.2. Part B

Boosting ethionamide efficacy in *M. tuberculosis*

3.2.1. Reversion of antibiotic resistance in *Mycobacterium tuberculosis* by spiroisoxazoline SMARt-420

Nicolas Blondiaux,[1] Martin Moune,[1] Matthieu Desroses,[2,3] Rosangela Frita,[1] Marion Flipo,[2] Vanessa Mathys,[4] Karine Soetaert,[4] Mehdi Kiass,[4] Vincent Delorme,[1,5] Kamel Djaout,[1] **Vincent Trebosc**,[6,7] Christian Kemmer,[6] René Wintjens,[8] AlexandreWohlkönig,[9,10] Rudy Antoine,[1] Ludovic Huot,[1] David Hot,[1] Mireia Coscolla,[11,12] Julia Feldmann,[11,12] Sebastien Gagneux,[11,12] Camille Locht,[1] Priscille Brodin,[1] Marc Gitzinger,[6] Benoit Déprez,[2] NicolasWilland,[2] Alain R. Baulard[1]

[1] Institut Pasteur de Lille, Univ. Lille, CNRS, Inserm, CHU Lille, U1019-UMR8204-CIIL-Centre d'Infection et d'Immunité de Lille, F-59000 Lille, France
[2] Univ. Lille, Inserm, Institut Pasteur de Lille, U1177 - Drugs and Molecules for living Systems, F-59000 Lille, France
[3] National Reference Center for Tuberculosis and Mycobacteria, Bacterial Diseases Service, Operational Direction Communicable and Infectious Diseases, Scientific Institute of Public Health, Brussels, Belgium
[4] Bioversys AG, Hochbergerstrasse 60C, 4057 Basel, Switzerland
[5] Laboratoire des biopolymères et des nanomatériaux supramoléculaires, Université Libre de Bruxelles, Brussels, Belgium
[6] VIB Center for Structural Biology, VIB, Pleinlaan 2, 1050 Brussels, Belgium
[7] Structural Biology Brussels, Vrije Universiteit Brussel, Pleinlaan 2, 1050 Brussels, Belgium
[8] Swiss Tropical and Public Health Institute, Basel, Switzerland
[9] University of Basel, Basel Switzerland

Status of the paper: published in Science

3.2.1.1. Abstract of the paper

Antibiotic resistance is one of the biggest threats to human health globally. Alarmingly, multidrug-resistant and extensively drug-resistant Mycobacterium tuberculosis have now spread worldwide. Some key antituberculosis antibiotics are prodrugs, for which resistance mechanisms are mainly driven by mutations in the bacterial enzymatic pathway required for their bioactivation. We have developed drug-like molecules that activate a cryptic alternative bioactivation pathway of ethionamide in M. tuberculosis, circumventing the classic activation pathway in which resistance mutations have now been observed. The first-of-its-kind molecule, named SMARt-420 (Small Molecule Aborting Resistance), not only fully reverses ethionamide-acquired resistance and clears ethionamide-resistant infection in mice, it also increases the basal sensitivity of bacteria to ethionamide.

3.2.1.2. Statement of my work

- Design and construction of the synthetic mammalian gene regulation system enabling to sense EthR2-DNA interactions
- Performing synthetic mammalian gene regulation system bioassay to assess compound efficacy and SEAP expression data analysis

3.2.1.3. Published paper

REPORT

ANTIBIOTICS

Reversion of antibiotic resistance in *Mycobacterium tuberculosis* by spiroisoxazoline SMARt-420

Nicolas Blondiaux,[1]* Martin Moune,[1]* Matthieu Desroses,[2,3]* Rosangela Frita,[1]* Marion Flipo,[2] Vanessa Mathys,[4] Karine Soetaert,[4] Mehdi Kiass,[4] Vincent Delorme,[1,5] Kamel Djaout,[1] Vincent Trebosc,[6,7] Christian Kemmer,[6] René Wintjens,[8] Alexandre Wohlkönig,[9,10] Rudy Antoine,[1] Ludovic Huot,[1] David Hot,[1] Mireia Coscolla,[11,12] Julia Feldmann,[11,12] Sebastien Gagneux,[11,12] Camille Locht,[1] Priscille Brodin,[1] Marc Gitzinger,[6] Benoit Déprez,[2]† Nicolas Willand,[2]*† Alain R. Baulard[1]*†

Antibiotic resistance is one of the biggest threats to human health globally. Alarmingly, multidrug-resistant and extensively drug-resistant *Mycobacterium tuberculosis* have now spread worldwide. Some key antituberculosis antibiotics are prodrugs, for which resistance mechanisms are mainly driven by mutations in the bacterial enzymatic pathway required for their bioactivation. We have developed drug-like molecules that activate a cryptic alternative bioactivation pathway of ethionamide in *M. tuberculosis*, circumventing the classic activation pathway in which resistance mutations have now been observed. The first-of-its-kind molecule, named SMARt-420 (Small Molecule Aborting Resistance), not only fully reverses ethionamide-acquired resistance and clears ethionamide-resistant infection in mice, it also increases the basal sensitivity of bacteria to ethionamide.

Antibiotic resistance is a rapidly growing health concern and is observed for many antibacterial agents, both in hospital and in community settings (*1*, *2*). The development of drug resistance—especially rifampicin resistance (RR), multidrug resistance (MDR) and extensive drug resistance (XDR)—is particularly worrisome for tuberculosis (TB) (*3*). Approximately 580,000 MDR/RR-TB cases have occurred in 2015, resulting in about 250,000 deaths. This situation seriously undermines efforts to control the global epidemic of TB and may soon counteract the slow but continuous annual decline of ~1.5% observed during the past 14 years (*4*).

Discovering new anti-TB therapeutics is difficult (*5*), and few new drugs have emerged during the past 30 years. Moreover, because current TB treatment requires poly-therapeutic approaches, losing key antibiotics because of the emergence of drug resistance may impair the efficacy of the whole combination.

Drug resistance in bacteria can occur through mutations in the antibiotic's target; the acquisition of enzymes that modify or degrade the drug, such as aminoglycoside-modifying enzymes or β-lactamases; their active expulsion from the bacteria; or alterations of the cell permeability (*6*). Sometimes, antibiotic resistance can be reversed—for example, through restoration of the antimicrobial activity of β-lactams by clavulanic acid, which inhibits enzymes responsible for their degradation (*7*). Unfortunately, there are so far no other examples of this 40-year-old paradigm.

Some of the most effective anti-TB antibiotics require bioactivation by *Mycobacterium tuberculosis* enzymes to acquire their antibacterial effect. These pro-antibiotics not only include the 40-year-old compounds isoniazid (INH), pyrazinamide (PZA), *p*-aminosalicylic acid (PAS) and ethionamide (ETH), but also the recently approved drug delamanid (OPC-67683) and the under-clinical-evaluation compound pretomanid (PA824). However, bioactivation of pro-antibiotics is vulnerable to mutational inactivation or attenuation of the corresponding bioactivating enzymes, as observed for INH-, PZA-, and ETH-resistant clinical isolates with mutations in *katG* (*8*), *pncA* (*9*), and *ethA* (*10*, *11*), respectively. Similarly, experimentally generated and clinical resistance to delamanid and to pretomanid pointed to enzymes and coenzymes involved in their bioactivation (*12*–*14*). Resistance to PAS also involves mutations in enzymes, such as dihydrofolate synthase, which is implicated in its bioactivation (*15*).

We have discovered a spiroisoxazoline family of Small Molecules Aborting Resistance (SMARt) that induces expression of an alternative bioactivation pathway of ETH, reverting acquired resistance of *M. tuberculosis* to this antibiotic.

The bioactivation of ETH in *M. tuberculosis* is normally catalyzed by the Baeyer-Villiger monooxygenase EthA (*10*, *11*, *16*). Transformation of ETH by EthA into highly reactive intermediates leads to the formation of a stable covalent adduct of ETH and nicotinamide adenine dinucleotide (NAD) (*10*, *17*). This adduct binds to and inhibits the enoyl reductase InhA involved in mycolic acid biosynthesis, one of the essential components in the mycobacterial cell wall (*18*, *19*). The production of EthA is regulated by the TetR-type transcriptional repressor EthR (*20*). Previously, we have shown that small-molecule inhibitors of EthR stimulate the transcription of the *ethA* gene (*21*–*24*), which improves the bioactivation of ETH and consequently boosts its antibiotic activity, both in vitro and in vivo (*25*). These booster molecules, such as BDM41906, reduce or reset the innate resistance of *M. tuberculosis* to ETH; however, as expected, they were unable to boost the bioactivation of ETH in strains harboring mutations in *ethA* (Table 1, panel B).

During optimization of first-generation EthR inhibitors, most derivatives revealed a good correlation between binding to EthR and ETH-boosting activity against the bacteria (*21*–*24*). However, unexpectedly, the replacement of the oxadiazole-piperidine motif by a more constrained, structurally divergent, spiroisoxazoline scaffold completely abolished the ability of the compounds to bind to EthR in vitro, whereas they remained highly effective in boosting ETH activity against *M. tuberculosis* (Fig. 1A).

Because these compounds had no antibacterial activity in the absence of ETH but boosted ETH activity independently of EthR, we hypothesized that they may trigger an alternative bioactivation pathway for ETH.

To identify this pathway, we studied the impact of SMARt-420, a representative member of the spiroisoxazoline family, on the transcriptome of *Mycobacterium bovis* Bacillus Calmette-Guérin (BCG) and compared it with the impact of the bona fide EthR-inhibitor BDM41906 (*23*).

When the mycobacteria were treated with BDM41906, overexpression of both *ethA* and *ethR* was observed (Fig. 1B), which is in agreement with previous reports showing that EthR represses both *ethA* and its own expression (*20*). No other major modification of the transcriptome was observed, suggesting that the inhibitory activity of BDM41906 is restricted to EthR. In contrast to BDM41906, SMARt-420 only weakly induced

[1]Univ. Lille, CNRS, Inserm, CHU Lille, Institut Pasteur de Lille, U1019-UMR8204-CIIL–Center for Infection and Immunity of Lille, F-59000 Lille, France. [2]Université Lille, Inserm, Institut Pasteur de Lille, U1177–Drugs and Molecules for Living Systems, F-59000 Lille, France. [3]Division of Translational Medicine and Chemical Biology, Science for Life Laboratory, Department of Medical Biochemistry and Biophysics, Karolinska Institutet, Stockholm, Sweden. [4]National Reference Center for Tuberculosis and Mycobacteria, Bacterial Diseases Service, Operational Direction Communicable and Infectious Diseases, Scientific Institute of Public Health (WIV-ISP), Brussels, Belgium. [5]Tuberculosis Research Laboratory, Institut Pasteur Korea, South Korea. [6]Bioversys AG, Hochbergerstrasse 60C, 4057 Basel, Switzerland. [7]Biozentrum, University of Basel, Basel, Switzerland. [8]Laboratoire des Biopolymères et des Nanomatériaux Supramoléculaires, Université Libre de Bruxelles, Brussels, Belgium. [9]VIB Center for Structural Biology, VIB, Pleinlaan 2, 1050 Brussels, Belgium. [10]Structural Biology Brussels, Vrije Universiteit Brussel (VUB), Pleinlaan 2, 1050 Brussels, Belgium. [11]Swiss Tropical and Public Health Institute, Basel, Switzerland. [12]University of Basel, Basel, Switzerland.
*These authors contributed equally to this work. **†Corresponding author. Email: benoit.deprez@univ-lille2.fr (B.D.); nicolas.willand@univ-lille2.fr (N.W.); alain.baulard@inserm.fr (A.R.B.)**

the expression of *ethA* and *ethR*. However, SMARt-420 strongly activated the expression of the distantly located group of genes *bcg_0107c–bcg_0108c*, corresponding to *rv0076c–rv0077c* (Fig. 1C) in *M. tuberculosis*. According to protein homology, Bcg_0108c is predicted to be a member of the large family of oxidoreductases (http://enzyme.expasy.org/EC/1.-.-.-), which also includes EthA. In silico analyses revealed that *bcg_0108c* is neighboring the tetR type transcriptional regulator gene *bcg_0109* (http://pfam.xfam.org/family/PF00440), indicating analogies between the *rv0076c-rv0078* and the *ethR-ethA* loci (*rv3854c-rv3855*). The genetic organization of the two loci is also similar: *rv0077c* and *rv0078*, like *ethA* and *ethR*, are divergent open reading frames, both separated by small intergenic regions [76 base pairs (bp) and 62 bp for *ethR-ethA* and *rv0077c-rv0078*, respectively] (Fig. 1C). By analogy with the transcriptional organization of the *ethA-ethR* regulon (*20*), these observations indicate that Rv0078 might regulate the expression of *rv0077c* by binding within the intergenic region. This hypothesis was confirmed with surface plasmon resonance experiments (SPR, Biacore), demonstrating the specific binding of Rv0078 to the intergenic region of *rv0077c-rv0078* (Fig. 2A). In contrast, no binding of EthR to the intergenic region of *rv0077c–rv0078* was observed, even at high concentrations of protein, thus excluding EthR for controlling the expression of the *rv0076c–rv0078* locus (Fig. 2B). Conversely, no interaction was detected between Rv0078 and the *ethA–ethR* intergenic region, indicating the absence of cross-talk between the two regulons (Fig. 2B). We assigned the names EthR2 and EthA2 to Rv0078 and Rv0077c, respectively.

The direct binding of SMARt-420 to EthR2 was analyzed in vitro by means of thermal shift assay. The dose-dependent thermal stabilization of EthR2 through binding to SMARt-420 is illustrated in Fig. 2C, whereas no interaction between BDM41906 and EthR2 was observed at equivalent concentrations, which is in agreement with the lack of effect of BDM41906 on the transcription of *ethA2*.

A detailed understanding of the interaction of SMARt-420 with EthR2 was obtained from the x-ray structure of the complex, which shows that EthR2 forms a homodimer in which one molecule of SMARt-420 is embedded in each monomer (Fig. 2D). The structure also confirmed EthR2 as a typical TetR-type regulator harboring two twistable helix-turn-helix (HTH) motifs that are typically involved in the binding of the homodimer to its DNA target (*26*). In this family of repressors, binding of ligands to the distant specific pockets located in the regulatory core of the homodimer induces allosteric reorganization of the architecture of the HTH motifs and thereby modifies the binding properties of the protein to its DNA target (*23*). In agreement with this paradigm, the EthR2–SMARt-420 cocrystal revealed that the distance separating the HTH motifs is far larger than the ±34 Å required for the binding of the regulator to DNA (*27–29*), thus providing the mechanism of action of SMARt-420 (Fig. 2D).

To quantify the inhibition of EthR2-binding to its DNA target by SMARt-420, we designed a synthetic mammalian gene circuit that senses the EthR2-DNA interaction in human cells and produces a quantitative reporter gene expression readout [*secreted alkaline phosphatase* (*SEAP*)] (Fig. 3A) (*30*). In contrast to its repressor role in mycobacteria, binding of EthR2 to the chimeric promoter used in this assay is expected to activate the expression of the *SEAP* reporter gene. In the absence of SMARt-420, we observed strong SEAP production, confirming the binding of EthR2 to its DNA promoter in this cellular context. Upon adding SMARt-420, a dose-dependent inhibition of SEAP production was observed, confirming that SMARt-420 impairs the DNA-binding properties of EthR2. In contrast and as expected, no effect was observed when the cells were incubated with BDM41906, confirming the specificity of the SMARt-420–EthR2 interaction (Fig. 3A). In vitro, SPR experiments showed that SMARt-420 inhibits in a dose-dependent manner

Table 1. Impact of BDM41906 and SMARt-420 on the ethionamide susceptibility of a selection of clinical strains. (**Panel A**) Antibiotic profile. Threshold concentrations above which bacteria are considered clinically resistant are indicated. The drug-sensitivity status of each strain is reported; green indicates "under the threshold concentration," and red indicates "above the threshold concentration." Specifically, for ETH, MICs have been defined by MGIT960 and are reported (values in micrograms per milliliter). All selected strains except the reference pan-susceptible laboratory strain H37Rv (group 1) are multidrug-resistant (INH- and RIF-resistant). Group 2 includes ETH-sensitive strains. Group 3 contains ETH-resistant strains without mutation in *ethA*. Group 4 contains ETH-resistant strains mutated in *ethA*. (**Panel B**) MIC of ETH in the presence of 10 μM first-generation booster BDM41906. (**Panel C**) MIC of ETH in the presence of 10 μM SMARt-420.

	Panel A							Panel B	Panel C
TB strains	INH 0.1 μg/ml	RIF 1 μg/ml	EMB 5 μg/ml	OFL 1 μg/ml	AMI 1 μg/ml	ETH 5 μg/ml	EthA status	ETH + BDM 41906	ETH + SMARt 420
Group 1. Pan-susceptible laboratory strain									
H37Rv						2	wt	0.01	0.05
Group 2. Ethionamide sensitive - MDR strains									
L4376						4	wt	0.1	0.05
LPN30			nd			2	nd	0.1	0.05
L1094						2	wt	0.1	0.05
P591			nd			2	nd	0.1	0.05
L0578						1	wt	0.05	0.25
Group 3. Ethionamide resistant - EthA wt - MDR strains									
B1166						64	wt	4	0.05
B1196						32	wt	0.25	0.25
B1004						32	wt	0.25	0.5
B1304						32	wt	1	0.025
P379						32	wt	4	0.05
B1001						32	wt	4	0.05
B0383						16	wt	1	0.5
B0391						8	wt	0.1	0.25
B0089						8	wt	0.25	0.5
LPN4						8	wt	0.5	0.025
P395						8	wt	1	0.025
P359						8	wt	2	0.05
P351						8	wt	2	0.05
Group 4. Ethionamide resistant - EthA mutated - MDR strains									
B1150						256	P230Q	> 64	0.5
B1602						256	R239G	> 64	0.5
B0775						256	Δa110	32	0.25
B0057						64	Δa110	64	0.25
L3556						64	Q165P	64	0.5
L0728						64	ins.c357	8	0.25

the binding of EthR2 to its DNA target (Fig. 3B), thus confirming that no other partner is required.

The expression of *ethA2* upon inhibition of EthR2 by SMARt-420 leads to efficient bioactivation of ETH in the bacteria. To evaluate the role of EthA2 in the SMARt-420–controlled bioactivation of ETH, *M. tuberculosis* H37Rv was engineered to overexpress *ethA2* by using the multicopy plasmid pMV261 (*31*). Under these conditions, the minimal inhibitory concentration (MIC) of ETH decreased from 2 to 0.25 μg/ml, suggesting that EthA2 takes part in the bioactivation of ETH when overexpressed, thus reducing the innate resistance of the bacteria to ETH (Fig. 3C).

SMARt-420 is the most active compound of a spiroisoxazoline series for which the binding to EthR2 (thermal shift assay) and the inhibition of the DNA binding of EthR2 (SEAP assay) were shown to be correlated to the ETH-boosting effect on sensitive and on ETH-resistant *M. tuberculosis* (fig. S2).

As indicated by the transcriptomic analyses, the basal expression level of *ethA2* in the absence of SMARt-420 is low in *M. tuberculosis*. We measured the relative abundance of mRNA by means of high-throughput RNA-sequencing (RNA-seq) in *M. tuberculosis* cells grown to mid-log phase. We found that *ethA2* belongs to the 10% least-expressed genes in *M. tuberculosis* (rank 3609 out of the 3973 TB genes), whereas *ethA* is among the 10% genes with the highest levels of expression. When compared with each other, *ethA2*-mRNAs were about 60 times less abundant than *ethA*-mRNAs in *M. tuberculosis* grown under standard conditions. Low expression of *ethA2* in the absence of EthR2 inhibitors is of clinical importance, offering an explanation as to why EthA2 has not been previously identified as involved in ETH activation, and therefore mutations in this gene have not been observed in clinical isolates resistant to ETH so far.

Human-adapted *M. tuberculosis* complex comprises seven main phylogenetically distinct lineages (*32*). We analyzed the genome sequences of 217 geographically diverse clinical strains representing all seven lineages (*33*) and confirmed the presence of the *rv0076c–rv0078* locus in all strains. In addition, the presence of the locus was confirmed in a collection of ETH-resistant (171) and ETH-sensitive (253) clinical isolates of *M. tuberculosis* (*34*). No mutation in this locus was observed in the ETH-sensitive population. Only

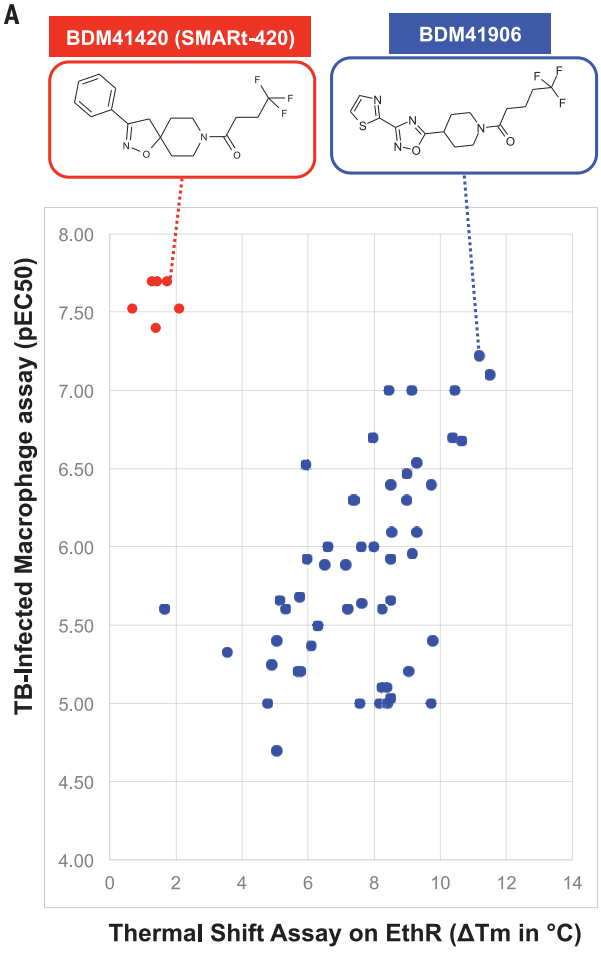

B

Gene Name		(1) RPKM control	(2) RPKM 41906	(2)/(1) FC	(3) RPKM Smart420	(3)/(1) FC
ethA	BCG_3917c	74	2250	30,41	184	2,49
ethR	BCG_3918	35	675	19,29	89	2,54
mmpS5	BCG_0726c	111	263	2,37	107	ns
-	BCG_0108c	23	57	2,48	6186	268,96
-	BCG_0107c	47	50	ns	4016	85,45
-	BCG_0269	89	157	1,76	242	2,72
-	BCG_1777	50	10	ns	126	2,52
nrdB	BCG_0270	78	125	1,60	188	2,41
mmpS4	BCG_0490c	127	110	ns	265	2,09

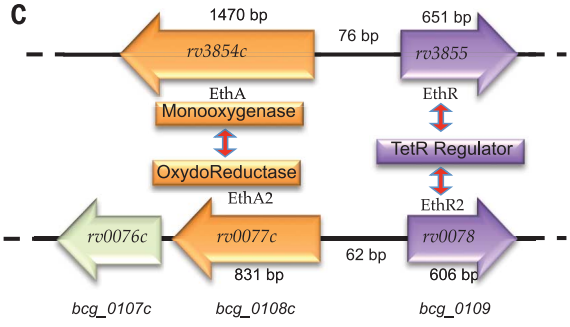

Fig. 1. SMARt family of molecules reveals alternative ETH bioactivation pathway. (**A**) Bidimensional representation of the properties of ETH-boosting compounds (BDM). The *x* axis indicates the shift in the melting temperature (ΔTm) of EthR in the presence of BDM compounds, which translates the capacity of the compounds to bind and thermostabilize EthR in vitro (values are provided in table S1). The *y* axis indicates the potency [expressed as the negative logarithm of the median effective concentration (EC_{50})] of a panel of compounds to increase ETH antibacterial activity on *M. tuberculosis*–infected macrophages. EC_{50} is the concentration of compound that allows ETH at 0.1 μg/mL (10 times less than the normal MIC) to inhibit 50% of *M. tuberculosis* growth in macrophages. Blue dots and red dots represent compounds of the oxadiazole-piperidine family (first-generation boosters) and of the spiroisoxazoline family (SMARt), respectively. (**B**) RNA-seq analysis of genes that are differentially expressed in *M. bovis BCG* exposed for 24 hours to 25 μM BDM41906 (2) or SMARt-420 (3) in comparison with dimethyl sulfoxide–treated bacteria (1). Only genes showing a minimum twofold change (FC) in transcript abundance in at least one condition are shown. RPKM, reads per kilobase per million mapped reads. Whereas BDM41906 specifically induce the expression of *ethA* and *ethR*, SMARt-420 massively induces the expression of *bcg_0108c* and *bcg_0107c*. A weak, but statistically significant, induction of *ethA* and *ethR* is also observed. (**C**) Comparison of the genetic organization and predicted function of the corresponding *M. tuberculosis* loci and proteins. Genes *bcg_0107c* and *bcg_108c* correspond to *rv0076c* and *rv0077c*, respectively. Rv0078 is predicted as a transcriptional repressor of the TetR family.

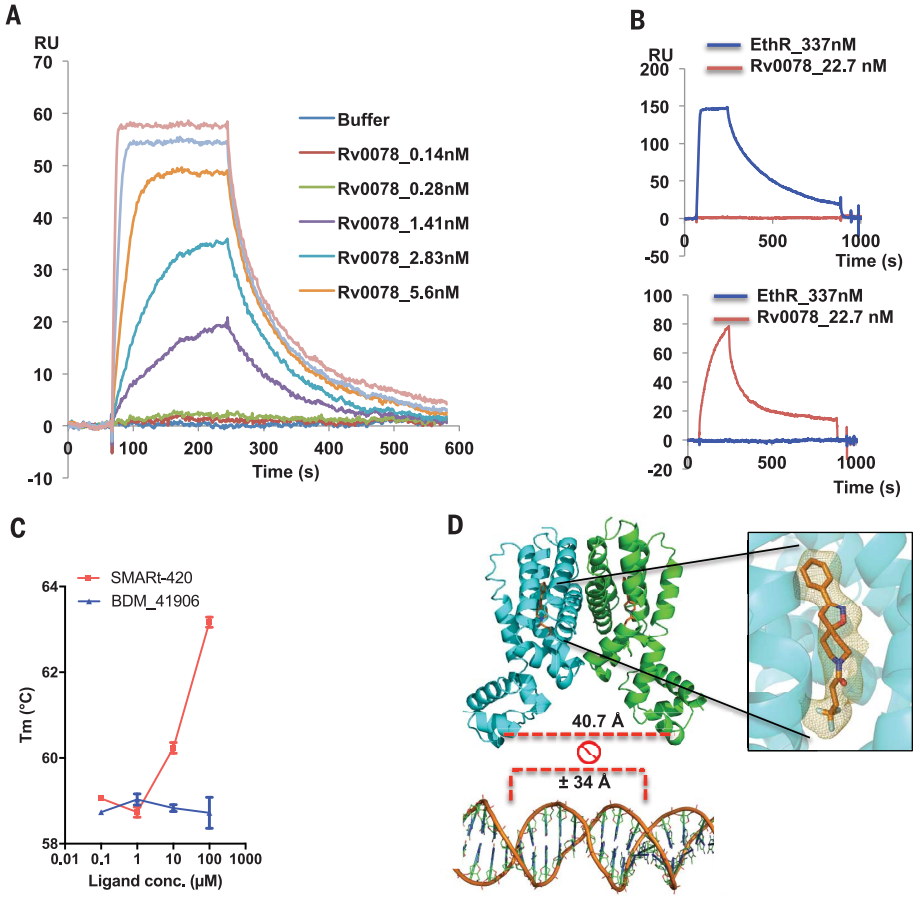

Fig. 2. SMARt-420 interacts with the transcriptional regulator EthR2. (**A**) Global affinity of the interaction between EthR2 and the *ethA2-ethR2* intergenic region measured with SPR. Sensorgrams of 22.7, 11.35, 5.60, 2.83, 1.41, and 0.28 nM EthR2 (Rv0078) injections over a sensor chip functionalized with 40 RU (resonance unit) of the biotinylated *ethA2-ethR2* intergenic DNA. (**B**) Comparison of the injection of EthR and EthR2 (Rv0078) over 2 sensor chips functionalized with *ethA-ethR* intergenic DNA (top) and with *ethA2-ethR2* intergenic DNA (bottom), respectively. (**C**) Binding of SMARt-420 and BDM41906 on EthR2 measured by determination of the melting temperature (T_m) of the complex (thermal-shift assay) (supplementary materials, materials and methods). (**D**) Crystal structure of the EthR2/SMARt-420 complex and illustration of the steric inability of binding of the repressor to DNA because the 40.7 Å spacing of the HTH motifs. The zoom onto the ligand binding pocket of the protein shows an omit map contoured at 1.2σ for one of the two SMARt-420 molecules embedded in each monomer of the EthR2 homodimer (statistics are provided in the supplementary materials, materials and methods, and table S2).

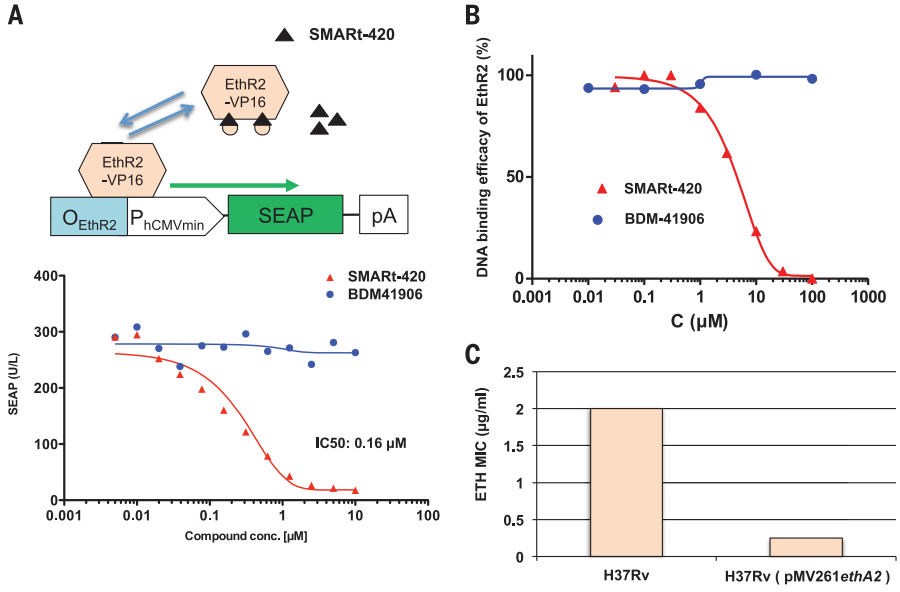

Fig. 3. SMARt-420 inhibits the DNA binding activity of EthR2. (**A**) Synthetic mammalian gene circuit designed to sense EthR2-DNA interactions (*ethA2–ethR2* intergenic region) that are required to induce expression of the reporter gene *SEAP*. The alkaline phosphatase induced by the EthR2-VP16 complex was inhibited in a dose-dependent manner by SMARt-420, whereas no effect was observed in the presence of BDM41906 (supplementary materials, materials and methods, and fig. S1). (**B**) Inhibition of the binding of EthR2 to the *ethA2–ethR2* intergenic region by SMARt-420 but not by BDM41906, measured with surface plasmon resonance. (**C**) Effect of the overexpression of *ethA2* (pMV261–*ethA2*) on the MIC of ETH in *M. tuberculosis*.

one ETH-resistant isolate shows a point mutation in *rv0078*, which also contains a Stop mutation in *ethA*, which is most probably responsible for the ETH-resistance phenotype (table S3). Then, a panel of ETH-sensitive and ETH-resistant MDR *M. tuberculosis* clinical isolates were tested by means of respirometry (*MGIT 960*) (*35*) for their sensitivity to ETH in the presence of SMARt-420. Treatment of ETH-sensitive strains with SMARt-420 (10 µM) decreased their ETH MIC (Table 1, panel C). Strains highly resistant to ETH, because of mutations in *ethA*, were also sensitive to ETH in the presence of SMARt-420 (Table 1, panel C, group 4). The combination SMARt-420 plus ETH was active against all ETH-resistant, MDR, and XDR isolates tested. Last, we showed that overexpression of *inhA* by using a multicopy plasmid modified the boosting effect of SMARt-420, suggesting that the new bioactivation pathway of ETH still targets InhA (fig. S3). We also verified that SMARt-420 does not affect the efficacy of other antibiotics (table S4).

Pharmacokinetic experiments performed in female Swiss mice showed that a single oral

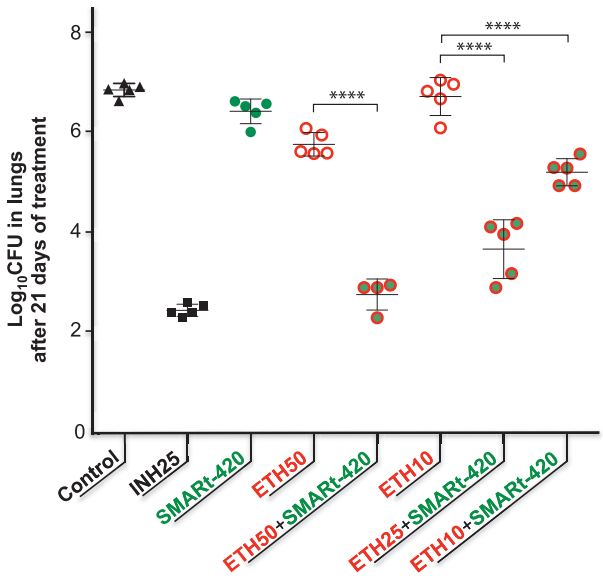

Fig. 4. Reversion of ETH resistance in tuberculosis-infected mice. Mice (five mice per group) infected with ETH-resistant bacteria were treated with the control antibiotic INH (25 mg/kg), ETH alone (50 mg/kg), SMARt-420 alone (50 mg/kg), or a combination of ETH and SMARt-420. Pulmonary bacillary loads were enumerated by colony-forming units (CFUs) after 3 weeks of treatment. Administration of up to 50 mg/kg of ETH did not reduce the pulmonary load of ETH-resistant mycobacteria, whereas coadministration of ETH and SMARt-420 showed a dose-dependent reduction, with a maximum of 4.6 log (control versus ETH50+SMARt-420). Details and statistics are available in "Bonferroni's multiple comparison test" in table S6.

dose of 30 mg/kg of SMARt-420 provides a circulating concentration of SMARt-420 higher than that required to boost ETH in vitro (table S5). Restoration of sensitivity to ETH by SMARt-420 was evaluated in C57BL6/J mice infected by aerosol with 10^5 ETH-resistant *M. tuberculosis* bacilli mutated in *ethA*. Seven days after infection, the mice were treated with ETH alone or with ETH in combination with SMARt-420. Daily administration of up to 50 mg/kg of ETH for 3 weeks was ineffective in significantly reducing the bacterial load in the lungs (Fig. 4), confirming the resistance to ETH of this strain. In contrast, mice treated with a combination of ETH and SMARt-420 (both at 50 mg/kg) showed a striking reduction of the bacterial load (4.6 log) in the lungs (Fig. 4). The absence of an effect observed with SMARt-420 administered alone, and a dose-response to ETH combined with SMARt-420, confirms that the anti-TB activity of the combination is specifically due to the restoration of ETH sensitivity of this strain.

We show that drug-resistance to the widely used antituberculosis drug ETH (*36*) can be circumvented by spiroisoxazoline SMARt-420, which activates cryptic drug-bioactivation pathways in drug-resistant pathogens. Other ETH activation pathways may exist in *M. tuberculosis*, including the recently described VirS-MymA (*37*), opening supplementary avenues for reversing ETH-resistance and boosting its activity.

Innovative treatment protocols could also be explored, in which noncontinuous but regular administration of SMARts to TB patients would periodically toggle the expression of alternative bioactivation pathways of pro-drugs. This approach could be used to limit the frequency of resistance by systematically destroying subpopulations of resistant bacteria that may emerge during treatment.

REFERENCES AND NOTES

1. B. Spellberg, D. N. Gilbert, *Clin. Infect. Dis.* **59** (suppl. 2), S71–S75 (2014).
2. World Health Organization (WHO), *Antimicrobial Resistance: Global Report on Surveillance* (WHO, 2014).
3. S. Hoffner, *Lancet* **380**, 1367–1369 (2012).
4. WHO, *Global Tuberculosis Report* (WHO, 2015).
5. C. Barry, *Science* **348**, 633–634 (2015).
6. C. Walsh, *Antibiotics: Actions, Origins, Resistance* (ASM Press, 2003).
7. C. Reading, M. Cole, *Antimicrob. Agents Chemother.* **11**, 852–857 (1977).
8. Y. Zhang, B. Heym, B. Allen, D. Young, S. Cole, *Nature* **358**, 591–593 (1992).
9. A. Scorpio, Y. Zhang, *Nat. Med.* **2**, 662–667 (1996).
10. A. E. DeBarber, K. Mdluli, M. Bosman, L. G. Bekker, C. E. Barry 3rd, *Proc. Natl. Acad. Sci. U.S.A.* **97**, 9677–9682 (2000).
11. A. R. Baulard *et al.*, *J. Biol. Chem.* **275**, 28326–28331 (2000).
12. U. H. Manjunatha *et al.*, *Proc. Natl. Acad. Sci. U.S.A.* **103**, 431–436 (2006).
13. M. Matsumoto *et al.*, *PLOS Med.* **3**, e466 (2006).
14. G. V. Bloemberg *et al.*, *N. Engl. J. Med.* **373**, 1986–1988 (2015).
15. J. Zheng *et al.*, *J. Biol. Chem.* **288**, 23447–23456 (2013).
16. T. A. Vannelli, A. Dykman, P. R. Ortiz de Montellano, *J. Biol. Chem.* **277**, 12824–12829 (2002).
17. X. Hanoulle *et al.*, *J. Antimicrob. Chemother.* **58**, 768–772 (2006).
18. F. Wang *et al.*, *J. Exp. Med.* **204**, 73–78 (2007).
19. A. Banerjee *et al.*, *Science* **263**, 227–230 (1994).
20. J. Engohang-Ndong *et al.*, *Mol. Microbiol.* **51**, 175–188 (2004).
21. N. Willand *et al.*, *ACS Chem. Biol.* **5**, 1007–1013 (2010).
22. M. Flipo *et al.*, *J. Med. Chem.* **54**, 2994–3010 (2011).
23. M. Flipo *et al.*, *J. Med. Chem.* **55**, 68–83 (2012).
24. M. Flipo *et al.*, *J. Med. Chem.* **55**, 6391–6402 (2012).
25. N. Willand *et al.*, *Nat. Med.* **15**, 537–544 (2009).
26. L. Cuthbertson, J. R. Nodwell, *Microbiol. Mol. Biol. Rev.* **77**, 440–475 (2013).
27. M. A. Schumacher *et al.*, *Science* **294**, 2158–2163 (2001).
28. F. Frénois, J. Engohang-Ndong, C. Locht, A. R. Baulard, V. Villeret, *Mol. Cell* **16**, 301–307 (2004).
29. F. Frénois, A. R. Baulard, V. Villeret, *Tuberculosis (Edinb.)* **86**, 110–114 (2006).
30. W. Weber *et al.*, *Proc. Natl. Acad. Sci. U.S.A.* **105**, 9994–9998 (2008).
31. C. K. Stover *et al.*, *Nature* **351**, 456–460 (1991).
32. M. Coscolla, S. Gagneux, *Semin. Immunol.* **26**, 431–444 (2014).
33. I. Comas *et al.*, *Nat. Genet.* **45**, 1176–1182 (2013).
34. N. Casali *et al.*, *Nat. Genet.* **46**, 279–286 (2014).
35. F. Ardito, B. Posteraro, M. Sanguinetti, S. Zanetti, G. Fadda, *J. Clin. Microbiol.* **39**, 4440–4444 (2001).
36. S. D. Ahuja *et al.*, *PLOS Med.* **9**, e1001300 (2012).
37. S. S. Grant *et al.*, *Cell Chem. Biol.* **23**, 666–677 (2016).

ACKNOWLEDGMENTS

All data and code to understand and assess the conclusions of this research are available in the main text, supplementary materials, and via the following repositories: The refined coordinates and the structure factors of Rv0078 were deposited in the Protein Data Bank under the accession numbers 5N1C (iodinated form), 5N1I (unliganded form), and 5ICJ (liganded form); raw data of RNA-seq analysis have been deposited in Datadryad.org under the doi 10.5061/dryad.mb463. We are indebted to the Soleil [Block Allocation Group (BAG) proposal 20141408] and the European Synchrotron Radiation Facility (BAG proposal MX-1677) synchrotrons for beam-time allocations on this project. Sequencing analyses were performed at the sciCORE (http://scicore.unibas.ch) scientific computing core facility at the University of Basel. The funders had no role in study design, data collection and analysis, decision to publish, or preparation of the manuscript. We are indebted to E. Willery for technical support in molecular biology, F. Leroux for screening management, L. Agouridas and N. Probst for chemical synthesis, and C. Piveteau for bioanalysis. This work was supported by l'Agence Nationale de la Recherche (ANR), France (Tea-4-Two, ANR-14-CE14-0027-01) (ANR-10-EQPX-04-01), by EU grants ERC-STG INTRACELLTB no 260901, the Feder (12001407 (D-AL), PRIM (NewBio4Tb), European Research Council (grant 309540-EVODRTB), SystemsX.ch, Institut National de la Santé et de la Recherche Médicale, Université de Lille, Institut Pasteur de Lille, Centre National de la Recherche Scientifique, the Région Hauts-de-France (convention no. 12000080), and Société d'Accélération du Transfert de Technologie Nord. R.W. is Research Associate at the National Fund for Scientific Research (FNRS-FRS) (Belgium). M.M. was supported by PRIM (NewBio4Tb), V.D. was supported by EU grant 260872, and V.T. was supported by the Marie Curie Initial Training Network (ITN-2013-607694-Translocation). The authors also thank the Unité Mixte de Recherche UMR 8199, Lille Integrated Genomics Network for Advanced Personalized Medicine (LIGAN-PM) Genomics platform (Lille, France), which belongs to the Federation de Recherche 3508 Labex EGID (European Genomics Institute for Diabetes; ANR-10-LABX-46) and was supported by the Agence Nationale de la Recherche (ANR) Equipex 2010 session (ANR-10-EQPX-07-01; LIGAN-PM). The LIGAN-PM Genomics platform is supported by the Fonds Européen de Développement Régional and the Region Hauts-de-France. We thank A. Wagner and Roquettes-Frères (Lestrem, France) for their gift of Cyclodextrine Kleptose HP. We greatly appreciate the fruitful discussions with all the members of the GlaxoSmithKline team "Diseases of the Developing World (DDW)" and their invaluable support in the continuation of this project. C.K. is employed at Bioversys; S.G. is a consultant for the Foundation of Innovative Diagnostics (FIND) in Geneva, Switzerland. M.G. is CEO of Bioversys and a Board Member of the BEAM Alliance, a group of Biopharmaceutical companies from Europe innovating in antimicrobial resistance research. The BEAM Alliance is a not-for-profit association, and there is no financial remuneration of any kind for its Board members. All companies included are working within the field of antimicrobial drug discovery. N.W., B.D., A.R.B., P.B., and M.D. are inventors on patent PCT/EP2013/077706, which covers BDM41420; WO/2014/096369. B.D., N.W., C.L., and A.R.B. are inventors on patent PCT/FR2007/001138; WO/2008/003861, which covers BDM41906. The facilities conformed to Directive 86/609/EEC on the Protection of Animals Used for Experimental and Other Scientific Purposes and norms published in the European Council ETS123 Appendix A. Facilities and procedures complied with the Belgian Law of 14 August 1986 on animal protection and welfare. Training of experimental leaders, biotechnicians, and animal caretakers was in accordance with Royal decree of 13 September 2004, which specifies the training of persons working with laboratory animals. All animal experimentation and procedures performed at the National Reference Center for Tuberculosis and Mycobacteria, Bacterial Diseases Service, Scientific Institute of Public Health (WIV-ISP), Brussels, Belgium, were validated and approved by the Ethical Committee of the IPH-VAR (Scientific Institute of Public Health–Veterinary and Agrochemical Research Centre, Belgium) under file no. 120323-01. The animal facilities and procedures were under the supervision of an expert on animal welfare in accordance with the Belgian Ministry of Health. pET-15b-*ethR2* and *pET-15b-ethR* are available from A.R.B. under a materials transfer agreement with Institut Pasteur de Lille. pCK289 and pCK287 are available from M.G. under a materials transfer agreement with Bioversys.

SUPPLEMENTARY MATERIAL

www.sciencemag.org/content/355/6330/1206/suppl/DC1
Materials and Methods
Figs. S1 to S5
Tables S1 to S6
References (*38–45*)
Database S1

14 May 2016; accepted 20 February 2017
10.1126/science.aag1006

www.sciencemag.org/content/355/6330/1206/suppl/DC1

Supplementary Material for

Reversion of antibiotic resistance in *Mycobacterium tuberculosis* by spiroisoxazoline SMARt-420

Nicolas Blondiaux, Martin Moune, Matthieu Desroses, Rosangela Frita, Marion Flipo, Vanessa Mathys, Karine Soetaert, Mehdi Kiass, Vincent Delorme, Kamel Djaout, Vincent Trebosc, Christian Kemmer, René Wintjens, Alexandre Wohlkönig, Rudy Antoine, Ludovic Huot, David Hot, Mireia Coscolla, Julia Feldmann, Sebastien Gagneux, Camille Locht, Priscille Brodin, Marc Gitzinger, Benoit Déprez,* Nicolas Willand,* Alain R. Baulard*

*Corresponding author. Email: benoit.deprez@univ-lille2.fr (B.D.); nicolas.willand@univ-lille2.fr (N.W.); alain.baulard@inserm.fr (A.R.B.)

Published 17 March 2017, *Science* **355**, 1206 (2017)
DOI: 10.1126/science.aag1006

This PDF file includes:

Other Supplementary Material for this manuscript includes the following:
(available at www.sciencemag.org/content/355/6330/1206/suppl/DC1)

Table S3 as a separate Excel file

Database S1 (transcriptomic data) is available as zipped archives deposited in Datadryad.org under the DOI 10.5061/dryad.mb463:
BCG_DMSO.fastq
BCG_BDM41906.fastq
BCG_SMARt-420.fastq

Materials and Methods

Transcriptomic analysis

Transcriptomic analys of *M. bovis* BCG treated or untreated with 25 µM BDM41906 or BDM41420 (SMARt-420).

mRNA extraction/purification.

Mycobacterium bovis BCG Pasteur 1173P2 was grown at 37°C in 60 mL Sauton broth (*38*) supplemented with 0.001 % $ZnSO_4$ and 0.25 % Triton WR1339 (Sigma) to an OD_{600nm} of 0.8. The culture was divided in two; BDM41906 and BDM41420 (SMARt-420) were added to each part (10 mL) to a final concentration of 25 µM. Incubation was continued for a further 24 h at 37°C. Mycobacteria were harvested by 10 min centrifugation at 5,000 g at 4°C, resuspended in 1 mL of RNApro™ (FastRNA® Pro Blue Kit, MP biomedicals) and homogenized in impact-resistant 2 mL tubes containing 0.1 mm silica spheres (Lysing Matrix B, MP biomedicals) using a FastPrep FP120 cell disrupter (Thermo Fisher Scientific) at 6.0 m/sec for 40 sec. The ribolysed cells were centrifuged at 12,000 g to remove cellular debris and RNA was purified following the manufacturer's instructions. Ribosomal RNA(rRNA) depletion was performed using magnetic beads (Ribo-Zero rRNA Removal kit-Bacteria; Epicentre) according to the manufacturer's protocol. Libraries for Illumina sequencing were prepared with the TruSeq RNA sample preparation kit version 2.0 rev. A (Illumina Inc.) according to the manufacturer's protocol. All cDNA libraries were uniquely indexed. cDNA libraries were sequenced using an Illumina NextSeq 500 system (Illumina Inc.) in high-output mode according to the manufacturer's protocols. All samples were multiplexed on one lane of the flow cell and sequenced in single-read sequencing mode with reads lengths of 150 bp. Raw RNA-seq reads were processed with Illumina quality control tools using default settings. Sequences shorter than 50 bp and/or that contained any 'Ns' and/or with a mean quality score lower than 30 were removed using PRINSEQ (http://prinseq.sourceforge.net/index.html). Next, residual rRNA-specific reads were filtered out by mapping all the reads on *M. tuberculosis* rRNAs sequences using Bowtie2 (http://bowtie-bio.sourceforge.net/bowtie2/index.shtml). Analysis of the RNA sequencing data was conducted using the Rockhopper open source software package with default parameters (http://cs.wellesley.edu/~btjaden/Rockhopper/). Rockhopper's RNA sequencing analysis platform is designed specifically for bacterial organisms. Transcript abundance levels were quantified using the Reads Per Kilobase per Million mapped reads (RPKM).

In figure 1.B. Only genes showing a minimum 2-fold change (FC) in transcript abundance in at least one condition are shown. Upon treatment of the mycobacteria with DMSO (control) or with BDM41906, low expression of BCG_0108c and BCG_0107c are shown.

For RNAseq raw data see the associated compressed folder: Additional "Databases S1" deposited in DataDRYAD.org under the doi:10.5061/dryad.mb463

Surface Plasmon Resonance (SPR)

A BIAcore3000 apparatus (BIAcore AB, Uppsala, Sweden) was used for real-time analysis of molecular interactions between His_6-EthR, His_6-EthR2 and the *ethA2-R2* promoter region.

Production of biotinylated double stranded DNA fragments: A 109-bp fragment overlapping the *ethA2-R2* intergenic region was obtained by PCR using *M. tuberculosis* H37Rv chromosomal DNA as template and the primer pair OpeRvx1/ OpeRvxbiot1 (OpeRvx1: 5'-CCTGGGTGCGTCTCTTGATTTC-3' and OpeRvxbiot1: Biotin-5'-GCACTAATGTCGATCGTCGACATG-3'. The amplified biotinylated fragment was purified on a QIAquick PCR purification Kit column (QIAGEN) before immobilization on a flow cell of a sensor Chip SA (GE Healthcare) using the standard protocol provided by the manufacturer.

A 106-bp fragment overlapping the *ethA-R* intergenic region was obtained by PCR using *M. tuberculosis* H37Rv chromosomal DNA as template and the primer pair O270/O271 (O270 : 5'-CGGTCATGGATCCACGCTATCAAC-3' and O271 : Biotin-5'-CTGACTGGCCGCGGAGGTGGT-3'). The amplified biotinylated DNA was purified on a QIAquick column (QIAGEN) before immobilization on a flow cell of a sensor Chip SA (GE Healthcare) using the standard protocol provided by the manufacturer.

A biotinylated double stranded 113-bp long irrelevant DNA fragment (+14 to +127 fragment of the *E. coli bla* gene PCR-amplified from pUC18) was obtained by PCR using the primer pair O343/O344 (O343:5'-TTTCCGTGTCGCCCTTATTCC-3' and O344: Biotin-5'-CCACTCGTGCACCCAACTGAT-3'). The amplified biotinylated fragment was purified on a QIAquick PCR purification Kit column (QIAGEN) before immobilization on a flow cell of a sensor Chip SA (GE Healthcare) using the standard protocol provided by the manufacturer. Briefly, the sensor surface was conditioned with three consecutive 1-minute injections of 1M NaCl, 50 mM NaOH before DNA immobilization. Several injections of biotinylated relevant or irrelevant DNA at 0.2µg/mL were performed so as to reach a stable level of 40 Resonance Unit (RU). Binding of His_6-EthR2 and His_6-EthR to the DNA was carried out at 25 °C in HBS-EP buffer: 10mM HEPES pH 7.4, 150mM NaCl, 3mM EDTA, 0.005% P20. His_6-EthR and His_6-EthR2 were injected for 3 minutes at the desired concentrations at 20µL/min in the running buffer. Based on the dissociation profiles recorded for the various combinations, the dissociation flow time was fixed to 5 min. The sensor chip was regenerated by a 30s injection of 0.03% SDS followed by 5 min buffer injection for basal signal stabilization. Final curves were obtained by subtraction of the signal corresponding to a control flow cell functionalized with the irrelevant DNA.

To measure the capacity of SMARt-420 to inhibit EthR2-DNA interaction, 22.7 nM of the purified protein (see Production and purification of His_6-EthR2) was incubated with serial dilutions of SMARt-420 or BDM41906 (in HBS-EP buffer), placed 5 min at 37 °C, and injected in BIAcore3000 at a flow rate of 20 µL/min for 3 min. RU were measured at the end of the injection period and used to calculate the inhibition of protein-DNA interaction. Dose response curve of SMARt-420 and BDM41906 were determined using GraphPad Prism. RU recorded during the binding EthR2 and DNA in absence of SMARt-420 was defined as "100% binding". Maximum efficacy of SMARt-420 was obtained at 100 µM (defined as 0% binding on the graph of fig.3B).

Thermal Shift Assays

Thermal Shift Assay on EthR2

The recombinant *M. tuberculosis* protein EthR2 (Rv0078) was used at a concentration of 10 µM. The fluorescent dye SYPRO® Orange (SigmaAldrich) was used to monitor EthR2 unfolding. This dye is environmentally sensitive and leads to an increase in fluorescence following exposure of hydrophobic regions during protein unfolding. The thermal shift assay was conducted in a Lightcycler 480 (Roche). The system contained a heating/cooling device for temperature control and a charge-coupled device (CCD) detector for real-time imaging of the fluorescence changes in the wells of the microplate. The final sample concentration was 10 µM EthR2, 2.5x SYPRO® Orange, 1% DMSO, and 20 µM ligand in the EthR2 buffer (20 mM HEPES, pH 7.5, 300 mM NaCl, 5% glycerol, 100 mM imidazole). The samples were heated from 37 to 85 °C with a heating rate of 0.04 °C/s. The fluorescence intensity was measured at Ex/Em = 465/510 nm. The data were processed using the algorithmic software Wavemetrics Igor by applying the following procedure: The fluorescence intensity of each well/sample is plotted as a function of the temperature. Then the 1D numerical derivative of these curves is calculated. Finally, the maximum data values, corresponding to the inflection points (T_m), are extracted.

Thermal Shift Assay on EthR

The procedure was performed in a similar manner than the one described for EthR2. Subtraction between the value of the respective Tm obtained with and without addition of ligand is defined as ΔTm and was used in the X axis of figure 1.A.

Production and purification of His6-EthR2

The DNA coding for EthR2 was amplified by PCR using *M. tuberculosis* H37Rv chromosomal DNA as template and oligonucleotides Rv0078up: 5'-GAAATCAAGAGACGCACCC-3' and Rv0078lo: 5'-TAGCCGTTAAGCATCCCGTCG-3' as primers. The PCR product was digested with *Nde*I and *Bam*HI, and inserted into pET-15b (Novagen), yielding pET-15b-*ethR2*. The *ethR2*-encoding fragment was sequenced on both strands. This plasmid encodes EthR2 containing an amino-terminal tag with the following sequence: $MGSSH_6SSGLVPRGSHM$ and was introduced into *E. coli* BL21 (DE3). *E. coli* BL21 (DE3) (pET-15b-*ethR2)* was grown in 2L LB broth to an $OD_{600\ nm}$ of 0.6-0.8. Isopropylthiogalactoside (IPTG) was added to a final concentration of 1 mM, and the culture was grown for an additional 3 hours. The cells were harvested by centrifugation at 12,000 x *g* at 4 °C. The pellet was frozen in liquid nitrogen and conserved at -20°C. After defrosting, the pellet was re-suspended in 40 mL of lysis buffer (20 mM HEPES, pH 7.5, 500 mM NaCl, 5% glycerol, 10 mM imidazole, Protease inhibitor cocktail (Roche)) and lysed by three passages through a French Pressure cell at 6.2 x 10^6 Pa. After centrifugation (15,000 x *g*, 30 min, 4 °C), the supernatant was recovered and His_6-EthR2 was separated from the whole-cell lysate using a 5 mL HisTrap affinity chromatography columns (GE healthcare). After extensive washing with 10, 20 and 40 mM imidazole in lysis buffer, His_6-EthR2 was eluted from the resin with 300 mM imidazole in lysis buffer

and dialysed overnight against "EthR2-buffer " (20 mM HEPES, pH 7.5, 300 mM NaCl, 5% glycerol, 100 mM imidazole). Approximately 5.9 mg/mL of purified protein was obtained as determined by the NanoVue^{TM} spectrophotometer (GE healthcare) using a molar extinction coefficient of ε=20910Lmol^{-1}cm^{-1}). Protein purity was determined by Coomassie blue staining after SDS-PAGE on a 12 % polyacrylamide gel. The purified protein was stored at – 80 °C until further use.

Crystal structure of EthR2 in complex with SMARt-420

EthR2 crystals were obtained by the vapour diffusion method at 293°K using a protein sample at 10 mg/mL and the following crystallization solution (200 mM NaCl, 200 mM Na citrate pH 4.2 and 15% polyethylene glycol monomethylether 5000). An iodine derivative for phasing was prepared using *in-crystal* iodination reaction that consisted in incubating a droplet containing EthR2 crystals in iodine vapour overnight at a temperature of 293°K. The iodinated EthR2 structure was then solved by Iodine-Single wavelength Anomalous Dispersion method (I-SAD). The structure of EthR2 was obtained in the absence of SMARt-420 (an unliganded form), by molecular replacement using the iodinated structure as search model. The structures of iodinated and unliganded EthR2 were deposited in the Protein Data Bank under accession codes **5n1c** and **5n1i**, respectively. Crystals of the complex EthR2/SMARt-420 were then prepared by soaking EthR2 crystals for ~1 min in the crystallization buffer containing 1 mM of SMARt-420. The X-ray diffraction data were collected on a Pilatus 6M detector using synchrotron radiation on the ESRF-ID23 beamline. Indexing was performed using the XDS program(*39*).The structure of the complex was solved by molecular replacement with MOLREP (*40*) using the unliganded structure of EthR2 as search model. The structure was refined with REFMAC5 (*41*) at 2.40 Å resolution. Initially SMARt-420 was automatically fitted in the electron density using FINDLIGAND tool of the CCP4 software suite (*42*) and then manually positioned using Coot (*43*). Geometrical and chemical restraints of SMARt-420 were generated from the SMILES string using LIBCHECK. The final R and R_{free} values are 21.2% and 26.0%, respectively. Data collection and refinement statistics are shown inTable S2. The refined coordinates and the structure factors were deposited in the Protein Data Bank under the accession number **5icj**.

The omit map shown in figure 2D of the manuscript was obtained by removing ligand from the structure, then randomly shaking up all coordinates by a small amount (between 0 and 0.3 Å) with PDBSET program and finally running 20 cycles of refinement with REFMAC5.

Mammalian SEAP reporter assay

Vector design. A chimeric mammalian transcriptional regulator was constructed by fusing the coding sequence of EthR2 (Rv0078) from *Mycobacterium tuberculosis* to the *Herpes simplex* derived transactivator protein VP16. The resulting ORF was sequence-optimized for expression in human/mouse, synthesized (Genscript) and introduced into pSEAP2-control (Clontech) using EcoRI/XbaI to generate the expression vector pCK289 (P_{SV40}-EthR2-VP16-HA-pA). To enable EthR2-VP16 based transcriptional control, we

designed a synthetic DNA by fusing the 61 nucleotide spanning intergenic region of *ethA2* (Rv0077c) and *ethR2* (Rv0078) upstream of a minimal variant of the human cytomegalovirus derived promotor ($P_{hCMVmin}$). This synthetic promoter was cloned into pSEAP2-basic (Clontech) by restriction (XhoI/EcoRI) and ligation to generate pCK287 (O_{EthR2}-$P_{hCMVmin}$-SEAP-pA), which enables EthR2-VP16 based control of human placental secreted alkaline phosphatase (SEAP) expression.

Cell culture. Baby hamster kidney cells (BHK-21, American Type Culture Collection CCL-10) were cultured in Dulbecco's modified Eagle's medium (DMEM, Gibco, catalog no. 41966) supplemented with 10% (v/v) heat-inactivated fetal bovine serum (FBS, Gibco, catalog no. 10500) and 1% (v/v) penicillin/streptomycin (Gibco, catalog no. 15140) in a humidified atmosphere with 5% CO_2 at 37°C. Prior to transfection, cells from a confluent grown culture dish were split 1:2 to a new petri dish and grown for 16hours. For transfection, 10µg of total plasmid DNA (5µg pCK287 and 5µg pCK289, ratio 1:1) were added to 1mL Opti-MEM reduced serum medium (Gibco, catalog no. 11058021), mixed with 30µL MegaTran 1.0 transfection reagent (Origene, catalog no. TT200003) and incubated for 15min at room temperature. The DNA mix was transferred to the cells and incubated for 6h for plasmid uptake. The cells were detached from the plate with 0.05% trypsin-EDTA (Gibco, catalog no. 25300), counted and diluted to 500.000 cells/mL using fresh culture medium. Hundred microliter of cell suspension was dispersed per well of a 96 well culture dish. Compound dilutions were prepared by adding 1.2µL compounds (10mM stock solution in DMSO) to 600µL culture medium, 1:2 dilution rows were prepared, and 100µL of compound dilutions were finally added to the cells. After incubation for 48h the SEAP expression was quantified from cell culture supernatants using a p-nitrophenyl phosphate based method (*44*).

Intracellular Assay

The detailed procedure is described in Delorme *et al.* (*45*). Briefly, Raw264.7 macrophages (10^8 cells) were infected with an H37Rv-GFP suspension at a multiplicity of infection (MOI) of 1:1 in 300 mL for 2 h at 37 °C with shaking (100 rpm). After two washes by centrifugation at 1100 rpm for 5 min, the remaining extracellular bacilli were killed by a 1 h amikacin (20 µM, Sigma, A2324-5G) treatment. After a final centrifugation step, 40 µL of *M. tuberculosis* H37Rv-GFP colonized macrophages were dispensed with a Wellmate (Matrix) into 384-well Evotec plates pre-plated with 10 µL of compound-mixture diluted in cell medium and incubated for 5 days at 37 °C, 5% CO_2. Macrophages were stained with SYTO 60 (Invitrogen, S11342) for 1 h followed by plate sealing. Confocal images were recorded on an automated fluorescent ultra-high-throughput microscope Opera (PerkinElmer). Images were acquired with a 20x water-immersion objective (NA = 0.70). A double laser excitation (488 and 635 nm) and dedicated dichroic mirrors were used to record green fluorescence of mycobacteria and red fluorescence of the macrophages on two independant cameras. A series of four pictures at the center of each well were taken, and each image was then processed using dedicated image analysis (Acapella Studio, Perkin Elmer). The percentage of infected cells and the number of cells are the two parameters extracted from image analysis as previously reported (*45*). Reported data are the average of two replicates.

Extracellular potency Assay of Test Compounds on *M. tuberculosis* (Ethionamide Concentration Fixed at 0.1 µg/mL, Serial Dilution of Test-Compounds).

Ethionamide (Sigma, E6005-5G) was diluted in DMSO at 0.1 mg/mL, and aliquots were stored frozen at −20 °C. Test-compounds were resuspended in DMSO at a concentration of 10 µM. Ethionamide and test-compounds were transferred to a 384-well low-volume polypropylene plate (Corning, no. 3672) and used to prepare essay plates. Briefly, ten 3-fold serial dilutions of compounds were performed into black Greiner 384-well clear bottom polystyrene plates (Greiner, no. 781091) using an Echo 550 liquid Handler (Labcyte). DMSO volume was compensated so that the concentration across all wells was equal (0.3%). Two independent replicates were made for each setting. Finally an equal volume of ethionamide (final concentration 0.1 µg/ml) was transferred to one of the 384-well replicates, using Echo. On the day of the experiment, 50 µL of *M. tuberculosis*-GFP culture diluted to an OD600 nm of 0.02 was transferred to each assay plate and incubated at 37ºC for 5 days. Fluorescent signal were acquired on a Victor multilabel plate reader (PerkinElmer), using exc=485nm/em=535nm.

Synthesis of SMARt-420 (BDM41420)

Chemical pathway:

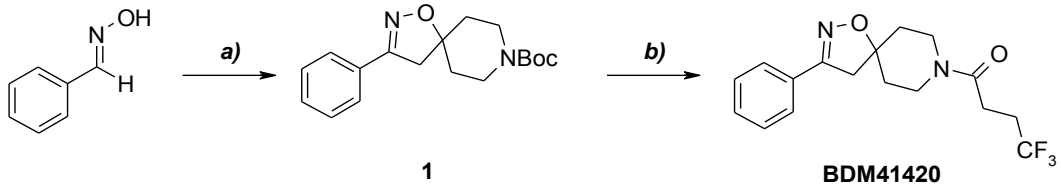

a) Synthesis of tert-butyl 3-phenyl-1-oxa-2,8-diazaspiro[4.5]dec-2-ene-8-carboxylate (1).

(E)-benzaldehyde oxime (2.77 ml, 25.34 mmol) was solubilized in dichloromethane (100 ml) and dimethylformamide (8 ml) was added. N-Chlorosuccinimide (3.72 g, 27.88 mmol) was added portion-wise over 30 min to the stirred mixture at 0°C. Tert-butyl 4-methylenepiperidine-1-carboxylate (5 g, 25.34 mmol) was then added to the mixture followed by the slow addition of triethylamine (10.61 ml, 76.03 mmol). The resulting solution was stirred at room temperature for 24 hours. After completion, the mixture was quenched with 1N HCl. The organic layer was extracted with DCM (2x100mL) then dried over magnesium sulfate, filtered and concentrated in *vacuo*. The crude residue was purified by flash column chromatography using cyclohexane / AcOEt as eluent to afford 4.3 g (50.8%) of tert-butyl 3-phenyl-1-oxa-2,8-diazaspiro[4.5]dec-2-ene-8-carboxylate.

NMR ^{1}H (CD_2Cl_2, 300 MHz) δ(ppm) 1.48 (s, 9H, CH_3 Boc), 1.72-1.93 (m, 4H, CH_2), 3.13 (s, 2H, CH_2 isoxazoline), 3.41-3.72 (m, 4H, CH_2), 7.44 (m, 3H, HAr), 7.67 (m, 2H, HAr). NMR ^{13}C (CD_2Cl_2, 75 MHz) δ (ppm) 28.2 (CH_3 Boc), 35.8, 45.0 (CH_2 pip), 79.3 (Cq Boc), 84.5 (CH_2 isoxazoline), 126.4, 126.7, 129.9, 130.1 (CAr), 154.4 (C=O Boc), 156.2 (C=N). LC-MS : $[M\text{-}tBu+H]^+$ 261, purity >99%.

b) Synthesis of 4,4,4-trifluoro-1-(3-phenyl-1-oxa-2,8-diazaspiro[4.5]dec-2-en-8-yl)butan-1-one BDM41420 (SMARt-420).

Tert-butyl 3-phenyl-1-oxa-2,8-diazaspiro[4.5]dec-2-ene-8-carboxylate (4.09 g, 12.92 mmol) was solubilized in dichloromethane (20 ml). Trifluoroacetic acid (20 ml, 261.35 mmol) was added dropwise. After completion, the mixture was quenched with aqueous saturated sodium carbonate solution. The organic layer was extracted with DCM (2x25 mL) and concentrated in *vacuo*. The resultant crude oil was then diluted in DMF. HBTU (7.35 g, 19.39 mmol) and 4,4,4-Triflurobutanoic acid (1.84 g, 12.92 mmol) were added to the stirred solution followed by a dropwise addition of DIEA (3.35 ml, 19.39 mmol). The mixture was stirred at room temperature for 24 hours. The resulting crude mixture was quenched with 100 ml saturated NH_4Cl and 100 ml Methyl tert-butyl ether (MTBE). The aqueous layer was then extracted with MTBE (3x100 ml). The organic layers were collected and evaporated in *vacuo*. The resulting oil was recrystallized using diethyl ether and isopropanol to yield 3.57 g of 4,4,4-trifluoro-1-(3-phenyl-1-oxa-2,8-diazaspiro[4.5]dec-2-en-8-yl)butan-1-one.

NMR ^{1}H (CD_2Cl_2, 300 MHz): δ*(ppm)* 1.72-1.83 (m, 2H), 1.90-2.04 (m, 2H), 2.45-2.61 (m, 4H), 3.16 (s, 2H), 3.42 (m, 1H), 3.56 (m, 2H), 4.18 (m, 1H), 7.47 (m, 3H), 7.70 (m, 2H). NMR ^{13}C (CD_2Cl_2, 75 MHz): δ*(ppm)* 25.8, 29.5 (q, *J*=29.1Hz), 35.5, 36.2, 39.0, 42.4, 45.3, 84.0, 126.4, 127.6 (q, *J*=273.7 Hz), 128.7, 130.0, 156.3, 167.8. $[M+H]^+$ 342, purity > 95%.

M. tuberculosis strain E1

The *M. tuberculosis* strain E1 used in the animal experiment (see fig.4), in experiment S2 and in experiment S4 is a derivative of the Beijing strain W4 that carries a Gly343Ala mutation in EthA, which causes resistance to ethionamide (MIC > 32µg/mL measured by MGIT960).

Antibiotic profile and lineage of the *M. tuberculosis* clinical strains used in this study.

Threshold concentrations above which bacteria are considered clinically resistant are indicated in parenthesis. The drug sensitivity status of each strain is reported, S (Sentitive) meaning "under the threshold concentration", and R (Resistant) meaning "above the threshold concentration". Specifically, for ETH, Minimal Inhibitory Concentrations have been defined by MGIT960 and are reported (values in µg/mL). Bacteria are considered sensitive (greenbox) when MIC is bellow 5µg/mL, and resistant (red box) when MIC is above this value.

TB strains	INH (0.1 µg/ml)	RIF (1 µg/ml)	EMB (5 µg/ml)	OFL (1 µg/ml)	AMI (1 µg/ml)	ETH (5 µg/ml)	EthA status	Strain lineage
H37Rv	**S**	**S**	**S**	**S**	**S**	**2**	wt	Euro-American
L4376	**R**	**R**	**R**			**4**	wt	nd
LPN30	**R**	**R**				**2**	nd	nd
L1094	**R**	**R**	**R**			**2**	wt	nd
P591	**R**	**R**				**2**	nd	nd
L0578	**R**	**R**	**S**			**1**	wt	nd
B1166	**R**	**R**	**R**	**S**	**R**	**64**	wt	Beijing
B1196	**R**	**R**	**S**	**S**	**S**	**32**	wt	CAS1_DELHI
B1004	**R**	**R**	**R**	**R**	**R**	**32**	wt	Beijing
B1304	**R**	**R**	**S**	**S**	**S**	**32**	wt	Beijing
P379	**R**	**R**				**32**	wt	nd
B1001	**R**	**R**	**R**	**S**	**S**	**32**	wt	Beijing
B0383	**R**	**R**	**S**	**S**	**S**	**16**	wt	Haarlem2
B0391	**R**	**R**	**R**	**R**	**R**	**8**	wt	Beijing
B0089	**R**	**R**	**R**	**S**	**S**	**8**	wt	T1
LPN4	**R**	**R**				**8**	wt	nd
P395	**R**	**R**	**S**			**8**	wt	nd
P359	**R**	**R**	**S**			**8**	wt	nd
P351	**R**	**R**				**8**	wt	nd
B1150	**R**	**R**	**R**	**R**	**S**	**256**	P230Q	Beijing
B1602	**R**	**R**	**R**	**R**	**R**	**256**	R239G	LAM9
B0775	**R**	**R**	**R**	**S**	**S**	**256**	Δa110	Beijing
B0057	**R**	**R**	**R**	**S**	**S**	**64**	Δa110	CAS1_DELHI
L3556	**R**	**R**				**64**	Q165P	nd
B0467	**R**	**R**	**R**	**S**	**S**	**64**	wt	Beijing
L0728	**R**	**R**	**R**			**64**	ins.c357	nd

Fig. S1.

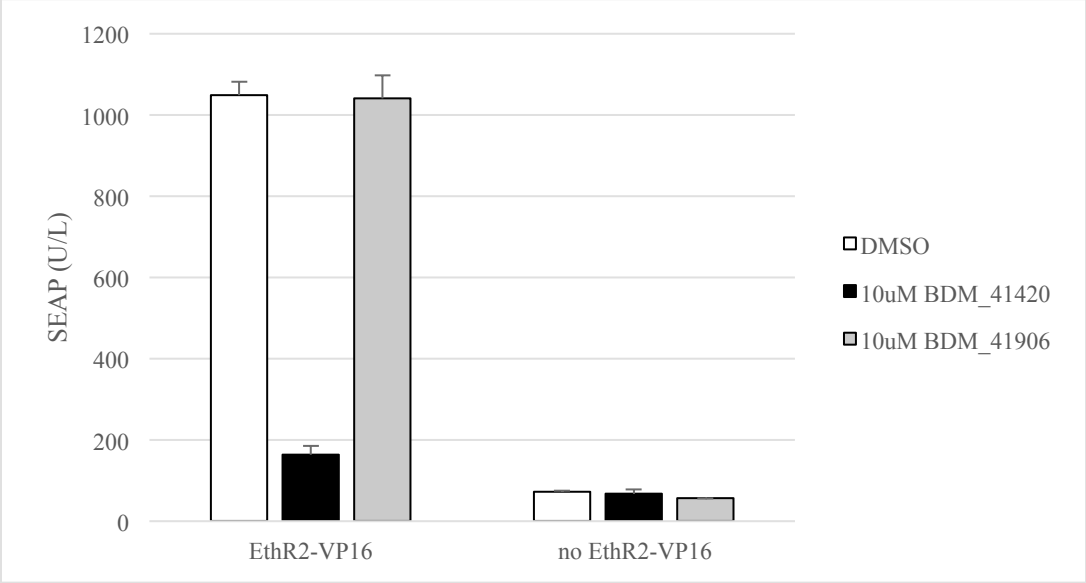

Extended controls on the Mammalian reporter assay

These additional data compares the SEAP activity in BHK-21 cells transfected with pCK287 (containing the DNA intergenic region of *ethA2-ethR2*), in combination with either pCK289 (expressing the EthR2-VP16 complex) or the equivalent empty vector (no EthR2-VP16). These two type of cells were treated with either DMSO (white bars), 10 µM BDM41420 (SMARt-420) (Black bars) or 10 µM BDM41906 (Grey bars). This additional control shows that SMARt-420 inhibits SEAP activity almost as completely as the one measured in cells that do not contain the transactivating complex EthR2-VP16. On the contrary, BDM41906 has no detectable effect, confirming the specificity of interaction of SMARt-420 with EthR2. Graphs show the average of two independent experiments.

Sixteen hours prior infection, 20.000 BHK-21 cells were seeded in 200µL medium to a 96 well plate. For transfection, 10µg of total plasmid DNA (5µg pCK287 were mixed with 5µg pCK289 or empty control vector pcDNA3.1, ratio 1:1) were added to 1mL Opti-MEM reduced serum medium (Gibco, catalog no. 11058021), mixed with 30µL MegaTran 1.0 transfection reagent (Origene, catalog no. TT200003) and incubated for 15min at room temperature. Twenty microliter of the DNA mixes were transferred to the cells and incubated for 6h for plasmid uptake. The medium discarded and replaced by fresh medium containing DMSO, 10µM BDM_41420 or BDM_41906, respectively. SEAP expression was determined after 48h of expression.

Fig. S2

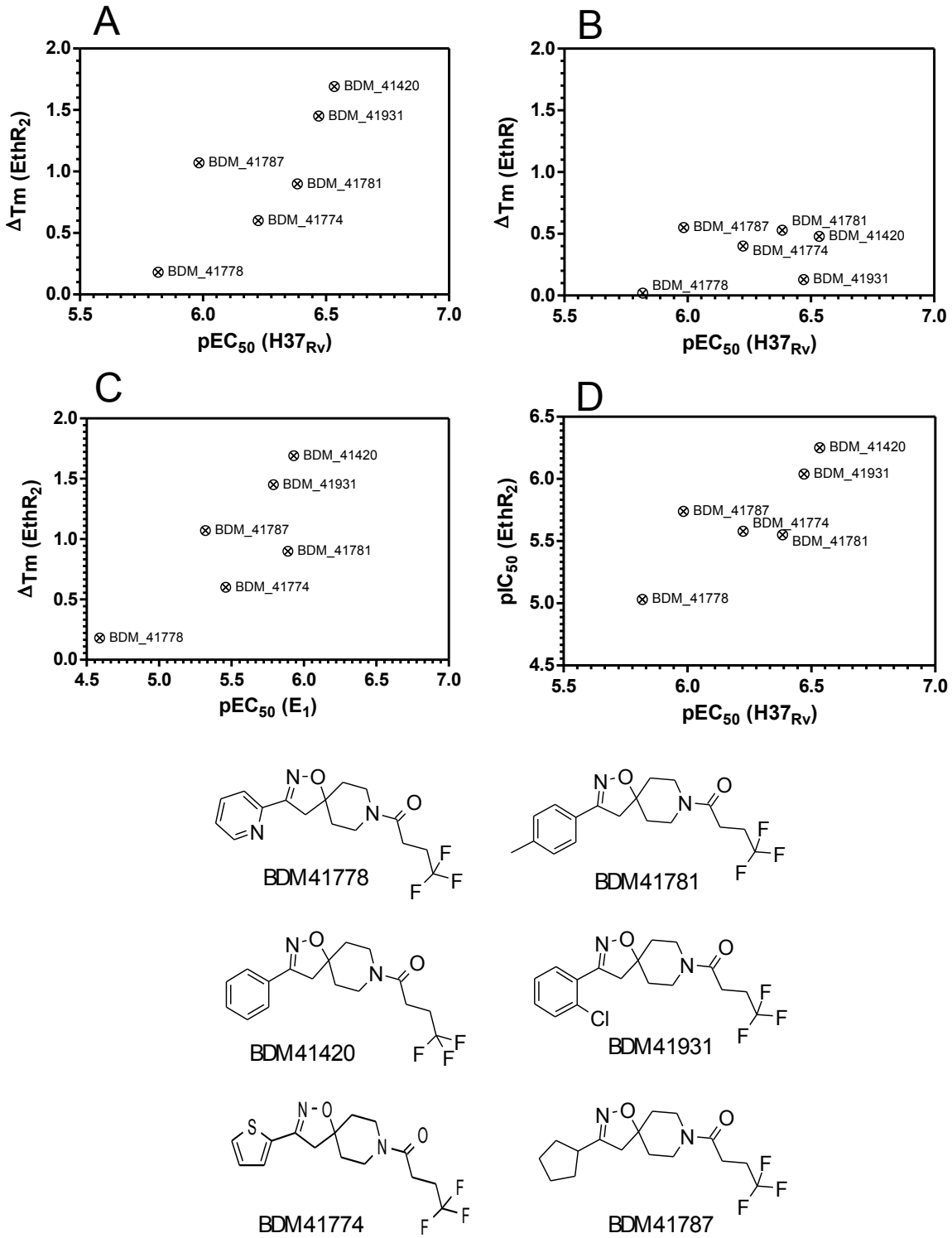
A
ΔTm (EthR2)
pEC50 (H37Rv)
BDM_41420
BDM_41931
BDM_41787
BDM_41781
BDM_41774
BDM_41778
B
ΔTm (EthR)
pEC50 (H37Rv)
BDM_41787
BDM_41781
BDM_41420
BDM_41774
BDM_41778
BDM_41931
C
ΔTm (EthR2)
pEC50 (E1)
BDM_41420
BDM_41931
BDM_41787
BDM_41781
BDM_41774
BDM_41778
D
pIC50 (EthR2)
pEC50 (H37Rv)
BDM_41420
BDM_41931
BDM_41787
BDM_41774
BDM_41781
BDM_41778
BDM41778
BDM41781
BDM41420
BDM41931
BDM41774
BDM41787

Multidimentionnal SAR in the Spiroisoxazoline family. Graphs of correlation between thermal shift assay (ΔTm, see fig. 2C), DNA binding assay (pIC_{50}, SEAP reporter assay, see fig. 3A), and boosting effect on bacteria (pEC50, as described in Section Material and Methods – Extracellular potency assay) for 5 direct analogues of SMARt-420 (BDM41420).
Graph A shows that the capacity of these 5 compounds to boost ETH in H37Rv (pEC_{50}) correlates with their binding efficacy to EthR2 (ΔTm), whereas no correlation is observed for EthR (Graph B). Graph C shows that mutation in EthA (TB strain E1, see description in Material and methods) do not modify this correlation. Graph D shows that the inhibition of the binding capacity of EthR2 onto its DNA operator (pIC_{50}) by these 5 compounds is correlated with their ETH-boosting effect. More precisely, introduction of a chlorine atom on the ortho-position of the phenyl ring (BDM41931) does not impair activity, while substitution of the para-position with a methyl group (BDM41781) leads to a decrease of activity.
These observations are in accordance with the X-ray structure of the $EthR_2$/SMARt-420 complex. Replacement of the phenyl ring with thiophenyl (BDM41774), or pyridinyl (BDM41778) and cyclopropyl (BDM41787) motifs leads to a loss of activity.

Fig. S3

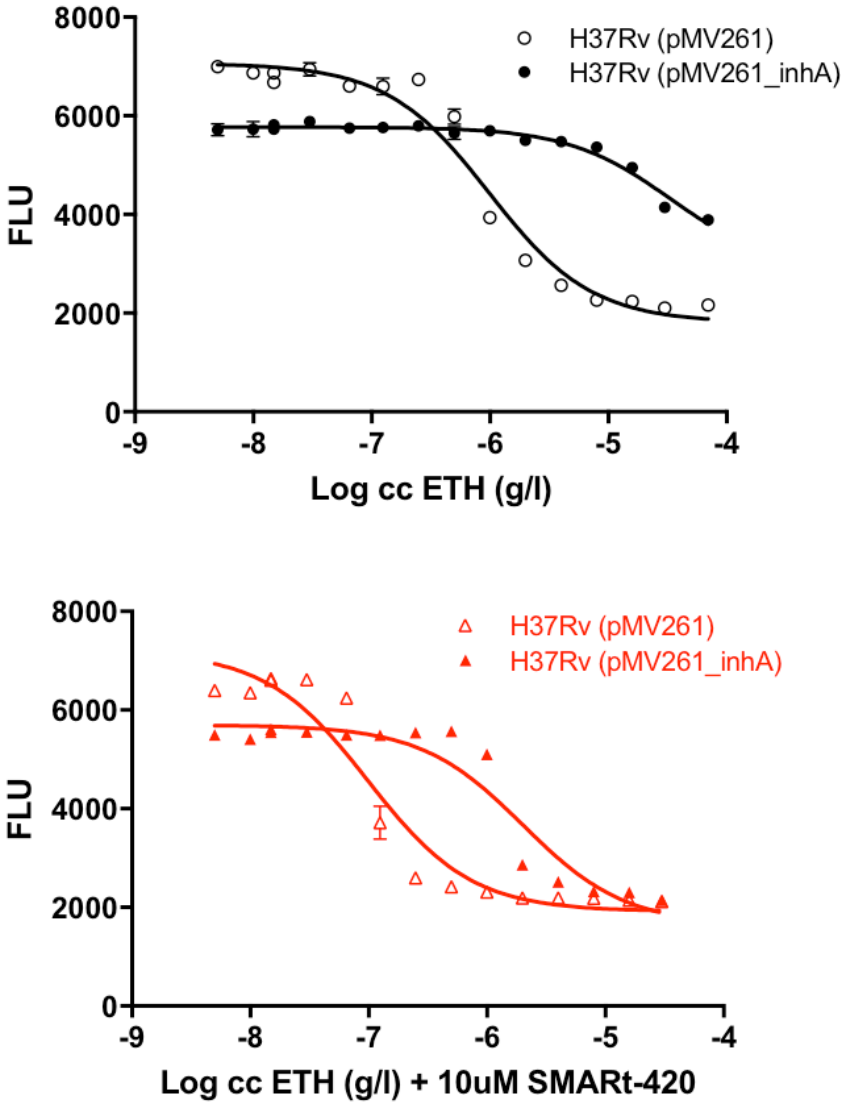

Effect of the overexpression of *inhA* onto the boosting effect of SMARt-420. The test is performed with an H37Rv derivative expressing GFP (H37Rv-GFP). FLU are arbitrary Units of Fluorescence measured after 5 days of growth, as described in Delorme *et al.* (*45*). Dose response curves ("Log cc" is the log of the concentration) of ETH (upper graph in black) versus ETH + fix dose (10 µM) of SMARt-420 (lower graph in red) measured on *M. tuberculosis* overexpressing InhA (pMV261-*inhA*) and on *M. tuberculosis* (empty plasmid pMV261). Black curves show that, as expected, overexpressing *inhA* impacts on the MIC of ETH. Red curves show that SMARt-420 reduces the MIC of ETH (open red triangles) and that overexpression of *inhA* impact on this MIC (plain red triangles). Altogether, these data strongly suggest that the bioactivation of ETH mediated by SMARt-420 keeps targeting InhA.

Fig. S4

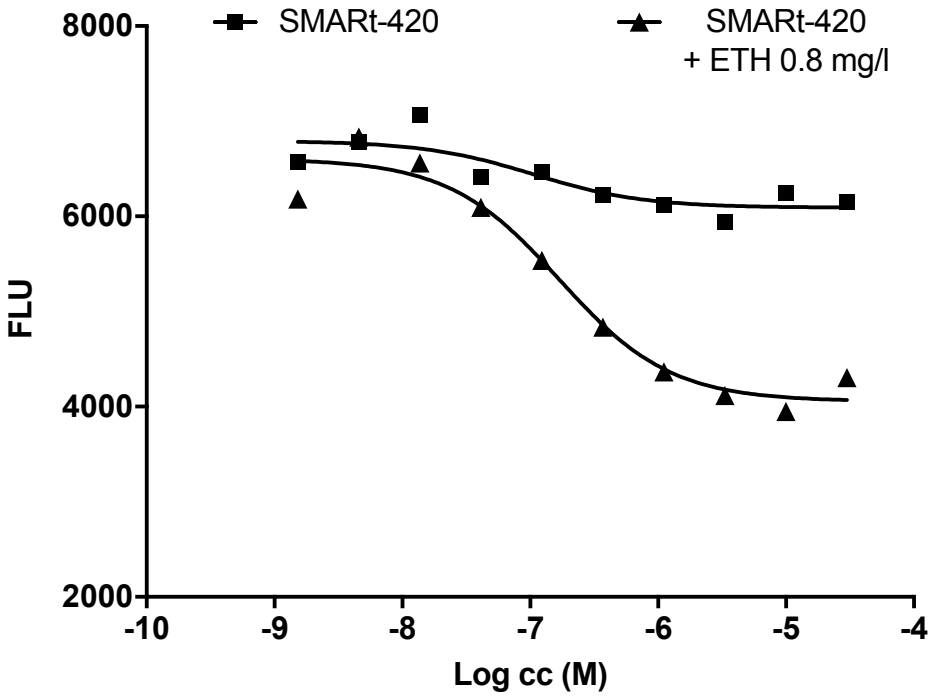

Dose response curve (DRC) of SMARt-420 alone (plain squares) or in the presence of a fix dose ETH (0.8 µg/mL) (plain triangles). The E1 strain (mutated in EthA) is resistant to high doses of ETH (> 25 µg/mL). This DRC of SMARt-420 was done in the presence of a sub-inhibitory dose of ETH (0.8 µg/mL). The dose of SMARt-420 that allows ETH at 0.8 µg/mL to inhibit the growth of the E1 strain is defined as the "Effective Concentration 50% " (EC50). Under such conditions, the EC50 of SMARt-420 was determined as 1.7 10^{-7}M. FLU are arbitrary Units of Fluorescence measured after 5 days of growth

Fig. S5

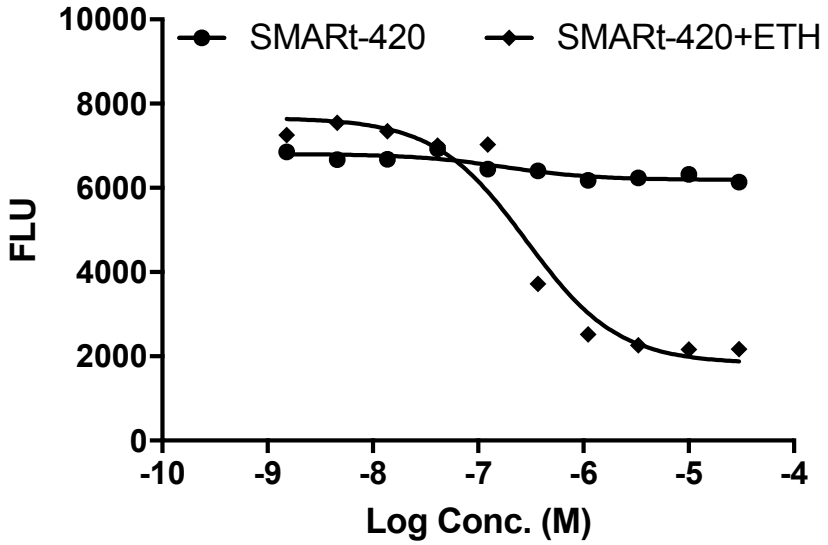

Dose response curve of SMARt-420 alone (plain circles) or in the presence of a fixed dose ETH (0.1 µg/mL) (plain diamonds). Compounds were tested for the antibacterial activity against H37Rv-GFP as previously described (*45*). FLU are arbitrary Units of Fluorescence measured after 5 days of growth

Table S1.

ID_STRUCTURE	Tm(EthR)	Tm (+ligand)	Unit	deltaTM	EC50	pEC50
BDM_14801	62.26	68.24	°C	5.98	1.20E-06	5.92E+00
BDM_31343	62.11	65.67	°C	3.56	4.70E-06	5.33E+00
BDM_31344	62.11	70.07	°C	7.96	2.00E-07	6.70E+00
BDM_31368	62.11	67.41	°C	5.3	2.50E-06	5.60E+00
BDM_31369	61.35	70.48	°C	9.13	1.00E-07	7.00E+00
BDM_31371	62.81	71.26	°C	8.45	1.00E-07	7.00E+00
BDM_31372	62.11	68.04	°C	5.93	3.00E-07	6.52E+00
BDM_31377	62.11	70.62	°C	8.51	4.00E-07	6.40E+00
BDM_31381	60.67	71.12	°C	10.45	1.00E-07	7.00E+00
BDM_41154	62.25	67.29	°C	5.04	2.00E-05	4.70E+00
BDM_41182	62.25	69.4	°C	7.15	1.30E-06	5.89E+00
BDM_41183	62.25	68.75	°C	6.5	1.30E-06	5.89E+00
BDM_41231	62.25	69.65	°C	7.4	5.00E-07	6.30E+00
BDM_41231	62.31	71.28	°C	8.97	5.00E-07	6.30E+00
BDM_41269	60.67	66.96	°C	6.29	3.20E-06	5.49E+00
BDM_41272	60.67	69.19	°C	8.52	8.00E-07	6.10E+00
BDM_41273	60.67	67.27	°C	6.6	1.00E-06	6.00E+00
BDM_41280	60.67	68.28	°C	7.61	1.00E-06	6.00E+00
BDM_41281	60.67	70.41	°C	9.74	4.00E-07	6.40E+00
BDM_41323	60.67	65.44	°C	4.77	1.00E-05	5.00E+00
BDM_41325	62.81	73.18	°C	10.37	2.00E-07	6.70E+00
BDM_41329	62.81	67.72	°C	4.91	5.70E-06	5.24E+00
BDM_41330	60.67	66.45	°C	5.78	6.30E-06	5.20E+00
BDM_41425	62.31	69.68	°C	7.37	5.00E-07	6.30E+00
BDM_41437	62.81	70.01	°C	7.2	2.50E-06	5.60E+00
BDM_41471	62.81	71.06	°C	8.25	2.50E-06	5.60E+00
BDM_41523	62.81	71.87	°C	9.06	6.30E-06	5.20E+00
BDM_41701	61.35	67.08	°C	5.73	2.10E-06	5.68E+00
BDM_41702	61.35	70.51	°C	9.16	1.10E-06	5.96E+00
BDM_41711	61.35	69.34	°C	7.99	1.00E-06	6.00E+00
BDM_41715	61.35	69.57	°C	8.22	7.90E-06	5.10E+00
BDM_41719	61.35	69.52	°C	8.17	1.00E-05	5.00E+00
BDM_41722	61.35	68.92	°C	7.57	1.00E-05	5.00E+00
BDM_41726	61.35	69.72	°C	8.37	1.00E-05	5.00E+00
BDM_41732	61.35	69.76	°C	8.41	1.00E-05	5.00E+00
BDM_41734	61.35	69.84	°C	8.49	2.20E-06	5.66E+00
BDM_41736	61.35	68.98	°C	7.63	2.30E-06	5.64E+00
BDM_41746	61.35	67.44	°C	6.09	4.30E-06	5.37E+00
BDM_41752	61.35	69.83	°C	8.48	9.30E-06	5.03E+00
BDM_41773	61.35	66.4	°C	5.05	4.00E-06	5.40E+00
BDM_41906	62.31	73.5	°C	11.19	6.00E-08	7.22E+00
BDM_41946	62.31	72.02	°C	9.71	1.00E-05	5.00E+00
BDM_41948	62.31	72.08	°C	9.77	4.00E-06	5.40E+00
BDM_41950	62.31	71.6	°C	9.29	8.00E-07	6.10E+00
BDM_41952	62.31	68	°C	5.69	6.30E-06	5.20E+00
BDM_41955	62.31	70.69	°C	8.38	7.90E-06	5.10E+00
BDM_41956	62.84	72.13	°C	9.29	2.90E-07	6.54E+00
BDM_43125	62.84	71.32	°C	8.48	1.20E-06	5.92E+00
BDM_43266	66.35	77.86	°C	11.51	8.00E-08	7.10E+00

BDM_31827	65.06	75.7	°C	10.64	2.10E-07	6.68E+00
BDM_32024	62.84	71.83	°C	8.99	3.40E-07	6.47E+00
BDM_31883	66.35	71.5	°C	5.15	2.20E-06	5.66E+00
BDM_41774	61.35	63.45	°C	2.1	3.00E-08	7.52E+00
BDM_41776	61.35	62.74	°C	1.39	4.00E-08	7.40E+00
BDM_41420	61.35	63.08	°C	1.73	2.00E-08	7.70E+00
BDM_41781	61.35	62.99	°C	1.64	2.50E-06	5.60E+00
BDM_41938	62.31	63.59	°C	1.28	2.00E-08	7.70E+00
BDM_41931	66.29	66.97	°C	0.68	3.00E-08	7.52E+00
BDM_43100	62.84	64.27	°C	1.43	2.00E-08	7.70E+00

Thermal shift values and EC_{50} from Intracellular Assay (described in Materials and Methods) presented in Fig. 1A

Table S2.

	I-derivative	unliganded	SMARt-420
PDB Accession number	**5n1c**	**5n1i**	**5icj**
Data Collection[a]			
X-ray generator	Rigaku Cu*K*□	Soleil-proxima1	ESRF-ID23
Detector	Saturn944+	Pilatus 6M	Pilatus 6M
Crystal-to-detector distance (mm)	70.00	344.6	312.9
Wavelength (Å)	1.5418	0.98011	0.97934
Number of images	1080	1000	720
Oscillation width (°)	1.0	0.2	0.5
Space group	$P2_12_12_1$	$P2_12_12_1$	$P2_12_12_1$
Unit cell parameters (Å)	59.7; 74.9; 87.5	59.6; 74.1; 89.1	59.8; 74.2; 88.1
Resolution range (Å)	60.0-2.6 (2.67-2.60)	50.0-2.4 (2.54-2.40)	60.0-2.4 (2.54-2.40)
Completeness (%)	99.6 (98.9)	99.0 (94.7)	99.8 (98.8)
No. of unique reflections	12520 (901)	16231 (2440)	15892 (2494)
Redundancy	38.5 (26.2)	7.0 (7.1)	12.8 (13.1)
R_{meas}[b]	0.234 (1.7)	0.083 (0.83)	0.121 (1.11)
$\langle I/\sigma(I)\rangle$[c]	19.3 (2.6)	14.5 (2.5)	19.2 (2.8)
$CC_{1/2}$[d]	0.999 (0.70)	0.999 (0.88)	0.999 (0.85)
Wilson B factor (Å^2)	49.3	60.4	52.2
Refinement data statistics			
Resolution limits (Å)	57.1-2.6	38.4-2.4	37.9-2.4
Number of reflections[e]	11878(626)	15361(809)	15053(793)
Number of refined atoms			
protein	2911	2861	2783
water	6	4	3
iodine	9	0	0
ligand	0	0	48
Final R_{work}[f]/R_{free}[g] (%)	24.3/30.8	22.2/26.9	21.2/26.0
RMSD bond lengths (Å)	0.012	0.012	0.013
RMSD bond angles (°)	1.553	1.515	1.578
Overall mean B factor (Å^2)			
protein	48.8	60.8	50.0
ligand	-	-	61.5
solvent	31.2	50.0	48.0
MolProbity statistics			
Ramachandran favoured (%)[h]	97.4	99.7	100.0
Ramachandran outliers (%)[h]	0.0	0.0	0.0
Clash score all-atom	5.32 (99th)	3.64 (99th)	2.67 (100th)
MolProbity score	1.80 (99th)	1.15 (100th)	1.32 (100th)

[a]For data-collection, the numbers in parentheses represent values for the highest resolution shell.

[b] $R_{meas} = \sum_{hkl} [N/(N-1)]^{1/2} \sum_i |I_i(hkl) - \langle I(hkl)\rangle| / \sum_{hkl} \sum_i I_i(hkl)$, is the multiplicity (N) independent R_{merge}, where I_i is the intensity of the ith observation and $\langle I \rangle$ is the mean intensity of the reflections.
[c] $\langle I/\sigma(I)\rangle$ = mean of I/σ(I)of unique reflections.
[d] The mean intensity correlation coefficient of half-datasets.
[e] Numbers in parentheses are the number of reflections in the free set.

Data collection and refinement statistics for X-ray data. "I-derivative" stands for EthR2 iodinated derivative, "unliganded" stands for the unliganded form of EthR2, "SMARt-420" stands for the form of EthR2 liganded with SMARt-420.

Table S3.

See separated associated file.

Locus Rv0077-Rv0078 of ETH^r and ETH^s clinical isolates. Snip analysis in Casali's dataset of ETH sensitive and ETH resistant clinical isolates. See interpretation of the data in the main text. Genomes analyzed in this work are from strains described in Casali et al (*30*).

Table S4.

AB + No cpd [1]		AB + cpd at 0.3 µM		AB + cpd at 2.5 µM	
	MIC90 (M)		MIC90 (M)		MIC90 (M)
MOX	6.53E-08	MOX + BDM41906	9.12E-08	MOX + BDM41906	9.37E-08
		MOX + SMARt-420	8.59E-08	MOX + SMARt-420	9.35E-08
LNZ	4.03E-07	LNZ + BDM41906	3.92E-07	LNZ + BDM41906	3.88E-07
		LNZ + SMARt-420	3.77E-07	LNZ + SMARt-420	3.98E-07
TMC207	1.52E-07	TMC207 + BDM41906	5.17E-07	TMC207 + BDM41906	3.75E-07
		TMC207 + SMARt-420	4.09E-07	TMC207 + SMARt-420	4.05E-07
EMB	3.89E-06	EMB + BDM41906	3.32E-06	EMB + BDM41906	3.28E-06
		EMB + SMARt-420	3.30E-06	EMB + SMARt-420	3.29E-06
PA284	2.81E-07	PA284 + BDM41906	1.30E-07	PA284 + BDM41906	1.24E-07
		PA284 + SMARt-420	1.25E-07	PA284 + SMARt-420	1.35E-07
INH	7.63E-07	INH + BDM41906	3.28E-07	INH + BDM41906	1.91E-07
		INH + SMARt-420	3.10E-07	INH + SMARt-420	2.70E-07

Effect of SMARt-420 onto the MIC of anti-TB compounds other than ETH. To verify the specificity of action of BDM41906 and SMARt-420, these compounds were tested in combination with Moxifloxacin, Linezolid, Bedaquiline, Ethambutol, PA824, Isoniazid against H37Rv-GFP, as previously described (*45*). Neither BDM41906 nor SMARt-420 changed significantly the MIC90 of these antibiotics. [1] "AB" stands for antibiotics and "cpd" means compound BDM41906 or SMARt-420
MIC have been determined using MGIT Bactec 960.

Table S5.

SMARt-420	MW	340.4 g/mol
	Solubility	44 µg/mL
	Human Cl_{int}	0.6 µL.min^{-1}/mg
	Mouse Cl_{int}	98 µL.min^{-1}/mg
	AUC*	2.63 µg.h/mL
	Cmax*	4.9 µg/mL
	$t_{1/2}$	19 min
	A-B permeability	75.7 10^{-6} cm/s
	B-A permeability	29.4 10^{-6} cm/s
	$t_{1/2}$ human plasma	>24h

*PO @ 30 mpk

Pharmacokinetic profile of SMARt-420. The cyclodextrine vehicle-solution was prepared by dissolving 4.015 g of HP-β-CD (MW=1481 g.mol^{-1}; Roquette, France) in 8 mL of milliQ-H_2O. The solution was sonicated until complete transparency was reached and filtered on PTFE 0.2µm. The preparation of a stock solution of SMARt-420 was made as follow: 3.13 mg of SMARt-420 was transferred in 2 mL tubes containing 1 mL of the cyclodextrine vehicle-solution. Tubes were sonicated for 4 min and shaken (1000 rpm) at 50°C for 4h. 200 µL of this solution were given to mice, which correspond to ±30 mg.kg^{-1} for 20g mice.

Seven Groups of Swiss female mice (SPF OF1) (18-21 g) were given 200 µL of SMARt-420 orally at 30 mg.kg^{-1}. Replicates of three mice were anesthetized with ketamine-xyalzine and bled at 10, 20, 30, 60,120, 240 and 480 minutes after administration of a single dose of SMARt-420. Blood was collected from the brachial vein. Blood samples were centrifuged (5000 g, 15 min) for plasma separation, and the serum was subjected to LC-MS/MS analysis. The LC-MS/MS system used was a UPLC I Class – Xevo TQD. Analytes in incubation mixtures were separated by HPLC using an Acquity BEH C18 50x2.1mm, 1.7µm column. The mobile phase solvents used were: (A) 0.1% formic acid in water; (B) 0.1% formic acid in acetonitrile. The injection volume was 1 µl, and the flow rate was 0.6 mL/min.

The facilities conformed to Directive 86/609/EEC on the Protection of Animals Used for Experimental and Other Scientific Purposes and norms published in the European Council ETS123 Appendix A. Facilities and procedures complied with the Belgian Law of 14th of August 1986 on animal protection and welfare. Training of experimental leaders, bio-technicians and animal caretakers was in accordance with Royal decree of 13/9/2004, which specifies the training of persons working with laboratory animals. All animal experimentation and procedures were validated and approved by the Local Ethics Committee (IPH – Pasteur – VAR), which answers to the National Deontological Committee. The animal facilities and procedures were under the supervision of an expert on animal welfare in accordance with the Belgian Ministry of Health.

Table S6.

log of CFU in the lungs after 3 weeks of treatment (7d/week)	**Control**	**INH25**	**420L50**	**ETH50**	**ETH25**	**ETH50+420L50**	**ETH25+420L50**	**ETH10+420L50**
	6.84	2.4	6.51	5.58	7.03	2.3	4.11	4.93
	6.97	2.4	6.61	5.94	6.81	0 (exclu.)	3.18	5.29
	6.9	2.54	6.56	6.07	6.95	2.95	3.96	5.56
	6.85	2.6	6.38	5.61	6.66	2.9	4.18	4.93
	6.62	2.3	6	5.57	6.08	2.9	2.9	5.28

	Control	**INH25**	**420L50**	**ETH50**	**ETH25**	**ETH50+420L50**	**ETH25+420L50**	**ETH10+420L50**
Number of Mice	5	5	5	5	5	4	5	5
Minimum	6.6	2.3	6	5.6	6.1	2.3	2.9	4.9
25% Percentile	6.7	2.4	6.2	5.6	6.4	2.5	3	4.9
Median	6.9	2.4	6.5	5.6	6.8	2.9	4	5.3
75% Percentile	6.9	2.6	6.6	6	7	2.9	4.1	5.4
Maximum	7	2.6	6.6	6.1	7	3	4.2	5.6
Mean	6.8	2.4	6.4	5.8	6.7	2.8	3.7	5.2
Std. Deviation	0.13	0.12	0.25	0.23	0.38	0.31	0.59	0.27
Std. Error	0.059	0.054	0.11	0.1	0.17	0.15	0.26	0.12
Lower 95% CI	6.7	2.3	6.1	5.5	6.2	2.3	2.9	4.9
Upper 95% CI	7	2.6	6.7	6	7.2	3.3	4.4	5.5

Statistical Analysis: One-way analysis of variance

P value	< 0.0001
P value summary	****
Are means signif. different? (P < 0.05)	Yes
Number of groups	8
F	151
R square	0.97

ANOVA Table	SS	df	MS
Treatment (between columns)	106	7	15
Residual (within columns)	3.1	31	0.1
Total	109	38	

Bonferroni's Multiple Comparison Test	Mean Diff.	t	Significant? P < 0.05?	Summary	95% CI of diff
Control vs INH25	4.4	22	Yes	****	3.7 to 5.1
Control vs 420L50	0.42	2.1	No	ns	-0.26 to 1.1
Control vs ETH50	1.1	5.4	Yes	***	0.40 to 1.8
Control vs ETH25	0.13	0.65	No	ns	-0.55 to 0.81
Control vs ETH50+420L50	4.1	19	Yes	****	3.3 to 4.8
Control vs ETH25+420L50	3.2	16	Yes	****	2.5 to 3.9
Control vs ETH10+420L50	1.6	8.2	Yes	****	0.95 to 2.3
INH25 vs 420L50	-4	20	Yes	****	-4.6 to -3.3
INH25 vs ETH50	-3.3	17	Yes	****	-4.0 to -2.6
INH25 vs ETH25	-4.3	21	Yes	****	-4.9 to -3.6
INH25 vs ETH50+420L50	-0.31	1.5	No	ns	-1.0 to 0.41
INH25 vs ETH25+420L50	-1.2	6.1	Yes	****	-1.9 to -0.53
INH25 vs ETH10+420L50	-2.8	14	Yes	****	-3.4 to -2.1
420L50 vs ETH50	0.66	3.3	No	ns	-0.026 to 1.3
420L50 vs ETH25	-0.29	1.5	No	ns	-0.98 to 0.39
420L50 vs ETH50+420L50	3.6	17	Yes	****	2.9 to 4.4
420L50 vs ETH25+420L50	2.7	14	Yes	****	2.1 to 3.4
420L50 vs ETH10+420L50	1.2	6.1	Yes	****	0.53 to 1.9
ETH50 vs ETH25	-0.95	4.8	Yes	**	-1.6 to -0.27
ETH50 vs ETH50+420L50	3	14	Yes	****	2.3 to 3.7
ETH50 vs ETH25+420L50	2.1	10	Yes	****	1.4 to 2.8
ETH50 vs ETH10+420L50	0.56	2.8	No	ns	-0.13 to 1.2
ETH25 vs ETH50+420L50	3.9	19	Yes	****	3.2 to 4.7
ETH25 vs ETH25+420L50	3	15	Yes	****	2.4 to 3.7
ETH25 vs ETH10+420L50	1.5	7.5	Yes	****	0.82 to 2.2
ETH50+420L50 vs ETH25+420L50	-0.9	4.3	Yes	**	-1.6 to -0.18
ETH50+420L50 vs ETH10+420L50	-2.4	11	Yes	****	-3.2 to -1.7
ETH25+420L50 vs ETH10+420L50	-1.5	7.7	Yes	****	-2.2 to -0.85

Pharmacodynamic of SMARt-420 in combination with ETH on mice infected with ETH-resistant *M. tuberculosis*. One week after infection (with 10^4 mycobacteria), either with strain H37Rv (control) or with strain E1 (see Materials and Methods), the mice (BalbC) were treated 7 days per week for 3 weeks with the indicated doses of ETH and SMARt-420 (420L) expressed in mg/kg in Table S6. Except for the mice of the first untreated group that were sacrificed at day 1 (D1), all the surviving mice were sacrificed at the end of the treatment (day 28) and the pulmonary mycobacterial load was enumerated by CFU counts. Values in table S6 are log of the mean of the bacterial loads as measured by CFU counts in the lungs. All animal experimentation and procedures performed at the National Reference Center for Tuberculosis and Mycobacteria, Bacterial Diseases Service, Scientific Institute of Public Health (WIV-ISP), Brussels, Belgium, were validated and approved by the Ethical Committee of the IPH-VAR (Belgium) under the file number 120323-01. The animal facilities and procedures were under the supervision of an expert on animal welfare in accordance with the Belgian Ministry of Health.

Databases S1 (separate file)

This compressed file has been deposited in DATADRYAD.org under accession number doi:10.5061/dryad.mb463

Raw data (demultiplexed and trimmed from their adaptors) of the RNAseq experiment. The compressed folder (.gz) contains 3 files (.fastq) corresponding to the RNAseq obtained upon treatment of the mycobacteria with DMSO (control), BDM41906, or SMARt-420, respectively, as described in Fig. 1B and in Material & Methods.

References and Notes

1. B. Spellberg, D. N. Gilbert, The future of antibiotics and resistance: A tribute to a career of leadership by John Bartlett. *Clin. Infect. Dis.* **59** (suppl. 2), S71–S75 (2014). doi:10.1093/cid/ciu392 Medline

2. World Health Organization (WHO), *Antimicrobial Resistance: Global Report on Surveillance* (WHO, 2014).

3. S. Hoffner, Unexpected high levels of multidrug-resistant tuberculosis present new challenges for tuberculosis control. *Lancet* **380**, 1367–1369 (2012). doi:10.1016/S0140-6736(12)61069-1 Medline

4. WHO, *Global Tuberculosis Report* (WHO, 2015).

5. C. Barry, More than just bugs in spit. *Science* **348**, 633–634 (2015). doi:10.1126/science.aaa2886 Medline

6. C. Walsh, *Antibiotics: Actions, Origins, Resistance* (ASM Press, 2003).

7. C. Reading, M. Cole, Clavulanic acid: A β-lactamase-inhiting β-lactam from *Streptomyces clavuligerus*. *Antimicrob. Agents Chemother.* **11**, 852–857 (1977). doi:10.1128/AAC.11.5.852 Medline

8. Y. Zhang, B. Heym, B. Allen, D. Young, S. Cole, The catalase-peroxidase gene and isoniazid resistance of *Mycobacterium tuberculosis*. *Nature* **358**, 591–593 (1992). doi:10.1038/358591a0 Medline

9. A. Scorpio, Y. Zhang, Mutations in pncA, a gene encoding pyrazinamidase/nicotinamidase, cause resistance to the antituberculous drug pyrazinamide in tubercle bacillus. *Nat. Med.* **2**, 662–667 (1996). doi:10.1038/nm0696-662 Medline

10. A. E. DeBarber, K. Mdluli, M. Bosman, L. G. Bekker, C. E. Barry 3rd, Ethionamide activation and sensitivity in multidrug-resistant *Mycobacterium tuberculosis*. *Proc. Natl. Acad. Sci. U.S.A.* **97**, 9677–9682 (2000). doi:10.1073/pnas.97.17.9677 Medline

11. A. R. Baulard, J. C. Betts, J. Engohang-Ndong, S. Quan, R. A. McAdam, P. J. Brennan, C. Locht, G. S. Besra, Activation of the pro-drug ethionamide is regulated in mycobacteria. *J. Biol. Chem.* **275**, 28326–28331 (2000). Medline

12. U. H. Manjunatha, H. Boshoff, C. S. Dowd, L. Zhang, T. J. Albert, J. E. Norton, L. Daniels, T. Dick, S. S. Pang, C. E. Barry 3rd, Identification of a nitroimidazo-oxazine-specific protein involved in PA-824 resistance in *Mycobacterium tuberculosis*. *Proc. Natl. Acad. Sci. U.S.A.* **103**, 431–436 (2006). doi:10.1073/pnas.0508392103 Medline

13. M. Matsumoto, H. Hashizume, T. Tomishige, M. Kawasaki, H. Tsubouchi, H. Sasaki, Y. Shimokawa, M. Komatsu, OPC-67683, a nitro-dihydro-imidazooxazole derivative with promising action against tuberculosis in vitro and in mice. *PLOS Med.* **3**, e466 (2006). doi:10.1371/journal.pmed.0030466 Medline

14. G. V. Bloemberg, P. M. Keller, D. Stucki, A. Trauner, S. Borrell, T. Latshang, M. Coscolla, T. Rothe, R. Hömke, C. Ritter, J. Feldmann, B. Schulthess, S. Gagneux, E. C. Böttger, Acquired resistance to bedaquiline and delamanid in therapy for tuberculosis. *N. Engl. J. Med.* **373**, 1986–1988 (2015). doi:10.1056/NEJMc1505196 Medline

15. J. Zheng, E. J. Rubin, P. Bifani, V. Mathys, V. Lim, M. Au, J. Jang, J. Nam, T. Dick, J. R. Walker, K. Pethe, L. R. Camacho, para-Aminosalicylic acid is a prodrug targeting

dihydrofolate reductase in *Mycobacterium tuberculosis*. *J. Biol. Chem.* **288**, 23447–23456 (2013). doi:10.1074/jbc.M113.475798 Medline

16. T. A. Vannelli, A. Dykman, P. R. Ortiz de Montellano, The antituberculosis drug ethionamide is activated by a flavoprotein monooxygenase. *J. Biol. Chem.* **277**, 12824–12829 (2002). doi:10.1074/jbc.M110751200 Medline

17. X. Hanoulle, J. M. Wieruszeski, P. Rousselot-Pailley, I. Landrieu, C. Locht, G. Lippens, A. R. Baulard, Selective intracellular accumulation of the major metabolite issued from the activation of the prodrug ethionamide in mycobacteria. *J. Antimicrob. Chemother.* **58**, 768–772 (2006). doi:10.1093/jac/dkl332 Medline

18. F. Wang, R. Langley, G. Gulten, L. G. Dover, G. S. Besra, W. R. Jacobs Jr., J. C. Sacchettini, Mechanism of thioamide drug action against tuberculosis and leprosy. *J. Exp. Med.* **204**, 73–78 (2007). doi:10.1084/jem.20062100 Medline

19. A. Banerjee, E. Dubnau, A. Quemard, V. Balasubramanian, K. S. Um, T. Wilson, D. Collins, G. de Lisle, W. R. Jacobs Jr., *inhA*, a gene encoding a target for isoniazid and ethionamide in *Mycobacterium tuberculosis*. *Science* **263**, 227–230 (1994). doi:10.1126/science.8284673 Medline

20. J. Engohang-Ndong, D. Baillat, M. Aumercier, F. Bellefontaine, G. S. Besra, C. Locht, A. R. Baulard, EthR, a repressor of the TetR/CamR family implicated in ethionamide resistance in mycobacteria, octamerizes cooperatively on its operator. *Mol. Microbiol.* **51**, 175–188 (2004). doi:10.1046/j.1365-2958.2003.03809.x Medline

21. N. Willand, M. Desroses, P. Toto, B. Dirié, Z. Lens, V. Villeret, P. Rucktooa, C. Locht, A. Baulard, B. Deprez, Exploring drug target flexibility using in situ click chemistry: Application to a mycobacterial transcriptional regulator. *ACS Chem. Biol.* **5**, 1007–1013 (2010). doi:10.1021/cb100177g Medline

22. M. Flipo, M. Desroses, N. Lecat-Guillet, B. Dirié, X. Carette, F. Leroux, C. Piveteau, F. Demirkaya, Z. Lens, P. Rucktooa, V. Villeret, T. Christophe, H. K. Jeon, C. Locht, P. Brodin, B. Déprez, A. R. Baulard, N. Willand, Ethionamide boosters: Synthesis, biological activity, and structure-activity relationships of a series of 1,2,4-oxadiazole EthR inhibitors. *J. Med. Chem.* **54**, 2994–3010 (2011). doi:10.1021/jm200076a Medline

23. M. Flipo, M. Desroses, N. Lecat-Guillet, B. Villemagne, N. Blondiaux, F. Leroux, C. Piveteau, V. Mathys, M.-P. Flament, J. Siepmann, V. Villeret, A. Wohlkönig, R. Wintjens, S. H. Soror, T. Christophe, H. K. Jeon, C. Locht, P. Brodin, B. Déprez, A. R. Baulard, N. Willand, Ethionamide boosters. 2. Combining bioisosteric replacement and structure-based drug design to solve pharmacokinetic issues in a series of potent 1,2,4-oxadiazole EthR inhibitors. *J. Med. Chem.* **55**, 68–83 (2012). doi:10.1021/jm200825u Medline

24. M. Flipo, N. Willand, N. Lecat-Guillet, C. Hounsou, M. Desroses, F. Leroux, Z. Lens, V. Villeret, A. Wohlkönig, R. Wintjens, T. Christophe, H. Kyoung Jeon, C. Locht, P. Brodin, A. R. Baulard, B. Déprez, Discovery of novel N-phenylphenoxyacetamide derivatives as EthR inhibitors and ethionamide boosters by combining high-throughput screening and synthesis. *J. Med. Chem.* **55**, 6391–6402 (2012). doi:10.1021/jm300377g Medline

25. N. Willand, B. Dirié, X. Carette, P. Bifani, A. Singhal, M. Desroses, F. Leroux, E. Willery, V. Mathys, R. Déprez-Poulain, G. Delcroix, F. Frénois, M. Aumercier, C. Locht, V. Villeret, B. Déprez, A. R. Baulard, Synthetic EthR inhibitors boost

antituberculous activity of ethionamide. *Nat. Med.* **15**, 537–544 (2009). doi:10.1038/nm.1950 Medline

26. L. Cuthbertson, J. R. Nodwell, The TetR family of regulators. *Microbiol. Mol. Biol. Rev.* **77**, 440–475 (2013). doi:10.1128/MMBR.00018-13 Medline

27. M. A. Schumacher, M. C. Miller, S. Grkovic, M. H. Brown, R. A. Skurray, R. G. Brennan, Structural mechanisms of QacR induction and multidrug recognition. *Science* **294**, 2158–2163 (2001). doi:10.1126/science.1066020 Medline

28. F. Frénois, J. Engohang-Ndong, C. Locht, A. R. Baulard, V. Villeret, Structure of EthR in a ligand bound conformation reveals therapeutic perspectives against tuberculosis. *Mol. Cell* **16**, 301–307 (2004). doi:10.1016/j.molcel.2004.09.020 Medline

29. F. Frénois, A. R. Baulard, V. Villeret, Insights into mechanisms of induction and ligands recognition in the transcriptional repressor EthR from *Mycobacterium tuberculosis*. *Tuberculosis (Edinb.)* **86**, 110–114 (2006). doi:10.1016/j.tube.2005.07.005 Medline

30. W. Weber, R. Schoenmakers, B. Keller, M. Gitzinger, T. Grau, M. Daoud-El Baba, P. Sander, M. Fussenegger, A synthetic mammalian gene circuit reveals antituberculosis compounds. *Proc. Natl. Acad. Sci. U.S.A.* **105**, 9994–9998 (2008). doi:10.1073/pnas.0800663105 Medline

31. C. K. Stover, V. F. de la Cruz, T. R. Fuerst, J. E. Burlein, L. A. Benson, L. T. Bennett, G. P. Bansal, J. F. Young, M. H. Lee, G. F. Hatfull, S. B. Snapper, R. G. Barletta, W. R. Jacobs Jr., B. R. Bloom, New use of BCG for recombinant vaccines. *Nature* **351**, 456–460 (1991). doi:10.1038/351456a0 Medline

32. M. Coscolla, S. Gagneux, Consequences of genomic diversity in *Mycobacterium tuberculosis*. *Semin. Immunol.* **26**, 431–444 (2014). doi:10.1016/j.smim.2014.09.012 Medline

33. I. Comas, M. Coscolla, T. Luo, S. Borrell, K. E. Holt, M. Kato-Maeda, J. Parkhill, B. Malla, S. Berg, G. Thwaites, D. Yeboah-Manu, G. Bothamley, J. Mei, L. Wei, S. Bentley, S. R. Harris, S. Niemann, R. Diel, A. Aseffa, Q. Gao, D. Young, S. Gagneux, Out-of-Africa migration and Neolithic coexpansion of *Mycobacterium tuberculosis* with modern humans. *Nat. Genet.* **45**, 1176–1182 (2013). doi:10.1038/ng.2744 Medline

34. N. Casali, V. Nikolayevskyy, Y. Balabanova, S. R. Harris, O. Ignatyeva, I. Kontsevaya, J. Corander, J. Bryant, J. Parkhill, S. Nejentsev, R. D. Horstmann, T. Brown, F. Drobniewski, Evolution and transmission of drug-resistant tuberculosis in a Russian population. *Nat. Genet.* **46**, 279–286 (2014). doi:10.1038/ng.2878 Medline

35. F. Ardito, B. Posteraro, M. Sanguinetti, S. Zanetti, G. Fadda, Evaluation of BACTEC Mycobacteria Growth Indicator Tube (MGIT 960) automated system for drug susceptibility testing of *Mycobacterium tuberculosis*. *J. Clin. Microbiol.* **39**, 4440–4444 (2001). doi:10.1128/JCM.39.12.4440-4444.2001 Medline

36. S. D. Ahuja, D. Ashkin, M. Avendano, R. Banerjee, M. Bauer, J. N. Bayona, M. C. Becerra, A. Benedetti, M. Burgos, R. Centis, E. D. Chan, C.-Y. Chiang, H. Cox, L. D'Ambrosio, K. DeRiemer, N. H. Dung, D. Enarson, D. Falzon, K. Flanagan, J. Flood, M. L. Garcia-Garcia, N. Gandhi, R. M. Granich, M. G. Hollm-Delgado, T. H. Holtz, M. D. Iseman, L. G. Jarlsberg, S. Keshavjee, H.-R. Kim, W.-J. Koh, J. Lancaster, C. Lange, W. C. M. de Lange, V. Leimane, C. C. Leung, J. Li, D. Menzies, G. B. Migliori, S. P. Mishustin, C. D. Mitnick, M. Narita, P. O'Riordan, M. Pai, D.

Palmero, S. K. Park, G. Pasvol, J. Peña, C. Pérez-Guzmán, M. I. D. Quelapio, A. Ponce-de-Leon, V. Riekstina, J. Robert, S. Royce, H. S. Schaaf, K. J. Seung, L. Shah, T. S. Shim, S. S. Shin, Y. Shiraishi, J. Sifuentes-Osornio, G. Sotgiu, M. J. Strand, P. Tabarsi, T. E. Tupasi, R. van Altena, M. Van der Walt, T. S. Van der Werf, M. H. Vargas, P. Viiklepp, J. Westenhouse, W. W. Yew, J.-J. Yim, Collaborative Group for Meta-Analysis of Individual Patient Data in MDR-TB, Multidrug resistant pulmonary tuberculosis treatment regimens and patient outcomes: An individual patient data meta-analysis of 9,153 patients. *PLOS Med.* **9**, e1001300 (2012). doi:10.1371/journal.pmed.1001300 Medline

37. S. S. Grant, S. Wellington, T. Kawate, C. A. Desjardins, M. R. Silvis, C. Wivagg, M. Thompson, K. Gordon, E. Kazyanskaya, R. Nietupski, N. Haseley, N. Iwase, A. M. Earl, M. Fitzgerald, D. T. Hung, Baeyer-Villiger monooxygenases EthA and MymA Are required for activation of replicating and non-replicating *Mycobacterium tuberculosis* inhibitors. *Cell Chem. Biol.* **23**, 666–677 (2016). doi:10.1016/j.chembiol.2016.05.011 Medline

38. M. B. Sauton, Sur la nutrition minérale du bacille tuberculeux. *C R Acad Sci Paris* **155**, 860–861 (1912).

39. W. Kabsch, Xds. *Acta Crystallogr. D Biol. Crystallogr.* **66**, 125–132 (2010). doi:10.1107/S0907444909047337 Medline

40. A. Vagin, A. Teplyakov, Molecular replacement with MOLREP. *Acta Crystallogr. D Biol. Crystallogr.* **66**, 22–25 (2010). doi:10.1107/S0907444909042589 Medline

41. A. A. Vagin, R. A. Steiner, A. A. Lebedev, L. Potterton, S. McNicholas, F. Long, G. N. Murshudov, REFMAC5 dictionary: Organization of prior chemical knowledge and guidelines for its use. *Acta Crystallogr. D Biol. Crystallogr.* **60**, 2184–2195 (2004). doi:10.1107/S0907444904023510 Medline

42. M. D. Winn, C. C. Ballard, K. D. Cowtan, E. J. Dodson, P. Emsley, P. R. Evans, R. M. Keegan, E. B. Krissinel, A. G. W. Leslie, A. McCoy, S. J. McNicholas, G. N. Murshudov, N. S. Pannu, E. A. Potterton, H. R. Powell, R. J. Read, A. Vagin, K. S. Wilson, Overview of the CCP4 suite and current developments. *Acta Crystallogr. D Biol. Crystallogr.* **67**, 235–242 (2011). doi:10.1107/S0907444910045749 Medline

43. P. Emsley, B. Lohkamp, W. G. Scott, K. Cowtan, Features and development of Coot. *Acta Crystallogr. D Biol. Crystallogr.* **66**, 486–501 (2010). doi:10.1107/S0907444910007493 Medline

44. S. Schlatter, M. Rimann, J. Kelm, M. Fussenegger, SAMY, a novel mammalian reporter gene derived from *Bacillus stearothermophilus* α-amylase. *Gene* **282**, 19–31 (2002). doi:10.1016/S0378-1119(01)00824-1 Medline

45. V. Delorme, O. R. Song, A. Baulard, P. Brodin, Testing chemical and genetic Modulators in *Mycobacterium tuberculosis* infected cells using phenotypic assays. *Methods Mol. Biol.* **1285**, 387–411 (2015). doi:10.1007/978-1-4939-2450-9_24 Medline

4. Discussion

Antibiotic resistance is a major and global threat for our health care system. The discovery of antibiotics enabled to cure previously deadly bacterial infectious diseases and revolutionized modern medicine. Indeed, without antibiotics physicians may no longer be able to perform immunosuppressing cancer chemotherapies or simple surgeries that rely on antibiotic prophylaxis (Teillant et al., 2015). The risk to enter a post-antibiotic era has been mentioned due to the emergence of infections caused by the so-called "superbugs" that do not respond to most of antibiotics available (Falagas and Bliziotis, 2007; WHO, 2014). The projections estimate that by 2050, drug-resistant infections could kill annualy more than 10 million people worldwide if no action are taken to tackle this problem (Review on Antimicrobial Resistance, 2016).

One way to tackle antibiotic resistance is to rescue the efficacy of approved antibiotic using antibiotic adjuvants that block resistances (Wright, 2016). This strategy has been successfully employed since years in the case of β-lactam antibiotics associated with β-lactamase inhibitors, such as clavulanic acid, which was discovered 40 years ago (Reading and Cole, 1977). However, thus far β-lactamase inhibitors are the only example of antibiotic resistance inhibitor in clinical use (Wright, 2016). Overall, our work studied the possibilities to extend this adjuvant drug approach to other antibiotics, such as tigecycline and colistin for the treatment of *A. baumannii* infections or ethionamide to target *M. tuberculosis*.

4.1. Genome editing platform

The first step of adjuvant drug development is to characterize the resistance mechanisms developed by bacteria during patient treatment in order to identify suitable targets to block resistances. This implies to study recently isolated MDR clinical strains instead of the old laboratory adapted strains routinely used, which are not representative of the population causing infection. Typically, the *A. baumannii* and *P. aeruginosa* reference strains ATCC-17978 and PAO1, respectively, were isolated more than 50 years ago and represent isolated clonal lineages that are not anymore present in the ICUs (Diancourt et al., 2010; Wiehlmann et al., 2007). The PAO1 strain has been extensively studied to get insight into *P. aeruginosa* colistin resistance mechanisms (Fernández et al., 2010, 2012, Macfarlane et al., 2000, 1999; McPhee et al., 2006). However, PAO1 encodes a truncated *cprA* gene, which is required for TCSs mediated colistin resistance, indicating that findings on PAO1 colistin resistance mechanisms may not be relevant for *P. aeruginosa* species (Gutu et al., 2015). To avoid this kind of incident and increase representativeness it is necessary to study resistance mechanisms in several clinical strains. In addition, antibiotic resistance mechanisms developed during antibiotic exposure *in vitro* do not necessarily represent the resistance development during patient treatment. For instance, *A. baumannii* exposed to colistin *in vitro* easily loses its LPS leading to colistin resistance (Moffatt et al., 2011). However, this resistance mechanism is not observed in colistin resistant strains isolated from patients most likely due to the high fitness cost engendered by LPS loss (Beceiro et al., 2014; García-Quintanilla et al., 2015). Similarly, *E. coli* exposed to fosfomycin *in vitro* shows a high resistance rate whereas resistance rate *in vivo* is very low, which can be explained by the high fitness cost of the resistant mutants obtained *in vitro* (Pan et al., 2017). In summary, relevant antibiotic resistance mechanisms must be studied on a panel of resistant strains isolated from patients to avoid misjudgement on target potential.

The study of antibiotic resistance in clinical strains is impeded by the lack of methods to genetically manipulate such strains. Indeed, strains that are resistant to clinically used antibiotics are generally resistant to classical antibiotics used for plasmid selection, such as ampicillin, kanamycin, tetracycline and chloramphenicol. The genome editing platform that was developed during this thesis is based on a two-step recombination method. Importantly, this method requires a single resistance cassette contrary to other methods, such as CRISPR/Cas9, λ-red system and other recombineering systems that require multiple selection markers making them not compatible with drug resistant strains (Jiang et al., 2013; Poteete, 2001; Tucker et al., 2014). We implemented a non-antibiotic selection cassette to overcome this limitation allowing to select for genomic plasmid integration even in drug resistant isolates. The expression of the gene *tpm* confers resistance to tellurite (TeO_3^{2-}) in *A. baumannii* as demonstrated in the section 2.1.1. of this thesis and it is also functional in *P. aeruginosa*, *K. pneumoniae* and *E. coli*. Tellurite is highly toxic for most microorganisms (Chasteen et al., 2009). Tellurite toxicity is thought to be due to its high oxidizing ability that leads to superoxide radicals generation and subsequent bacterial oxidative burst (Prigent-Combaret et al., 2012). Most bacteria can reduce tellurite into elementary tellurium (Te), which is less toxic than the tellurite oxyanion and accumulates as black deposit in the cells (Chasteen et al., 2009). However, *tpm* encodes a thiopurine S-methyltransferase that methylates tellurium to produce volatile dimethyl telluride (CH_3TeCH_3) resulting in complete detoxification thus conferring resistance (Prigent-Combaret et al., 2012). In our method, tellurite was very efficient in selecting *tpm* expressing bacteria on agar plates after conjugation. Nevertheless, we have noticed that liquid culture growth of *tpm* expressing bacteria in the presence of tellurite was associated with strong fitness cost, even when the tellurite concentration was reduced to 10 µg/ml. Therefore, we recommend to use this resistance marker only for agar plate-based selection.

The second step of the genome editing method consists of plasmid removal from the genome by homologous recombination. To overcome the low efficiency of the SacB/sucrose counter selection system, we implemented a Tdk/AZT system whose expression is inducible by IPTG. The thymidine kinase encoded by *tdk* can phosphorylate the non-functional thymidine analogue AZT. AZT has an azido (-N3) group at the 3' position instead of the thymidine 3' hydroxyl (-OH) group, which is required to form the phosphodiester bond with the next nucleotide (Figure 13). Upon phosphorylation by Tdk, AZT is incorporated into DNA and replaces endogenous thymide finally leading to the termination of DNA elongation. AZT incorporation in DNA is highly toxic and thus allows plasmid removal counter selection. This counter selection system is very efficient in selecting plasmid removal in *A. baumannii* as demonstrated in section 2.1.1. We have further shown that this counterselection method is also functional in *P. aeruginosa*. In contrast, Tdk/AZT counter selection system cannot be applied in *Enterobacteriaceae* because these species endogenously encode Tdk and they are therefore susceptible to AZT even in absence of Tdk expressing plasmid. Universal counter selection system might reside in endonucleases that catalyse targeted double strand breaks, such as Cas9 and SceI enzymes (Colleaux et al., 1988; Jinek et al., 2012). Double strand break targeted to the plasmid sequence would select for plasmid removal from the genome by inducing recombination. The major drawback of such counter selection system is the absolute necessity for a tight expression regulation of the system in order to avoid mutational inactivation.

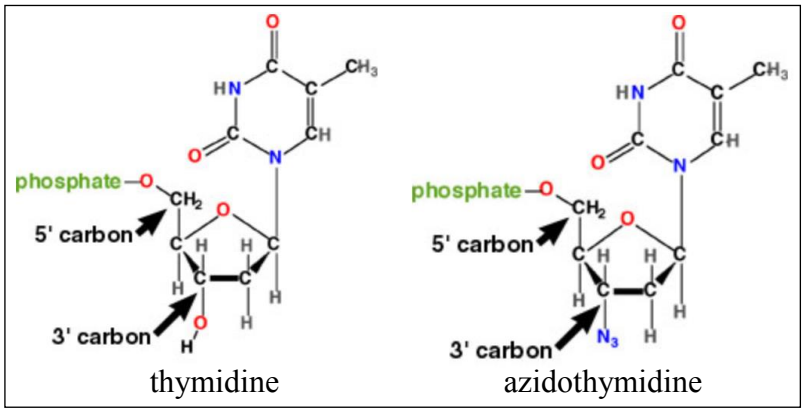

Figure 13: Schematic structure of thymidine and its non-functional analogue azidothymidine (AZT)

The backbone of the genome editing platform is based on the Standard European Vector Architecture (SEVA) platform (Silva-Rocha et al., 2013). Consequently, the platform has a modular architecture that allows the rapid exchange of the individual genetic building blocks enabling the customization to target other important Gram-negative pathogens (Figure 14). In addition to selection and counter selection marker, the origin of replication can also be replaced to extend the applicability of the method to *Enterobacteriaceae*. The described plasmid platform is designed with a ColE1 origin of replication that is not replicative in *A. baumannii* and *P. aeruginosa*. In contrast, ColE1 origin of replication is functional in *Enterobacteriaceae*, which does not allow genomic plasmid integration in these species. Replacement of the ColE1 origin of replication with an R6K origin of replication that is functional only in λpir phage lysogenised strains, would allow to target *Enterobacteriaceae* pathogenic species, such as *E. coli* and *K. pneumoniae*.

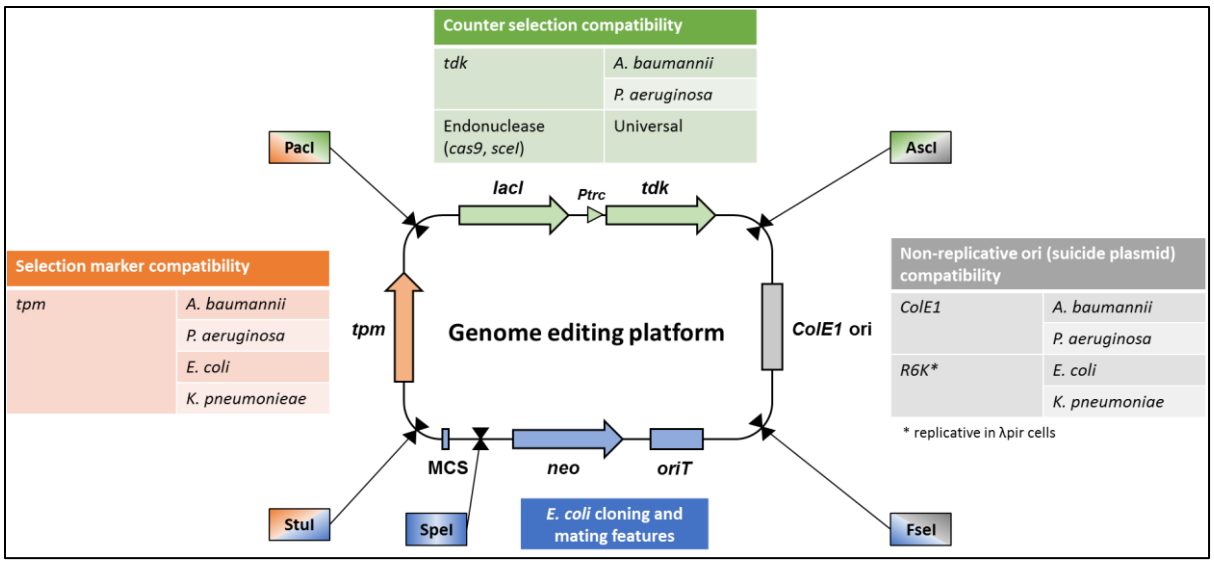

Figure 14: Modularity of the genome editing platform.
The main building blocks of the genome editing platform and their compatibility for the expansion to other species are presented.

In addition to its high modularity, the genome editing platform is very versatile. The method can be employed to produce markeless deletions, insertions (knockin) and point mutations in only three days (Figure 15). Altogether, we believe that the developed genome editing platform is the most powerful method to edit the genome of Gram-negative without distinction between laboratory and clinical strains.

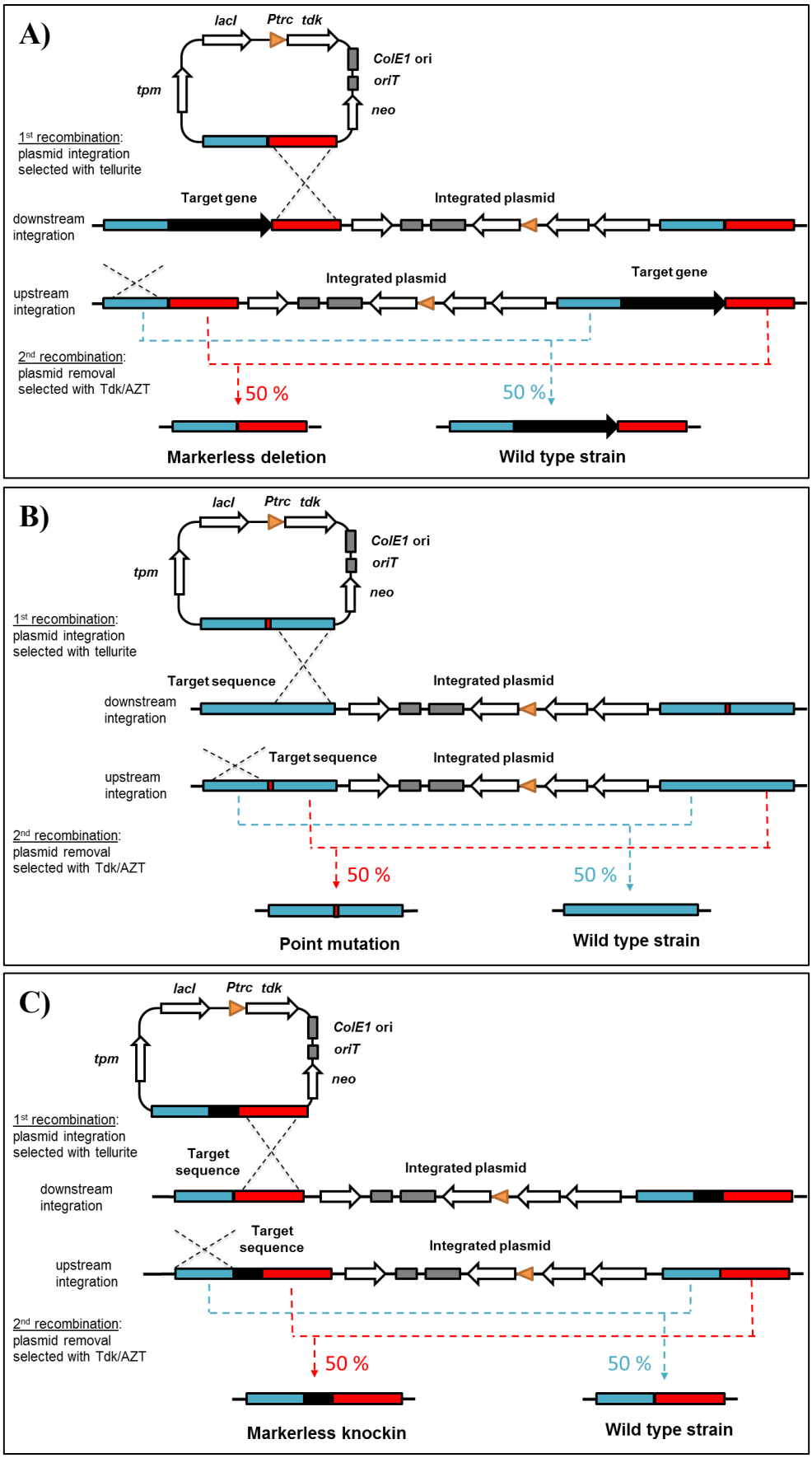

Figure 15: Genome editing platform applications.
The first and second recombination steps are represented in the case of genomic markerless **A)** deletion, **B)** point mutation and **C)** insertion (knockin).

4.2. Adjuvant drug targets to overcome antibiotic resistance

4.2.1. *Acinetobacter baumannii*

TCSs have been suggested as potential drug targets to overcome antibiotic resistance or to reduce virulence (Worthington et al., 2013). TCSs are bacterial signal transduction pathways that allow to sense environmental changes and rapidly respond to these perturbations in order to survive and proliferate. TCSs are not found in higher eukaryotic organisms whereas they are ubiquitous in bacteria. Gram-negative pathogens, such as *P. aeruginosa* and *E. coli*, encode over 30 ordinary TCSs in their genome while the Gram-positive pathogen *S. aureus* encodes 16 TCSs (García-Calderón et al., 2007; Gooderham and Hancock, 2009; Xue et al., 2011). Most of these TCSs are not essential for survival in classical *in vitro* conditions. However, TCSs have significant impact on bacterial survival to specific stress conditions, such as those encountered during infection, making TCSs attractive targets for novel antibacterial therapeutic approaches (Stephenson and Hoch, 2002). On another hand, many TCSs have been associated with antibiotic resistance regulation in pathogenic bacteria (Worthington et al., 2013). Our work focused on two different TCSs, the AdeRS and PmrAB TCSs, that were shown to be involved in *A. baumannii* tigecycline and polymyxin resistance, respectively (Adams et al., 2009; Hornsey et al., 2010).

4.2.1.1. Efflux pump systems

We demonstrated that AdeRS mediated AdeABC efflux pump expression is the major tigecycline resistance mechanism in *A. baumannii* clinical isolates as previously suggested in the literature (Hornsey et al., 2010; Peleg et al., 2007; Ruzin et al., 2007; Sun et al., 2010). However, we demonstrated that some clinical strains have an alternative resistance mechanism, which is independent of AdeRS and AdeABC expression, and confers moderate tigecycline resistance. This observation is in accordance with resistance mechanisms to other antibiotics where efflux pumps are rarely the unique mechanism. For instance, aminoglycosides are substrates of the AdeABC efflux pump and upregulation of AdeABC confers aminoglycoside resistance to *A. baumannii* (Magnet et al., 2001; Yoon et al., 2015). However, a recent study showed that 94 % aminoglycoside non-susceptible *A. baumannii* isolated from clinical settings harboured at least one AMEs, suggesting that the major *A. baumannii* aminoglycoside resistance resides in AMEs expression and that efflux pumps expression is secondary (Sheikhalizadeh et al., 2017). The same observation was done in *P. aeruginosa* clinical isolate where efflux pump expression interplays with AME expression to confer high level aminoglycoside resistance (Morita et al., 2012). A similar phenomenon applies to fluoroquinolone resistance. Fluoroquinolones are substrate of the AdeABC efflux pump and overexpression of AdeABC has been associated with fluoroquinolone resistance (Magnet et al., 2001; Yoon et al., 2015). However, all ciprofloxacin resistant *A. baumannii* clinical strains, which were isolated in two independent studies, harboured at least one mutation in DNA gyrase or topoisomerase whereas the ciprofloxacin susceptible isolates had wildtype gyrase and topoisomerase (Lee et al., 2005; Vila et al., 1997). These data indicate that, although efflux pumps might be involved in ciprofloxacin resistance development, it has only a secondary role in clinical strains. The secondary role of the AdeABC efflux pump in *A. baumannii* antibiotic resistance disproved our initial hypothesis, which consisted in AdeRS mediated AdeABC

expression inhibition to overcome antibiotic resistance. Furthermore, global efflux pump inhibition strategies may not be sufficient to overcome antibiotic resistance in *A. baumannii*.

4.2.1.2. Phosphoethanolamine transferases

In our second project we applied the developed gene knockout platform to investigate the polymyxin resistance in *A. baumannii*. It has been proposed that the main colistin resistance mechanism in *A. baumannii* is based on the addition of PetN to lipid A, which is catalysed by the PetN transferase enzyme PmrC (Adams et al., 2009; Arroyo et al., 2011; Olaitan et al., 2014). The response regulator PmrA triggers *pmrC* overexpression when phosphorylated by the pmrB sensor kinase (Park et al., 2011b). Therefore, inhibition of PmrA might revert colistin resistance in *A. baumannii*. This hypothesis has been confirmed by the development of PmrAB small molecule inhibitors that break colistin resistance in *A. baumannii* (Harris et al., 2014). However, our data revealed that PmrA mediated overexpression of *pmrC* is an important but not the exclusive colistin resistance mechanism in *A. baumannii* clinical isolates. Indeed, we found clinical isolates where colistin resistance was mediated by the overexpression of the PmrC homologue EptA due to IS*AbaI* element insertion. This finding indicates that PmrAB small molecule inhibitor would not be efficient on EptA mediated colistin resistant *A. baumannii* strains. Nevertheless, our results suggest PetN transferase enzymes as potential targets to restore colistin sensitivity in *A. baumannii*.

PetN transferases are associated with colistin resistance in other clinically relevant Gram-negative pathogens, such as *P. aeruginosa* and *Enterobacteriaceae* (Olaitan et al., 2014). However, in contrast to *A. baumannii*, PetN transferase expression is not the exclusive resistance mechanism in other Gram-negative pathogens. In addition to PetN lipid A modification, *P. aeruginosa* and *Enterobacteriaceae* colistin resistance can be mediated by aminoarabinose (AraN) addition to lipid A (Needham and Trent, 2013). The AraN lipid A decoration is mediated by the AraN transferase ArnT and is independent of PetN transferase, which indicates that PetN transferase inhibitors would not be efficient on strains harboring AraN modified lipid A.

Plasmid mediated expression of *mcr-1*, which codes for another PetN transferase, has been recently identified in colistin resistant *E. coli* clinical strains in China (Liu et al., 2016). Since then, plasmid mediated colistin resistant strains have been reported all over the world (Poirel et al., 2017). The *mcr-1* gene has been identified predominantly in *E. coli* and in several other *Enterobacteriaceae*, but not in *A. baumannii* and *P. aeruginosa* so far. It is interesting to note that *mcr-1* could be retrospectively identified in animal samples isolated 30 years ago and that the *mcr-1* outbreak started in 2009 indicating that *mcr-1* dissemination might not be as sudden as suggested directly after its worldwide identification (Shen et al., 2016b).

The genomic organisation of the plasmid encoded *mcr-1* shares similarities with the *A. baumannii* chromosomally encoded *eptA* identified in our work. Both genes present an upstream IS element, IS*Apl1* and IS*AbaI* upstream *mcr-1* and *eptA*, respectively. They most likely provide a promoter for PetN transferase expression. In addition, *mcr-1* has been identified with both upstream and downstream IS*Apl1* indicating its presence in a transposable element (Snesrud et al., 2016). Our work suggests that *eptA* is also present in a mobile element due to its duplication in the genome of a clinical strain. Unfortunately, we could not resolve the

sequence downstream the duplicated *eptA* but whole genome sequencing of this clinical strain would allow to verify this hypothesis. Overall, *mcr-1* expression in *E. coli* leads to a 4- to 8-fold increase in colistin MIC whereas *eptA* expression in *A. baumannii* leads up to a 254-fold increase in colistin MIC. Despite the lower ability of *mcr-1* expression to increase colistin resistance, *mcr-1* expression does not require additional mechanisms to confer colistin resistance in *Enterobacteriaceae*. Alarmingly, *mcr-1* has been identified in plasmid harbouring multiple resistance genes and plasmid mediated *mcr-1* colistin resistance has been reported in carbapenem resistant *Enterobacteriaceae* (Du et al., 2016; Falgenhauer et al., 2016; Poirel et al., 2016; Yao et al., 2016; Zhong et al., 2017). In summary, the contribution of PmrC in *P. aeruginosa* polymyxin resistance, the emergence of plasmid mediated *mcr-1* polymyxin resistance in *Enterobacteriaceae* and the exclusive role of PmrC and EptA in *A. baumannii* polymyxin resistance make PetN transferases attractive targets to rescue the activity of polymyxins in Gram-negative pathogens.

PetN transferases are composed by a transmembrane domain, that anchors the enzyme to the cytoplasmic membrane, attached to a soluble catalytic domain located in the periplasm (Anandan et al., 2017). The three-dimensional structure of the catalytic domain of *Campylobacter jejuni* (cEptC), *Neisseria meningitidis* (cLptA) and MCR-1 (cMCR-1) PetN transferases have been determined (Figure 16) (Fage et al., 2014; Stojanoski et al., 2016; Wanty et al., 2013).

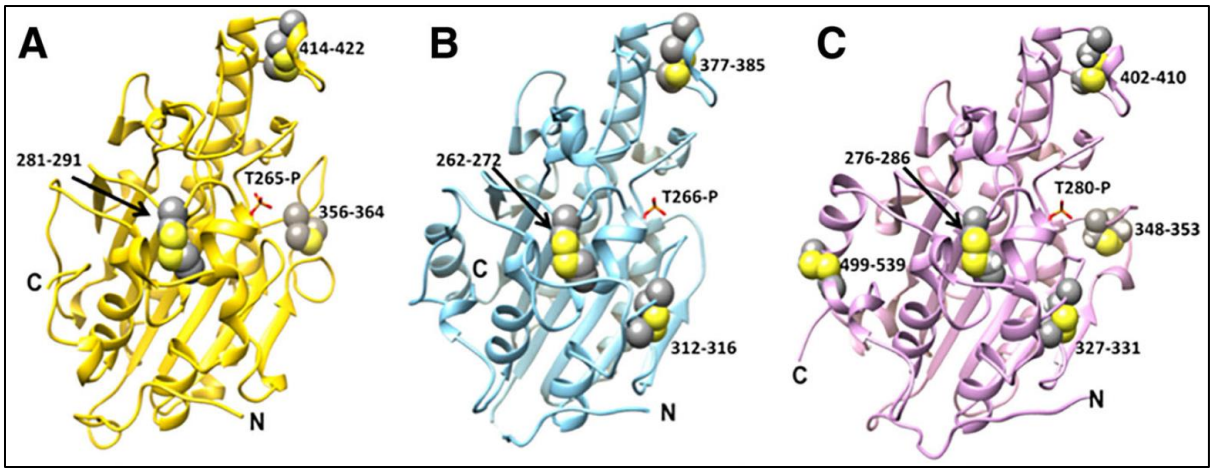

Figure 16: Three-dimensional structure of bacterial PetN transferases (Stojanoski et al., 2016).
Crystal structure of **A)** cMCR-1, **B)** cEptC and **C)** cLptA. The disulphide bounds are shown as spare-fill spheres in the three structures as well as the active site threonine in its phosphorylated state in red.

Overall, the three catalytic domains present a similar fold. The active site and most of the disulphide bonds are conserved among the three proteins. As expected, the three protein catalytic domains have conserved primary amino acid sequences. This sequence similarity can be expanded to the catalytic domain of the *A. baumannii* PmrC and EptA PetN transferases, which conserve all the active sites residues and the cysteine forming disulphide bounds (Figure 17). This analysis suggests that the catalytic domain of all these PetN transferases are very similar and may potentially allow the development of broad spectrum PetN transferase inhibitor.

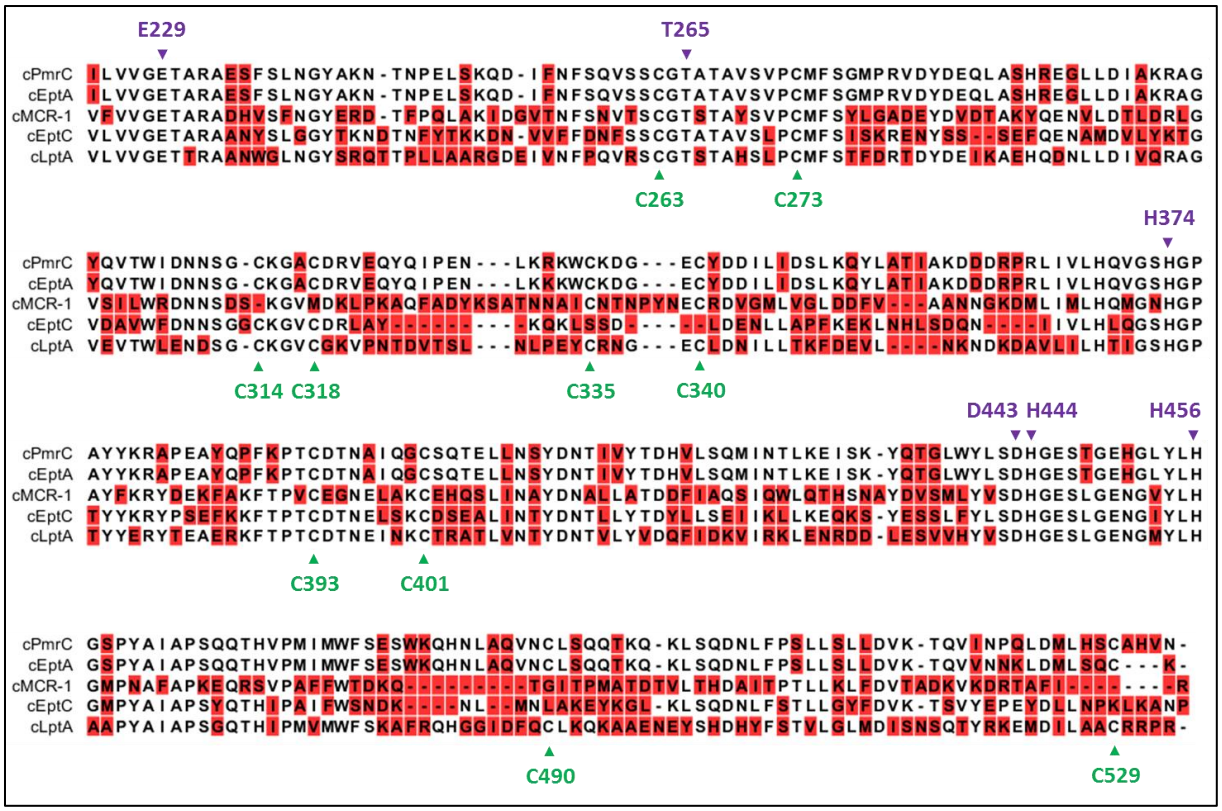

Figure 17: Amino acid sequence alignment of PetN transferases catalytic domain.
PetN transferase catalytic domain amino acid sequence of PmrC ($PmrC_{224-533}$), EptA ($EptA_{221-527}$), MCR-1 ($MCR\text{-}1_{241-541}$), EptC ($EptC_{222-512}$) and LptA ($LptA_{235-544}$) were aligned using CLC Main Workbench. Active site residues (purple) and cysteine forming disulphide bounds (green) are numbered according to the PmrC amino acid sequence.

4.2.2. *Mycobacterium tuberculosis*

We have previously shown that antibiotic resistance mechanisms are complex and can be mediated by multiple pathways. This observation holds true for *M. tuberculosis* ethionamide resistance, as presented in the introduction section 1.2.3. of this thesis. The two major mechanisms reside in alteration of the ethionamide target InhA or loss of function of the bioactivation enzyme EthA (Vilchèze and Jacobs, 2014).

The mutations affecting InhA result in InhA overexpression or a decreased affinity of ethionamide for InhA, which in both cases do not abolish ethionamide activity but dilute out the drug (Vilchèze et al., 2006). Therefore, increasing drug concentration may overcome this type of resistance. Indeed, high dose regiment of isoniazid, which targets InhA, is expected to successfully treat low isoniazid resistant *M. tuberculosis* strains (Schaaf et al., 2007). However, ethionamide high dose regiment cannot be applied due to the adverse effects of the drug (Holdiness, 1987; Weinstein et al., 1962).

In constrast, enhanced intracellular active ethionamide concentrations can be achieved by boosting the ethionamide bioactivation pathway. Indeed, Willand and colleagues developed EthR inhibitors to derepress the expression of *ethA* and thereby boost the activation of ethionamide (Willand et al., 2009). Co-administration of EthR inhibitors with ethionamide in *M. tuberculosis*-infected mice allowed a three-fold decrease in the dosage of ethionamide. The EthR inhibitor BDM41906 reverts ethionamide resistance mediated through non EthA mutations, but was not efficient in reverting ethionamide resistance mediated by EthA

mutations. Therefore, the identification of the alternative ethionamide bioactivation pathway EthA2-EthR2 and the development of EthR2 inhibitors allow to revert ethionamide resistance in *M. tuberculosis*, regardless of the resistance mechanism.

4.2.2.1. Synthetic mammalian gene regulation system

In this project, we designed and developed the EthR2 based synthetic mammalian gene regulation system. This system was designed to sense the binding of EthR2 to its DNA operator and monitor the compound-mediated inhibition of this protein-DNA interaction. The gene regulation system consists in two vectors co-transfected in mammalian host cells. The first vector is an expression plasmid, which allows the constitutive expression of EthR2 fused to the VP16 transactivation domain of *Herpes simplex*. The second vector is a reporter plasmid, which enables the EthR2-VP16 regulated expression of the serum alkaline phosphatase (SEAP) reporter gene. Indeed, the reporter plasmid was constructed in a way that the intergenic region between *ethA2* and *ethR2*, which contains the EthR2 operator, is placed upstream of the SEAP gene driven by the minimal variant of the human cytomegalovirus derived promotor (P_{CMVmin}). Because VP16 activates the P_{CMVmin} promoter, the binding of EthR2-VP16 to its DNA operator induces the quantifiable expression of SEAP. This system enables to evaluate the ability of compounds to inhibit the binding of EthR2 to its operator, which is expected to translate into the ability of compounds to boost ethionamide activation in *M. tuberculosis*.
The implementation of the synthetic gene regulation system in mammalian cells enables to keep track on target specificity, cytotoxicity and bioavailability of the tested compounds. First, the use of a non-*Mycobacterium* background avoids potential unspecific interaction with the EthR2 regulation system thereby limiting the possibility of off-target compound effect. Second, the use of mammalian cells as host for the EthR2 based regulation system allows to monitor compound cytotoxicity and mimics the infectious environment of *M. tuberculosis,* which is an intracellular pathogen. Finally, working with *M. tuberculosis* or its non-pathogenic related species *Mycobacterium smegmatis* is very cumbersome due to their low growth rate and therefore mammalian cells appear as appropriate host to bypass this hurdle.
A similar mammalian gene regulation system has been developed for EthR based regulation (Weber et al., 2008). The assessment of newly synthesised compounds on the two EthR- and EthR2-dependent systems enables the distinction between EthR and EthR2 specific ethionamide boosting compounds.

4.2.2.2. Bioactivation pathway as drug target

In contrast to the multiplicity of resistance mechanisms that impedes the development of adjuvant drug to overcome resistance, the two independent ethionamide bioactivation pathways are a major asset for the development of adjuvant drug to boost ethionamide. Indeed, the EthA2-EthR2 bioactivation pathway appears to be ubiquitous in *M. tuberculosis* despite the low expression of *ethA2*. The low expression level of *ethA2* may explain the absence of mutations in its coding sequence, which makes this bioactivation pathway a perfect switch to boost ethionamide efficacy. Nevertheless, *M. tuberculosis* resistance through EthA2 loss of function mutation may arise due to selection pressure during treatment with the combination of ethionamide-EthR2 inhibitor. The development of EthR/EthR2 dual-inhibitor may drastically reduce the frequency of resistance. Indeed, EthA or EthA2 loss of function mutation alone would not be sufficient to confer resistance to the combination ethionamide-dual inhibitor.

Therefore, resistance would need to be mediated by at least two independent mutations, in both EthA and EthA2. This delayed resistance development is exemplified by two well-known class of multitarget antibiotics, the β-lactams that inhibit penicillin-binding proteins and the quinolones that inhibit the DNA topoisomerases (East and Silver, 2013).

Ethionamide is one of the most potent *M. tuberculosis* second-line drug and it is recommended for the treatment of MDR *M. tuberculosis* strains. However, to limit the adverse effects ethionamide is used at concentrations relatively close to its MIC, which impairs treatment efficiency and favors the selection of resistance (Zhu et al., 2002). The EthR2 inhibitor compound SMARt-420 not only reverts ethionamide resistance but also boost ethionamide activity on *M. tuberculosis* susceptible strains. Decreasing the dose of ethionamide by co-administration of EthR/EthR2 dual inhibitors, might, on one hand, lower the toxicity of the treatment and improve the quality of life of the patients, and, on the other hand, improve the treatment efficacy and potentially reduce the treatment time. This would allow clinicians to consider placing the combination ethionamide-EthR/EthR2 inhibitors as a first-line drug to treat *M. tuberculosis* infections.

5. Conclusion

Antimicrobial resistance is a serious threat for public health worldwide. The risk to enter a post-antibiotic era has been raised due to the emergence of pathogens resistant to most of available antibiotics. In the last decades, many of the big pharmaceutical companies pulled away from antibiotic discovery due to a lower expectation of profits compared to other therapeutic areas. The strong reduction in antibacterial research lead to empty pipelines and a lack of innovation in the antibiotic field. Without increasing efforts the risk is high to enter a post-antibiotic era where simple infections by drug resistant pathogens may be hazardous due to a lack of treatment options. Beside research on novel antibiotics, innovative approaches may provide another solution to overcome this lack.

One of the innovative approach resides in adjuvant therapies that have the capability to revert antibiotic resistances. Molecules inhibiting antibiotic resistance mechanisms can prolong the life time of currently used antibiotics by delaying the onset of resistance or even revive old antibiotics that were left aside due to the high frequency of resistant strains in the environment. This approach has been successfully applied during decades with β-lactams inhibitors but never expanded to other antibiotics.

The genome engineering method developed during this thesis allowed us to characterize the different mechanisms employed by *A. baumannii* to resist the antibacterial action of tigecycline and colistin antibiotics during patient treatment. Overall, we showed that the mechanisms employed to resist the action of a specific antibiotic may be diverse due to the treatment history of the individual clinical strains. This impairs the development of adjuvant drug to overcome tigecycline and colistin resistances in *A. baumannii* and it implies a careful evaluation of drug target relevance before to develop inhibitors that are specific of one resistance pathway. Nevertheless, we propose PetN transferases as attractive targets to restore polymyxin sensitivity.
In contrast to the two studied targets in *A. baumannii*, we successfully demonstrated that an adjuvant approach has the potential to overcome resistance and boost the activity of the antibiotic ethionamide in *M. tuberculosis*. By using the synthetic mammalian gene regulation system designed during this thesis we developed EthR2-specific inhibitory compounds that boost the newly discovered *M. tuberculosis* ethionamide bioactivation pathway. These compounds not only revert ethionamide resistance in MDR *M. tuberculosis,* but also boost the ethionamide efficacy in drug susceptible strains, rendering ethionamide into a more potent antibiotic. These adjuvant compounds are very promising chemical entities and they are currently in pre-clinical development.

The research performed in this thesis demonstrated that the development of adjuvant therapeutic approaches is not straightforward and that special attention should be paid to drug target evaluation. The non-essential nature of these drug targets promotes a higher diversity and heterogeneity and careful target validation is required before starting a drug development program. However, the successful development of ethionamide boosting compounds that also switch off bacterial resistance traits demonstrates the potential of novel therapeutic adjuvant approaches.

References

Adams, M.D., Goglin, K., Molyneaux, N., Hujer, K.M., Lavender, H., Jamison, J.J., MacDonald, I.J., Martin, K.M., Russo, T., Campagnari, A.A., et al. (2008). Comparative genome sequence analysis of multidrug-resistant Acinetobacter baumannii. J. Bacteriol. 190, 8053–8064.

Adams, M.D., Nickel, G.C., Bajaksouzian, S., Lavender, H., Murthy, A.R., Jacobs, M.R., and Bonomo, R.A. (2009). Resistance to Colistin in Acinetobacter baumannii Associated with Mutations in the PmrAB Two-Component System. Antimicrob. Agents Chemother. 53, 3628–3634.

Adams-Haduch, J.M., Paterson, D.L., Sidjabat, H.E., Pasculle, A.W., Potoski, B.A., Muto, C.A., Harrison, L.H., and Doi, Y. (2008). Genetic basis of multidrug resistance in Acinetobacter baumannii clinical isolates at a tertiary medical center in Pennsylvania. Antimicrob. Agents Chemother. 52, 3837–3843.

Akers, K.S., Chaney, C., Barsoumian, A., Beckius, M., Zera, W., Yu, X., Guymon, C., Keen, E.F., Robinson, B.J., Mende, K., et al. (2010). Aminoglycoside resistance and susceptibility testing errors in Acinetobacter baumannii-calcoaceticus complex. J. Clin. Microbiol. 48, 1132–1138.

Al Atrouni, A., Joly-Guillou, M.-L., Hamze, M., and Kempf, M. (2016). Reservoirs of Non-baumannii Acinetobacter Species. Front. Microbiol. 7.

Al-Agamy, M.H., Khalaf, N.G., Tawfick, M.M., Shibl, A.M., and El Kholy, A. (2014). Molecular characterization of carbapenem-insensitive Acinetobacter baumannii in Egypt. Int. J. Infect. Dis. IJID Off. Publ. Int. Soc. Infect. Dis. 22, 49–54.

Alyamani, E.J., Khiyami, M.A., Booq, R.Y., Alnafjan, B.M., Altammami, M.A., and Bahwerth, F.S. (2015). Molecular characterization of extended-spectrum beta-lactamases (ESBLs) produced by clinical isolates of Acinetobacter baumannii in Saudi Arabia. Ann. Clin. Microbiol. Antimicrob. 14, 38.

Anandan, A., Evans, G.L., Condic-Jurkic, K., O'Mara, M.L., John, C.M., Phillips, N.J., Jarvis, G.A., Wills, S.S., Stubbs, K.A., Moraes, I., et al. (2017). Structure of a lipid A phosphoethanolamine transferase suggests how conformational changes govern substrate binding. Proc. Natl. Acad. Sci. 114, 2218–2223.

Anstey, N.M., Currie, B.J., and Withnall, K.M. (1992). Community-Acquired Acinetobacter Pneumonia in the Northern Territory of Australia. Clin. Infect. Dis. 14, 83–91.

Antunes, L.C.S., Imperi, F., Towner, K.J., and Visca, P. (2011). Genome-assisted identification of putative iron-utilization genes in Acinetobacter baumannii and their distribution among a genotypically diverse collection of clinical isolates. Res. Microbiol. 162, 279–284.

Aranda, J., Bardina, C., Beceiro, A., Rumbo, S., Cabral, M.P., Barbé, J., and Bou, G. (2011). Acinetobacter baumannii RecA Protein in Repair of DNA Damage, Antimicrobial Resistance, General Stress Response, and Virulence ▿. J. Bacteriol. 193, 3740–3747.

Arroyo, L.A., Herrera, C.M., Fernandez, L., Hankins, J.V., Trent, M.S., and Hancock, R.E.W. (2011). The pmrCAB operon mediates polymyxin resistance in Acinetobacter baumannii ATCC 17978 and clinical isolates through phosphoethanolamine modification of lipid A. Antimicrob. Agents Chemother. 55, 3743–3751.

Atasoy, A.R., Ciftci, I.H., and Petek, M. (2015). Modifying enzymes related aminoglycoside: analyses of resistant Acinetobacter isolates. Int. J. Clin. Exp. Med. 8, 2874–2880.

Bakour, S., Alsharapy, S.A., Touati, A., and Rolain, J.-M. (2014). Characterization of Acinetobacter baumannii clinical isolates carrying bla(OXA-23) carbapenemase and 16S rRNA methylase armA genes in Yemen. Microb. Drug Resist. Larchmt. N 20, 604–609.

Banerjee, A., Dubnau, E., Quemard, A., Balasubramanian, V., Um, K.S., Wilson, T., Collins, D., de Lisle, G., and Jacobs, W.R. (1994). inhA, a gene encoding a target for isoniazid and ethionamide in Mycobacterium tuberculosis. Science 263, 227–230.

Bartual, S.G., Seifert, H., Hippler, C., Luzon, M.A.D., Wisplinghoff, H., and Rodríguez-Valera, F. (2005). Development of a multilocus sequence typing scheme for characterization of clinical isolates of Acinetobacter baumannii. J. Clin. Microbiol. 43, 4382–4390.

Basler, M. (2015). Type VI secretion system: secretion by a contractile nanomachine. Phil Trans R Soc B 370, 20150021.

Bassetti, M., Merelli, M., Temperoni, C., and Astilean, A. (2013). New antibiotics for bad bugs: where are we? Ann. Clin. Microbiol. Antimicrob. 12, 22.

Baulard, A.R., Betts, J.C., Engohang-Ndong, J., Quan, S., McAdam, R.A., Brennan, P.J., Locht, C., and Besra, G.S. (2000). Activation of the pro-drug ethionamide is regulated in mycobacteria. J. Biol. Chem. 275, 28326–28331.

Beceiro, A., Moreno, A., Fernández, N., Vallejo, J.A., Aranda, J., Adler, B., Harper, M., Boyce, J.D., and Bou, G. (2014). Biological cost of different mechanisms of colistin resistance and their impact on virulence in Acinetobacter baumannii. Antimicrob. Agents Chemother. 58, 518–526.

Beijerinck, M.W. (1911). Uber Pigmentbildung bei Essigbakterien. Cent. Bakteriol. Parasitenk. Abt.II 29:169-176.

Bergogne-Bérézin, E. (2008). Importance of Acinetobacter spp. In Acinetobacter Biology and Pathogenesis, E. Bergogne-Bérézin, H. Friedman, and M. Bendinelli, eds. (Springer US), pp. 1–18.

Berlau, J., Aucken, H., Malnick, H., and Pitt, T. (1999a). Distribution of Acinetobacter species on skin of healthy humans. Eur. J. Clin. Microbiol. Infect. Dis. Off. Publ. Eur. Soc. Clin. Microbiol. 18, 179–183.

Berlau, J., Aucken, H.M., Houang, E., and Pitt, T.L. (1999b). Isolation of Acinetobacter spp. including A. baumannii from vegetables: implications for hospital-acquired infections. J. Hosp. Infect. 42, 201–204.

Blair, J.M.A., Webber, M.A., Baylay, A.J., Ogbolu, D.O., and Piddock, L.J.V. (2015). Molecular mechanisms of antibiotic resistance. Nat. Rev. Microbiol. 13, 42–51.

Blot, S., Vandewoude, K., and Colardyn, F. (2003). Nosocomial bacteremia involving Acinetobacter baumannii in critically ill patients: a matched cohort study. Intensive Care Med. 29, 471–475.

Boll, J.M., Tucker, A.T., Klein, D.R., Beltran, A.M., Brodbelt, J.S., Davies, B.W., and Trent, M.S. (2015). Reinforcing Lipid A Acylation on the Cell Surface of Acinetobacter baumannii Promotes Cationic Antimicrobial Peptide Resistance and Desiccation Survival. mBio 6, e00478-15.

Bonnin, R.A., Potron, A., Poirel, L., Lecuyer, H., Neri, R., and Nordmann, P. (2011). PER-7, an Extended-Spectrum β-Lactamase with Increased Activity toward Broad-Spectrum Cephalosporins in Acinetobacter baumannii. Antimicrob. Agents Chemother. 55, 2424–2427.

Bonnin, R.A., Rotimi, V.O., Al Hubail, M., Gasiorowski, E., Al Sweih, N., Nordmann, P., and Poirel, L. (2013). Wide dissemination of GES-type carbapenemases in Acinetobacter baumannii isolates in Kuwait. Antimicrob. Agents Chemother. 57, 183–188.

Boonaiam, S., Chaiprasert, A., Prammananan, T., and Leechawengwongs, M. (2010). Genotypic analysis of genes associated with isoniazid and ethionamide resistance in MDR-TB isolates from Thailand. Clin. Microbiol. Infect. Off. Publ. Eur. Soc. Clin. Microbiol. Infect. Dis. 16, 396–399.

Bou, G., and Martínez-Beltrán, J. (2000). Cloning, nucleotide sequencing, and analysis of the gene encoding an AmpC beta-lactamase in Acinetobacter baumannii. Antimicrob. Agents Chemother. 44, 428–432.

Boucher, H.W., Talbot, G.H., Benjamin, D.K., Bradley, J., Guidos, R.J., Jones, R.N., Murray, B.E., Bonomo, R.A., Gilbert, D., and America, for the I.D.S. of (2013). 10 × ’20 Progress—Development of New Drugs Active Against Gram-Negative Bacilli: An Update From the Infectious Diseases Society of America. Clin. Infect. Dis. 56, 1685–1694.

Bouvet, P.J.M., and Grimont, P.A.D. (1986). Taxonomy of the Genus Acinetobacter with the Recognition of Acinetobacter baumannii sp. nov., Acinetobacter haemolyticus sp. nov., Acinetobacter johnsonii sp. nov., and Acinetobacter junii sp. nov. and Emended Descriptions of Acinetobacter calcoaceticus and Acinetobacter lwoffii. Int. J. Syst. Evol. Microbiol. 36, 228–240.

de Breij, A., Gaddy, J., van der Meer, J., Koning, R., Koster, A., van den Broek, P., Actis, L., Nibbering, P., and Dijkshoorn, L. (2009). CsuA/BABCDE-dependent pili are not involved in the adherence of Acinetobacter baumannii ATCC19606T to human airway epithelial cells and their inflammatory response. Res. Microbiol. 160, 213–218.

de Breij, A., Eveillard, M., Dijkshoorn, L., van den Broek, P.J., Nibbering, P.H., and Joly-Guillou, M.-L. (2012). Differences in Acinetobacter baumannii Strains and Host Innate Immune Response Determine Morbidity and Mortality in Experimental Pneumonia. PLoS ONE 7.

Brigante, G., Migliavacca, R., Bramati, S., Motta, E., Nucleo, E., Manenti, M., Migliorino, G., Pagani, L., Luzzaro, F., and Viganò, F.E. (2012). Emergence and spread of a multidrug-resistant Acinetobacter baumannii clone producing both the carbapenemase OXA-23 and the 16S rRNA methylase ArmA. J. Med. Microbiol. 61, 653–661.

Brisou, J., and Prevot, A.R. (1954). [Studies on bacterial taxonomy. X. The revision of species under Acromobacter group]. Ann. Inst. Pasteur 86, 722–728.

Brossier, F., Veziris, N., Truffot-Pernot, C., Jarlier, V., and Sougakoff, W. (2006). Performance of the Genotype MTBDR Line Probe Assay for Detection of Resistance to Rifampin and Isoniazid in Strains of Mycobacterium tuberculosis with Low- and High-Level Resistance. J. Clin. Microbiol. 44, 3659–3664.

Brossier, F., Veziris, N., Truffot-Pernot, C., Jarlier, V., and Sougakoff, W. (2011). Molecular Investigation of Resistance to the Antituberculous Drug Ethionamide in Multidrug-Resistant Clinical Isolates of Mycobacterium tuberculosis. Antimicrob. Agents Chemother. 55, 355–360.

Brown, J.M., Dorman, D.C., and Roy, L.P. (1970). Acute renal failure due to overdosage of colistin. Med. J. Aust. 2, 923–924.

Bruhn, K.W., Pantapalangkoor, P., Nielsen, T., Tan, B., Junus, J., Hujer, K.M., Wright, M.S., Bonomo, R.A., Adams, M.D., Chen, W., et al. (2015). Host fate is rapidly determined by innate effector-microbial interactions during Acinetobacter baumannii bacteremia. J. Infect. Dis. 211, 1296–1305.

Carvalho, V.C. de, Oliveira, P.R.D. de, Dal-Paz, K., Paula, A.P. de, Félix, C. da S., and Lima, A.L.L.M. (2012). Gram-negative osteomyelitis: clinical and microbiological profile. Braz. J. Infect. Dis. Off. Publ. Braz. Soc. Infect. Dis. 16, 63–67.

Catel-Ferreira, M., Nehmé, R., Molle, V., Aranda, J., Bouffartigues, E., Chevalier, S., Bou, G., Jouenne, T., and Dé, E. (2012). Deciphering the function of the outer membrane protein OprD homologue of Acinetobacter baumannii. Antimicrob. Agents Chemother. 56, 3826–3832.

CDC (2013). Antibiotic resistance threats in the United States, 2013.

Chabane, Y.N., Marti, S., Rihouey, C., Alexandre, S., Hardouin, J., Lesouhaitier, O., Vila, J., Kaplan, J.B., Jouenne, T., and Dé, E. (2014). Characterisation of Pellicles Formed by Acinetobacter baumannii at the Air-Liquid Interface. PLOS ONE 9, e111660.

Chasteen, T.G., Fuentes, D.E., Tantaleán, J.C., and Vásquez, C.C. (2009). Tellurite: history, oxidative stress, and molecular mechanisms of resistance. FEMS Microbiol. Rev. 33, 820–832.

Chen, C.-H., Chang, C.-Y., Lin, L.-J., Chen, W.L., Chang, Y.-J., Wang, S.-H., Cheng, C.-Y., and Yen, H.-C. (2016). Risk factors associated with postcraniotomy meningitis: A retrospective study. Medicine (Baltimore) 95.

Chen, M.-Z., Hsueh, P.-R., Lee, L.-N., Yu, C.-J., Yang, P.-C., and Luh, K.-T. (2001). Severe Community-Acquired Pneumonia due to Acinetobacter baumannii. Chest 120, 1072–1077.

Chihi, H., Bonnin, R.A., Bourouis, A., Mahrouki, S., Besbes, S., Moussa, M.B., Belhadj, O., and Naas, T. (2016). GES-11-producing Acinetobacter baumannii clinical isolates from Tunisian hospitals: Long-term dissemination of GES-type carbapenemases in North Africa. J. Glob. Antimicrob. Resist. 5, 47–50.

Chin, C.-Y., Gregg, K.A., Napier, B.A., Ernst, R.K., and Weiss, D.S. (2015). A PmrB-Regulated Deacetylase Required for Lipid A Modification and Polymyxin Resistance in Acinetobacter baumannii. Antimicrob. Agents Chemother. 59, 7911–7914.

Cho, Y.J., Moon, D.C., Jin, J.S., Choi, C.H., Lee, Y.C., and Lee, J.C. (2009). Genetic basis of resistance to aminoglycosides in Acinetobacter spp. and spread of armA in Acinetobacter baumannii sequence group 1 in Korean hospitals. Diagn. Microbiol. Infect. Dis. 64, 185–190.

Choi, C.H., Lee, E.Y., Lee, Y.C., Park, T.I., Kim, H.J., Hyun, S.H., Kim, S.A., Lee, S.-K., and Lee, J.C. (2005). Outer membrane protein 38 of Acinetobacter baumannii localizes to the mitochondria and induces apoptosis of epithelial cells. Cell. Microbiol. 7, 1127–1138.

Choi, C.H., Hyun, S.H., Lee, J.Y., Lee, J.S., Lee, Y.S., Kim, S.A., Chae, J.-P., Yoo, S.M., and Lee, J.C. (2008). Acinetobacter baumannii outer membrane protein A targets the nucleus and induces cytotoxicity. Cell. Microbiol. 10, 309–319.

Chopra, I., and Roberts, M. (2001). Tetracycline Antibiotics: Mode of Action, Applications, Molecular Biology, and Epidemiology of Bacterial Resistance. Microbiol. Mol. Biol. Rev. 65, 232–260.

Clark, R.B. (1996). Imipenem resistance among Acinetobacter baumannii: association with reduced expression of a 33-36 kDa outer membrane protein. J. Antimicrob. Chemother. 38, 245–251.

Colleaux, L., D'Auriol, L., Galibert, F., and Dujon, B. (1988). Recognition and cleavage site of the intron-encoded omega transposase. Proc. Natl. Acad. Sci. 85, 6022–6026.

Coyne, S., Rosenfeld, N., Lambert, T., Courvalin, P., and Périchon, B. (2010). Overexpression of Resistance-Nodulation-Cell Division Pump AdeFGH Confers Multidrug Resistance in Acinetobacter baumannii. Antimicrob. Agents Chemother. 54, 4389–4393.

Crubézy, E., Ludes, B., Poveda, J.D., Clayton, J., Crouau-Roy, B., and Montagnon, D. (1998). Identification of Mycobacterium DNA in an Egyptian Pott's disease of 5,400 years old. C. R. Acad. Sci. III 321, 941–951.

Cuellar, L.E., Fernandez-Maldonado, E., Rosenthal, V.D., Castaneda-Sabogal, A., Rosales, R., Mayorga-Espichan, M.J., Camacho-Cosavalente, L.A., and Castillo-Bravo, L.I. (2008). Device-associated infection rates and mortality in intensive care units of Peruvian hospitals: findings of the International Nosocomial Infection Control Consortium. Rev. Panam. Salud Publica Pan Am. J. Public Health 24, 16–24.

Daniel, T.M. (2004). René Théophile Hyacinthe Laënnec and the founding of pulmonary medicine [Founders of Our Knowledge]. Int. J. Tuberc. Lung Dis. 8, 517–518.

Daniel, T.M. (2006). The history of tuberculosis. Respir. Med. 100, 1862–1870.

Davis, J.S., McMillan, M., Swaminathan, A., Kelly, J.A., Piera, K.E., Baird, R.W., Currie, B.J., and Anstey, N.M. (2014). A 16-Year Prospective Study of Community-Onset Bacteremic Acinetobacter Pneumonia: Low Mortality With Appropriate Initial Empirical Antibiotic Protocols. Chest 146, 1038–1045.

Davis, K.A., Moran, K.A., McAllister, C.K., and Gray, P.J. (2005). Multidrug-Resistant Acinetobacter Extremity Infections in Soldiers. Emerg. Infect. Dis. 11, 1218–1224.

DeBarber, A.E., Mdluli, K., Bosman, M., Bekker, L.G., and Barry, C.E. (2000). Ethionamide activation and sensitivity in multidrug-resistant Mycobacterium tuberculosis. Proc. Natl. Acad. Sci. U. S. A. 97, 9677–9682.

Decousser, J.W., Jansen, C., Nordmann, P., Emirian, A., Bonnin, R.A., Anais, L., Merle, J.C., and Poirel, L. (2013). Outbreak of NDM-1-producing Acinetobacter baumannii in France, January to May 2013. Euro Surveill. Bull. Eur. Sur Mal. Transm. Eur. Commun. Dis. Bull. 18.

Dexter, C., Murray, G.L., Paulsen, I.T., and Peleg, A.Y. (2015). Community-acquired Acinetobacter baumannii: clinical characteristics, epidemiology and pathogenesis. Expert Rev. Anti Infect. Ther. 13, 567–573.

Diancourt, L., Passet, V., Nemec, A., Dijkshoorn, L., and Brisse, S. (2010). The population structure of Acinetobacter baumannii: expanding multiresistant clones from an ancestral susceptible genetic pool. PloS One 5, e10034.

Dijkshoorn, L., van Aken, E., Shunburne, L., van der Reijden, T.J.K., Bernards, A.T., Nemec, A., and Towner, K.J. (2005). Prevalence of Acinetobacter baumannii and other Acinetobacter spp. in faecal samples from non-hospitalised individuals. Clin. Microbiol. Infect. 11, 329–332.

Dijkshoorn, L., Nemec, A., and Seifert, H. (2007). An increasing threat in hospitals: multidrug-resistant Acinetobacter baumannii. Nat. Rev. Microbiol. 5, 939–951.

Doi, Y., and Arakawa, Y. (2007). 16S Ribosomal RNA Methylation: Emerging Resistance Mechanism against Aminoglycosides. Clin. Infect. Dis. 45, 88–94.

Dorman, S.E., and Chaisson, R.E. (2007). From magic bullets back to the Magic Mountain: the rise of extensively drug-resistant tuberculosis. Nat. Med. 13, 295–298.

Dortet, L., Poirel, L., and Nordmann, P. (2014). Worldwide Dissemination of the NDM-Type Carbapenemases in Gram-Negative Bacteria. BioMed Res. Int. 2014, e249856.

Du, H., Chen, L., Tang, Y.-W., and Kreiswirth, B.N. (2016). Emergence of the mcr-1 colistin resistance gene in carbapenem-resistant Enterobacteriaceae. Lancet Infect. Dis. 16, 287–288.

Dueñas, L., Bran de Casares, A., Rosenthal, V.D., and Jesús Machuca, L. (2011). Device-associated infections rates in pediatrics and neonatal intensive care units in El Salvador: findings of the INICC. J. Infect. Dev. Ctries. 5, 445–451.

Dupont, M., Pagès, J.-M., Lafitte, D., Siroy, A., and Bollet, C. (2005). Identification of an OprD homologue in Acinetobacter baumannii. J. Proteome Res. 4, 2386–2390.

East, S.P., and Silver, L.L. (2013). Multitarget ligands in antibacterial research: progress and opportunities. Expert Opin. Drug Discov. 8, 143–156.

ECDC (2012). Surveillance of healthcare-associated infections in Europe, 2007.

ECDC (2013). Point prevalence survey of healthcareassociated infections and antimicrobial use in European acute care hospitals.

ECDC (2015). Annual epidemiological report 2014. Antimicrobial resistance and healthcare-associated infections.

ECDC (2017). Antimicrobial resistance surveillance in Europe 2015. Annual Report of the European Antimicrobial Resistance Surveillance Network (EARS-Net).

Eijkelkamp, B.A., Stroeher, U.H., Hassan, K.A., Paulsen, I.T., and Brown, M.H. (2014). Comparative analysis of surface-exposed virulence factors of Acinetobacter baumannii. BMC Genomics 15, 1020.

Eldholm, V., and Balloux, F. (2016). Antimicrobial Resistance in Mycobacterium tuberculosis: The Odd One Out. Trends Microbiol. 24, 637–648.

El-Sayed-Ahmed, M.A.E.-G., Amin, M.A., Tawakol, W.M., Loucif, L., Bakour, S., and Rolain, J.-M. (2015). High prevalence of bla(NDM-1) carbapenemase-encoding gene and 16S rRNA armA methyltransferase gene among Acinetobacter baumannii clinical Isolates in Egypt. Antimicrob. Agents Chemother. 59, 3602–3605.

Endimiani, A., Luzzaro, F., Migliavacca, R., Mantengoli, E., Hujer, A.M., Hujer, K.M., Pagani, L., Bonomo, R.A., Rossolini, G.M., and Toniolo, A. (2007). Spread in an Italian Hospital of a Clonal Acinetobacter baumannii Strain Producing the TEM-92 Extended-Spectrum β-Lactamase. Antimicrob. Agents Chemother. 51, 2211–2214.

Esterly, J.S., Richardson, C.L., Eltoukhy, N.S., Qi, C., and Scheetz, M.H. (2011). Genetic Mechanisms of Antimicrobial Resistance of Acinetobacter baumannii. Ann. Pharmacother. 45, 218–228.

Eveillard, M., Soltner, C., Kempf, M., Saint-André, J.-P., Lemarié, C., Randrianarivelo, C., Seifert, H., Wolff, M., and Joly-Guillou, M.-L. (2010). The virulence variability of different Acinetobacter baumannii strains in experimental pneumonia. J. Infect. 60, 154–161.

Fage, C.D., Brown, D.B., Boll, J.M., Keatinge-Clay, A.T., and Trent, M.S. (2014). Crystallographic study of the phosphoethanolamine transferase EptC required for polymyxin resistance and motility in Campylobacter jejuni. Acta Crystallogr. D Biol. Crystallogr. 70, 2730–2739.

Falagas, M.E., and Bliziotis, I.A. (2007). Pandrug-resistant Gram-negative bacteria: the dawn of the post-antibiotic era? Int. J. Antimicrob. Agents 29, 630–636.

Falagas, M.E., and Kasiakou, S.K. (2005). Colistin: the revival of polymyxins for the management of multidrug-resistant gram-negative bacterial infections. Clin. Infect. Dis. Off. Publ. Infect. Dis. Soc. Am. 40, 1333–1341.

Falagas, M.E., Bliziotis, I.A., and Siempos, I.I. (2006). Attributable mortality of Acinetobacter baumannii infections in critically ill patients: a systematic review of matched cohort and case-control studies. Crit. Care 10, R48.

Falgenhauer, L., Waezsada, S.-E., Yao, Y., Imirzalioglu, C., Käsbohrer, A., Roesler, U., Michael, G.B., Schwarz, S., Werner, G., Kreienbrock, L., et al. (2016). Colistin resistance gene mcr-1 in extended-spectrum β-lactamase-producing and carbapenemase-producing Gram-negative bacteria in Germany. Lancet Infect. Dis. 16, 282–283.

Fallah, F., Noori, M., Hashemi, A., Goudarzi, H., Karimi, A., Erfanimanesh, S., and Alimehr, S. (2014). Prevalence of blaNDM, blaPER, blaVEB, blaIMP, and blaVIM Genes among Acinetobacter baumannii Isolated from Two Hospitals of Tehran, Iran. Scientifica 2014.

Fernández, L., Gooderham, W.J., Bains, M., McPhee, J.B., Wiegand, I., and Hancock, R.E.W. (2010). Adaptive Resistance to the "Last Hope" Antibiotics Polymyxin B and Colistin in Pseudomonas aeruginosa Is Mediated by the Novel Two-Component Regulatory System ParR-ParS. Antimicrob. Agents Chemother. 54, 3372–3382.

Fernández, L., Jenssen, H., Bains, M., Wiegand, I., Gooderham, W.J., and Hancock, R.E.W. (2012). The Two-Component System CprRS Senses Cationic Peptides and Triggers Adaptive Resistance in Pseudomonas aeruginosa Independently of ParRS. Antimicrob. Agents Chemother. 56, 6212–6222.

Fiester, S.E., Nwugo, C.C., Penwell, W.F., Neary, J.M., Beckett, A.C., Arivett, B.A., Schmidt, R.E., Geiger, S.C., Connerly, P.L., Menke, S.M., et al. (2015). Role of the Carboxy Terminus of SecA in Iron Acquisition, Protein Translocation, and Virulence of the Bacterial Pathogen Acinetobacter baumannii. Infect. Immun. 83, 1354–1365.

Figueiredo, S., Poirel, L., Papa, A., Koulourida, V., and Nordmann, P. (2009). Overexpression of the Naturally Occurring blaOXA-51 Gene in Acinetobacter baumannii Mediated by Novel Insertion Sequence ISAba9. Antimicrob. Agents Chemother. 53, 4045–4047.

Fonseca, E.L., Scheidegger, E., Freitas, F.S., Cipriano, R., and Vicente, A.C.P. (2013). Carbapenem-resistant Acinetobacter baumannii from Brazil: role of carO alleles expression and blaOXA-23 gene. BMC Microbiol. 13, 245.

Fournier, P.-E., Vallenet, D., Barbe, V., Audic, S., Ogata, H., Poirel, L., Richet, H., Robert, C., Mangenot, S., Abergel, C., et al. (2006). Comparative genomics of multidrug resistance in Acinetobacter baumannii. PLoS Genet. 2, e7.

Fraaije, M.W., Kamerbeek, N.M., Heidekamp, A.J., Fortin, R., and Janssen, D.B. (2004). The prodrug activator EtaA from Mycobacterium tuberculosis is a Baeyer-Villiger monooxygenase. J. Biol. Chem. 279, 3354–3360.

Gaddy, J.A., Tomaras, A.P., and Actis, L.A. (2009). The Acinetobacter baumannii 19606 OmpA protein plays a role in biofilm formation on abiotic surfaces and in the interaction of this pathogen with eukaryotic cells. Infect. Immun. 77, 3150–3160.

Gaddy, J.A., Arivett, B.A., McConnell, M.J., López-Rojas, R., Pachón, J., and Actis, L.A. (2012). Role of Acinetobactin-Mediated Iron Acquisition Functions in the Interaction of Acinetobacter baumannii Strain ATCC 19606T with Human Lung Epithelial Cells, Galleria mellonella Caterpillars, and Mice. Infect. Immun. 80, 1015–1024.

Gales, A.C., Jones, R.N., and Sader, H.S. (2011). Contemporary activity of colistin and polymyxin B against a worldwide collection of Gram-negative pathogens: results from the SENTRY Antimicrobial Surveillance Program (2006–09). J. Antimicrob. Chemother. 66, 2070–2074.

García-Calderón, C.B., Casadesús, J., and Ramos-Morales, F. (2007). Rcs and PhoPQ Regulatory Overlap in the Control of Salmonella enterica Virulence. J. Bacteriol. 189, 6635–6644.

García-Quintanilla, M., Carretero-Ledesma, M., Moreno-Martínez, P., Martín-Peña, R., Pachón, J., and McConnell, M.J. (2015). Lipopolysaccharide loss produces partial colistin dependence and collateral sensitivity to azithromycin, rifampicin and vancomycin in Acinetobacter baumannii. Int. J. Antimicrob. Agents.

Garnacho, J., Sole-Violan, J., Sa-Borges, M., Diaz, E., and Rello, J. (2003). Clinical impact of pneumonia caused by Acinetobacter baumannii in intubated patients: a matched cohort study. Crit. Care Med. 31, 2478–2482.

Geisinger, E., and Isberg, R.R. (2015). Antibiotic Modulation of Capsular Exopolysaccharide and Virulence in Acinetobacter baumannii. PLOS Pathog. 11, e1004691.

Giammanco, A., Calà, C., Fasciana, T., and Dowzicky, M.J. (2017). Global Assessment of the Activity of Tigecycline against Multidrug-Resistant Gram-Negative Pathogens between 2004 and 2014 as Part of the Tigecycline Evaluation and Surveillance Trial. mSphere 2.

Glew, R.H., Moellering, R.C., and Kunz, L.J. (1977). Infections with Acinetobacter calcoaceticus (Herellea vaginicola): clinical and laboratory studies. Medicine (Baltimore) 56, 79–97.

Gooderham, W.J., and Hancock, R.E.W. (2009). Regulation of virulence and antibiotic resistance by two-component regulatory systems in Pseudomonas aeruginosa. FEMS Microbiol. Rev. 33, 279–294.

Gordon, N.C., and Wareham, D.W. (2010). Multidrug-resistant Acinetobacter baumannii: mechanisms of virulence and resistance. Int. J. Antimicrob. Agents 35, 219–226.

Group, B.M.J.P. (1948). Streptomycin Treatment of Pulmonary Tuberculosis. Br Med J 2, 769–782.

Guanche-Garcell, H., Requejo-Pino, O., Rosenthal, V.D., Morales-Pérez, C., Delgado-González, O., and Fernández-González, D. (2011). Device-associated infection rates in adult intensive care units of Cuban university hospitals: International Nosocomial Infection Control Consortium (INICC) findings. Int. J. Infect. Dis. 15, e357–e362.

Guardabassi, L., Dijkshoorn, L., Collard, J.M., Olsen, J.E., and Dalsgaard, A. (2000). Distribution and in-vitro transfer of tetracycline resistance determinants in clinical and aquatic Acinetobacter strains. J. Med. Microbiol. 49, 929–936.

Gutierrez, M.C., Brisse, S., Brosch, R., Fabre, M., Omaïs, B., Marmiesse, M., Supply, P., and Vincent, V. (2005). Ancient Origin and Gene Mosaicism of the Progenitor of Mycobacterium tuberculosis. PLOS Pathog. 1, e5.

Gutu, A.D., Rodgers, N.S., Park, J., and Moskowitz, S.M. (2015). Pseudomonas aeruginosa High-Level Resistance to Polymyxins and Other Antimicrobial Peptides Requires cprA, a Gene That Is Disrupted in the PAO1 Strain. Antimicrob. Agents Chemother. 59, 5377–5387.

Hamouda, A., and Amyes, S.G.B. (2004). Novel gyrA and parC point mutations in two strains of Acinetobacter baumannii resistant to ciprofloxacin. J. Antimicrob. Chemother. 54, 695–696.

Harris, G., Lee, R.K., Lam, C.K., Kanzaki, G., Patel, G.B., Xu, H.H., and Chen, W. (2013). A Mouse Model of Acinetobacter baumannii-Associated Pneumonia Using a Clinically Isolated Hypervirulent Strain. Antimicrob. Agents Chemother. 57, 3601–3613.

Harris, T.L., Worthington, R.J., Hittle, L.E., Zurawski, D.V., Ernst, R.K., and Melander, C. (2014). Small molecule downregulation of PmrAB reverses lipid A modification and breaks colistin resistance. ACS Chem. Biol. 9, 122–127.

Hayman, J. (1984). Mycobacterium ulcerans: an infection from Jurassic time? Lancet Lond. Engl. 2, 1015–1016.

Héritier, C., Poirel, L., and Nordmann, P. (2006). Cephalosporinase over-expression resulting from insertion of ISAba1 in Acinetobacter baumannii. Clin. Microbiol. Infect. Off. Publ. Eur. Soc. Clin. Microbiol. Infect. Dis. 12, 123–130.

Higgins, P.G., Wisplinghoff, H., Stefanik, D., and Seifert, H. (2004). Selection of topoisomerase mutations and overexpression of adeB mRNA transcripts during an outbreak of Acinetobacter baumannii. J. Antimicrob. Chemother. 54, 821–823.

Higgins, P.G., Dammhayn, C., Hackel, M., and Seifert, H. (2010). Global spread of carbapenem-resistant Acinetobacter baumannii. J. Antimicrob. Chemother. 65, 233–238.

Hinshaw, C., Feldman, W.H., and Pfuetze, K.H. (1946). TREATMENT OF TUBERCULOSIS WITH STREPTOMYCIN: A Summary of Observations on One Hundred Cases. J. Am. Med. Assoc. 132, 778–782.

Hirai, Y. (1991). Survival of bacteria under dry conditions; from a viewpoint of nosocomial infection. J. Hosp. Infect. 19, 191–200.

Holdiness, M.R. (1987). Neurological manifestations and toxicities of the antituberculosis drugs. A review. Med. Toxicol. 2, 33–51.

Holmberg, S.D. (1990). The Rise of Tuberculosis in America before 1820. Am. Rev. Respir. Dis. 142, 1228–1232.

Hong, S.B., Shin, K.S., Ha, J., and Han, K. (2013). Co-existence of blaOXA-23 and armA in multidrug-resistant Acinetobacter baumannii isolated from a hospital in South Korea. J. Med. Microbiol. 62, 836–844.

Hornsey, M., Ellington, M.J., Doumith, M., Thomas, C.P., Gordon, N.C., Wareham, D.W., Quinn, J., Lolans, K., Livermore, D.M., and Woodford, N. (2010). AdeABC-mediated efflux and tigecycline MICs for epidemic clones of Acinetobacter baumannii. J. Antimicrob. Chemother. 65, 1589–1593.

Houang, E.T., Sormunen, R.T., Lai, L., Chan, C.Y., and Leong, A.S. (1998). Effect of desiccation on the ultrastructural appearances of Acinetobacter baumannii and Acinetobacter lwoffii. J. Clin. Pathol. 51, 786–788.

Hu, D., Liu, B., Dijkshoorn, L., Wang, L., and Reeves, P.R. (2013). Diversity in the Major Polysaccharide Antigen of Acinetobacter Baumannii Assessed by DNA Sequencing, and Development of a Molecular Serotyping Scheme. PLoS ONE 8.

Hu, Y., He, L., Tao, X., Meng, F., and Zhang, J. (2016). Biofilm may not be Necessary for the Epidemic Spread of Acinetobacter baumannii. Sci. Rep. 6, 32066.

Hujer, K.M., Hujer, A.M., Hulten, E.A., Bajaksouzian, S., Adams, J.M., Donskey, C.J., Ecker, D.J., Massire, C., Eshoo, M.W., Sampath, R., et al. (2006). Analysis of antibiotic resistance genes in multidrug-resistant Acinetobacter sp. isolates from military and civilian patients treated at the Walter Reed Army Medical Center. Antimicrob. Agents Chemother. 50, 4114–4123.

Huys, G., Cnockaert, M., Vaneechoutte, M., Woodford, N., Nemec, A., Dijkshoorn, L., and Swings, J. (2005a). Distribution of tetracycline resistance genes in genotypically related and unrelated multiresistant Acinetobacter baumannii strains from different European hospitals. Res. Microbiol. 156, 348–355.

Huys, G., Cnockaert, M., Nemec, A., Dijkshoorn, L., Brisse, S., Vaneechoutte, M., and Swings, J. (2005b). Repetitive-DNA-element PCR fingerprinting and antibiotic resistance of pan-European multi-resistant Acinetobacter baumannii clone III strains. J. Med. Microbiol. 54, 851–856.

Iacono, M., Villa, L., Fortini, D., Bordoni, R., Imperi, F., Bonnal, R.J.P., Sicheritz-Ponten, T., De Bellis, G., Visca, P., Cassone, A., et al. (2008). Whole-Genome Pyrosequencing of an Epidemic Multidrug-Resistant Acinetobacter baumannii Strain Belonging to the European Clone II Group. Antimicrob. Agents Chemother. 52, 2616–2625.

Imperi, F., Antunes, L.C.S., Blom, J., Villa, L., Iacono, M., Visca, P., and Carattoli, A. (2011). The genomics of Acinetobacter baumannii: Insights into genome plasticity, antimicrobial resistance and pathogenicity. IUBMB Life 63, 1068–1074.

Jahani-Sherafat, S., Razaghi, M., Rosenthal, V.D., Tajeddin, E., Seyedjavadi, S., Rashidan, M., Alebouyeh, M., Rostampour, M., Haghi, A., Sayarbayat, M., et al. (2015). Device-associated infection rates and bacterial resistance in six academic teaching hospitals of Iran: Findings from the International Nocosomial Infection Control Consortium (INICC). J. Infect. Public Health 8, 553–561.

Jarlier, V., and Nikaido, H. (1994). Mycobacterial cell wall: Structure and role in natural resistance to antibiotics. FEMS Microbiol. Lett. 123, 11–18.

Jawad, A., Seifert, H., Snelling, A.M., Heritage, J., and Hawkey, P.M. (1998). Survival of Acinetobacter baumannii on Dry Surfaces: Comparison of Outbreak and Sporadic Isolates. J. Clin. Microbiol. 36, 1938–1941.

Jellinek, K. (1949). Streptomycin in the Treatment of Extrapulmonary Tuberculosis. N. Engl. J. Med. 240, 680–683.

Jeong, S.H., Bae, I.K., Kwon, S.B., Lee, K., Yong, D., Woo, G.J., Lee, J.H., Jung, H.I., Jang, S.J., Sung, K.H., et al. (2005). Investigation of a nosocomial outbreak of Acinetobacter baumannii producing PER-1 extended-spectrum beta-lactamase in an intensive care unit. J. Hosp. Infect. 59, 242–248.

Jiang, W., Bikard, D., Cox, D., Zhang, F., and Marraffini, L.A. (2013). RNA-guided editing of bacterial genomes using CRISPR-Cas systems. Nat. Biotechnol. 31, 233–239.

Jinek, M., Chylinski, K., Fonfara, I., Hauer, M., Doudna, J.A., and Charpentier, E. (2012). A Programmable Dual-RNA–Guided DNA Endonuclease in Adaptive Bacterial Immunity. Science 337, 816–821.

Johnson, T.L., Waack, U., Smith, S., Mobley, H., and Sandkvist, M. (2016). Acinetobacter baumannii Is Dependent on the Type II Secretion System and Its Substrate LipA for Lipid Utilization and In Vivo Fitness. J. Bacteriol. 198, 711–719.

Jones, C.L., Clancy, M., Honnold, C., Singh, S., Snesrud, E., Onmus-Leone, F., McGann, P., Ong, A.C., Kwak, Y., Waterman, P., et al. (2015). Fatal Outbreak of an Emerging Clone of Extensively Drug-Resistant Acinetobacter baumannii With Enhanced Virulence. Clin. Infect. Dis. 61, 145–154.

Kanj, S., Kanafani, Z., Sidani, N., Alamuddin, L., Zahreddine, N., and Rosenthal, V. (2012). International Nosocomial Infection Control Consortium Findings of Device-Associated Infections Rate in an Intensive Care Unit of a Lebanese University Hospital. J. Glob. Infect. Dis. 4, 15–21.

Karah, N., Haldorsen, B., Hermansen, N.O., Tveten, Y., Ragnhildstveit, E., Skutlaberg, D.H., Tofteland, S., Sundsfjord, A., and Samuelsen, Ø. (2011). Emergence of OXA-carbapenemase- and 16S rRNA methylase-producing international clones of Acinetobacter baumannii in Norway. J. Med. Microbiol. 60, 515–521.

Kenyon, J.J., and Hall, R.M. (2013). Variation in the Complex Carbohydrate Biosynthesis Loci of Acinetobacter baumannii Genomes. PLoS ONE 8.

Keshavjee, S., and Farmer, P.E. (2012). Tuberculosis, Drug Resistance, and the History of Modern Medicine. N. Engl. J. Med. 367, 931–936.

Kim, D.H., Choi, J.-Y., Kim, H.W., Kim, S.H., Chung, D.R., Peck, K.R., Thamlikitkul, V., So, T.M.-K., Yasin, R.M.D., Hsueh, P.-R., et al. (2013). Spread of Carbapenem-Resistant Acinetobacter baumannii Global Clone 2 in Asia and AbaR-Type Resistance Islands. Antimicrob. Agents Chemother. 57, 5239–5246.

Knapp, S., Wieland, C.W., Florquin, S., Pantophlet, R., Dijkshoorn, L., Tshimbalanga, N., Akira, S., and van der Poll, T. (2006). Differential Roles of CD14 and Toll-like Receptors 4and 2 in Murine Acinetobacter Pneumonia. Am. J. Respir. Crit. Care Med. 173, 122–129.

Koch-Weser, J., Sidel, V.W., Federman, E.B., Kanarek, P., Finer, D.C., and Eaton, A.E. (1970). Adverse effects of sodium colistimethate. Manifestations and specific reaction rates during 317 courses of therapy. Ann. Intern. Med. 72, 857–868.

Koeleman, J.G., van der Bijl, M.W., Stoof, J., Vandenbroucke-Grauls, C.M., and Savelkoul, P.H. (2001). Antibiotic resistance is a major risk factor for epidemic behavior of Acinetobacter baumannii. Infect. Control Hosp. Epidemiol. 22, 284–288.

Laganà, P., Melcarne, L., and Delia, S. (2015). Acinetobacter baumannii and endocarditis, rare complication but important clinical relevance. Int. J. Cardiol. 187, 678–679.

Lean, S.-S., Yeo, C.C., Suhaili, Z., and Thong, K.-L. (2015). Whole-genome analysis of an extensively drug-resistant clinical isolate of Acinetobacter baumannii AC12: insights into the mechanisms of resistance of an ST195 clone from Malaysia. Int. J. Antimicrob. Agents 45, 178–182.

Leblebicioglu, H., Rosenthal, V.D., Arikan, O.A., Ozgültekin, A., Yalcin, A.N., Koksal, I., Usluer, G., Sardan, Y.C., Ulusoy, S., and Turkish Branch of INICC (2007). Device-associated hospital-acquired infection rates in Turkish intensive care units. Findings of the International Nosocomial Infection Control Consortium (INICC). J. Hosp. Infect. 65, 251–257.

Lee, J.C., Koerten, H., van den Broek, P., Beekhuizen, H., Wolterbeek, R., van den Barselaar, M., van der Reijden, T., van der Meer, J., van de Gevel, J., and Dijkshoorn, L. (2006). Adherence of Acinetobacter baumannii strains to human bronchial epithelial cells. Res. Microbiol. 157, 360–366.

Lee, J.K., Lee, Y.S., Park, Y.K., and Kim, B.S. (2005). Mutations in the gyrA and parC Genes in Ciprofloxacin-Resistant Clinical Isolates of Acinetobacter baumannii in Korea. Microbiol. Immunol. 49, 647–653.

Lee, J.S., Choi, C.H., Kim, J.W., and Lee, J.C. (2010). Acinetobacter baumannii outer membrane protein a induces dendritic cell death through mitochondrial targeting. J. Microbiol. 48, 387–392.

Lee, N.-Y., Lee, H.-C., Ko, N.-Y., Chang, C.-M., Shih, H.-I., Wu, C.-J., and Ko, W.-C. (2007). Clinical and economic impact of multidrug resistance in nosocomial Acinetobacter baumannii bacteremia. Infect. Control Hosp. Epidemiol. 28, 713–719.

Lees-Miller, R.G., Iwashkiw, J.A., Scott, N.E., Seper, A., Vinogradov, E., Schild, S., and Feldman, M.F. (2013). A common pathway for O-linked protein-glycosylation and synthesis of capsule in Acinetobacter baumannii. Mol. Microbiol. 89, 816–830.

Lei, B., Wei, C.-J., and Tu, S.-C. (2000). Action mechanism of antitubercular isoniazid activation by mycobacterium tuberculosis KatG, isolation, and characterization of InhA inhibitor. J. Biol. Chem. 275, 2520–2526.

Lesho, E., Yoon, E.-J., McGann, P., Snesrud, E., Kwak, Y., Milillo, M., Onmus-Leone, F., Preston, L., Clair, K.S., Nikolich, M., et al. (2013). Emergence of Colistin-Resistance in Extremely Drug-Resistant Acinetobacter baumannii Containing a Novel pmrCAB Operon During Colistin Therapy of Wound Infections. J. Infect. Dis. 208, 1142–1151.

Leung, K.L., Yip, C.W., Yeung, Y.L., Wong, K.L., Chan, W.Y., Chan, M.Y., and Kam, K.M. (2010). Usefulness of resistant gene markers for predicting treatment outcome on second-line anti-tuberculosis drugs. J. Appl. Microbiol. 109, 2087–2094.

Leung, W.-S., Chu, C.-M., Tsang, K.-Y., Lo, F.-H., Lo, K.-F., and Ho, P.-L. (2006). Fulminant Community-Acquired Acinetobacter baumannii Pneumonia as a Distinct Clinical Syndrome. Chest 129, 102–109.

Li, H., Liu, F., Zhang, Y., Wang, X., Zhao, C., Chen, H., Zhang, F., Zhu, B., Hu, Y., and Wang, H. (2015). Evolution of carbapenem-resistant Acinetobacter baumannii revealed through whole-genome sequencing and comparative genomic analysis. Antimicrob. Agents Chemother. 59, 1168–1176.

Li, J., Nation, R.L., Turnidge, J.D., Milne, R.W., Coulthard, K., Rayner, C.R., and Paterson, D.L. (2006). Colistin: the re-emerging antibiotic for multidrug-resistant Gram-negative bacterial infections. Lancet Infect. Dis. 6, 589–601.

Lin, L., Tan, B., Pantapalangkoor, P., Ho, T., Baquir, B., Tomaras, A., Montgomery, J.I., Reilly, U., Barbacci, E.G., Hujer, K., et al. (2012). Inhibition of LpxC Protects Mice from Resistant Acinetobacter baumannii by Modulating Inflammation and Enhancing Phagocytosis. mBio 3, e00312-12.

Liou, M.-L., Chen, K.-H., Yeh, H.-L., Lai, C.-Y., and Chen, C.-H. (2017). Persistent nasal carriers of Acinetobacter baumannii in long-term-care facilities. Am. J. Infect. Control 0.

Litake, G.M., Ghole, V.S., Niphadkar, K.B., and Joshi, S.G. (2009). PER-1-type extended-spectrum β-lactamase-producing Acinetobacter baumannii clinical isolates from India. Int. J. Antimicrob. Agents 34, 388–389.

Liu, F., Zhu, Y., Yi, Y., Lu, N., Zhu, B., and Hu, Y. (2014). Comparative genomic analysis of Acinetobacter baumannii clinical isolates reveals extensive genomic variation and diverse antibiotic resistance determinants. BMC Genomics 15, 1163.

Liu, Y.-Y., Wang, Y., Walsh, T.R., Yi, L.-X., Zhang, R., Spencer, J., Doi, Y., Tian, G., Dong, B., Huang, X., et al. (2016). Emergence of plasmid-mediated colistin resistance mechanism MCR-1 in animals and human beings in China: a microbiological and molecular biological study. Lancet Infect. Dis. 16, 161–168.

Loehfelm, T.W., Luke, N.R., and Campagnari, A.A. (2008). Identification and characterization of an Acinetobacter baumannii biofilm-associated protein. J. Bacteriol. 190, 1036–1044.

Longo, F., Vuotto, C., and Donelli, G. (2014). Biofilm formation in Acinetobacter baumannii. New Microbiol. 37, 119–127.

Lopes, B.S., and Amyes, S.G.B. (2012). Role of ISAba1 and ISAba125 in governing the expression of blaADC in clinically relevant Acinetobacter baumannii strains resistant to cephalosporins. J. Med. Microbiol. 61, 1103–1108.

Lupo, A., Vogt, D., Seiffert, S.N., Endimiani, A., and Perreten, V. (2014). Antibiotic resistance and phylogenetic characterization of Acinetobacter baumannii strains isolated from commercial raw meat in Switzerland. J. Food Prot. 77, 1976–1981.

Macfarlane, E.L., Kwasnicka, A., and Hancock, R.E. (2000). Role of Pseudomonas aeruginosa PhoP-phoQ in resistance to antimicrobial cationic peptides and aminoglycosides. Microbiol. Read. Engl. 146 (Pt 10), 2543–2554.

Macfarlane, E.L.A., Kwasnicka, A., Ochs, M.M., and Hancock, R.E.W. (1999). PhoP–PhoQ homologues in Pseudomonas aeruginosa regulate expression of the outer-membrane protein OprH and polymyxin B resistance. Mol. Microbiol. 34, 305–316.

Madani, N., Rosenthal, V.D., Dendane, T., Abidi, K., Zeggwagh, A.A., and Abouqal, R. (2009). Health-care associated infections rates, length of stay, and bacterial resistance in an intensive care unit of Morocco: Findings of the International Nosocomial Infection Control Consortium (INICC). Int. Arch. Med. 2, 29.

Magiorakos, A.-P., Srinivasan, A., Carey, R.B., Carmeli, Y., Falagas, M.E., Giske, C.G., Harbarth, S., Hindler, J.F., Kahlmeter, G., Olsson-Liljequist, B., et al. (2012). Multidrug-resistant, extensively drug-resistant and pandrug-resistant bacteria: an international expert proposal for interim standard definitions for acquired resistance. Clin. Microbiol. Infect. 18, 268–281.

Magnet, S., Courvalin, P., and Lambert, T. (2001). Resistance-Nodulation-Cell Division-Type Efflux Pump Involved in Aminoglycoside Resistance in Acinetobacter baumannii Strain BM4454. Antimicrob. Agents Chemother. 45, 3375–3380.

Mak, J.K., Kim, M.-J., Pham, J., Tapsall, J., and White, P.A. (2009). Antibiotic resistance determinants in nosocomial strains of multidrug-resistant Acinetobacter baumannii. J. Antimicrob. Chemother. 63, 47–54.

del Mar Tomás, M., Beceiro, A., Pérez, A., Velasco, D., Moure, R., Villanueva, R., Martínez-Beltrán, J., and Bou, G. (2005). Cloning and functional analysis of the gene encoding the 33- to 36-kilodalton outer membrane protein associated with carbapenem resistance in Acinetobacter baumannii. Antimicrob. Agents Chemother. 49, 5172–5175.

Maragakis, L.L., and Perl, T.M. (2008). Acinetobacter baumannii: epidemiology, antimicrobial resistance, and treatment options. Clin. Infect. Dis. Off. Publ. Infect. Dis. Soc. Am. 46, 1254–1263.

Marrakchi, H., Lanéelle, G., and Quémard, A. (2000). InhA, a target of the antituberculous drug isoniazid, is involved in a mycobacterial fatty acid elongation system, FAS-II. Microbiol. Read. Engl. 146 (Pt 2), 289–296.

Marti, S., Nait Chabane, Y., Alexandre, S., Coquet, L., Vila, J., Jouenne, T., and Dé, E. (2011). Growth of Acinetobacter baumannii in Pellicle Enhanced the Expression of Potential Virulence Factors. PLoS ONE 6.

Martinez, T., Martinez, I., Vazquez, G.J., Aquino, E.E., and Robledo, I.E. (2016). Genetic environment of the KPC gene in Acinetobacter baumannii ST2 clone from Puerto Rico and genomic insights into its drug resistance. J. Med. Microbiol. 65, 784–792.

McConnell, M.J., Actis, L., and Pachón, J. (2013). Acinetobacter baumannii: human infections, factors contributing to pathogenesis and animal models. FEMS Microbiol. Rev. 37, 130–155.

McPhee, J.B., Bains, M., Winsor, G., Lewenza, S., Kwasnicka, A., Brazas, M.D., Brinkman, F.S.L., and Hancock, R.E.W. (2006). Contribution of the PhoP-PhoQ and PmrA-PmrB Two-Component Regulatory Systems to Mg2+-Induced Gene Regulation in Pseudomonas aeruginosa. J. Bacteriol. 188, 3995–4006.

Mehta, A., Rosenthal, V.D., Mehta, Y., Chakravarthy, M., Todi, S.K., Sen, N., Sahu, S., Gopinath, R., Rodrigues, C., Kapoor, P., et al. (2007). Device-associated nosocomial infection rates in intensive care units of seven Indian cities. Findings of the International Nosocomial Infection Control Consortium (INICC). J. Hosp. Infect. 67, 168–174.

Milan, A., Furlanis, L., Cian, F., Bressan, R., Luzzati, R., Lagatolla, C., Deiana, M.L., Knezevich, A., Tonin, E., and Dolzani, L. (2016). Epidemic Dissemination of a Carbapenem-Resistant Acinetobacter baumannii Clone Carrying armA Two Years After Its First Isolation in an Italian Hospital. Microb. Drug Resist. Larchmt. N 22, 668–674.

Miller, G.H., Sabatelli, F.J., Naples, L., Hare, R.S., and Shaw, K.J. (1995). The most frequently occurring aminoglycoside resistance mechanisms- combined results of surveys in eight regions of the world. The aminoglycoside resistance study groups. 7, 17–30.

Moffatt, J.H., Harper, M., Adler, B., Nation, R.L., Li, J., and Boyce, J.D. (2011). Insertion sequence ISAba11 is involved in colistin resistance and loss of lipopolysaccharide in Acinetobacter baumannii. Antimicrob. Agents Chemother. 55, 3022–3024.

Moreno, C.Á., Rosenthal, V.D., Olarte, N., Gomez, W.V., Sussmann, O., Agudelo, J.G., Rojas, C., Osorio, L., Linares, C., Valderrama, A., et al. (2006). Device-Associated Infection Rate and Mortality in Intensive Care Units of 9 Colombian Hospitals: Findings of the International Nosocomial Infection Control Consortium. Infect. Control Hosp. Epidemiol. 27, 349–356.

Mori, G., Chiarelli, L.R., Riccardi, G., and Pasca, M.R. (2017). New prodrugs against tuberculosis. Drug Discov. Today 22, 519–525.

Morita, Y., Tomida, J., and Kawamura, Y. (2012). Primary mechanisms mediating aminoglycoside resistance in the multidrug-resistant Pseudomonas aeruginosa clinical isolate PA7. Microbiol. Read. Engl. 158, 1071–1083.

Morlock, G.P., Metchock, B., Sikes, D., Crawford, J.T., and Cooksey, R.C. (2003). ethA, inhA, and katG Loci of Ethionamide-Resistant Clinical Mycobacterium tuberculosis Isolates. Antimicrob. Agents Chemother. 47, 3799–3805.

Morris, R.P., Nguyen, L., Gatfield, J., Visconti, K., Nguyen, K., Schnappinger, D., Ehrt, S., Liu, Y., Heifets, L., Pieters, J., et al. (2005). Ancestral antibiotic resistance in Mycobacterium tuberculosis. Proc. Natl. Acad. Sci. U. S. A. 102, 12200–12205.

Mortensen, B.L., and Skaar, E.P. (2013). The contribution of nutrient metal acquisition and metabolism to Acinetobacter baumannii survival within the host. Front. Cell. Infect. Microbiol. 3.

Moubareck, C., Brémont, S., Conroy, M.-C., Courvalin, P., and Lambert, T. (2009). GES-11, a novel integron-associated GES variant in Acinetobacter baumannii. Antimicrob. Agents Chemother. 53, 3579–3581.

Mugnier, P.D., Poirel, L., and Nordmann, P. (2009). Functional Analysis of Insertion Sequence ISAba1, Responsible for Genomic Plasticity of Acinetobacter baumannii. J. Bacteriol. 191, 2414–2418.

Naas, T., Coignard, B., Carbonne, A., Blanckaert, K., Bajolet, O., Bernet, C., Verdeil, X., Astagneau, P., Desenclos, J.-C., Nordmann, P., et al. (2006a). VEB-1 Extended-spectrum beta-lactamase-producing Acinetobacter baumannii, France. Emerg. Infect. Dis. 12, 1214–1222.

Naas, T., Bogaerts, P., Bauraing, C., Degheldre, Y., Glupczynski, Y., and Nordmann, P. (2006b). Emergence of PER and VEB extended-spectrum beta-lactamases in Acinetobacter baumannii in Belgium. J. Antimicrob. Chemother. 58, 178–182.

Naas, T., Nordmann, P., and Heidt, A. (2007a). Intercountry transfer of PER-1 extended-spectrum beta-lactamase-producing Acinetobacter baumannii from Romania. Int. J. Antimicrob. Agents 29, 226–228.

Naas, T., Kernbaum, S., Allali, S., and Nordmann, P. (2007b). Multidrug-resistant Acinetobacter baumannii, Russia. Emerg. Infect. Dis. 13, 669–671.

Naas, T., Namdari, F., Réglier-Poupet, H., Poyart, C., and Nordmann, P. (2007c). Panresistant extended-spectrum β-lactamase SHV-5-producing Acinetobacter baumannii from New York City. J. Antimicrob. Chemother. 60, 1174–1176.

Nahid, P., Dorman, S.E., Alipanah, N., Barry, P.M., Brozek, J.L., Cattamanchi, A., Chaisson, L.H., Chaisson, R.E., Daley, C.L., Grzemska, M., et al. (2016). Official American Thoracic Society/Centers for Disease Control and Prevention/Infectious Diseases Society of America Clinical Practice Guidelines: Treatment of Drug-Susceptible Tuberculosis. Clin. Infect. Dis. 63, e147–e195.

Navoa-Ng, J.A., Berba, R., Galapia, Y.A., Rosenthal, V.D., Villanueva, V.D., Tolentino, M.C.V., Genuino, G.A.S., Consunji, R.J., and Mantaring, J.B.V. (2011). Device-associated infections rates in adult, pediatric, and neonatal intensive care units of hospitals in the Philippines: International Nosocomial Infection Control Consortium (INICC) findings. Am. J. Infect. Control 39, 548–554.

Needham, B.D., and Trent, M.S. (2013). Fortifying the barrier: the impact of lipid A remodelling on bacterial pathogenesis. Nat. Rev. Microbiol. 11, 467–481.

Nemec, A., Dolzani, L., Brisse, S., van den Broek, P., and Dijkshoorn, L. (2004). Diversity of aminoglycoside-resistance genes and their association with class 1 integrons among strains of pan-European Acinetobacter baumannii clones. J. Med. Microbiol. 53, 1233–1240.

Nerlich, A.G., Haas, C.J., Zink, A., Szeimies, U., and Hagedorn, H.G. (1997). Molecular evidence for tuberculosis in an ancient Egyptian mummy. The Lancet 350, 1404.

Nguyen, L. (2016). Antibiotic resistance mechanisms in M. tuberculosis: an update. Arch. Toxicol. 90, 1585–1604.

Nie, L., Lv, Y., Yuan, M., Hu, X., Nie, T., Yang, X., Li, G., Pang, J., Zhang, J., Li, C., et al. (2014). Genetic basis of high level aminoglycoside resistance in Acinetobacter baumannii from Beijing, China. Acta Pharm. Sin. B 4, 295–300.

Noppe-Leclercq, I., Wallet, F., Haentjens, S., Courcol, R., and Simonet, M. (1999). PCR detection of aminoglycoside resistance genes: a rapid molecular typing method for Acinetobacter baumannii. Res. Microbiol. 150, 317–322.

Olaitan, A.O., Morand, S., and Rolain, J.-M. (2014). Mechanisms of polymyxin resistance: acquired and intrinsic resistance in bacteria. Front. Microbiol. 5, 643.

Ong, C.W.M., Lye, D.C.B., Khoo, K.L., Chua, G.S.W., Yeoh, S.F., Leo, Y.S., Tambyah, P.A., and Chua, A.C. (2009). Severe community-acquired Acinetobacter baumannii pneumonia: An emerging highly lethal infectious disease in the Asia–Pacific. Respirology 14, 1200–1205.

Ou, H.-Y., Kuang, S.N., He, X., Molgora, B.M., Ewing, P.J., Deng, Z., Osby, M., Chen, W., and Xu, H.H. (2015). Complete genome sequence of hypervirulent and outbreak-associated Acinetobacter baumannii strain LAC-4: epidemiology, resistance genetic determinants and potential virulence factors. Sci. Rep. 5, 8643.

Palomino, J.C., and Martin, A. (2014). Drug Resistance Mechanisms in Mycobacterium tuberculosis. Antibiot. Basel Switz. 3, 317–340.

Pan, A., Mei, Q., Ye, Y., Li, H., Liu, B., and Li, J. (2017). Validation of the mutant selection window hypothesis with fosfomycin against Escherichia coli and Pseudomonas aeruginosa: an in vitro and in vivo comparative study. J. Antibiot. (Tokyo) 70, 166–173.

Park, S., Lee, K.M., Yoo, Y.S., Yoo, J.S., Yoo, J.I., Kim, H.S., Lee, Y.S., and Chung, G.T. (2011a). Alterations of gyrA, gyrB, and parC and Activity of Efflux Pump in Fluoroquinolone-resistant Acinetobacter baumannii. Osong Public Health Res. Perspect. 2, 164–170.

Park, Y.K., Choi, J.Y., Shin, D., and Ko, K.S. (2011b). Correlation between overexpression and amino acid substitution of the PmrAB locus and colistin resistance in Acinetobacter baumannii. Int. J. Antimicrob. Agents 37, 525–530.

Pasterán, F., Rapoport, M., Petroni, A., Faccone, D., Corso, A., Galas, M., Vázquez, M., Procopio, A., Tokumoto, M., and Cagnoni, V. (2006). Emergence of PER-2 and VEB-1a in Acinetobacter baumannii Strains in the Americas. Antimicrob. Agents Chemother. 50, 3222–3224.

Patel, G., Perez, F., Hujer, A.M., Rudin, S.D., Augustine, J.J., Jacobs, G.H., Jacobs, M.R., and Bonomo, R.A. (2015). Fulminant endocarditis and disseminated infection caused by carbapenem-resistant Acinetobacter baumannii in a renal-pancreas transplant recipient. Transpl. Infect. Dis. Off. J. Transplant. Soc. 17, 289–296.

Paterson, D.L., and Harris, P.N.A. (2015). The New Acinetobacter Equation: Hypervirulence plus Antibiotic Resistance Equals Big Trouble. Clin. Infect. Dis. civ227.

Patil, J.R., and Chopade, B.A. (2001). Distribution and in vitro antimicrobial susceptibility of Acinetobacter species on the skin of healthy humans. Natl. Med. J. India 14, 204–208.

Peleg, A.Y., and Hooper, D.C. (2010). Hospital-Acquired Infections Due to Gram-Negative Bacteria. N. Engl. J. Med. 362, 1804–1813.

Peleg, A.Y., Adams, J., and Paterson, D.L. (2007). Tigecycline Efflux as a Mechanism for Nonsusceptibility in Acinetobacter baumannii. Antimicrob. Agents Chemother. 51, 2065–2069.

Peleg, A.Y., Seifert, H., and Paterson, D.L. (2008). Acinetobacter baumannii: Emergence of a Successful Pathogen. Clin. Microbiol. Rev. 21, 538–582.

Pendleton, J.N., Gorman, S.P., and Gilmore, B.F. (2013). Clinical relevance of the ESKAPE pathogens. Expert Rev. Anti Infect. Ther. 11, 297–308.

Penwell, W.F., Arivett, B.A., and Actis, L.A. (2012). The Acinetobacter baumannii entA Gene Located Outside the Acinetobactin Cluster Is Critical for Siderophore Production, Iron Acquisition and Virulence. PLOS ONE 7, e36493.

Pieren, M., and Tigges, M. (2012). Adjuvant strategies for potentiation of antibiotics to overcome antimicrobial resistance. Curr. Opin. Pharmacol. 12, 551–555.

Pogue, J.M., Cohen, D.A., and Marchaim, D. (2015). Editorial commentary: Polymyxin-resistant Acinetobacter baumannii: urgent action needed. Clin. Infect. Dis. Off. Publ. Infect. Dis. Soc. Am. 60, 1304–1307.

Poirel, L., and Nordmann, P. (2006). Carbapenem resistance in Acinetobacter baumannii: mechanisms and epidemiology. Clin. Microbiol. Infect. 12, 826–836.

Poirel, L., Naas, T., and Nordmann, P. (2010). Diversity, Epidemiology, and Genetics of Class D β-Lactamases. Antimicrob. Agents Chemother. 54, 24–38.

Poirel, L., Kieffer, N., Liassine, N., Thanh, D., and Nordmann, P. (2016). Plasmid-mediated carbapenem and colistin resistance in a clinical isolate of Escherichia coli. Lancet Infect. Dis. 16, 281.

Poirel, L., Jayol, A., and Nordmann, P. (2017). Polymyxins: Antibacterial Activity, Susceptibility Testing, and Resistance Mechanisms Encoded by Plasmids or Chromosomes. Clin. Microbiol. Rev. 30, 557–596.

Post, V., White, P.A., and Hall, R.M. (2010). Evolution of AbaR-type genomic resistance islands in multiply antibiotic-resistant Acinetobacter baumannii. J. Antimicrob. Chemother. 65, 1162–1170.

Poteete, A.R. (2001). What makes the bacteriophage lambda Red system useful for genetic engineering: molecular mechanism and biological function. FEMS Microbiol. Lett. 201, 9–14.

Potron, A., Munoz-Price, L.S., Nordmann, P., Cleary, T., and Poirel, L. (2011). Genetic Features of CTX-M-15-Producing Acinetobacter baumannii from Haiti ▿. Antimicrob. Agents Chemother. 55, 5946–5948.

Potron, A., Poirel, L., and Nordmann, P. (2015). Emerging broad-spectrum resistance in Pseudomonas aeruginosa and Acinetobacter baumannii: Mechanisms and epidemiology. Int. J. Antimicrob. Agents 45, 568–585.

Prigent-Combaret, C., Sanguin, H., Champier, L., Bertrand, C., Monnez, C., Colinon, C., Blaha, D., Ghigo, J.-M., and Cournoyer, B. (2012). The bacterial thiopurine methyltransferase tellurite resistance process is highly dependent upon aggregation properties and oxidative stress response. Environ. Microbiol. 14, 2645–2660.

Pym, A.S., Domenech, P., Honoré, N., Song, J., Deretic, V., and Cole, S.T. (2001). Regulation of catalase-peroxidase (KatG) expression, isoniazid sensitivity and virulence by furA of Mycobacterium tuberculosis. Mol. Microbiol. 40, 879–889.

Rafei, R., Hamze, M., Pailhoriès, H., Eveillard, M., Marsollier, L., Joly-Guillou, M.-L., Dabboussi, F., and Kempf, M. (2015). Extrahuman Epidemiology of Acinetobacter baumannii in Lebanon. Appl. Environ. Microbiol. 81, 2359–2367.

Ramirez, M.S., and Tolmasky, M.E. (2010). Aminoglycoside Modifying Enzymes. Drug Resist. Updat. Rev. Comment. Antimicrob. Anticancer Chemother. 13, 151–171.

Ramirez Barba, E.J., Rosenthal, V.D., Higuera, F., Oropeza, M.S., Hernández, H.T., López, M.S., Lona, E.L., Duarte, P., Ruiz, J., Hernandez, R.R., et al. (2006). Device-associated nosocomial infection rates in intensive care units in four Mexican public hospitals. Am. J. Infect. Control 34, 244–247.

Rawat, R., Whitty, A., and Tonge, P.J. (2003). The isoniazid-NAD adduct is a slow, tight-binding inhibitor of InhA, the Mycobacterium tuberculosis enoyl reductase: adduct affinity and drug resistance. Proc. Natl. Acad. Sci. U. S. A. 100, 13881–13886.

Reading, C., and Cole, M. (1977). Clavulanic Acid: a Beta-Lactamase-Inhibiting Beta-Lactam from Streptomyces clavuligerus. Antimicrob. Agents Chemother. 11, 852–857.

Repizo, G.D., Gagné, S., Foucault-Grunenwald, M.-L., Borges, V., Charpentier, X., Limansky, A.S., Gomes, J.P., Viale, A.M., and Salcedo, S.P. (2015). Differential Role of the T6SS in Acinetobacter baumannii Virulence. PLOS ONE 10, e0138265.

Review on antimicrobial resistance (2016). Tackling drug-resistant infections globally: final report and recommendations.

Ribera, A., Roca, I., Ruiz, J., Gibert, I., and Vila, J. (2003). Partial characterization of a transposon containing the tet(A) determinant in a clinical isolate of Acinetobacter baumannii. J. Antimicrob. Chemother. 52, 477–480.

Ristow, M., Möhlig, M., Rifai, M., Schatz, H., Feldmann, K., and Pfeiffer, A. (1995). New isoniazid/ethionamide resistance gene mutation and screening for multidrug- resistant Mycobacterium tuberculosis strains. The Lancet 346, 502–503.

Robledo, I.E., Aquino, E.E., Santé, M.I., Santana, J.L., Otero, D.M., León, C.F., and Vázquez, G.J. (2010). Detection of KPC in Acinetobacter spp. in Puerto Rico. Antimicrob. Agents Chemother. 54, 1354–1357.

Rolain, J.-M., Kempf, M., Leangapichart, T., Chabou, S., Olaitan, A.O., Page, S.L., Morand, S., and Raoult, D. (2016). Plasmid-mediated mcr-1 gene in colistin-resistant clinical isolates of Klebsiella pneumoniae in France and Laos. Antimicrob. Agents Chemother. AAC.00960-16.

Rosenthal, V.D. (2016). International Nosocomial Infection Control Consortium (INICC) resources: INICC multidimensional approach and INICC surveillance online system. Am. J. Infect. Control 44, e81–e90.

Russo, T.A., Luke, N.R., Beanan, J.M., Olson, R., Sauberan, S.L., MacDonald, U., Schultz, L.W., Umland, T.C., and Campagnari, A.A. (2010). The K1 Capsular Polysaccharide of Acinetobacter baumannii Strain 307-0294 Is a Major Virulence Factor. Infect. Immun. 78, 3993–4000.

Ruzin, A., Keeney, D., and Bradford, P.A. (2007). AdeABC multidrug efflux pump is associated with decreased susceptibility to tigecycline in Acinetobacter calcoaceticus-Acinetobacter baumannii complex. J. Antimicrob. Chemother. 59, 1001–1004.

Ryan, K.J., Schainuck, L.I., Hickman, R.O., and Striker, G.E. (1969). Colistimethate toxicity. Report of a fatal case in a previously healthy child. JAMA 207, 2099–2101.

Sahl, J.W., Del Franco, M., Pournaras, S., Colman, R.E., Karah, N., Dijkshoorn, L., and Zarrilli, R. (2015). Phylogenetic and genomic diversity in isolates from the globally distributed Acinetobacter baumannii ST25 lineage. Sci. Rep. 5, 15188.

Salo, W.L., Aufderheide, A.C., Buikstra, J., and Holcomb, T.A. (1994). Identification of Mycobacterium tuberculosis DNA in a pre-Columbian Peruvian mummy. Proc. Natl. Acad. Sci. U. S. A. 91, 2091–2094.

Salomao, R., Rosenthal, V.D., Grimberg, G., Nouer, S., Blecher, Buchner-Ferreira, S., Vianna, R., and Maretti-da-Silva, M.Â. (2008). Device-associated infection rates in intensive care units of Brazilian hospitals: datos de la Comunidad Científica Internacional de Control de Infecciones Nosocomiales. Rev. Panam. Salud Pública 24, 195–202.

Schaaf, H.S., Victor, T.C., Engelke, E., Brittle, W., Marais, B.J., Hesseling, A.C., Helden, P.D. van, and Donald, P.R. (2007). Minimal inhibitory concentration of isoniazid in isoniazid-resistant Mycobacterium tuberculosis isolates from children. Eur. J. Clin. Microbiol. Infect. Dis. 26, 203–205.

Schatz, A., Bugie, E., and Waksman, S.A. (2005). Streptomycin, a substance exhibiting antibiotic activity against gram-positive and gram-negative bacteria. 1944. Clin. Orthop. 3–6.

Schweppe, D.K., Harding, C., Chavez, J.D., Wu, X., Ramage, E., Singh, P.K., Manoil, C., and Bruce, J.E. (2015). Host-Microbe Protein Interactions during Bacterial Infection. Chem. Biol. 22, 1521–1530.

Scorpio, A., and Zhang, Y. (1996). Mutations in pncA, a gene encoding pyrazinamidase/nicotinamidase, cause resistance to the antituberculous drug pyrazinamide in tubercle bacillus. Nat. Med. 2, 662–667.

Scott, N.E., Kinsella, R.L., Edwards, A.V.G., Larsen, M.R., Dutta, S., Saba, J., Foster, L.J., and Feldman, M.F. (2014). Diversity Within the O-linked Protein Glycosylation Systems of Acinetobacter Species. Mol. Cell. Proteomics 13, 2354–2370.

Seifert, H., Dijkshoorn, L., Gerner-Smidt, P., Pelzer, N., Tjernberg, I., and Vaneechoutte, M. (1997). Distribution of Acinetobacter species on human skin: comparison of phenotypic and genotypic identification methods. J. Clin. Microbiol. 35, 2819–2825.

Sheikhalizadeh, V., Hasani, A., Ahangarzadeh Rezaee, M., Rahmati-yamchi, M., Hasani, A., Ghotaslou, R., and Goli, H.R. (2017). Comprehensive study to investigate the role of various aminoglycoside resistance mechanisms in clinical isolates of Acinetobacter baumannii. J. Infect. Chemother. 23, 74–79.

Shen, M., Luan, G., Wang, Y., Chang, Y., Zhang, C., Yang, J., Deng, S., Ling, B., and Jia, X. (2016a). Coexistence of blaOXA-23 with armA in quinolone-resistant Acinetobacter baumannii from a Chinese university hospital. Diagn. Microbiol. Infect. Dis. 84, 230–231.

Shen, Z., Wang, Y., Shen, Y., Shen, J., and Wu, C. (2016b). Early emergence of mcr-1 in Escherichia coli from food-producing animals. Lancet Infect. Dis. 16, 293.

Silva-Rocha, R., Martínez-García, E., Calles, B., Chavarría, M., Arce-Rodríguez, A., Heras, A. de las, Páez-Espino, A.D., Durante-Rodríguez, G., Kim, J., Nikel, P.I., et al. (2013). The Standard European Vector Architecture (SEVA): a coherent platform for the analysis and deployment of complex prokaryotic phenotypes. Nucleic Acids Res. 41, D666–D675.

Singh, G., Singh, G., Jadeja, D., and Kaur, J. (2010). Lipid hydrolizing enzymes in virulence: Mycobacterium tuberculosis as a model system. Crit. Rev. Microbiol. 36, 259–269.

Sipahi, O.R., Nazli Zeka, A., Taşbakan, M., Pullukçu, H., Arda, B., Yamazhan, T., Sipahi, H., and Ulusoy, S. (2017). Pooled analysis of 899 nosocomial meningitis episodes from Turkey. Turk. J. Med. Sci. 47, 29–33.

Snesrud, E., He, S., Chandler, M., Dekker, J.P., Hickman, A.B., McGann, P., and Dyda, F. (2016). A Model for Transposition of the Colistin Resistance Gene mcr-1 by ISApl1. Antimicrob. Agents Chemother. 60, 6973–6976.

Snitkin, E.S., Zelazny, A.M., Montero, C.I., Stock, F., Mijares, L., Program, N.C.S., Murray, P.R., Segre, J.A., Mullikin, J., Blakesley, R., et al. (2011). Genome-wide recombination drives diversification of epidemic strains of Acinetobacter baumannii. Proc. Natl. Acad. Sci. 108, 13758–13763.

Spellberg, B., and Bonomo, R.A. (2014). The Deadly Impact of Extreme Drug Resistance in Acinetobacter baumannii*. Crit. Care Med. 42, 1289–1291.

Spellberg, B., and Rex, J.H. (2013). The value of single-pathogen antibacterial agents. Nat. Rev. Drug Discov. 12, 963–963.

Srinivasan, V.B., Rajamohan, G., and Gebreyes, W.A. (2009). Role of AbeS, a novel efflux pump of the SMR family of transporters, in resistance to antimicrobial agents in Acinetobacter baumannii. Antimicrob. Agents Chemother. 53, 5312–5316.

Stephenson, K., and Hoch, J.A. (2002). Virulence- and antibiotic resistance-associated two-component signal transduction systems of Gram-positive pathogenic bacteria as targets for antimicrobial therapy. Pharmacol. Ther. 93, 293–305.

Stojanoski, V., Sankaran, B., Prasad, B.V.V., Poirel, L., Nordmann, P., and Palzkill, T. (2016). Structure of the catalytic domain of the colistin resistance enzyme MCR-1. BMC Biol. 14, 81.

Strateva, T., Todorova, A., Ouzounova-Raykova, V., and Mitov, I. (2008). Emergence of a PER-1 extended-spectrum beta-lactamase-producing Acinetobacter baumannii clinical isolate in Bulgaria. J. Chemother. Florence Italy 20, 391–392.

Strateva, T., Markova, B., Marteva-Proevska, Y., Ivanova, D., and Mitov, I. (2012). Widespread dissemination of multidrug-resistant Acinetobacter baumannii producing OXA-23 carbapenemase and ArmA 16S ribosomal RNA methylase in a Bulgarian university hospital. Braz. J. Infect. Dis. 16, 307–310.

Su, X.-Z., Chen, J., Mizushima, T., Kuroda, T., and Tsuchiya, T. (2005). AbeM, an H+-coupled Acinetobacter baumannii multidrug efflux pump belonging to the MATE family of transporters. Antimicrob. Agents Chemother. 49, 4362–4364.

Subashchandrabose, S., Smith, S., DeOrnellas, V., Crepin, S., Kole, M., Zahdeh, C., and Mobley, H.L.T. (2016). Acinetobacter baumannii Genes Required for Bacterial Survival during Bloodstream Infection. mSphere 1.

Sun, J.-R., Chan, M.-C., Chang, T.-Y., Wang, W.-Y., and Chiueh, T.-S. (2010). Overexpression of the adeB gene in clinical isolates of tigecycline-nonsusceptible Acinetobacter baumannii without insertion mutations in adeRS. Antimicrob. Agents Chemother. 54, 4934–4938.

Sun, J.-R., Perng, C.-L., Chan, M.-C., Morita, Y., Lin, J.-C., Su, C.-M., Wang, W.-Y., Chang, T.-Y., and Chiueh, T.-S. (2012). A Truncated AdeS Kinase Protein Generated by ISAba1 Insertion Correlates with Tigecycline Resistance in Acinetobacter baumannii. PLoS ONE 7, e49534.

Sunenshine, R.H., Wright, M.-O., Maragakis, L.L., Harris, A.D., Song, X., Hebden, J., Cosgrove, S.E., Anderson, A., Carnell, J., Jernigan, D.B., et al. (2007). Multidrug-resistant Acinetobacter Infection Mortality Rate and Length of Hospitalization. Emerg. Infect. Dis. 13, 97–103.

Szabó, D., Szentandrássy, J., Juhász, Z., Katona, K., Nagy, K., and Rókusz, L. (2008). Imported PER-1 producing Pseudomonas aeruginosa, PER-1 producing Acinetobacter baumanii and VIM-2-producing Pseudomonas aeruginosa strains in Hungary. Ann. Clin. Microbiol. Antimicrob. 7, 12.

Tada, T., Miyoshi-Akiyama, T., Kato, Y., Ohmagari, N., Takeshita, N., Hung, N.V., Phuong, D.M., Thu, T.A., Binh, N.G., Anh, N.Q., et al. (2013). Emergence of 16S rRNA methylase-producing Acinetobacter baumannii and Pseudomonas aeruginosa isolates in hospitals in Vietnam. BMC Infect. Dis. 13, 251.

Tada, T., Miyoshi-Akiyama, T., Shimada, K., Shimojima, M., and Kirikae, T. (2014). Dissemination of 16S rRNA methylase ArmA-producing acinetobacter baumannii and emergence of OXA-72 carbapenemase coproducers in Japan. Antimicrob. Agents Chemother. 58, 2916–2920.

Tada, T., Miyoshi-Akiyama, T., Shimada, K., Nga, T.T.T., Thu, L.T.A., Son, N.T., Ohmagari, N., and Kirikae, T. (2015). Dissemination of clonal complex 2 Acinetobacter baumannii strains co-producing carbapenemases and 16S rRNA methylase ArmA in Vietnam. BMC Infect. Dis. 15, 433.

Takayama, K., Wang, L., and David, H.L. (1972). Effect of isoniazid on the in vivo mycolic acid synthesis, cell growth, and viability of Mycobacterium tuberculosis. Antimicrob. Agents Chemother. 2, 29–35.

Tao, L., Hu, B., Rosenthal, V.D., Gao, X., and He, L. (2011). Device-associated infection rates in 398 intensive care units in Shanghai, China: International Nosocomial Infection Control Consortium (INICC) findings. Int. J. Infect. Dis. IJID Off. Publ. Int. Soc. Infect. Dis. 15, e774-780.

Teillant, A., Gandra, S., Barter, D., Morgan, D.J., and Laxminarayan, R. (2015). Potential burden of antibiotic resistance on surgery and cancer chemotherapy antibiotic prophylaxis in the USA: a literature review and modelling study. Lancet Infect. Dis. 15, 1429–1437.

Thabit, A.K., Crandon, J.L., and Nicolau, D.P. (2015). Antimicrobial resistance: impact on clinical and economic outcomes and the need for new antimicrobials. Expert Opin. Pharmacother. 16, 159–177.

Thom, K.A., Johnson, J.K., Lee, M.S., and Harris, A.D. (2011). Environmental contamination because of multidrug-resistant Acinetobacter baumannii surrounding colonized or infected patients. Am. J. Infect. Control 39, 711–715.

Tomaras, A.P., Dorsey, C.W., Edelmann, R.E., and Actis, L.A. (2003). Attachment to and biofilm formation on abiotic surfaces by Acinetobacter baumannii: involvement of a novel chaperone-usher pili assembly system. Microbiol. Read. Engl. 149, 3473–3484.

Trebosc, V., Gartenmann, S., Royet, K., Manfredi, P., Tötzl, M., Schellhorn, B., Pieren, M., Tigges, M., Lociuro, S., Sennhenn, P.C., et al. (2016). A Novel Genome-Editing Platform for Drug-Resistant Acinetobacter baumannii Reveals an AdeR-Unrelated Tigecycline Resistance Mechanism. Antimicrob. Agents Chemother. 60, 7263–7271.

Tucker, A.T., Nowicki, E.M., Boll, J.M., Knauf, G.A., Burdis, N.C., Trent, M.S., and Davies, B.W. (2014). Defining Gene-Phenotype Relationships in Acinetobacter baumannii through One-Step Chromosomal Gene Inactivation. mBio 5, e01313-14.

Turton, J.F., Woodford, N., Glover, J., Yarde, S., Kaufmann, M.E., and Pitt, T.L. (2006a). Identification of Acinetobacter baumannii by Detection of the blaOXA-51-like Carbapenemase Gene Intrinsic to This Species. J. Clin. Microbiol. 44, 2974–2976.

Turton, J.F., Ward, M.E., Woodford, N., Kaufmann, M.E., Pike, R., Livermore, D.M., and Pitt, T.L. (2006b). The role of ISAba1 in expression of OXA carbapenemase genes in Acinetobacter baumannii. FEMS Microbiol. Lett. 258, 72–77.

Udwadia, Z.F. (2012). MDR, XDR, TDR tuberculosis: ominous progression. Thorax 67, 286–288.

Vahaboglu, H., Oztürk, R., Aygün, G., Coşkunkan, F., Yaman, A., Kaygusuz, A., Leblebicioglu, H., Balik, I., Aydin, K., and Otkun, M. (1997). Widespread detection of PER-1-type extended-spectrum beta-lactamases among nosocomial Acinetobacter and Pseudomonas aeruginosa isolates in Turkey: a nationwide multicenter study. Antimicrob. Agents Chemother. 41, 2265–2269.

Valencia, R., Arroyo, L.A., Conde, M., Aldana, J.M., Torres, M.-J., Fernández-Cuenca, F., Garnacho-Montero, J., Cisneros, J.M., Ortíz, C., Pachón, J., et al. (2009). Nosocomial outbreak of infection with pan-drug-resistant Acinetobacter baumannii in a tertiary care university hospital. Infect. Control Hosp. Epidemiol. 30, 257–263.

Valentine, S.C., Contreras, D., Tan, S., Real, L.J., Chu, S., and Xu, H.H. (2008). Phenotypic and Molecular Characterization of Acinetobacter baumannii Clinical Isolates from Nosocomial Outbreaks in Los Angeles County, California. J. Clin. Microbiol. 46, 2499–2507.

Vila, J., Ruiz, J., Goñi, P., Marcos, A., and Jimenez de Anta, T. (1995). Mutation in the gyrA gene of quinolone-resistant clinical isolates of Acinetobacter baumannii. Antimicrob. Agents Chemother. 39, 1201–1203.

Vila, J., Ruiz, J., Goñi, P., and Jimenez de Anta, T. (1997). Quinolone-resistance mutations in the topoisomerase IV parC gene of Acinetobacter baumannii. J. Antimicrob. Chemother. 39, 757–762.

Vilacoba, E., Almuzara, M., Gulone, L., Traglia, G.M., Montaña, S., Rodríguez, H., Pasteran, F., Pennini, M., Sucari, A., Gómez, N., et al. (2016). Widespread dispersion of the resistance element tet(B)::ISCR2 in XDR Acinetobacter baumannii isolates. Epidemiol. Infect. 144, 1574–1578.

Vilchèze, C., and Jacobs, W. (2014). Resistance to Isoniazid and Ethionamide in Mycobacterium tuberculosis: Genes, Mutations, and Causalities. Microbiol. Spectr. 2.

Vilchèze, C., Morbidoni, H.R., Weisbrod, T.R., Iwamoto, H., Kuo, M., Sacchettini, J.C., and Jacobs, W.R. (2000). Inactivation of the inhA-encoded fatty acid synthase II (FASII) enoyl-acyl carrier protein reductase induces accumulation of the FASI end products and cell lysis of Mycobacterium smegmatis. J. Bacteriol. 182, 4059–4067.

Vilchèze, C., Wang, F., Arai, M., Hazbón, M.H., Colangeli, R., Kremer, L., Weisbrod, T.R., Alland, D., Sacchettini, J.C., and Jacobs, W.R. (2006). Transfer of a point mutation in Mycobacterium tuberculosis inhA resolves the target of isoniazid. Nat. Med. 12, 1027–1029.

Wang, F., Langley, R., Gulten, G., Dover, L.G., Besra, G.S., Jacobs, W.R., and Sacchettini, J.C. (2007). Mechanism of thioamide drug action against tuberculosis and leprosy. J. Exp. Med. 204, 73–78.

Wang, N., Ozer, E.A., Mandel, M.J., and Hauser, A.R. (2014). Genome-Wide Identification of Acinetobacter baumannii Genes Necessary for Persistence in the Lung. mBio 5, e01163-14.

Wang, Y., Shen, M., Yang, J., Dai, M., Chang, Y., Zhang, C., Luan, G., Ling, B., and Jia, X. (2016). Prevalence of carbapenemases among high-level aminoglycoside-resistant Acinetobacter baumannii isolates in a university hospital in China. Exp. Ther. Med. 12, 3642–3652.

Wang, Z., Ye, S., Li, J., Zheng, B., Bao, M., and Ning, G. (2011). Fusion primer and nested integrated PCR (FPNI-PCR): a new high-efficiency strategy for rapid chromosome walking or flanking sequence cloning. BMC Biotechnol. 11, 109.

Wanty, C., Anandan, A., Piek, S., Walshe, J., Ganguly, J., Carlson, R.W., Stubbs, K.A., Kahler, C.M., and Vrielink, A. (2013). The structure of the neisserial lipooligosaccharide phosphoethanolamine transferase A (LptA) required for resistance to polymyxin. J. Mol. Biol. 425, 3389–3402.

Weber, B.S., Harding, C.M., and Feldman, M.F. (2015a). Pathogenic Acinetobacter: from the cell surface to infinity and beyond. J. Bacteriol. JB.00906-15.

Weber, B.S., Ly, P.M., Irwin, J.N., Pukatzki, S., and Feldman, M.F. (2015b). A multidrug resistance plasmid contains the molecular switch for type VI secretion in Acinetobacter baumannii. Proc. Natl. Acad. Sci. 201502966.

Weber, W., Schoenmakers, R., Keller, B., Gitzinger, M., Grau, T., Baba, M.D.-E., Sander, P., and Fussenegger, M. (2008). A synthetic mammalian gene circuit reveals antituberculosis compounds. Proc. Natl. Acad. Sci. 105, 9994–9998.

Weiner, L.M., Webb, A.K., Limbago, B., Dudeck, M.A., Patel, J., Kallen, A.J., Edwards, J.R., and Sievert, D.M. (2016). Antimicrobial-Resistant Pathogens Associated With Healthcare-Associated Infections: Summary of Data Reported to the National Healthcare Safety Network at the Centers for Disease Control and Prevention, 2011-2014. Infect. Control Hosp. Epidemiol. 37, 1288–1301.

Weinstein, H.J., Hallett, W.Y., and Sarauw, A.S. (1962). The absorption and toxicity of ethionamide. Am. Rev. Respir. Dis. 86, 576–578.

Whitman, T.J., Qasba, S.S., Timpone, J.G., Babel, B.S., Kasper, M.R., English, J.F., Sanders, J.W., Hujer, K.M., Hujer, A.M., Endimiani, A., et al. (2008). Occupational Transmission of Acinetobacter baumannii from a United States Serviceman Wounded in Iraq to a Health Care Worker. Clin. Infect. Dis. Off. Publ. Infect. Dis. Soc. Am. 47, 439–443.

WHO (2014). Antimicrobial resistance: global report on surveillance.

WHO (2016). Global tuberculosis report 2016.

WHO (2017). Global priority list of antibiotic-resistant bacteria to guide research, discovery, and development of new antibiotics.

Wiehlmann, L., Wagner, G., Cramer, N., Siebert, B., Gudowius, P., Morales, G., Köhler, T., van Delden, C., Weinel, C., Slickers, P., et al. (2007). Population structure of Pseudomonas aeruginosa. Proc. Natl. Acad. Sci. U. S. A. 104, 8101–8106.

Willand, N., Dirié, B., Carette, X., Bifani, P., Singhal, A., Desroses, M., Leroux, F., Willery, E., Mathys, V., Déprez-Poulain, R., et al. (2009). Synthetic EthR inhibitors boost antituberculous activity of ethionamide. Nat. Med. 15, 537–544.

Winder, F.G., Collins, P.B., and Whelan, D. (1971). Effects of ethionamide and isoxyl on mycolic acid synthesis in Mycobacterium tuberculosis BCG. J. Gen. Microbiol. 66, 379–380.

Wong, D., Nielsen, T.B., Bonomo, R.A., Pantapalangkoor, P., Luna, B., and Spellberg, B. (2017). Clinical and Pathophysiological Overview of Acinetobacter Infections: a Century of Challenges. Clin. Microbiol. Rev. 30, 409–447.

World Health Organization (2014). Treatment strategies for MDR-TB and XDR-TB (World Health Organization).

Worthington, R.J., Blackledge, M.S., and Melander, C. (2013). Small-molecule inhibition of bacterial two-component systems to combat antibiotic resistance and virulence. Future Med. Chem. 5, 1265–1284.

Wright, G.D. (2016). Antibiotic Adjuvants: Rescuing Antibiotics from Resistance. Trends Microbiol. 24, 862–871.

Xue, T., You, Y., Hong, D., Sun, H., and Sun, B. (2011). The Staphylococcus aureus KdpDE Two-Component System Couples Extracellular K+ Sensing and Agr Signaling to Infection Programming ▿. Infect. Immun. 79, 2154–2167.

Yadegarynia, D., Gachkar, L., Fatemi, A., Zali, A., Nobari, N., Asoodeh, M., and Parsaieyan, Z. (2014). Changing pattern of infectious agents in postneurosurgical meningitis. Casp. J. Intern. Med. 5, 170–175.

Yao, X., Doi, Y., Zeng, L., Lv, L., and Liu, J.-H. (2016). Carbapenem-resistant and colistin-resistant Escherichia coli co-producing NDM-9 and MCR-1. Lancet Infect. Dis. 16, 288–289.

Yezli, S., Shibl, A.M., and Memish, Z.A. (2015). The molecular basis of β-lactamase production in Gram-negative bacteria from Saudi Arabia. J. Med. Microbiol. 64, 127–136.

Yoon, E.-J., Chabane, Y.N., Goussard, S., Snesrud, E., Courvalin, P., Dé, E., and Grillot-Courvalin, C. (2015). Contribution of resistance-nodulation-cell division efflux systems to antibiotic resistance and biofilm formation in Acinetobacter baumannii. mBio 6.

Yun, H.C., Branstetter, J.G., and Murray, C.K. (2008). Osteomyelitis in military personnel wounded in Iraq and Afghanistan. J. Trauma 64, S163–168; discussion S168.

Zarrilli, R., Pournaras, S., Giannouli, M., and Tsakris, A. (2013). Global evolution of multidrug-resistant Acinetobacter baumannii clonal lineages. Int. J. Antimicrob. Agents 41, 11–19.

Zavascki, A.P., Goldani, L.Z., Li, J., and Nation, R.L. (2007). Polymyxin B for the treatment of multidrug-resistant pathogens: a critical review. J. Antimicrob. Chemother. 60, 1206–1215.

Zawilska, J.B., Wojcieszak, J., and Olejniczak, A.B. (2013). Prodrugs: A challenge for the drug development. Pharmacol. Rep. 65, 1–14.

Zhang, Y., and Yew, W.-W. (2015). Mechanisms of drug resistance in Mycobacterium tuberculosis: update 2015. Int. J. Tuberc. Lung Dis. 19, 1276–1289.

Zhang, J.P., Zhu, W., Tian, S.F., Chu, Y.Z., and Chen, B.Y. (2010). Molecular characteristics and resistant mechanisms of imipenem-resistant Acinetobacter baumannii isolates in Shenyang, China. J. Microbiol. Seoul Korea 48, 689–694.

Zhang, W.-J., Lu, Z., Schwarz, S., Zhang, R.-M., Wang, X.-M., Si, W., Yu, S., Chen, L., and Liu, S. (2013). Complete sequence of the blaNDM-1-carrying plasmid pNDM-AB from Acinetobacter baumannii of food animal origin. J. Antimicrob. Chemother. 68, 1681–1682.

Zhang, Y., Heym, B., Allen, B., Young, D., and Cole, S. (1992). The catalase-peroxidase gene and isoniazid resistance of Mycobacterium tuberculosis. Nature 358, 591–593.

Zheng, J., Rubin, E.J., Bifani, P., Mathys, V., Lim, V., Au, M., Jang, J., Nam, J., Dick, T., Walker, J.R., et al. (2013). para-Aminosalicylic acid is a prodrug targeting dihydrofolate reductase in Mycobacterium tuberculosis. J. Biol. Chem. 288, 23447–23456.

Zhong, L.-L., Zhang, Y.-F., Doi, Y., Huang, X., Zhang, X.-F., Zeng, K.-J., Shen, C., Patil, S., Xing, Y., Zou, Y., et al. (2017). Coproduction of MCR-1 and NDM-1 by Colistin-Resistant Escherichia coli Isolated from a Healthy Individual. Antimicrob. Agents Chemother. 61, e01962-16.

Zhu, M., Namdar, R., Stambaugh, J.J., Starke, J.R., Bulpitt, A.E., Berning, S.E., and Peloquin, C.A. (2002). Population pharmacokinetics of ethionamide in patients with tuberculosis. Tuberc. Edinb. Scotl. 82, 91–96.

Zimbler, D.L., Arivett, B.A., Beckett, A.C., Menke, S.M., and Actis, L.A. (2013). Functional Features of TonB Energy Transduction Systems of Acinetobacter baumannii. Infect. Immun. 81, 3382–3394.

Zimmerman, M.R. (1979). Pulmonary and osseous tuberculosis in an Egyptian mummy. Bull. N. Y. Acad. Med. 55, 604–608.

Zowawi, H.M., Harris, P.N.A., Roberts, M.J., Tambyah, P.A., Schembri, M.A., Pezzani, M.D., Williamson, D.A., and Paterson, D.L. (2015). The emerging threat of multidrug-resistant Gram-negative bacteria in urology. Nat. Rev. Urol. 12, 570–584.

M100-S24: Performance Standards for Antimicrobial Susceptibility Testing; Twenty-Fourth Informational Supplement - CLSI_M100-S24.pdf.

M07-A9: Methods for Dilution Antimicrobial Susceptibility Tests for Bacteria That Grow Aerobically; Approved Standard—Ninth Edition - 03-CLSI-M07-A9-2012.pdf.